

AD-A020 500

INFLUENCE OF ELASTOHYDRODYNAMIC LUBRICATION ON THE LIFE
AND OPERATION OF URBINE ENGINE BALL BEARINGS.
BEARING DESIGN MANUAL

J. I. McCool, et al

SKF Industries, Incorporated

Prepared for:

Air Force Aero Propulsion Laboratory

May 1975

DISTRIBUTED BY:

NTIS

National Technical Information Service
U. S. DEPARTMENT OF COMMERCE

RDAC20500

049136

Reproduced by
NATIONAL TECHNICAL
INFORMATION SERVICE
U.S. Department of Commerce
Springfield, VA 22151

049136
ADA020500

FINAL TECHNICAL REPORT
ON
INFLUENCE OF ELASTOHYDRODYNAMIC LUBRICATION
ON THE LIFE AND OPERATION OF TURBINE ENGINE BALL BEARINGS
-BEARING DESIGN MANUAL-

Contributors

J. I. McCool
Y. P. Chiu
W. J. Crecelius
J. Y. Liu
J. W. Rosenlieb

Prepared: *J. I. McCool*

Approved:

Released:

Air Force Contract No. F33615-72-C-1467
Navy MIPR No. M62376-3-000007
S K F Report: AL75P014
S K F Reg 414 2

SUBMITTED TO:

AIR FORCE AERO PROPULSION LABORATORY
WRIGHT-PATTERSON AIR FORCE BASE
DAYTON, OHIO 45433

AND

NAVAL AIR PROPULSION TEST CENTER
TRENTON, NEW JERSEY 08628

RESEARCH LABORATORY
SKF INDUSTRIES, INC.
ENGINEERING AND RESEARCH CENTER
KING OF PRUSSIA, PA.

1. TITLE	2. AUTHOR
3. PERFORMING ORGANIZATION	4. REPORT NUMBER
5. AUTHORING ORGANIZATION	6. PERFORMING ORGANIZATION
7. AUTHORING ORGANIZATION	8. PERFORMING ORGANIZATION
9. AUTHORING ORGANIZATION	10. PERFORMING ORGANIZATION
11. AUTHORING ORGANIZATION	12. PERFORMING ORGANIZATION
13. AUTHORING ORGANIZATION	14. PERFORMING ORGANIZATION
15. AUTHORING ORGANIZATION	16. PERFORMING ORGANIZATION
17. AUTHORING ORGANIZATION	18. PERFORMING ORGANIZATION
19. AUTHORING ORGANIZATION	20. PERFORMING ORGANIZATION
21. AUTHORING ORGANIZATION	22. PERFORMING ORGANIZATION
23. AUTHORING ORGANIZATION	24. PERFORMING ORGANIZATION
25. AUTHORING ORGANIZATION	26. PERFORMING ORGANIZATION
27. AUTHORING ORGANIZATION	28. PERFORMING ORGANIZATION
29. AUTHORING ORGANIZATION	30. PERFORMING ORGANIZATION
31. AUTHORING ORGANIZATION	32. PERFORMING ORGANIZATION
33. AUTHORING ORGANIZATION	34. PERFORMING ORGANIZATION
35. AUTHORING ORGANIZATION	36. PERFORMING ORGANIZATION
37. AUTHORING ORGANIZATION	38. PERFORMING ORGANIZATION
39. AUTHORING ORGANIZATION	40. PERFORMING ORGANIZATION
41. AUTHORING ORGANIZATION	42. PERFORMING ORGANIZATION
43. AUTHORING ORGANIZATION	44. PERFORMING ORGANIZATION
45. AUTHORING ORGANIZATION	46. PERFORMING ORGANIZATION
47. AUTHORING ORGANIZATION	48. PERFORMING ORGANIZATION
49. AUTHORING ORGANIZATION	50. PERFORMING ORGANIZATION
51. AUTHORING ORGANIZATION	52. PERFORMING ORGANIZATION
53. AUTHORING ORGANIZATION	54. PERFORMING ORGANIZATION
55. AUTHORING ORGANIZATION	56. PERFORMING ORGANIZATION
57. AUTHORING ORGANIZATION	58. PERFORMING ORGANIZATION
59. AUTHORING ORGANIZATION	60. PERFORMING ORGANIZATION
61. AUTHORING ORGANIZATION	62. PERFORMING ORGANIZATION
63. AUTHORING ORGANIZATION	64. PERFORMING ORGANIZATION
65. AUTHORING ORGANIZATION	66. PERFORMING ORGANIZATION
67. AUTHORING ORGANIZATION	68. PERFORMING ORGANIZATION
69. AUTHORING ORGANIZATION	70. PERFORMING ORGANIZATION
71. AUTHORING ORGANIZATION	72. PERFORMING ORGANIZATION
73. AUTHORING ORGANIZATION	74. PERFORMING ORGANIZATION
75. AUTHORING ORGANIZATION	76. PERFORMING ORGANIZATION
77. AUTHORING ORGANIZATION	78. PERFORMING ORGANIZATION
79. AUTHORING ORGANIZATION	80. PERFORMING ORGANIZATION
81. AUTHORING ORGANIZATION	82. PERFORMING ORGANIZATION
83. AUTHORING ORGANIZATION	84. PERFORMING ORGANIZATION
85. AUTHORING ORGANIZATION	86. PERFORMING ORGANIZATION
87. AUTHORING ORGANIZATION	88. PERFORMING ORGANIZATION
89. AUTHORING ORGANIZATION	90. PERFORMING ORGANIZATION
91. AUTHORING ORGANIZATION	92. PERFORMING ORGANIZATION
93. AUTHORING ORGANIZATION	94. PERFORMING ORGANIZATION
95. AUTHORING ORGANIZATION	96. PERFORMING ORGANIZATION
97. AUTHORING ORGANIZATION	98. PERFORMING ORGANIZATION
99. AUTHORING ORGANIZATION	100. PERFORMING ORGANIZATION

A

D D C
RECEIVED
MAY 12 1975
DISTRIBUTION

DISTRIBUTION STATEMENT
Approved for Public Release
Distribution Unlimited

FINAL TECHNICAL REPORT
ON
INFLUENCE OF ELASTOHYDRODYNAMIC LUBRICATION
ON THE LIFE AND OPERATION OF TURBINE ENGINE BALL BEARINGS
-BEARING DESIGN MANUAL-

Contributors

J. I. McCool
Y. P. Chiu
W. J. Crecelius
J. Y. Liu
J. W. Rosenlieb

Prepared: *John I. McCool*

Air Force Contract No. F33615-72-C-1467
Navy MIPR No. M62376-3-000007
S K F Report: AL75PO14
S K F Reg 414 2

Approved: *[Signature]*

Released: *[Signature]*

SUBMITTED TO:

AIR FORCE AERO PROPULSION LABORATORY
WRIGHT-PATTERSON AIR FORCE BASE
DAYTON, OHIO 45433

AND

NAVAL AIR PROPULSION TEST CENTER
TRENTON NEW JERSEY 08628

RESEARCH LABORATORY
SKF INDUSTRIES, INC.
ENGINEERING AND RESEARCH CENTER
KING OF PRUSSIA, PA

PH-4158 (Rev. 1-60)

1. TITLE	2. AUTHOR
3. SUBJECT	4. DISTRIBUTION STATEMENT
5. ABSTRACT	6. NOTES
7. REFERENCES	8. OTHER
9. INDEXING	10. SPECIAL

A

D D C
RECEIVED
JUN 12 1975
RECEIVED

DISTRIBUTION STATEMENT
Approved for public release
Distribution Unlimited

NOTICE

When Government drawings, specifications, or other data are used for any purpose other than in connection with a definitely related Government procurement operation, the United States Government thereby incurs no responsibility nor any obligation whatsoever; and the fact that the government may have formulated, furnished, or in any way supplied the said drawings, specifications, or other data, is not to be regarded by implication or otherwise as in any manner licensing the holder or any other person or corporation, or conveying any rights or permission to manufacture, use, or sell any patented invention that may in any way be related thereto.

Publication of this report does not constitute Air Force approval of the reports findings or conclusions. It is published only for the exchange and stimulation of ideas.

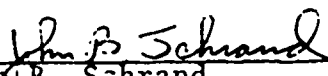
This report describes the work performed by S K F Industries, Inc. at its Technology Center in King of Prussia, Pa. for the United States Air Force Systems Command, Air Force Aero Propulsion Laboratory, Wright-Patterson Air Force Base, Ohio and for the Naval Air Propulsion Test Center, Trenton, N. J. The work was performed over a thirty-six month period starting in March 1972 under U. S. Air Force Contract No. F33615-72-C-1467 and Navy MIPR No. M62376-3-000007. Mr. John Jenkins and Mr. John Schrand administered the project for the Air Force and Mr. Raymond Valori administered the project for the Navy.

The project was conducted at S K F under the direction of Messrs. L. B. Sibley, P. S. Given and T. E. Tallian. The S K F report designation is No. AL75P014.


The report contains the results of an analytical modelling, computer program development and full-scale bearing test effort.

This report has been reviewed by the Information Office, (ASD/OIP) and is releasable to the National Technical Information Service (NTIS). At NTIS, it will be available to the general public, including foreign nations.

This technical report has been reviewed and is approved for publication.

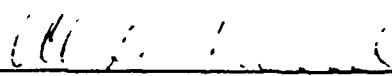

John B. Schrand
Project Engineer

FOR THE COMMANDER


Howard F. Jones
Chief, Lubrication Branch
Fuels and Lubrication Division
Air Force Aero Propulsion Laboratory


Raymond Valori
Project Engineer

FOR THE COMMANDING OFFICER


Al Lockwood, Supervisor
Lubricants and Power Drive
Systems Division, Naval Air
Propulsion Test Center

UNCLASSIFIED

SECURITY CLASSIFICATION OF THIS PAGE (When Data Entered)

REPORT DOCUMENTATION PAGE		READ INSTRUCTIONS BEFORE COMPLETING FORM
1. REPORT NUMBER AFAPL-TR-75-25	2. GOVT ACCESSION NO.	3. RECIPIENT'S CATALOG NUMBER
4. TITLE (and Subtitle) Influence of Elastohydrodynamic Lubrication on the Life and Operation of Turbine Engine Ball Bearings - Bearing Design Manual		5. TYPE OF REPORT & PERIOD COVERED Final Technical Report March '72-March '75
7. AUTHOR(s) J. I. McCool Y. P. Chiu W. J. Crecelius		6. PERFORMING ORG. REPORT NUMBER AL75P014
9. PERFORMING ORGANIZATION NAME AND ADDRESS SKF Industries, Inc., Technology Center 1100 First Ave. King of Prussia, Pa. 19406		8. CONTRACT OR GRANT NUMBER(s) AF Contract No. F33615-72-C-1467 Navy MIPR No. M62376-3-000007
11. CONTROLLING OFFICE NAME AND ADDRESS Air Force Aero Propulsion Laboratory Air Force Systems Command Wright-Patterson Air Force Base, Ohio		10. PROGRAM ELEMENT, PROJECT, TASK AREA & WORK UNIT NUMBERS
14. MONITORING AGENCY NAME & ADDRESS (if different from Controlling Office) Air Force Aero Propulsion Laboratory and Naval Air Propulsion Test Center Trenton, New Jersey 08628		12. REPORT DATE May 1975
16. DISTRIBUTION STATEMENT (of this Report) Approved for public release; distribution unlimited		13. NUMBER OF PAGES 303
17. DISTRIBUTION STATEMENT (of the abstract entered in Block 20, if different from Report)		15. SECURITY CLASS. (of this report) Unclassified
18. SUPPLEMENTARY NOTES		15a. DECLASSIFICATION/DOWNGRADING SCHEDULE
19. KEY WORDS (Continue on reverse side if necessary and identify by block number) Bearing Dynamics, Elastohydrodynamics (EHD), EHD Starvation, EHD Traction, Partial EHD, Surface Asperity Contact, Asperity Traction, Coulomb Friction, Boundary Lubrication, Hydrodynamic Lubrication, Cage Lubrication, Cage Dynamics, Shaft/Bearing Systems, Bearing Heat Generation, Steady-State Heat Transfer, Transient Heat Transfer.		
20. ABSTRACT (Continue on reverse side if necessary and identify by block number) This report is a self contained manual describing the rationale, use and predictive accuracy of an advanced state-of-the-art ball bearing analysis computer program. This program embodies mathematical models describing the lubricant's role in bearing behavior that were developed or adopted for this purpose. Mathematical descriptions of these models are set forth along with a detailed description of the program's organization, method of solution and		

DD FORM 1 JAN 73 1473

EDITION OF 1 NOV 65 IS OBSOLETE

UNCLASSIFIED

SECURITY CLASSIFICATION OF THIS PAGE (When Data Entered)

i-b

UNCLASSIFIED

SECURITY CLASSIFICATION OF THIS PAGE (When Data Entered)

20. ABSTRACT

convergence criteria. Input data preparation forms and program output are discussed in detail and examples of each are included.

Comparisons are given of the program's predictions and the values of heat generation rate, film thickness, and cage and ball rotational speeds measured in tests of a 125-mm bore angular-contact ball bearing operating at various axial loads at speeds up to 3.1×10^6 DN.

Parametric runs of the program in which key variables are systematically altered are included and interpreted.

UNCLASSIFIED

SECURITY CLASSIFICATION OF THIS PAGE (When Data Entered)

TABLE OF CONTENTS

SECTION		PAGE
1	INTRODUCTION AND SUMMARY	1
2	COMPUTER PROGRAM ORGANIZATION AND SCOPE	5
	2.1 PROGRAM GUIDELINES	5
	2.2 GENERAL PROGRAM	5
	2.3 A TYPICAL SYSTEM	6
	2.4 GENERAL LOGIC DIAGRAM - SYSTEM LEVEL	8
	2.5 LOGIC DIAGRAM SHAFT-BEARING EQUILIBRIUM CALCULATION	10
	2.6 HIERARCHICAL FLOW CHART	12
3	ANALYTICAL FORMULATION	15
	3.1 THE BALL BEARING SOLUTION	15
	3.1.1 BALL MOTIONS	15
	3.1.2 THE UNKNOWNNS FOR A BALL BEARING PROBLEM	20
	3.2 FORCES ACTING ON A BALL	20
	3.3 INERTIA FORCES AND MOMENTS ACTING ON A BALL	21
	3.4 CAGE MODEL	23
	3.5 BEARING GENERATED HEAT	25
	3.5.1 CONTACT REGIONS	26
	3.5.2 INLET REGIONS	26
	3.5.3 CAGE-LAND	27
	3.5.4 FLUID DRAG	27
	3.5.5 SUMMARIZATION OF HEAT GENERA- TION RATES	27

TABLE OF CONTENTS (CONTD)

SECTION		PAGE
3.6	TEMPERATURE DISTRIBUTION CALCULATION	28
3.6.1	STEADY STATE TEMPERATURES	28
3.6.2	TRANSIENT TEMPERATURES	28
3.7	CALCULATION OF HEAT TRANSFER RATE	30
3.7.1	GENERATED HEAT	30
3.7.2	CONDUCTION	31
3.7.3	FREE CONVECTION	31
3.7.4	FORCED CONVECTION	32
3.7.5	RADIATION	33
3.7.6	FLUID FLOW	34
3.7.7	TOTAL HEAT TRANSFERRED	35
3.8	CONDUCTION THROUGH A BEARING	36
3.8.1	THERMAL RESISTANCE	36
3.9	SOLUTION SCHEMES AND CONVERGENCE CRITERIA	39
3.9.1	TEMPERATURE EQUILIBRIUM CONVERGENCE CRITERIA	40
3.9.2	BEARING DIAMETRAL CLEARANCE CHANGE ANALYSIS	41
3.9.3	BEARING INNER RING EQUILIBRIUM	42
3.9.4	BEARING QUASI-DYNAMIC SOLUTION	45
3.10	METHOD FOR SOLVING BEARING EQUILI- BRIUM EQUATIONS	48
4	MATHEMATICAL MODELS	52
4.1	SCOPE	52
4.2	LUBRICANT PROPERTY MODELS	52
4.3	LUBRICANT FILM THICKNESS	53

TABLE OF CONTENTS (CONTD)

SECTION		PAGE
	4.3.1 INLET HEATING FACTOR ϕ_t	55
	4.3.2 STARVATION REDUCTION FACTOR ϕ_s	57
	4.3.3 FILM REPLENISHMENT	59
	4.3.4 FILM REPLENISHMENT MODEL FOR A FULL SCALE BEARING	60
4.4	TRACTION IN BALL-RACE CONTACTS	61
	4.4.1 ASPERITY TRACTION MODEL	62
	4.4.2 FLUID TRACTION COEFFICIENT μ_{EHD}	63
	4.4.3 COMPUTING TRACTION FORCE FOR A HERTZIAN CONTACT	68
4.5	CALCULATION OF CAGE POCKET NORMAL FORCES	71
	4.5.1 ELASTOHYDRODYNAMIC (EHD) CONTACT	75
	4.5.2 HYDRODYNAMIC (HD) CONTACT	75
4.6	CALCULATION OF HYDRODYNAMIC FRICTION FORCES IN POINT CONTACT	76
4.7	BALL DRAG FORCE IN AMBIENT LUBRICANT	86
4.8	BEARING LIFE REDUCTION DUE TO ASPERITY INTERACTION	87
5	INPUT DATA PREPARATION	89
	5.1 TYPES OF INPUT DATA	89
	5.2 DATA SET I - TITLE CARDS	90
	5.2.1 TITLE CARD 1	90
	5.2.2 TITLE CARD 2	90
	5.3 DATA SET II - BEARING DATA	92
	5.3.1 CARD TYPE 1	93

TABLE OF CONTENTS (CONTD)

SECTION	PAGE
5.3.2 CARD TYPE 2	94
5.3.3 CARD TYPE 3	94
5.3.3.1 BALL BEARING GEOMETRY INPUT	94
5.3.3.2 CYLINDRICAL ROLLER BEARING CONTACT GEOMETRY DATA	97
5.3.4 CARD TYPE 4	99
5.3.5 CARD TYPES 5 & 6	99
5.3.6 CARD TYPE 7	99
5.3.7 CARD TYPES 8, 9, 10, 11, 12	99
5.3.8 CARD TYPE 13	100
5.3.9 CARD TYPE 14	100
5.4 DATA SET III - THERMAL MODEL DATA	102
5.4.1 CARD TYPE 1	102
5.4.2 CARD TYPE 2	105
5.4.3 CARD TYPE 3	105
5.4.4 CARD TYPE 4	105
5.4.5 CARD TYPE 5	105
5.4.6 CARD TYPE 6	106
5.4.7 CARD TYPE 7	106
5.4.8 CARD TYPE 8	107
5.4.9 CARD TYPE 9	108
5.5 DATA SET IV - SHAFT INPUT DATA	108
5.5.1 CARD TYPE 1	108
5.5.2 CARD TYPE 2	109

TABLE OF CONTENTS (CONTD)

SECTION	PAGE
5.5.3 CARD TYPE 3	109
6 COMPUTER PROGRAM OUTPUT	110
6.1 INTRODUCTION	110
6.2 BEARING OUTPUT	111
6.2.1 LINEAR AND ANGULAR DEFLECTIONS	111
6.2.2 FORCES AND MOMENTS	111
6.2.3 FRICTION HEAT GENERATION RATE (WATTS)	111
6.2.4 TORQUE	112
6.2.5 FATIGUE LIFE (HOURS)	112
6.2.6 h/σ	112
6.2.7 LIFE MULTIPLIERS	112
6.2.7.1 LUBRICATION	112
6.2.7.2 MATERIAL	112
6.2.8 EHD FILM DATA FOR THE MOST HEAVILY LOADED ROLLING ELEMENT	112
6.2.8.1 FRICTION COEFFICIENT	112
6.2.8.2 CORRECTED FILM	113
6.2.8.3 THERMAL REDUCTION FACTOR	113
6.2.8.4 STARVATION REDUCTION FACTOR	113
6.2.8.5 MENISCUS DISTANCE (MM)	113
6.2.9 LUBRICANT TEMPERATURES AND PHYSICAL PROPERTIES	113

TABLE OF CONTENTS (CONTD)

SECTION		PAGE
	6.2.10 RING SPEEDS	113
	6.2.11 CALCULATED CAGE SPEED	113
	6.2.12 EPICYCLIC CAGE SPEED	114
	6.2.13 PERCENT DIFFERENCE	114
	6.2.14 FIT PRESSURES	114
	6.2.15 CLEARANCES	114
	6.2.16 SPEED GIVING ZERO FIT PRESSURE (BETWEEN THE SHAFT AND INNER RING)	114
6.3	ROLLING ELEMENT OUTPUT	114
	6.3.1 BALL SPEEDS	115
	6.3.2 SPEED VECTOR ANGLES	115
	6.3.3 NORMAL FORCES	115
	6.3.4 HERTZ STRESS	115
	6.3.5 LOAD RATIO Q_{asp}/Q_{tot}	115
	6.3.6 CONTACT ANGLES	116
6.4	THERMAL DATA	116
6.5	PROGRAM ERROR MESSAGES	116
	6.5.1 FROM SUBROUTINE ALLT	116
	6.5.2 FROM SUBROUTINE SHABE	116
	6.5.3 FROM SUBROUTINE SOLVXX	117
	6.5.4 FROM SUBROUTINE INTFIT	118
6.6	GUIDES TO PROGRAM USE	118
7	DISCUSSION OF PREDICTIVE ACCURACY	120
	7.1 TEST RIG DESCRIPTION	120
	7.1.1 RIG STRUCTURAL COMPONENTS	120

TABLE OF CONTENTS (CONTD)

SECTION		PAGE
7.1.2	THRUST APPLICATION AND MEASUREMENT SYSTEM	120
7.1.3	TORQUE MEASUREMENT SYSTEM	122
7.1.4	RIG DRIVE SYSTEM	122
7.1.5	TEST OIL RECIRCULATING AND CONDITIONING SYSTEM	124
7.1.6	BEARING INNER RING MOUNTING SLEEVES	125
7.1.7	INSTRUMENTATION USED IN FULL SCALE BEARING TESTING	127
7.2	EXPERIMENTAL EVALUATION OF CAGE AND BALL ANGULAR VELOCITIES	128
7.3	DESIGN OF THE TESTS	130
7.4	TEST BEARING HEAT GENERATION RATES	132
7.5	COMPUTER PREDICTIONS FOR FULL SCALE TESTS	138
7.5.1	INPUT PARAMETER VALUES	138
7.5.1.1	GEOMETRY DATA	138
7.5.1.2	TEMPERATURE DATA	139
7.5.1.3	OTHER INPUT PARAMETER VALUES	139
7.5.2	COMPARISON OF PREDICTED AND MEASURED VALUES - MIL-L-7808G LUBRICANT	140
7.5.2.1	HEAT GENERATION RATE PREDICTION - MIL-L-7808G LUBRICANT	140
7.5.2.2	BALL AND CAGE KINEMATIC PREDICTIONS - MIL-L-7808G LUBRICANT	143
7.5.2.3	FILM THICKNESS PREDICTIONS - MIL-L-7808G LUBRICANT	145

TABLE OF CONTENTS (CONTD)

SECTION		PAGE
	7.5.3 COMPARISON OF PREDICTED AND MEASURED VALUES - MIL-L-23699 LUBRICANT	152
	7.5.4 SUMMARY OF PROGRAM ACCURACY ASSESSMENT	156
8	PARAMETRIC STUDIES AND DISCUSSION OF PROGRAM BEHAVIOR	157
	8.1 INTRODUCTION	157
	8.2 DATA SET I - COMPUTER PREDICTIONS FOR FULL SCALE TEST CONDITIONS	165
	8.2.1 FILM THICKNESS	165
	8.2.2 ASPERITY FRICTION	166
	8.2.3 CAGE SLIP, TEST NO. 4	167
	8.2.4 RACEWAY CONTROL	172
	8.3 DATA SET II - PARAMETRIC STUDIES OF FLUID RESISTANCE, FILM REPLENISHMENT AND CONTACT ANGLE	173
	8.3.1 LUBRICANT MEDIUM DENSITY STUDY	173
	8.3.2 $\Delta\zeta$ VARIATION	174
	8.3.3 CONTACT ANGLE VARIATIONS	174
	8.4 DATA SET III - PARAMETRIC STUDIES OF THE RACEWAY CONTROL ASSUMPTION	178
	8.5 OVERVIEW OF THE DATA	184
REFERENCES		186
APPENDIX A	HEAT TRANSFER INFORMATION	189
APPENDIX B	INPUT DATA PREPARATION FORMS AND EXAMPLE	197
APPENDIX C	SAMPLE BALL BEARING PROGRAM OUTPUT	251
APPENDIX D	SAMPLE THERMAL ANALYSIS OUTPUT	264

LIST OF ILLUSTRATIONS

FIGURE		PAGE
2-1	TYPICAL SHAFT-BEARING SYSTEM	7
2-2	GENERAL PROGRAM FLOW CHART	9
2-3	FLOW-CHART OF SHAFT BEARING EQUILIBRIUM CALCULATION	11
2-4	HIERARCHICAL FLOW CHART	13
3-1	BEARING INERTIAL (XYZ) AND ROLLING ELEMENT (xyz) COORDINATE SYSTEMS	16
3-2	RADIAL SECTION AT AZIMUTH LOCATION ϕ	17
3-3	ROLLING ELEMENT SPEEDS AND DISPLACEMENTS	19
3-4	CAGE GEOMETRY	24
3-5	CONVECTIVE HEAT TRANSFER	34
3-6	DIVIDED FLUID FLOW FROM NODE i	35
3-7	CONTACT GEOMETRY AND TEMPERATURES	38
4-1	FILM GEOMETRY	58
4-2	TYPICAL TRACTION CURVES	64
4-3	μ_r VERSUS x	66
4-4	CALCULATION OF TRACTION FORCE COMPONENTS	70
4-5	CAGE POCKET GEOMETRY	72
4-6	LOAD CAPACITY VERSUS FILM THICKNESS FOR HYDRODYNAMIC AND ELASTOHYDRODYNAMIC OPERATING REGIMES	74
4-7	NOTATION FOR ROLLING SLIDING POINT CONTACT	78
4-8	FRICTION FORCES ON SLIDING AND/OR ROLLING DISKS	79
4-9	VARIATION OF F_S WITH ρ_1	82

LIST OF ILLUSTRATIONS (CONTD)

FIGURE		PAGE
4-10	VARIATION OF F_R WITH THE DIMENSIONLESS MENISCUS DISTANCE ρ_1 .	83
4-11	CONFIGURATION OF CONTACTS	85
5-1	SPLIT INNER RING AND ANGULAR CONTACT BALL BEARINGS UNDER AXIAL LOAD	95
5-2	SPLIT INNER RING BALL BEARING	96
5-3	ANGULAR CONTACT BALL BEARING	98
5-4	FRICTION COEFFICIENT VERSUS SLIDING VELOCITY	101
7-1	TEST RIG FOR FULL-SCALE BEARING TESTS	121
7-2	TEST RIG - GENERAL PLAN VIEW	123
7-3	BEARING INNER RACE MOUNTING SLEEVE	126
7-4	SEARCH COIL DESIGN	129
7-5	BEARING AND LUBRICATION TEMPERATURE (TEST 11)	137
7-6	HEAT GENERATION, MIL-L-7808G, TEST NO. 11, P=3280	142
7-7	EXPERIMENTAL AND CALCULATED HEAT GENERATION RATES, MIL-L-7808G, SKIDDING TEST NO. 4, 10,000 RPM.	144
7-8	COMPARISON OF PREDICTED AND OBSERVED CAGE ROTATIONAL VELOCITY, MIL-L-7808G, TEST NO. 4, 10,000 RPM.	146
7-9	THEORETICAL RELATION BETWEEN T/T_0 AND FILM THICKNESS FOR 1000 LBS. THRUST LOAD AT 4000 RPM.	149
7-10	MEASURED T/T_0 VERSUS CALCULATED OUTER RING FILM THICKNESS, MIL-L-7808G.	151
7-11	MEASURED T/T_0 VERSUS CALCULATED OUTER RING FILM THICKNESS, MIL-L-23699.	155

LIST OF ILLUSTRATIONS (CONTD)

FIGURE		PAGE
8-1	PROGRAM PREDICTED HEAT GENERATION RATES FOR EXPERIMENTAL TEST NO. 1 VERSUS SHAFT SPEED	168
8-2	PROGRAM PREDICTED HEAT GENERATION RATES FOR EXPERIMENTAL TEST NO. 11 VERSUS SHAFT SPEED	169
8-3	PROGRAM PREDICTED HEAT GENERATION RATES FOR EXPERIMENTAL TEST NO. 2 VERSUS SHAFT SPEED	170
8-4	PROGRAM PREDICTED CAGE-TO-SHAFT SPEED RATIO AND HEAT GENERATION RATES FOR EXPERIMENTAL TEST NO. 4 VERSUS APPLIED AXIAL LOAD	171
8-5	PROGRAM PREDICTED HEAT GENERATION RATE VERSUS $\Delta\zeta$	175
8-6	PROGRAM PREDICTED OUTER RACE DATA	176
8-7	PROGRAM PREDICTED INNER RACE DATA	177
8-8	BEARING HEAT GENERATION RATES AND CAGE-TO- SHAFT SPEED RATIO VERSUS UNMOUNTED CONTACT ANGLE	179
8-9	BEARING AND RACEWAY L ₁₀ FATIGUE LIFE VERSUS UNMOUNTED CONTACT ANGLE	180
8-10	BALL SPEED VECTOR PITCH ANGLE VERSUS SHAFT SPEED	182
8-11	BALL SPEED VECTOR PITCH ANGLE VERSUS SHAFT SPEED	183

LIST OF TABLES

TABLE		PAGE
4-1	LUBRICANT PROPERTIES OF FOUR OILS USED IN PROGRAM AT74Y001	54
4-2	TABULATION OF CONSTANTS FOR FOUR OILS	69
7-1	BEARING TEST MATRIX	131
7-2	SKIDDING TESTS. MIL-L-7808G, 10,000 RPM	133
7-3	EXPERIMENTAL BEARING HEAT GENERATION RATES	135
7-4	MIL-L-7808G TEST AND PROGRAM COMPARISON	141
7-5	MEASURED T/T ₀ - VARNISHED AND UNVARNISHED BEARINGS	153
7-6	MIL-L-23699 TEST AND PROGRAM COMPARISON	154
8-1	EXPANDED OUTPUT LIST FULL SCALE TEST PROGRAM	158
8-2	PARAMETRIC RUNS - 125 mm BORE ANGULAR CONTACT BALL BEARING, MIL-L-7808G. 10,000 RPM, 1000 LBS. LOAD	160
8-3	PARAMETRIC RUNS - 45 mm BORE ANGULAR CONTACT BALL BEARING, MIL-L-7808G LUBRICANT	162

NOMENCLATURE

<u>Symbol</u>	<u>Definition</u>	<u>Units*</u>
A	a constant in Walther's equation	(-)
A	surface of contact between media	(mm ²)
A _c	cage-land surface area	(mm ² or in. ²)
A _e	area of outer cylindrical surface	(mm ²)
A _i	area of inner cylindrical surface	(mm ²)
A _v	ball frontal area	(mm ²)
B	auxiliary variable	(-)
B	B = $\Delta\chi/\alpha$, a constant in Walther's equation	(-)
C	a constant tabulation by Fresco	(mm ² /N or in. ² /lb)
C _o	a non dimensional fluid-geometry parameter	(-)
C _p	specific heat at constant pressure	(W/kg-DegC)
C _r	cage pocket clearance	(mm)
C _v	drag coefficient	(-)
D	ball or roller diameter	(mm)
D	a constant tabulated by Fresco	(mm ² /N or in. ² /lb)
E	a constant tabulated by Fresco	(mm ² /N or in. ² /lb)
E ₁ , E ₂	Young's modulus for the contacting bodies	(N/mm ² or psi)
F _A	axial force	(-)
F _{n1} , F _{n2}	normal components of resultant force of the inlet pressure distribution	(N or lb)

*Where multiple units are indicated, the first units given are those associated with the computer program input and output.

NOMENCLATURE (CONTD)

<u>Symbol</u>	<u>Definition</u>	<u>Units*</u>
F_R	sliding force acting on the ball	(N or lb)
F_{R1}, F_{R2}	pumping forces acting on the ball	(N or lb)
F_{R3}, F_{S3}	tangential forces due to inlet rolling and shearing between ball and cage	(N or lb)
F_S	shearing force acting on the ball	(N or lb)
F_{S1}, F_{S2}	inlet friction forces	(N or lb)
F_x, F_y, F_z	force components in the x,y,z coordinate system	(N or lb)
F_w	windage force or drag force	(N or lb)
\vec{F}	the vector of inertia and drag forces	(N or lb)
\vec{F}_m	the vector sum of the hydrodynamic forces acting on the ball at the m-th contact	(N or lb)
\vec{FM}_b	a vector of bearing loads and moments	(N or lb & mm-N or in.-lb)
\vec{FM}_{si}	a vector of shaft loads and moments	(N or lb. & mm-N or in.-lb)
G	lubricant coefficient of thermal expansion	(1/DegC or 1/DegF)
H	non dimensional film thickness parameter	(-)
J	moment of inertia of the ball	kg-mm ²
K_f	conductivity of the film	(lb/degF-sec)
K_{ij}	the proportion of the heat flow from node i going to node j.	(-)
K_9, K_{10}	constants in expression for heat transfer coefficient	(-)
L	characteristic length	(mm or in.)
$L_{10\infty}$	full film fatigue life	(hrs)
M_c	moment due to fluid friction between the cage and the ring land	(mm-N or in.-lb)

*Where multiple units are indicated, the first units given are those associated with the computer program input and output.

NOMENCLATURE (CONTD)

<u>Symbol</u>	<u>Definition</u>	<u>Units*</u>
M_x, M_y, M_z	ball moment components in the x,y,z coordinate system	(mm-N or in.-lb)
\vec{M}	ball moment vector	(mm-N or in.-lb)
N_u	Nusselt's number	(-)
P_r	Prandtl's number	(-)
PD	diametral clearance	(mm or in.)
PE	bearing end play	(mm or in.)
P_1, P_2	forces acting normal to the ball surface within the outer and inner raceway contact ellipse	(N or lb)
P_3	ball-cage normal force	(N or lb)
Q	load	(N or lb)
Q_a	average asperity borne load	(N or lb)
Q_r	the radial component of the minimum rolling element-race normal force	(N or lb)
\bar{Q}	non dimensional load parameter	(-)
\vec{Q}_m	the vector normal load per unit length of the contact ellipse	(N/mm or lb/in.)
R	radius of outer ring groove centers	(mm)
R_e	Reynold's number	(-)
R_x, R_y	effective radii of curvature parallel and transverse to the rolling direction respectively	(mm or in.)
S	coordinate along the contact in the direction perpendicular to rolling friction	(mm or in.)

*Where multiple units are indicated, the first units given are those associated with the computer program input and output.

NOMENCLATURE (CONTD)

<u>Symbol</u>	<u>Definition</u>	<u>Units*</u>
Sd	diametral play	(mm or in.)
T	time	(sec)
T _o	long time duration	(sec)
T _s	starting time	(sec)
T ₁ , T ₂	traction forces	(N or lb)
\vec{T}	traction force vector at a general location within the contact	(N or lb)
U	characteristic speed	(m/sec or in./sec)
V	fluid entrainment velocity at the contact center	(m/sec or in./sec)
V	volume of the nodal element	(m ³ or in. ³)
V	voltage	(volt)
V _i	volume flow rate through node i	(m ³ /sec)
V _o	voltage over long time duration	(volt)
V _x	rolling velocity in x direction	(m/sec or in./sec)
V _y	rolling velocity in y direction	(m/sec or in./sec)
X, Y, Z	inertial coordinate system	(-)
DCL	diametral clearance	(mm or in.)
EPSFIT	user specified convergence criterion	(-)
EP1, EP2	a user supplied convergence criterion	(-)
EQ	temperature equilibrium convergence criteria for Eq. (3-41)	(-)
NEQ	number of equations in bearing solution	(-)
XCAV	volume fraction of lubricant in bearing cavity oil/air mixture	(-)

*Where multiple units are indicated, the first units given are those associated with the computer program input and output.

NOMENCLATURE (CONTD)

<u>Symbol</u>	<u>Definition</u>	<u>Units*</u>
a	a constant coefficient in Nusselt's number	(-)
a	contact ellipse semi-major axis	(in. or mm)
a	free convection temperature-exponent	(-)
b	an exponent in Nusselt's number	(-)
b	half the contact width	(in. or mm)
c	an exponent in Nusselt's number	(-)
c	coefficient of specific heat	(w/kg-DegC)
d	exponent in free convection heat transfer equations	(-)
d_l	cage-land diameter	(mm)
d_m	bearing pitch diameter	(mm or in.)
\vec{f}_m	the vector of friction force per unit length of the contact ellipse	(N/mm)
g	gravitational constant	(m/sec ² /or in./sec ²)
h	elastohydrodynamic film thickness	(mm or μ -in.)
h_c	critical value of film thickness	(mm or μ -in.)
h_f	the film thickness under fully flooded conditions	(mm or μ -in.)
h_s	starved plateau thickness	(mm or μ -in.)
$h_{a.c.}$	film thickness calculated by Archard-Cowking formula	(mm or μ -in.)
i j	indices of heat flow nodes	(-)

*Where multiple units are indicated, the first units given are those associated with the computer program input and output.

NOMENCLATURE (CONTD)

<u>Symbol</u>	<u>Definition</u>	<u>Units*</u>
l	separation distance between temperature nodes	(mm)
l_{re}	contact length, or in the case of an elliptical contact area, 0.8 times the contact length	(mm)
n	number of balls, total number of heat flow nodes	(-)
p_o	maximum contact pressure	(N/mm ² or psi)
q	heat generation rate, net heat transfer	(W)
q_c	heat generated by fluid shearing between the cage and land	(W)
q_f	fluid drag heat	(W)
q_I	heat generated by shearing force in the ball-raceway and ball-cage inlet region	(W)
q_i	heat energy in the i-th nodal element	(W)
q_T	heat generated by traction in the contact zone	(W)
q_{ti}	heat carried by mass flow from node i	(W)
q_{gi}	heat generated at node i	(W)
q_{oi}	heat flow from all neighboring nodes to node i	(W)
$q_{Ri,j}$	the heat energy transferred by radiation between nodes i and j	(W)
$q_{ci,j}$	heat flow transferred by conduction from node i to node j	(W)
$q_{ui,j}$	the heat flow between nodes i and j	(W)
$q_{vi,j}$	heat flow transferred by free convection from node i to node j	(W)

*Where multiple units are indicated, the first units given are those associated with the computer program input and output.

NOMENCLATURE (CONTD)

<u>Symbol</u>	<u>Definition</u>	<u>Units*</u>
$q_{wi,j}$	heat flow by forced convection from node i to node j	(W)
r	groove radius	(N or mm)
\vec{r}_m	a vector from the rolling element center to the point of contact	(mm or in.)
r^*	meniscus distance from center of contact along direction of rolling	(mm or -in.)
t	temperature	(degF or degK)
u	sliding velocity at the contact center	(m/sec or in./sec)
\vec{u}	sliding velocity vector	(m/sec or in./sec)
u_1, u_2	surface velocity of bodies 1 and 2 relative to the contact	(m/sec or in./sec)
u_s	sliding speed	(m/sec or in./sec)
u_s^*	sliding speed at which traction coefficient is a maximum	(m/sec or in./sec)
x, y, z	a local coordinate system established at each ball location	(-)
x	sliding velocity scaled by u_s^*	(m/sec or in./sec)
x_1	ball axial position relative to the outer race	(mm or in.)
x_m	maximum variation of x	(mm)
y_1	ball radial position relative to the outer race	(mm or in.)
y_m	maximum variation of y	(mm)

*Where multiple units are indicated, the first units given are those associated with the computer program input and output.

NOMENCLATURE (CONTD)

<u>Symbol</u>	<u>Definition</u>	<u>Units*</u>
z_c	ball center-cage pocket offset	(mm or in.)
Δ	diametral clearance between cage and land	(mm or in.)
$\vec{\Delta}$	shaft displacement at a bearing location	(mm or in.)
ΔDCL	change in bearing diametral clearance	(mm or in.)
ΔT	a small increment of time	(sec)
$\Delta \phi$	angular distance between rolling elements	(deg)
$\vec{\Delta}_b$	bearing deflection vector	(mm or rad)
$\Delta \zeta$	lubricant replenishment layer thickness	(mm)
$\Phi(\cdot)$	cumulative distribution function of standard normal distribution	(-)
Ω	resistance of heat flow	(degC/W)
Ω	angular velocity	(rad/sec)
Ω_c	cage angular velocity	(rad/sec)
Ω_{res}	resultant resistance to heat flow	(degC/W)
α	contact angle	(deg)
α	scaling factor in modified Newton-Raphson technique	(-)
α	pressure-viscosity index	(in. ² /lb)
α_i	inner race contact angle	(deg)
α_o	outer race contact angle	(deg)
α_o	auxiliary contact angle	(deg)
α_v	film coefficient of heat transfer by free convection	(W/m ² -degC ^a)

*Where multiple units are indicated, the first units given are those associated with the computer program input and output.

NOMENCLATURE (CONTD)

<u>Symbol</u>	<u>Definition</u>	<u>Units*</u>
α_w	film coefficient of heat transfer by forced convection	(W/m ² -degC)
β	temperature viscosity coefficient	(1/degF)
β	ball speed vector pitch angle	(deg)
δ	the first variation	(-)
δ_e	elastic deformation	(mm)
$\delta_x, \delta_y, \delta_z$	the linear deflection components of $\vec{\Delta}_b$	(mm)
ϵ	surface emissivity	(-)
ϵ	a small arbitrary constant	(-)
η	dynamic viscosity	(lb-sec/in.)
θ_y, θ_z	the angular deflection components of $\vec{\Delta}_b$	(rad)
λ	thermal conductivity	(W/M-degC)
λ	a viscoelastic constant (oil parameter)	(-)
u	traction coefficient	(-)
μ_a	coulomb friction coefficient	(-)
μ_r	u scaled by μ^*	(-)
μ_{EHD}	fluid traction coefficient	(-)
μ^*	maximum EHD traction coefficient	(-)
ν	kinematic viscosity	(m ² /sec)
ν_1, ν_2	Poisson's ratio for contacting bodies	(-)

*Where multiple units are indicated, the first units given are those associated with the computer program input and output.

NOMENCLATURE (CONTD)

<u>Symbol</u>	<u>Definition</u>	<u>Units*</u>
ρ	density	(kg/m ³)
ρ_o	density of the oil	(kg/m ³)
ρ_1	dimensionless meniscus distance	(-)
σ	Stefan-Boltzmann radiation constant	(W/m ² -DegK*)
σ_θ	RMS value of the distribution of asperity slope angles	(deg)
ϕ	azimuth angle	(Deg)
$\phi(\cdot)$	density function of standard normal distribution	(-)
ϕ_s	starvation reduction factor	(-)
ϕ_t	the film thickness reduction factor, due to heating	(-)
ψ	thermal diffusivity	(mm ² /sec)
ω_c	cage orbital velocity	(rad/sec)
ω_o	ball orbital velocity	(rad/sec)
ω_x	ball angular velocity component about the x axis	(rad/sec)
ω_y	ball angular velocity component about the y axis	(rad/sec)
ω_z	ball angular velocity component about the z axis	(rad/sec)
$\dot{\omega}_o$	first derivative of ω_o with respect to time	(rad/sec ²)
ω	angular velocity of ball in x,y,z coordinate system	(rad/sec)

*Where multiple units are indicated, the first units given are those associated with the computer program input and output.

SUBSCRIPTS

<u>Symbol</u>	<u>Definition</u>
B	refers to point where traction curve becomes nonlinear
C	refers to cage or conduction
N	refers to current iteration
R	refers to rolling or radiation
a, asp	denotes asperity effect
f	refers to fluid or flooded
i	denotes the i-th ball, i-th node, inner ring
j	denotes j-th node
k	index denoting a specific time interval
m	an index-denoting bearing component
o	denotes outer ring
s	refers to sliding, starvation effect, or shaft
t	refers to thermal effect
v	refers to free convection
w	refers to forced convection
x,y,z	denotes components of vector quantities with respect to x, y, and z coordinates
1,2	refers to bodies 1 and 2

SECTION 1

INTRODUCTION AND SUMMARY

Present as well as anticipated future operating requirements of high speed gas turbine engines functioning as aircraft power plants demand a sophistication in the bearing design and selection that is unprecedented in the history of mechanical engineering. The bearing's characteristics as a heat generator affects the engine cooling requirements; deflection characteristics are critical to rotor system stability; life and skidding characteristics are a chief determinant of the engine's reliability and maintainability performance.

The thermal, elastic and reliability performance of a bearing is the net result of a complex series of interactions between the bearing design parameters, material and surface finish characteristics, operating conditions and lubricant properties. Consequently, bearing design engineers have come to rely upon digital computer programs to help fathom these interactions and assess and predict bearing performance.

The earliest of such programs essentially solved the statically indeterminant problem of finding the load distribution at the equilibrium position of the bearing rings, considering only the forces of elastic deformation on the ball set. Life prediction due to the subsurface originated contact fatigue failure mode was calculated using Lundberg-Palmgren theory. Through an assumption regarding ball kinematics, heat generation rates were predicted using a Coulomb friction model.

Subsequently programs were developed that 1) calculated EHD film thickness wherefrom the likelihood of surface originated spalling failure could be gaged, 2) treated the bearing balls as six degree-of-freedom rotators acted upon by fluid drag forces resulting from the resistance of a lubricant-air mixture and viscous forces due to Newtonian shearing of lubricant in the contact zone.

Improvements in bearing analysis computer programs were accompanied by parallel developments in lubrication research that brought greater illumination of the role of lubrication in rolling contact systems. In particular the non-Newtonian nature of the contact traction in the lubricated contacts was confirmed by many researchers. Additionally, the occurrence of lubricant film starvation was observed and explained and quantitative methods were developed for assessing the magnitude of the life reduction due to operation in the partial EHD regime i.e., where the ratio of the elastohydrodynamic film thickness

to the composite surface roughness of the controlling bodies is less than 3.0.

The objective of USAF Contract No. F33615-72-C-1467 (Navy MIPR No. M62376-3-000007) was to put the latest lubrication research results in the hands of the bearing designer by providing him with a thoroughly contemporary bearing analysis computer program that incorporates these models as modular subroutines.

The work required to fulfill this objective involved both the adaptation of existing models and the development of new theoretical extensions. Additionally, it involved the determination of model parameters and model corroboration via tests conducted in an optical EHD rig equipped to measure contact traction.

The models in final form were incorporated into a Fortran IV bearing analysis computer program designated AT74Y00i and applied, first to bearing test data compiled under NASA sponsorship for preliminary appraisal, and then to the results of a specially conducted series of full scale tests at speeds up to 3×10^6 DN, for final validation.

Specifically, the new models are as follows:

- 1) An EHD film thickness model that accounts for
i) thermal heating in the contact inlet using a regression fit to results obtained by Cheng {1}
and ii) lubricant film starvation using theoretical results derived in the present program.
- 2) A new semi-empirical model for fluid traction in an EHD contact is combined with an asperity load sharing model developed by Tallian {2} to yield a model for traction in concentrated contacts that reflects the state of lubrication as it varies from boundary, through partial EHD to the full EHD regime.
- 3) A new model for the hydrodynamic rolling and shear forces in the inlet zone of lubricated contacts accounting for the degree of lubricant film starvation.
- 4) Normal and friction forces between a ball and a cage pocket are modelled in a way that accounts for the transition between the hydrodynamic and elastohydrodynamic regimes of lubrication.

Numbers in brackets refer to list of references at the end of this report.

- 5) A model for the effect on fatigue life of the ratio of the EHD plateau film thickness to the composite surface roughness.

Additionally models for temperature viscosity and pressure viscosity variation as functions of temperature given by Walther {3} and Fresco {4} respectively, have been adopted.

The computer program in which the mathematical models have been incorporated is a very general one which is structured to analyze system performance of an arbitrary flexible shaft configuration supported by up to five bearings. In the present program embodiment, the models developed under this contract, and reported herein, have been incorporated into the ball bearing solution, and have been checked under pure axial loading. Operation of the program under conditions of combined thrust, radial and moment loading remains to be performed. The roller bearing routine requires a different form of input from that which the program is presently written to accept, consequently, revisions to the program are necessary prior to obtaining roller bearing solutions with these new models.

This volume is a design manual that fully describes the use and operation of the powerful design tool and Computer Program AT74Y001 represents.

Section 2 contains a general discussion of the bearing analysis computer program highlighting its organization, scope and options.

Section 3 contains analytical details of the ball bearing problem formulation technique, including the calculation of ball orbital speed variation that justifies the sobriquet "quasidynamic" for the ball bearing solution. Section 3 also contains a description of the friction and normal forces and analytical expressions for the inertia force components acting on a ball. Finally it contains the details of the equilibrium calculation for the bearing cage and the calculation of heat transfer coefficients and thermal equilibrium.

Summary descriptions of the models developed and employed in this program are given in Section 4.

Section 5 contains the detailed instructions for preparing program input data.

Section 6 is a detailed description of the output provided by the program.

Section 7 is a comparison of the program's predicted values for several key variables to the values actually measured in full scale tests of 125 mm bore angular contact bearings conducted over a wide range of loads and speeds.

Section 8 contains a discussion of the results of parametric runs of the computer program elucidating the effect of load, speed, lubricant replenishment, amount of lubricant in the bearing cavity and free contact angle upon various predicted quantities. Interpretations are advanced in terms of the characteristics of the mathematical models employed.

Appendix A contains added background material applicable to using the program's thermal options. Appendix B contains the input data preparation forms and an example of their preparation. Appendix C is a sample set of program output for a thrust loaded ball bearing solution. Appendix D is a sample set of output from the thermal solution.

Additional material on the details of model development, the design and instrumentation of the rig for full scale bearing tests and the model corroborative tests is contained in two interim reports {6, 7}.

Computer program AT74Y001 is available to qualified users for government purposes. Requests may be addressed to AFAPL/SFL, WPAFB, Ohio 45433.

SECTION 2

COMPUTER PROGRAM ORGANIZATION AND SCOPE

2.1 PROGRAM GUIDELINES

In selecting a ball bearing analysis program into which to build the mathematical models developed under Contract No. F33615-72-C-1467, the choice was made to use computer program AE72Y003 assembled under a U. S. Army Contract (No. DAADO5-73-C-0011). Program AE72Y003 is applicable to the analysis of a complete shaft-bearing system containing up to five ball and non-thrust-carrying cylindrical roller bearings.

The modified program has been given the number AT74Y001 and enjoys the same latent capability as program AE72Y003, however at this writing the mathematical models developed under Contract F33615-72-C-1467 are only accessed by the ball bearing routine of AE72Y003. The roller bearing routine requires a different type of data input and therefore cannot be used in its present form.

The program is structured to make the cylindrical bearing portions operational with minimal additional work. Input and other functional descriptions presented in this Design Manual accordingly make provision to include the cylindrical bearing.

Guidelines followed in developing Program AE72Y003 and in the modification under the present contract were as follows:

1. Maximized use of modular subroutines to facilitate program updating
2. Maximized programming emphasis on ease of user input
3. Utilization of Fortran variable identification immediately recognizable by the engineer user
4. Liberal use of comment statements, in engineering language, throughout the program
5. Emphasis on direct, and simple, programming techniques for ease in future program refinements and updating.
6. Definition of output data in clear, concise, and titled formats.

2.2 GENERAL PROGRAM

At its most general application the program simulates the behavior of a system having up to five ball or roller bearings supporting

a flexible solid or hollow shaft of arbitrary design. Under the action of a prescribed set of point, distributed and moment loads, the elastic deflection curve of the shaft is determined as the unique shape for which the applied forces on the shaft equilibrate the angular and radial reactions exerted on the shaft by the bearings, as the bearing rings undergo relative angular, radial and axial deflections.

Additionally the heat generated by the bearings due to lubricant and asperity friction in the contacts between rolling elements and raceways and by lubricant friction 1) in the contact inlet region, 2) at the rolling element-cage pocket contacts and 3) over the cage-ring contact region is calculated and added to the heat generated by windage between the rotating ball set and the oil-air mixture that fills the bearing cavity.

The heat generated at the bearings and from any other specified heat sources (such as gears) having a known heat generation rate, is used in a system thermal balance to yield either the steady state or the transient temperature distribution throughout the mechanical system in which the shaft-bearing system functions.

Additionally the program accounts for the effect on bearing clearance of the initial shaft and housing fits, radial thermal gradient, centrifugal expansion and radial deflection under the rolling element loads.

Inasmuch as changes in bearing clearance affect the ring equilibrium positions and heat generation rates, the program may be used in an iterative mode to determine a self-consistent final solution. At the user's option several intermediate levels of problem simplification may be elected when the full solution is not needed or desired. For example the temperature calculation can be dispensed with and the solution found under a known or assumed steady state temperature distribution. Additionally it is possible to consider only the equilibrium of the elastic and centrifugal forces (i.e. neglect friction and other inertia forces) in calculating bearing equilibrium position, leading to a rapidly convergent first approximation solution.

2.3 A TYPICAL SYSTEM

Figure 2-1 illustrates a typical system to which the thermal analysis portion of this program may be applied (the bearing analysis portion of the program in its present form is limited to ball bearings only). The shaft is hollow, irregularly shaped and has an integral bevel gear.

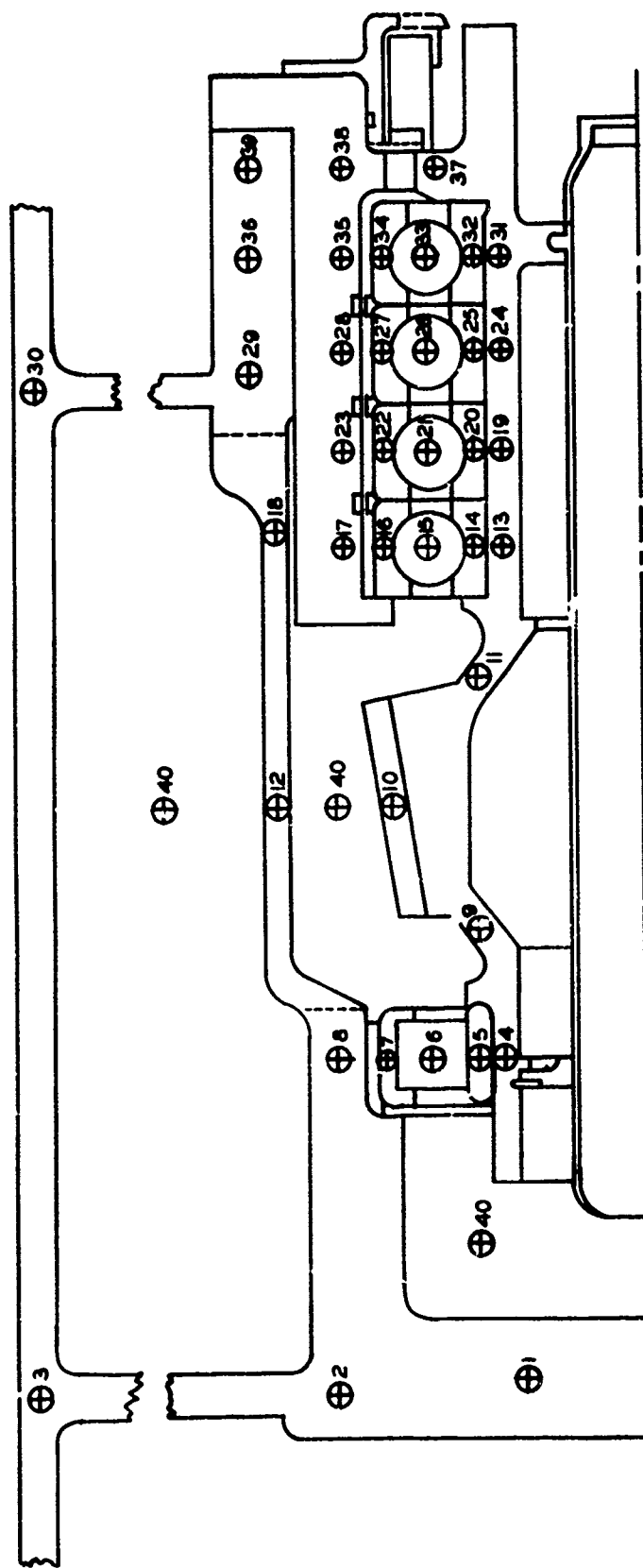


FIGURE 2-1
TYPICAL SHAFT-BEARING SYSTEM

The gear tooth load gives rise to axial and radial load components on the shaft.

Under the action of these forces the shaft will deflect and the rings of the ball bearings will undergo relative radial, axial and angular deflections. The rings of the cylindrical bearing will undergo relative radial and angular deflections. Axial translations of the rings are not considered since the inner ring is flangeless.

The relative ring deflections result, in turn, in deflections of the balls and rollers. In the deflected shape finally assumed by the shaft the forces and moments applied to the shaft by the bearing reactions will equilibrate the applied loads (the gear tooth loads in the present context).

Simultaneously the ball and roller loads due to elastic contact, inertia and friction forces acting upon the bearing are reacted by the inner ring and are in equilibrium with the forces that the deflected shaft imposes on the inner ring.

In its equilibrium position each bearing will generate heat due to lubricant shearing and windage. This heat will be dissipated throughout the structure via convection, conduction, radiation and fluid flow (mass transport) and the structure's temperature will rise until each point in the structure reaches a steady state or thermal equilibrium temperature.

The program calculates the steady state or transient temperature distribution of a collection of points or "nodes" established by the user throughout the structure via user supplied data describing how heat is transmitted between the various nodes. A typical node selection scheme is illustrated in Fig. 2-1. Selection of nodes is discussed in {2} in general terms for heat flow analysis, and in specific terms to the computer program in Sections 3.7, 3.8, 3.9, 5.1 and 5.4.

2.4 GENERAL LOGIC DIAGRAM - SYSTEM LEVEL

Figure 2-2 is a general flow chart of the solution scheme. Referring to this flow chart, it is seen that subsequent to reading the input data, the system variables that depend upon temperature, i.e., lubricant viscosity and temperature viscosity coefficient are calculated. These calculations are performed using the assumed system temperatures, if no temperature distribution is to be calculated, and initial guesses at system temperature, if an iterative calculation of the temperature distribution is to be performed.

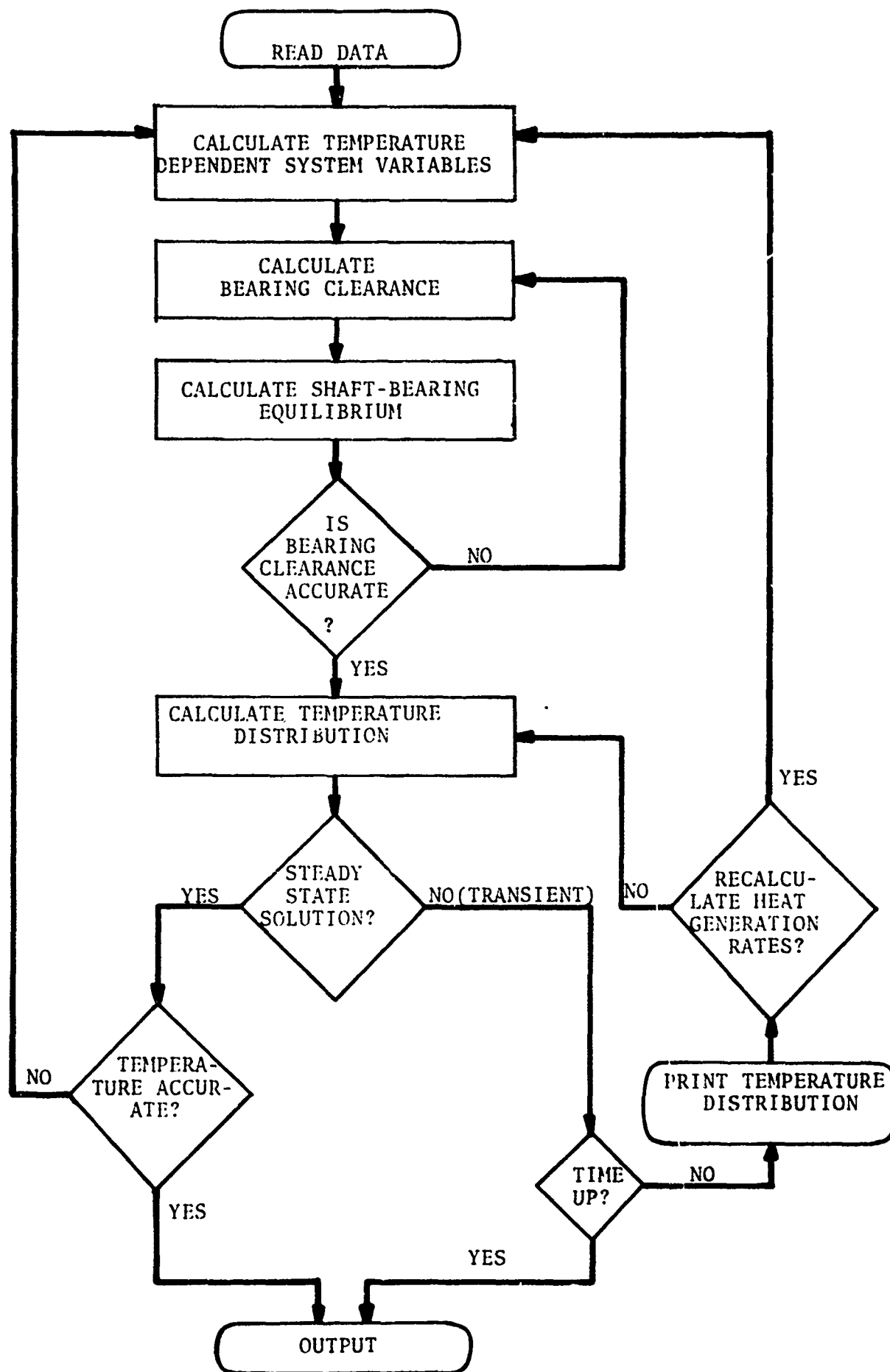


FIGURE 2-2
GENERAL PROGRAM FLOW CHART

The program next calculates the bearing operating clearance accounting for thermal, centrifugal and elastic expansion using approximations for the ball and cage speeds and loads.

Thereafter the program calculates the shaft and bearing deflections and other bearing operating parameters. (This calculation may be performed at several levels of complexity and is discussed later in this Section.)

Having solved for shaft-bearing equilibrium, the bearing clearance is rechecked and if it is too far different, according to a user specified accuracy criterion, from the initial value, the calculation is repeated with a modified clearance.

When the clearance accuracy requirement is met, the program proceeds to calculate a temperature distribution, if required. If a steady state solution is sought the temperatures are compared with those initially assumed and if too far different as judged by a user specified criterion, the entire calculation is repeated as indicated on the flow chart. When the results are sufficiently accurate, the program output is printed.

If a transient solution is desired the program calculates and prints the temperature distribution at time intervals specified by the user until it has been calculated at the latest time of interest. At intermediate times in the transient solution the program will loop through the initial part of the program in order to calculate updated heat generation rates with a frequency specified by the user. When time-up is achieved the complete shaft-bearing output is printed as well as the temperature distribution.

2.5 LOGIC DIAGRAM SHAFT-BEARING EQUILIBRIUM CALCULATION

Figure 2-3 is a more detailed flow chart of the section of the program shown as the shaft-bearing equilibrium calculation in Figure 2-2.

The calculation begins with a determination of the relative positions of the bearing rings. Approximations are used initially and are then refined as calculation proceeds.

If the user wishes a full solution considering all friction, inertia and elastic contact forces acting on the rolling element and cage, the right hand branch is followed.

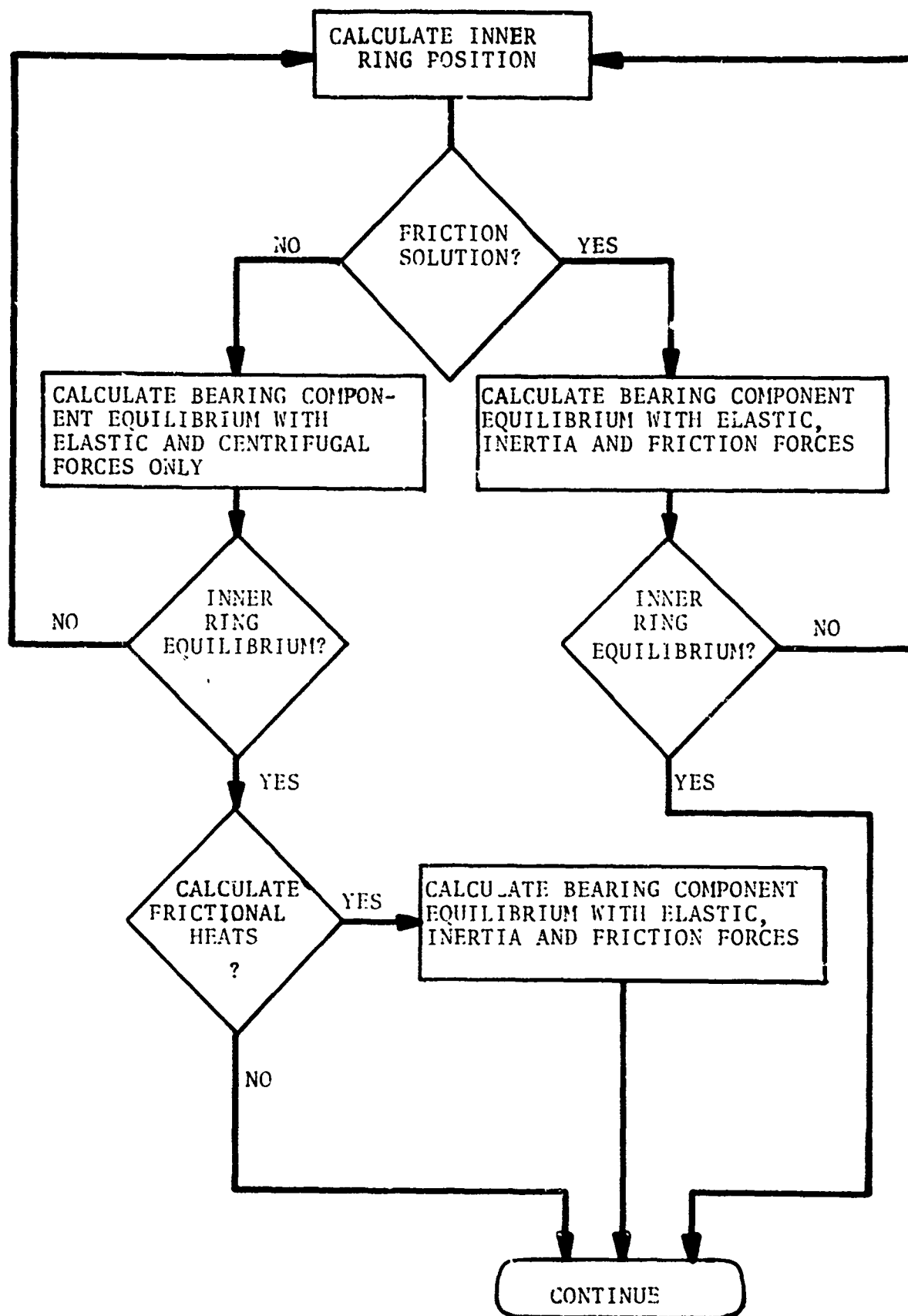


FIGURE 2-3

FLOW CHART OF SHAFT-BEARING EQUILIBRIUM CALCULATION

Having calculated the forces that the ball and cage transmit to the inner ring, inner ring equilibrium is checked. The assumed inner ring position is then modified if necessary until an accuracy criterion is met.

Two less stringent levels of solution are possible and often useful. They involve the omission of the friction and all but the centrifugal force among the inertia forces from the inner ring equilibrium calculation. Having satisfied inner ring equilibrium under these conditions the user may then 1) evaluate the bearing component equilibrium and heat generation rates using all of the forces, but without rechecking for inner ring equilibrium or 2) omit this additional evaluation and proceed.

2.6 HIERARCHICAL FLOW CHART

The hierarchical type flow chart given in Fig. 2-4 presents the program structure, listing the program elements in the order in which they would be called to solve the shaft-bearing dynamic, as well as steady state and transient temperature distribution problems. The various solution loops are indicated, as well as notes which indicate the functions of various subroutine groupings.

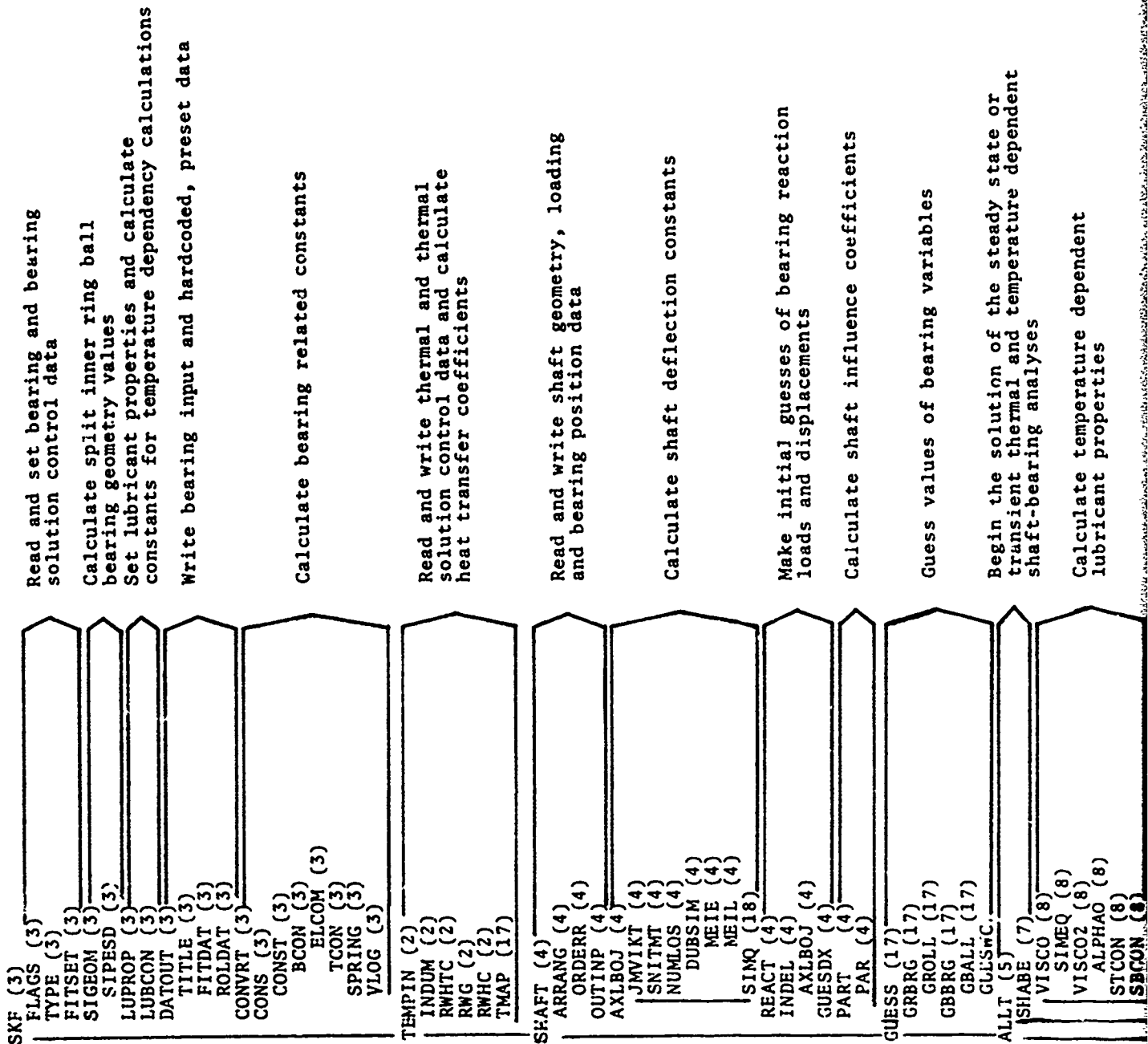
Each line in the flow chart represents a program element, subroutine, function or the main program ALWAYS. The call of one subroutine by another is denoted by indenting the called subroutine relative to the routine doing the calling. As an example, subroutine SKF calls subroutines FLAGS, TYPE, FITSET, SIGEOM, LUPROP, LUBCON, DATOUT, CONVRT and CONS. Subroutine CONS calls CONST, SPRING and VLOG. CONST calls BCON and TCON, and BCON calls ELCOM.

The first mention of a subroutine within the flow chart includes the entire list of subordinate program elements. At subsequent calls to that subroutine the list of subordinate elements is omitted but the elements are called nevertheless. As an example the first call to subroutine AXLBOJ is followed by the subordinate elements JMVKT, SNITMT, NUMLOS, DUBSIM, MEIE, MEIL and SIMQ. After the call of AXLBOJ from INDEL, the subordinate elements are not listed but are, nevertheless, employed. The list of subordinate program elements are omitted in repeated calls of subroutines GUESS, BEAR, CGBAL, SOLVXX and DELIVR as well as AXLBOJ.

The program occupies just under 100,000 words in a Univac 1108. If the program is too large to fit in its entirety on the user's computer, segments of the program may be "overlaid".

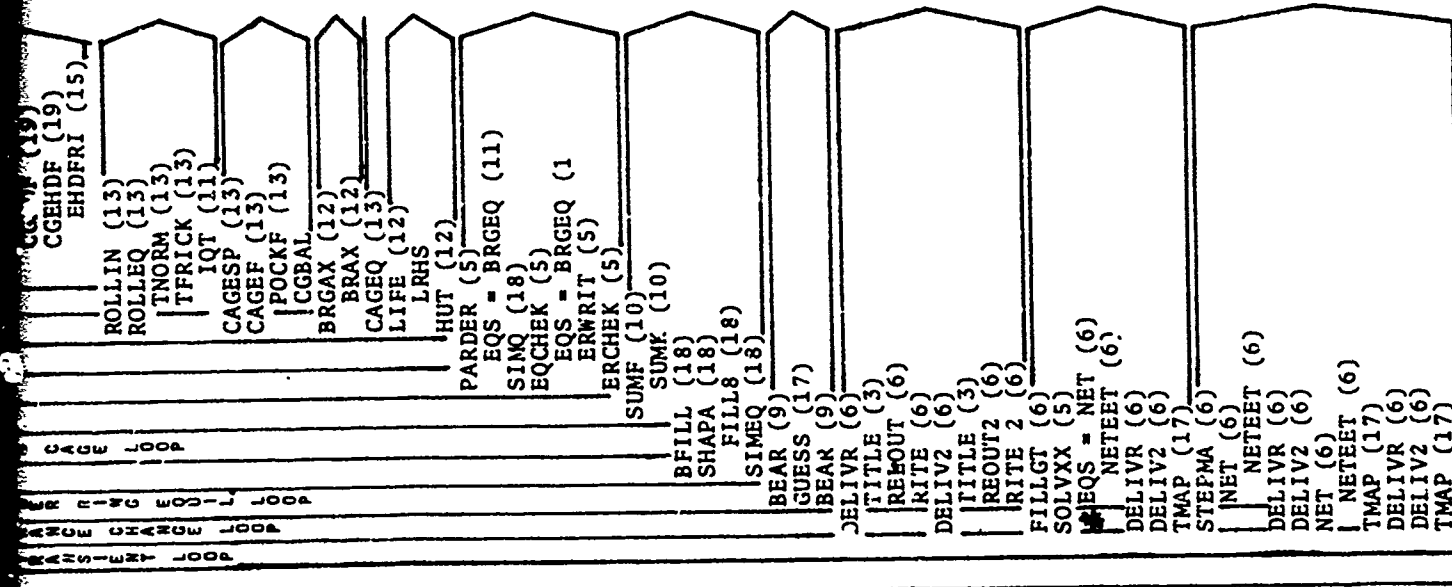
FLOW CHART

ALWAYS (1)



GBRG (17)	Begin the solution of the steady state or transient thermal and temperature dependent shaft-bearing analyses
GBALL (17)	
GLLSWC	
ALLT (5)	
SHABE (7)	
VISCO (8)	Calculate temperature dependent lubricant properties
SIMEQ (8)	
VISCO2 (8)	
ALPHA0 (8)	
STCON (8)	
SBCON (8)	
FIT (8)	
INTFIT (8)	
SIMEQ (18)	Calculate bearing diametral clearance
SONRI (9)	Establish iteration scheme to satisfy inner ring equilibrium
BEARC (9)	
BEAR (9)	
PREPAR (10)	
SOLVXX (5)	
INSOLV (5)	
EQS = BRGEQ (11)	
BEAREQ (11)	
BALLIN (13)	
BALLEQ (14)	
DRAG (16)	
FMIX (15)	
TINT (15)	
THERFC (15)	
STARFC (15)	
HOHI (15)	
HDFRIC (15)	
ASLOAD (15)	
EHDTRI (15)	
FRICTN (15)	
CGBAL (19)	Calculate ball-race film thickness plus the hydrodynamic and concentrated contact friction forces
CGNORM (19)	
CGHDP (19)	
CGHDP (19)	
CGFRIC (19)	
CGHDF (19)	
CGHDF (19)	
EHDTRI (15)	
ROLLIN (13)	
ROLLEQ (13)	
TNORM (13)	
TFRICK (13)	
IQT (11)	
CAGESP (13)	
CAGEF (13)	
POCKF (13)	
CGBAL	
BRGAX (12)	
BRAX (12)	
CAGEQ (13)	
LIFE (12)	
LRHS	
HUT (12)	
PARDER (5)	
EQS = BRGEQ (11)	
SINQ (18)	
EQCHEK (5)	
EQS = BRGEQ (11)	
ERWRIT (5)	
ERCHEK (5)	
SUMF (10)	
SUMK (10)	
BFILL (18)	
SHAPA (18)	
FILL (18)	

Sum the forces and moments acting on the bearing inner ring, thus creating the inner ring equilibrium equations. Solve the equations.



Calculate the raceway normal and all friction forces acting on each roller

Calculate cage speed and cage-rolling element pocket forces at all rolling elements

Calculate rolling element inertia terms excluding centrifugal force
Calculate cage equilibrium equation

Calculate bearing fatigue life and bearing heat transfer coefficients

Solve the rolling element and cage quasistatic dynamic equilibrium equations

Sum the forces and moments acting on the bearing inner ring, thus creating the inner ring equilibrium equations. Solve the equations.

Upon satisfying bearing inner ring equilibrium recalculate bearing operating parameters using the correct values of inner ring displacement

Write roller bearing output

Write ball bearing output

Calculate steady state temperature distribution and write results

Calculate transient temperature distribution and write results

For this purpose the Program is subdivided into nineteen (19) numbered modules which can be sequentially "overlaid". The number in parentheses to the right of the element name, corresponds to the module in which the given element belongs.

The Program segments SKF, TEMPIN, SHAFT and GUESS all perform initiation functions and with the exception of GUESS, are called only once per program execution.

The real problem solving portion of the program is embodied in segment ALLT. Within this segment the shaft bearing solution is obtained through the call to SHABE, then the steady state or transient temperature distributions are obtained. This scheme is repeated until the end objective, steady state thermal equilibrium or time up for the transient scheme, is realized.

The nonlinear equation solver SOLVXX is central to the program and deserves special discussion as related to the flow chart. The first call to SOLVXX is from BEAR. Only for this first call are all of the SOLVXX subordinate subroutines listed as noted earlier. These include INSOLV, EQS, PARDER, SIMQ, EQCHEK, and ERCHEK. In the subsequent call to SOLVXX in which the steady state temperatures are being calculated, the above listed subroutines are again called but these calls, with the exception of EQS, are not listed on the flow charts.

EQS is the name given by SOLVXX to either of two subroutines which set up the system of equations to be solved. EQS is brought into SOLVXX through the argument list. When the bearing equations are being solved, subroutine BRGEQ is brought into SOLVXX and within SOLVXX is referenced by the name EQS. When the heat transfer equations are being solved as a consequence of the call of SOLVXX from ALLT, NET is brought into SOLVXX and is referenced as EQS.

SECTION 3

ANALYTICAL FORMULATION

3.1 THE BALL BEARING SOLUTION

Figure 3-1 shows a coordinate system (XYZ) fixed at the geometric center of the plane of the outer ring groove centers of a ball bearing. The angular coordinate (azimuth angle) ϕ locates a radial plane through the center of one of the balls.

A local coordinate system x, y, z is established at each ball location with origin at the outer ring groove center. This coordinate system rotates with the ball. The z direction is tangential to the direction of rolling, the y direction is radial and the x direction is parallel to the outer ring centerline (i.e. parallel to the X direction).

Figure 3-2 shows a radial section at an arbitrary azimuth angle ϕ through an angular contact ball bearing. The contact angles between the ball and the inner and outer races are shown as α_i and α_o , respectively.

In the local coordinate system the ball center has coordinates x and y . In general the coordinates of the ball center in the local system will vary with azimuth angle ϕ , i.e., the balls, as they travel around the ring, will undergo small radial and axial excursions. We indicate the dependence of the ball center position on azimuth angle by writing its coordinates as $x(\phi)$ and $y(\phi)$.

3.1.1 Ball Motions

Returning to Fig. 3-1, the rotational velocity with which the moving coordinate system rotates about the X axis is designated ω_o and is also assumed to be a function of azimuth angle i.e. $\omega_o = \omega_o(\phi)$.

The ball is assumed to rotate relative to each of the axes in the moving system of coordinates. The angular velocities about each of the axes x, y, z are denoted ω_x, ω_y and ω_z respectively and are shown as the orthogonal components of the ball auto rotational velocity vector ω in Fig. 3-1.

$(z_c)_1$ denotes the circumferential displacement between the center of the ball arbitrarily designated ball No. 1 at azimuth location $\phi = \phi_1$, and the cage pocket center.

The value of the ball center-cage pocket center offset z_c applicable at other ball positions is deduced in terms of the

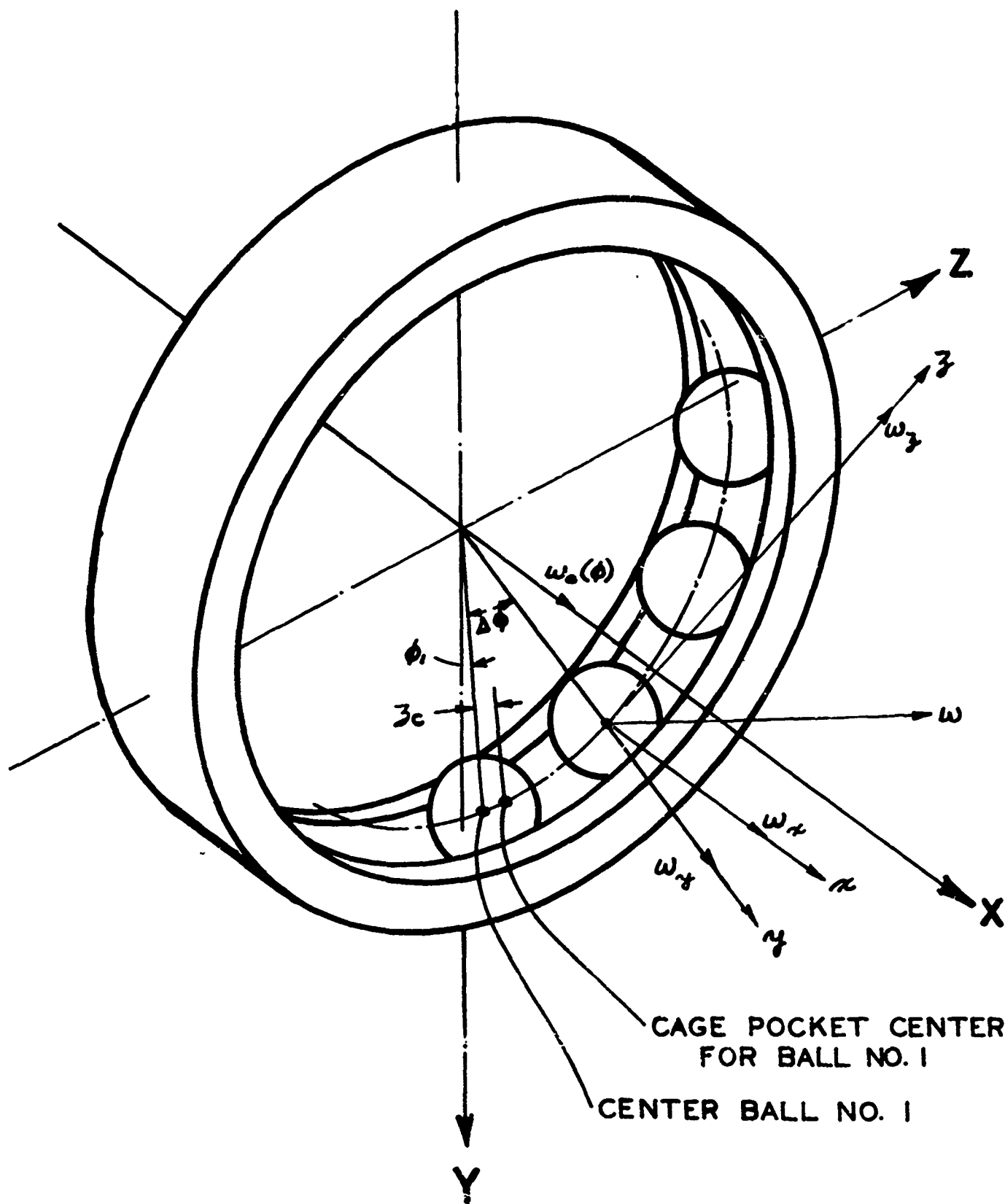


FIGURE 3-1
BEARING INERTIAL (XYZ) AND ROLLING ELEMENT (xyz),
COORDINATE SYSTEMS

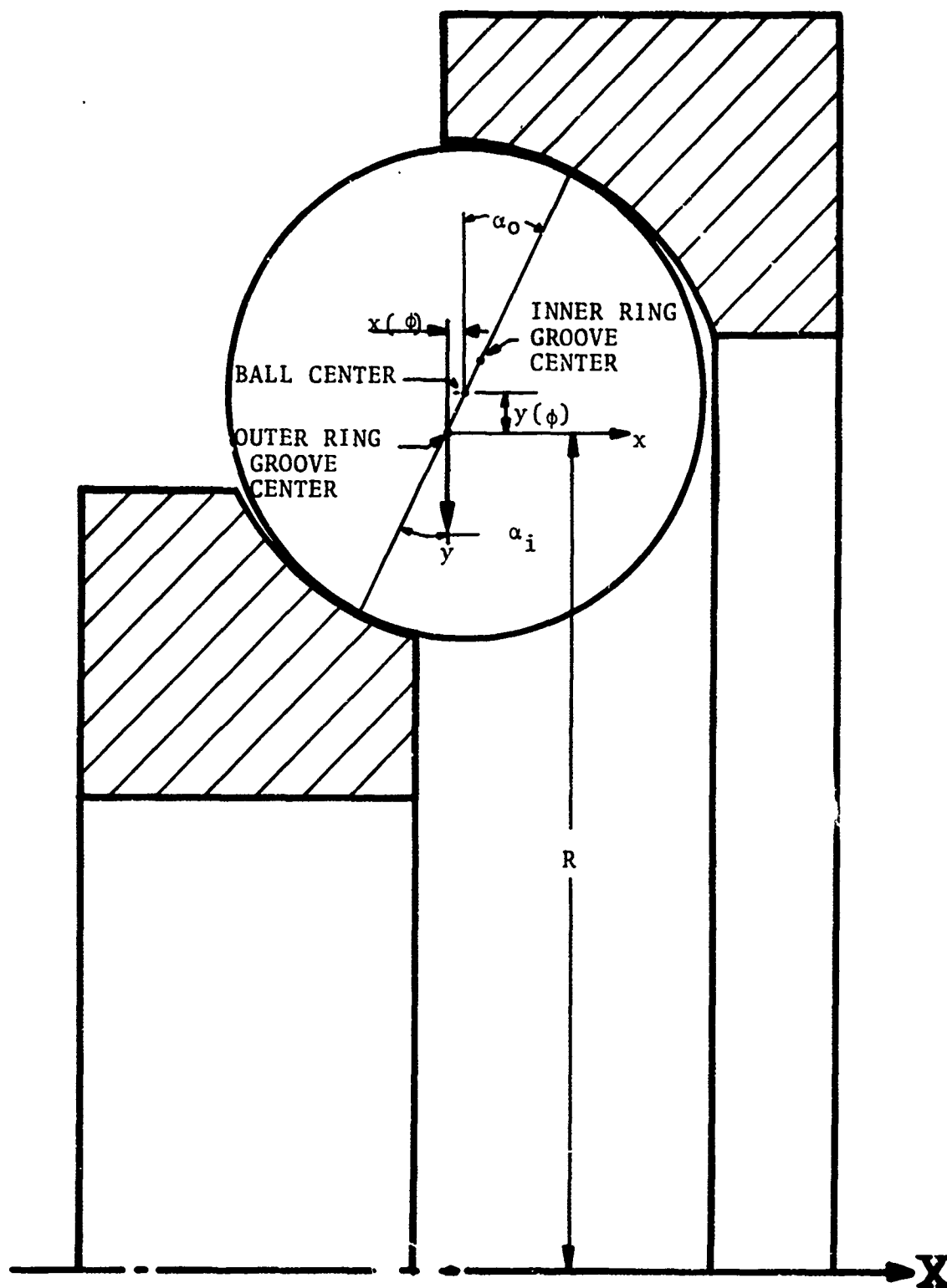


FIGURE 3-2

RADIAL SECTION AT AZIMUTH LOCATION ϕ

value z_{c1} at ball position No. 1 and the orbital speeds.

In so doing it is assumed that a ball's orbital velocity remains constant as it traverses the distance corresponding to half a ball spacing on either side of the ball's nominal azimuth position. As it enters the azimuth location of the next adjacent ball the orbital speed undergoes a step change. This is illustrated in Fig. 3-3 for ball Nos. 1 and 2. The top half of Figure 3-3 is a plot of the assumed variation of orbital velocity with respect to ball position.

The cage orbital velocity is denoted by ω_c and is assumed uniform and equal to the average of the ball orbital velocities i.e.

$$\omega_c = \frac{1}{n} \sum_{i=1}^n (\omega_o)_i \quad (3-1)$$

where n is the number of balls

The distance between ball positions is the quotient of the circumference πd_m of the locus of ball centers (neglecting small excursions) and the number of balls n . The time ΔT for the cage to traverse this distance is then

$$\Delta T = \frac{\pi d_m}{n} / \left(\frac{d_m}{2} \cdot \omega_c \right) = \frac{2\pi}{n \omega_c} \quad (3-2)$$

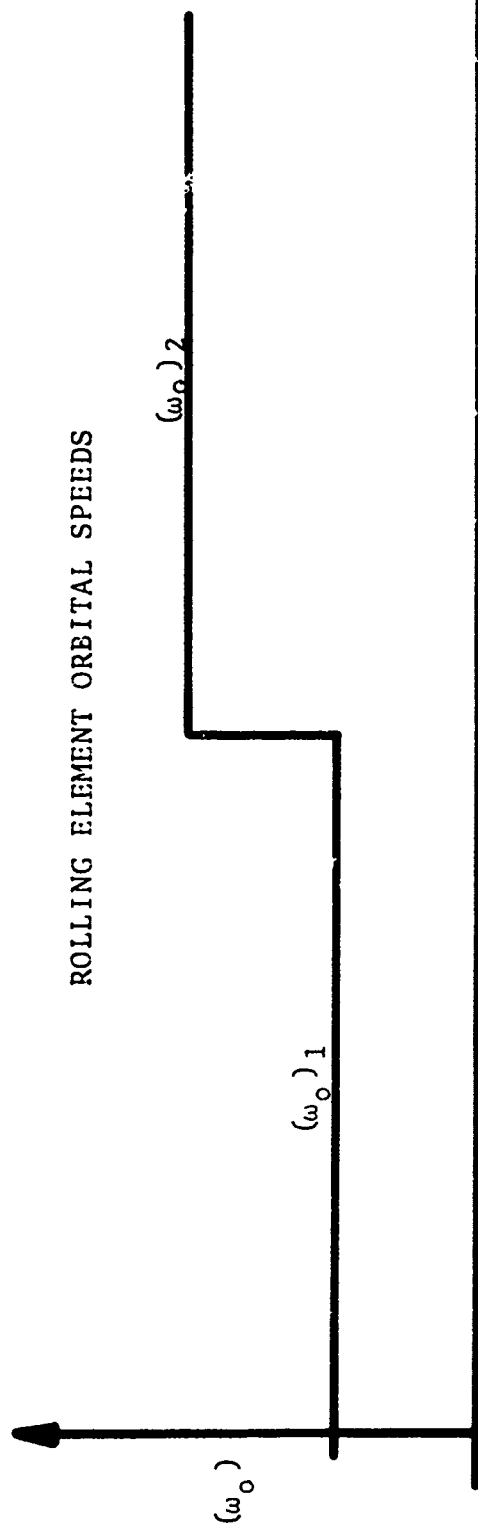
In this time period the center of ball No. 1 moves a distance of

$$\frac{d_m}{2} \cdot (\omega_o)_1 \cdot \left(\frac{\Delta T}{2} \right) + \frac{d_m}{2} \cdot (\omega_o)_2 \cdot \left(\frac{\Delta T}{2} \right) = \frac{d_m \Delta T}{4} [(\omega_o)_1 + (\omega_o)_2] \quad (3-3)$$

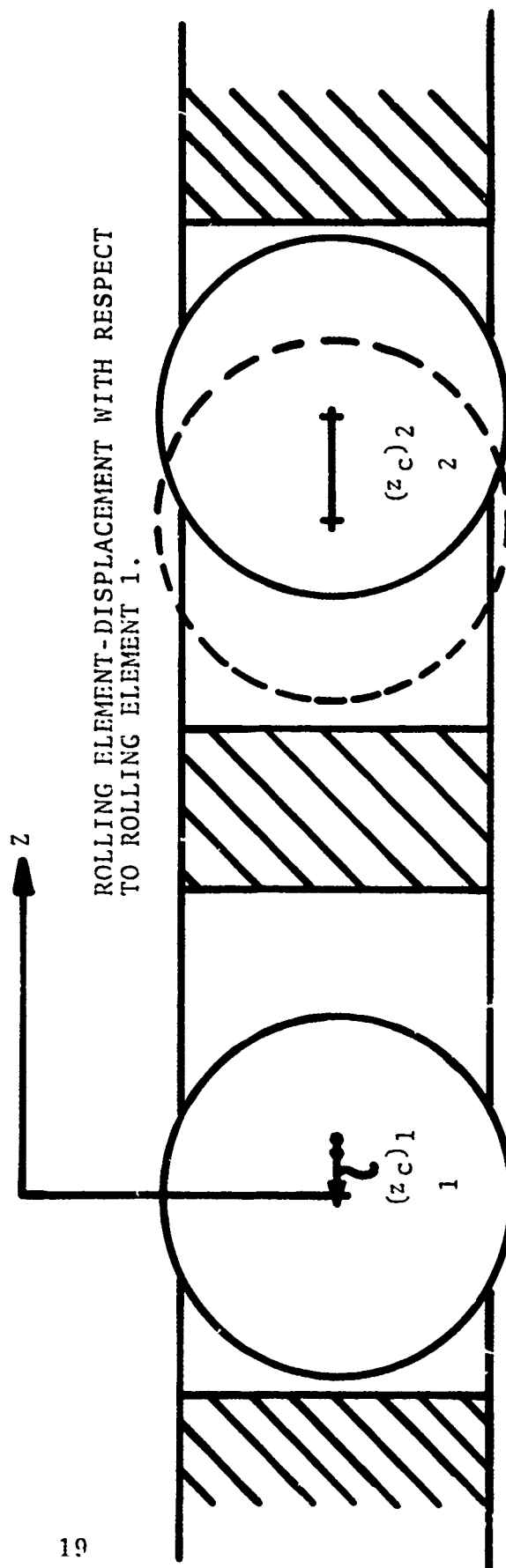
The distance between ball and cage pocket centers at ball position No. 2 is then given as the sum of the initial separation $(z_c)_1$, the distance the cage center moved, less the distance the ball center moved, i.e.

$$(z_c)_2 = (z_c)_1 + \frac{\pi d_m}{n} - \frac{d_m \Delta T}{4} [(\omega_o)_1 + (\omega_o)_2] \quad (3-4)$$

ROLLING ELEMENT ORBITAL SPEEDS



19



ROLLING ELEMENT-DISPLACEMENT WITH RESPECT TO ROLLING ELEMENT 1.

FIGURE 3-3
ROLLING ELEMENT SPEEDS AND DISPLACEMENTS

or, using $\Delta T = 2\pi/n\omega c$

$$(z_c)_2 = (z_c)_1 + \frac{\pi d_m}{n} \left[1 - \frac{(\omega_o)_1 + (\omega_o)_2}{2\omega c} \right] \quad (3-5)$$

3.1.2 The Unknowns for a Ball Bearing Problem

Equation 3-5 is applied successively to give the distances between the ball and cage pocket centers at succeeding azimuth positions. If the six quantities x , y , ω_o , ω_x , ω_y , ω_z for each value of ϕ (i.e. at each of the n balls) and the additional quantity $(z_c)_1$ were known, the complete system of forces on the bearing and cage could be determined. x and y for example govern the amount of elastic contact deformation and hence contact force at each contact. The velocities and their rate of change govern the lubricant shear forces and inertia forces and $(z_c)_1$ determines cage-pocket normal force at each of the contacts.

Solving the ball bearing problem consists of finding the value of these $6n + 1$ quantities for which the balls and cage are in equilibrium under an assumed relative displacement of the bearing rings. This is done by an iterative scheme in which the values of the unknowns are assumed, the forces calculated and equilibrium checked.

Having converged to a solution the associated forces acting on the inner ring are re-solved and tested for equilibrium with the forces imposed by the shaft on the inner ring. The assumed relative ring displacements are then modified and the process repeated until inner ring equilibrium is achieved as discussed above.

3.2 FORCES ACTING ON A BALL

At a given azimuth location a ball is acted upon by normal and friction forces whose magnitudes and directions are directly expressible in terms of the azimuth dependent unknown velocity and displacement components, x , y , ω_o , ω_x , ω_y , ω_z and z_c .

These forces are described as follows. Subscripts 1, 2 and 3 refer to ball/outer race, ball/inner race and ball/cage web forces respectively.

1. The normal forces P_1 and P_2 act normal to the ball surface within the outer and inner raceway contact ellipses. These forces are related to the displacements $x(\phi)$ and $y(\phi)$ by the equations of contact elasticity {6}.

2. The ball-cage normal force P_3 is directed along the circumferential direction coincident with the z axis of the ball. Its calculation is given in Section 4.
3. The windage force F_w acts through the center of the ball in the z direction. It is related to ω_o .
4. Pumping forces F_{R1} and F_{R2} act in the outer and inner race contacts in the plane perpendicular to a line passing through the center of each ellipse and the ball center. These forces arise as a result of the lubricant being pumped into the high pressure Hertzian contacts.
5. Traction forces T_1 and T_2 arise within the contact region due to a combination of fluid and asperity traction. These forces are calculated by summing the values calculated on individual subelements of each contact ellipse using a partial EHD model. The line of action of these forces makes an angle with the rolling direction.
6. Inlet friction forces F_{S1} and F_{S2} arise from fluid shear when gross sliding is present. The direction coincides with the ball-race sliding velocity vector at the center of the contact.
7. The normal components F_{N1} and F_{N2} of the resultant force of the inlet pressure distribution act opposite to the direction of rolling.
8. The tangential forces F_{R3} and F_{S3} due to inlet rolling and shearing resistance between the ball and the cage web act radially on the cage pockets.

Analytical expressions for the forces described in terms 2-8 above are given in Section 4.

3.3 INERTIA FORCES AND MOMENTS ACTING ON A BALL

As discussed above, the ball, in travelling between azimuth locations, is forced to undergo changes in its auto-rotational velocity components ω_x , ω_y , and ω_z as well as in its orbital velocity ω_o about the X axis of the stationary coordinate system. The forces which must act on a ball to produce time variations in its auto rotational and orbital velocities may be deduced

from Newton's Laws of motion as follows:

$$\vec{F} = \begin{bmatrix} F_x \\ F_y \\ F_z \end{bmatrix} = m \begin{bmatrix} \ddot{x} \\ \ddot{y} - \omega_o^2(R+y) \\ 2\omega_o\dot{y} + \dot{\omega}_o(R+y) \end{bmatrix} \quad (3-6)$$

where F_x , F_y and F_z are the components of the forces in the rotating coordinate system attached to the ball, m is the ball mass and x and y are the ball center displacements shown in Fig. 3-2, and R is the radius of outer ring groove centers.

A rough estimation assuming stable operation yields that the term x is smaller than $\omega_o^2(R+y)$ by a factor of the order of x_m/R , where x_m is the maximum variation of x . Similarly, the terms y and $2\dot{\omega}_o y$ are smaller than $\omega_o^2 R$ by a factor in the order of y_m/R where y_m is the maximum variation of y . Note that both x_m/R and y_m/R are very small in magnitude. The second derivatives with respect to time of x and y are thus neglected as is the Coriolis term $2\omega_o\dot{y}$. The term $\dot{\omega}_o$ is expressible as follows;

$$\dot{\omega}_o = \frac{d\omega_o}{dT} = \frac{d\omega_o}{d\phi} \cdot \frac{d\phi}{dT} = \omega_o \frac{d\omega_o}{d\phi} \quad (3-7)$$

The term $\frac{d\omega_o}{d\phi}$ is approximated for ball i as follows;

$$\left[\frac{d\omega_o}{d\phi} \right]_i = \frac{(\omega_o)_{i+1} - (\omega_o)_{i-1}}{2\Delta\phi} \quad (3-8)$$

where $\Delta\phi$ is the angular distance between rolling elements.

The moments necessary to cause the ball velocity to change are as follows;

$$\vec{M} = \begin{bmatrix} M_x \\ M_y \\ M_z \end{bmatrix} = J \begin{bmatrix} \dot{\omega}_x \\ \dot{\omega}_y - \omega_o \omega_z \\ \dot{\omega}_z + \omega_o \omega_y \end{bmatrix} \quad (3-9)$$

where J is the moment of inertia of the ball given by

$$J = MD^2/10 \quad (3-10)$$

and D is the ball diameter.

The time variation of the autorotational velocity components ω_x , ω_y and ω_z are approximated in the same manner as ω_o e.g.

$$\dot{\omega}_x \approx \left[\frac{(\omega_x)_{i+1} - (\omega_x)_{i-1}}{2\Delta\phi} \right] \omega_o \quad (3-11)$$

Using D'Alembert's principle, forces $-\vec{F}$ and moments $-\vec{M}$ calculated as described above are imposed on the ball along with the other forces and moments due to frictional and contact forces. The combined system of forces is then regarded as being in static equilibrium.

Because the time rates of change of ω_o , ω_x , ω_y and ω_z are included by approximation as described above, the analytical treatment is considered to be quasi-dynamic as distinct from analyses wherein these terms are neglected and only the centrifugal force $m \omega_o^2(R+y)$ and gyratory moments $J\omega_o \omega_z$ and $-J\omega_o \omega_y$ are considered. The description "quasi-static" has been applied to solutions of this type.

3.4 CAGE MODEL

Program AT74Y001 contains a model for either an inner ring or an outer ring guided cage.

Figure 3-4 shows a schematic representation of an inner ring riding cage. The diametral clearance between the cage and the land is denoted by Δ .

The cage pocket webs are acted upon by normal and tangential forces which are applied to the leading or trailing edge of the pocket depending upon whether the ball is driving or being driven by the cage at a given azimuth position.

For cage equilibrium the sum of the pocket force components in the Y and Z directions will be equilibrated by a hydrodynamic force acting on the cage/ring guide surfaces which is developed by the cage's moving out of concentricity with respect to the ring.

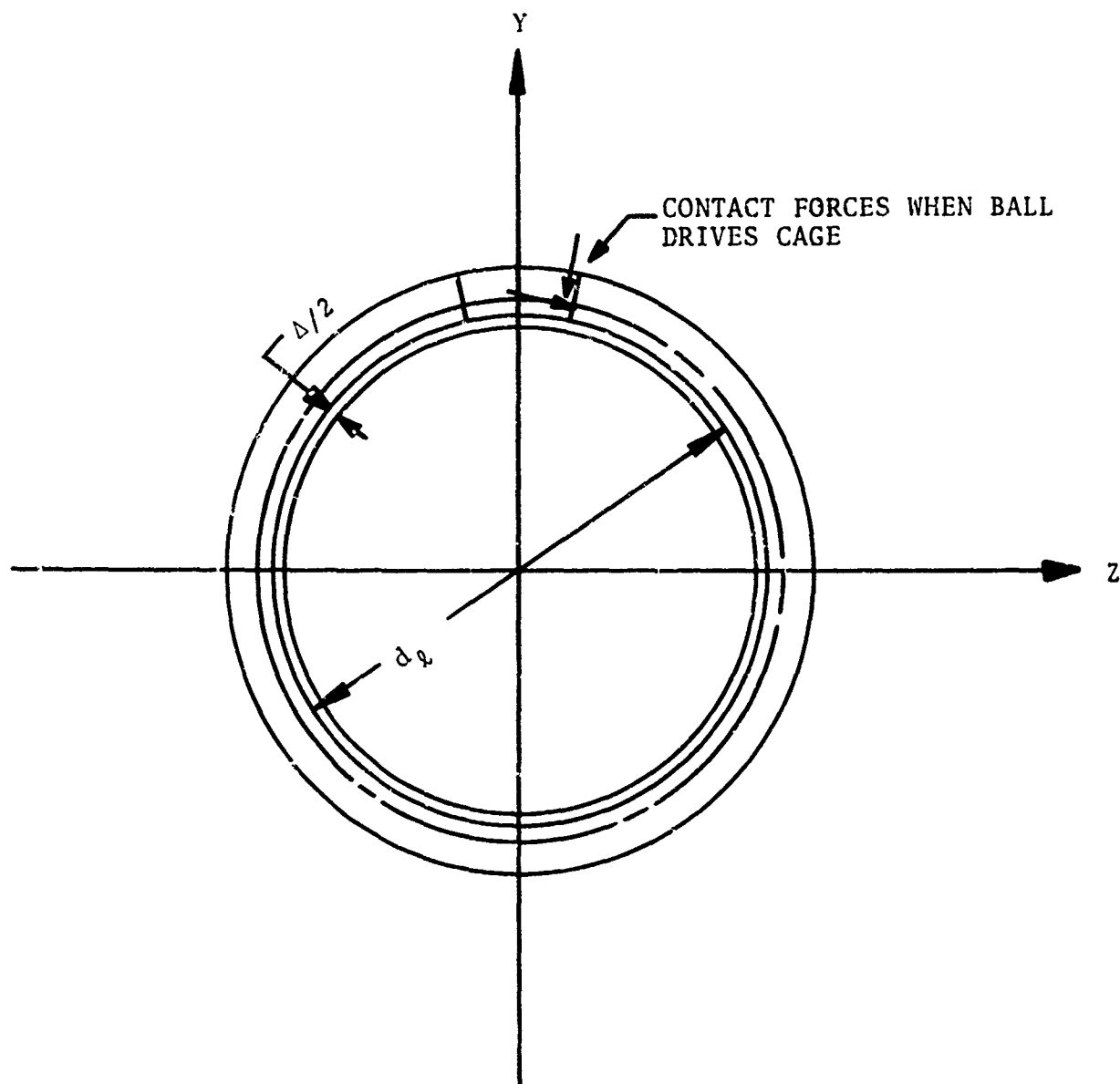


FIGURE 3-4
CAGE GEOMETRY

Expressions for the Y and Z components of cage reaction force as well as the moment about the bearing axis were developed as a function of cage eccentricity using the theory of short journal bearings. These results are given in the First Interim report {5}.

The assumption has been made in Computer Program AT74Y001 that the cage pocket forces are in near equilibrium i.e., the resultant cage/land normal force is negligibly small and the cage remains concentric with the ring. It is additionally assumed that the cage and the bearing ring that guides it, undergo no relative out-of-plane rotation.

The only condition thus remaining for cage equilibrium is that the resultant moment about the cage axis due to the cage pocket forces equilibrate the moment M_C due to fluid friction between the cage and the ring land.

For a concentric rotator, M_C is given by,

$$M_C = \frac{\eta |\omega - \omega_C| A_C d_L^2}{2} \quad (3-12)$$

where:

M_C = Torque acting on the cage, (in-lb)

ω = Angular velocity of the ring (inner or outer) that guides the cage (rad/sec)

ω_C = Cage angular velocity (rad/sec)

η = Dynamic viscosity (lb-sec/in)

A_C = Cage-land surface area (in²)

d_L = Cage-land diameter (in.)

Δ = Cage-land diametral clearance (in.)

3.5 BEARING GENERATED HEAT

The bearing generates heat at the following locations:

- 1) In the ball-race contact regions due to frictional sliding

- 2) In the ball-race contact inlets due to fluid pumping and shearing forces
- 3) In the ball-cage pocket contact inlets due to fluid pumping and shearing forces
- 4) Between the cage and land due to fluid shearing
- 5) At the ball-lubricant interface due to fluid drag

3.5.1 Contact Regions

The heat generated by traction in the contact zone is computed as

$$q_T = \int_{-a}^a \vec{T} \cdot \vec{u} \, ds \quad (3-13)$$

where \vec{T} = traction force vector at a general location within the contact

\vec{u} = sliding velocity vector associated with the same location as \vec{T}

s = coordinate along the contact in direction perpendicular to rolling

a = contact ellipse semi-major axis

The calculation of the traction vector \vec{T} is considered in Section 4.4.

3.5.2 Inlet Regions

In the ball-race and ball-cage inlet regions the heat generated due to the shearing force F_S and sliding force F_R is calculated as,

$$q_I = 2F_R V + F_S u \quad (3-14)$$

where V = fluid entrainment velocity at the contact center

u = sliding velocity at the contact center

Calculation of F_R and F_S is discussed in Section 4.6.

3.5.3 Cage-Land

The heat generated by fluid shearing between the cage and land is calculated as the product of the cage friction moment and rotational speed, i.e.,

$$q_c = M_c \cdot |\omega - \omega_c| \quad (3-15)$$

where M_c is given by Eq. (3-12) and $|\omega - \omega_c|$ is the absolute value of the difference between the cage speed and the speed of the ring that guides the cage.

3.5.4 Fluid Drag

The heat generated at the bearing by the fluid drag force is the product of the drag force F_w and the cage speed i.e.

$$q = F_w \cdot \frac{d_m}{2} \cdot \omega_c \quad (3-16)$$

where d_m is bearing pitch diameter
 ω_c is the cage angular speed
 F_w is the fluid drag force described in Section 4.7

3.5.5 Summarization of Heat Generation Rates

Program AT74Y001 calculates and prints the heat generated at the outer and inner ring contacts by summing q_r and q_i computed by Eq. (3-13) over all balls. Similarly the values of q_l at all cage-ball contacts are summed and printed as a separate item.

The cage land heat generation rate and the ball drag heat generation rate summed over all the balls, are printed as separate items.

Further, the total heat generation is calculated and printed.

If a thermal analysis is to be performed to determine the transient or steady state temperature distribution in a structure using calculated heat generation rates, the user has the option of separately apportioning the inner race, outer race, cage-land and combined drag and ball-cage pocket heat generation

rates between user designated points distributed within the structure. This point is discussed in more detail in Section 5, INPUT DATA PREPARATION.

3.6 TEMPERATURE DISTRIBUTION CALCULATION

Program AT74Y001 is capable of determining the steady state or equilibrium temperature distribution within a structure of general shape, as well as its transient temperature distribution i.e. the temperature distribution at selected time intervals after some arbitrary "start up" time.

The structure to be analyzed is conceptually divided into a number of elements or nodes. The net heat flow q_i into any node i is a function of the temperature of node i and the temperatures of all the other nodes that communicate thermally with node i . The form of the function depends upon how heat is transferred between the other nodes and node i . Conduction, radiation, convection and mass transport or fluid flow are all possible mechanisms for the transferral of heat from node j to node i . Expressions for the amount of heat transferred by these various mechanisms are given subsequently.

3.6.1 Steady State Temperatures

When the system is in thermal equilibrium the net heat energy q_i into the i -th nodal element is zero. The steady state temperature distribution is thus found by solving the system of equations,

$$q_i = 0 \qquad i = 1, 2 \dots n \qquad (3-17)$$

where n is the total number of nodes established
 q_i is a function of some subset of the nodal steady state temperatures.

3.6.2 Transient Temperatures

In the transient case the net heat q_i transferred to a node i heats the element. It is thus necessary for heat balance at node i that the following equations are satisfied.

$$\rho C_p V_i \frac{dt_i}{dT_i} = q_i \qquad (3-18)$$

where ρ = density
 C_p = specific heat
 V = volume of the element
 t = temperature
 T = time

The temperatures, t_{oi} , at the time of initiation $T = T_s$ are assumed to be known, that is

$$t_i(T_s) = t_{oi} \quad i = 1, 2, \dots, n \quad (3-19)$$

The problem of calculating the transient temperature distribution in a bearing arrangement thus becomes a problem of solving a system of non-linear differential equations of the first order with certain initial values given. The equations are non-linear since they contain terms of radiation and free convection, which are non-linear with temperature as will be shown later. The simplest and most economical way of solving these equations is to calculate the rate of temperature increase at the time $T = T_k$ from equation 3-18 and then calculate the temperatures at time $T_k + \Delta T$ from

$$t_{k+1} = t_k + \frac{dt_k}{dT} \Delta T = t_k + \frac{q_k}{\rho C_p V} \Delta T \quad (3-20)$$

If the time step ΔT used as program input is chosen too large, the temperatures will oscillate, and if it is chosen too small the calculation will be costly. It is therefore desirable to choose the largest possible time step that does not give an oscillating solution. The program optionally calculates such a time step. The step is obtained from the condition, {10}

$$\frac{dt_{i,k+1}}{dt_{i,k}} \geq 0 \quad i = 1, 2, \dots, n \quad (3-21)$$

If this derivative were negative, the implication would be that the local temperature at node i has a negative effect on its future value. This would be tantamount to asserting that the hotter a region is now, the colder it will be after an equal time interval. An oscillating solution would result.

Differentiating equation (3-20) for node i , one has as condition (3-21),

$$\frac{dt_{i,k+1}}{dt_{i,k}} = 1 + \frac{\Delta T_i}{\rho_i C_{pi} V_i} \cdot \frac{dq_i}{dt_i} = 0, \quad i = 1, 2, \dots, n \quad (3-22)$$

The derivative dq_i/dt_i is calculated numerically

$$\frac{dq_i}{dt_i} = \frac{q_i(t_i + \Delta t_i) - q_i(t_i)}{\Delta t_i} \quad (3-23)$$

For each node the value of ΔT_i giving a value of zero to the right hand side of Eqn. (3-22) is calculated.

A value of ΔT rounded off to one significant digit smaller than the smallest of the ΔT_i given by Eq. (3-22) is used.

3.7 CALCULATION OF HEAT TRANSFER RATE

The transfer of heat within a medium or between two media can occur by conduction, convection, radiation and fluid flow.

All these types of heat transfer occur in a bearing application as the following examples show.

1. Heat is transferred by conduction between inner ring and shaft and between outer ring and housing.
2. Heat is transferred by convection between the surface of the housing and the surrounding air.
3. Heat is transferred by radiation between the shaft and the housing.
4. When the bearing is lubricated and cooled by circulating oil, heat is transferred by fluid flow.

Therefore, in calculating the net flow to a node all the above mentioned modes of heat transfer will be considered.

3.7.1 Generated Heat

There may be a heat source at node i giving rise to a heat flow to be added to the heat flowing from the neighboring nodes.

In the case that the heat source is a bearing, it may either be considered to produce known amounts of power, in which case constant numbers are entered as input to the program, or the shaft-bearing program may be used to calculate the bearing generated heat as a function of bearing temperatures as discussed in Section 3.5.

3.7.2 Conduction

The heat flow $q_{ci,j}$ which is transferred by conduction from node i to node j , is proportional to the difference in temperature $(t_i - t_j)$ and the cross-sectional area A and is inversely proportional to the distance ℓ between the two points, thus

$$q_{ci,j} = \frac{\lambda A}{\ell} (t_i - t_j) \quad (3-24)$$

where λ = the thermal conductivity of the medium.

3.7.3 Free Convection

Between a solid medium such as a metallic body and a liquid or gas, heat transfer is by free or forced convection. Heat transfer by free convection is caused by the setting in motion of the liquid or gas as a result of a change in density arising from a temperature differential in the medium. With free convection between a solid medium and air, the heat energy $q_{vi,j}$ transferred between nodes i and j can be calculated from the equation, { 2 }

$$q_{vi,j} = \alpha_v A |t_i - t_j|^d \cdot \text{SIGN}(t_i - t_j) \quad (3-25)$$

where α_v = the film coefficient of heat transfer by free convection

A = the surface area of contact between the media

d = is an exponent, usually : 1.25, but any value can be specified as input to the program

$$\text{sign}(t_i - t_j) = \begin{cases} 1 & \text{if } t_i \geq t_j \\ -1 & \text{if } t_i < t_j \end{cases}$$

The last factor is included to give the expression $q_{vi,j}$ a correct sign.

The value of α_v can be calculated for various cases, see Jacob and Hawkins, {10}.

3.7.4 Forced Convection

Heat transfer by forced convection takes place when liquid or gas moves around a solid body, for example, when the liquid is forced to flow by means of a pump or when the solid body is moved through the liquid or gas. The heat flow $q_{wi,j}$ transferred by forced convection can be obtained from the following equation.

$$q_{wi,j} = \alpha_w A(t_i - t_j) \quad (3-26)$$

where α_w is the film coefficient of heat transfer during forced convection. This value is dependent on the actual shape, the surface condition of the body, the difference in speed, as well as the properties of the liquid or gas.

In most cases, it is possible to calculate the coefficient of forced convection from a general relationship of the form,

$$N_u = a R_e^b P_r^c \quad (3-27)$$

where a , b , and c are constants obtained from handbooks, such as {2}. R_e and P_r are dimensionless numbers defined by

N_u = Nusselt's number = $\alpha_w L / \lambda$

L = characteristic length

λ = conductivity of the fluid

R_e = Reynold's number = $UL\rho/\eta$

U = characteristic speed

ρ = density of the fluid

η = dynamic viscosity of the fluid

P_r = Prandtl's number = $\eta C_p / \lambda$

C_p = specific heat

The program can use a value of the coefficient of convection, or let it vary with actual temperatures, the variation being determined by how the viscosity varies. Input can be given in one of four ways, for each coefficient.

Constant viscosity

1. Values of the parameters of equation (3-27) are given as input and a constant value of α_w is calculated by the program.

Temperature dependent viscosity

2. The coefficient α_w for turbulent flow and heating of petroleum oils {25} is given by

$$\alpha_w = k_9 \cdot \eta(t)^{k_{10}} \quad (3-28)$$

where k_9 and k_{10} are given as input together with viscosity at two different temperatures.

3. Values of the parameters of equation (3-27) are given as input. Viscosity is given at two different temperatures.

3.7.5 Radiation

If two flat parallel, similar surfaces are placed close together and have the same surface area A , the heat energy transferred by radiation between nodes i and j representing those bodies, will be,

$$q_{Ri,j} = \epsilon \sigma A [(t_i + 273)^4 - (t_j + 273)^4] \quad (3-29)$$

where ϵ is the surface emissivity. The value of the coefficient ϵ is an input variable and varies between 1 for a completely black surface and 0 for an absolutely clean surface. In addition σ is Stefan-Boltzmann's radiation constant which has the value 5.76×10^{-8} watts/m²(°K)⁴ and t_i and t_j are the temperatures at points i and j .

Heat transfer by radiation under other conditions can also be calculated, {10}. The following equation, for instance, applies

between two concentric cylindrical surfaces

$$q_{Ri,j} = \frac{\epsilon \sigma A_i [(t_i + 273)^4 - (t_j + 273)^4]}{1 + (1 - \epsilon) (A_i / A_e)} \quad (3-30)$$

where A_i is the area of the inner cylindrical surface
 A_e is the area of the outer cylindrical surface

3.7.6 Fluid Flow

Between nodes established in fluids, heat is transferred by transportation of the fluid itself and the heat it contains.

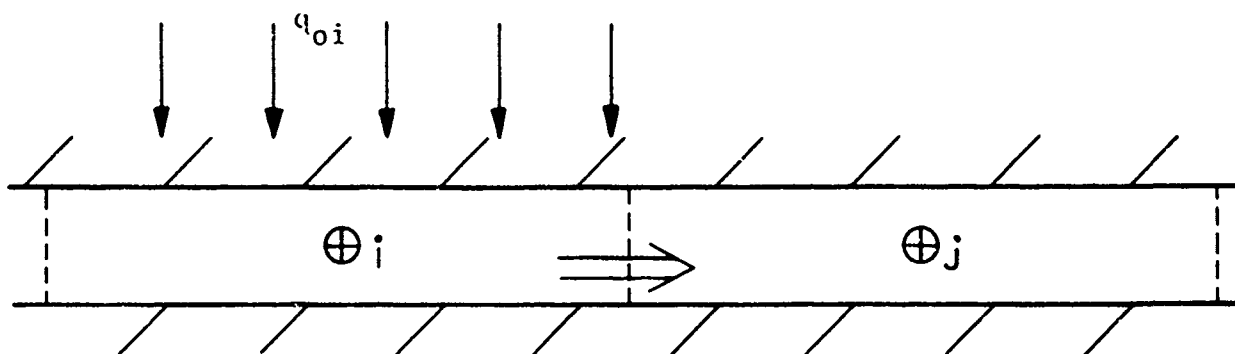


Figure 3-5 Convective Heat Transfer

Figure 3-5 shows nodes i and j at the midpoints of consecutive segments established in a stream of flowing fluid.

The heat flow $q_{ui,j}$ through the boundary between nodes i and j can be calculated as the sum of the heat flow q_{fi} through the middle of the element i , and half the heat flow q_{oi} transferred to node i by other means, such as convection.

The heat carried by mass flow is,

$$q_{fi} = \rho_i C_{p_i} V_i t_i = K_i t_i \quad (3-31)$$

where V_i = the volume flow rate through node i

The heat input to node i is the sum of the heat generated at node i (if any) and the sum over all other nodes of the heat transferred to node i by conduction, radiation, free and forced convection.

$$q_{oi} = q_{G,i} + \sum_j (q_{ci,j} + q_{vi,j} + q_{wi,j} + q_{Ri,j}) \quad (3-32)$$

The heat flow between the nodes of Fig. 3-6 is then,

$$q_{ui,j} = q_{fi} + q_{oi}/2 \quad (3-33)$$

If the flow is dividing between node i and j , Figure 3-6 then the heat flow is calculated from

$$q_{ui,j} = K_{ij} (q_{fi} + q_{oi}/2) \quad (3-34)$$

where K_{ij} = the proportion of the flow at i going to node j , $0 < K_{ij} \leq 1$. K_{ij} is specified at input.

$$k_k = k_{ik} \cdot k_i$$

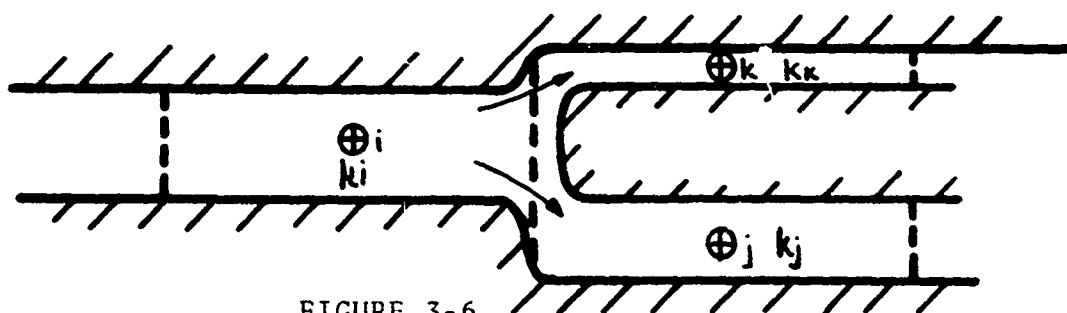


FIGURE 3-6

DIVIDED FLUID FLOW FROM NODE i

3.7.7 Total Heat Transferred

The net heat flow rate to node i can be expressed as,

$$q_i = q_{G,i} + \sum_j (q_{ci,j} + q_{ui,j} + q_{vi,j} + q_{wi,j} + q_{Ri,j}) \quad (3-35)$$

The summation should include all nodes j , both with unknown temperatures as well as boundary nodes, at which the temperature is known so long as they have a direct heat exchange with node i .

This expression is a non-linear function of temperatures because of the terms q_w and q_r . Therefore the equations to be solved for a steady state solution are non-linear. The subprogram SOLVXX for solving non-linear simultaneous equations is used for this purpose.

3.8 CONDUCTION THROUGH A BEARING

As described in Section 3.7 the conduction between two nodes is governed by the thermal conductivity parameter λ of the medium through which conduction takes place. The value of λ is specified at input.

An exception is when one of the nodes represents a bearing ring and the other a set of rolling elements. In this case the conduction is separately calculated using the principles described below.

3.8.1 Thermal Resistance

It is assumed that the rolling speeds of the rolling elements are so high that the bulk temperatures of the rolling elements are the same at both the inner and outer races, except in a volume close to the surface. The resistance to heat flow can then be calculated as the sum of the resistance across the surface and the resistance of the material close to the surface.

The resistance Ω is defined implicitly by

$$\Delta t = \Omega \cdot q \quad (3-36)$$

where

Δt is temperature difference
 q is heat flow

The resistance due to conduction through the EHD film is calculated as

$$\Omega_1 = (h/\lambda) \cdot A \quad (3-37)$$

where h is taken to be the calculated plateau film thickness

A is the Hertzian contact area at the specific rolling element-ring contact under consideration. λ is the conductivity of the oil.

The geometry is shown in Figure 3-7(a). Asperity conduction is not considered.

So far, a constant temperature difference between the surfaces has been assumed. But during the time period of contact, the difference will decrease because of the finite thermal diffusivity of the material near the surface, Fig. 3-7(b).

To points at a distance from the surface this phenomenon will have the same effect as an additional resistance Ω_2 acting in series with Ω_1 .

This resistance was estimated in {9} as,

$$\Omega_2 = \frac{1}{\lambda \ell_{re,i}} \left(\frac{\pi \psi}{2b_i V} \right)^{1/2} \quad (3-38)$$

where ℓ_{re} = contact length, or in the case of an elliptical contact area, 0.8 times the major axis

λ = heat conductivity

ψ = thermal diffusivity = $\lambda / (\rho \cdot C_p)$

ρ = density

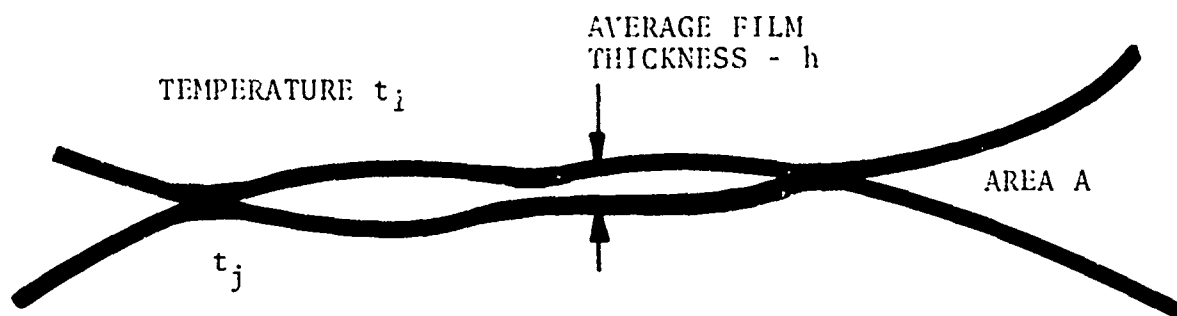
C_p = specific heat

b = half the contact width

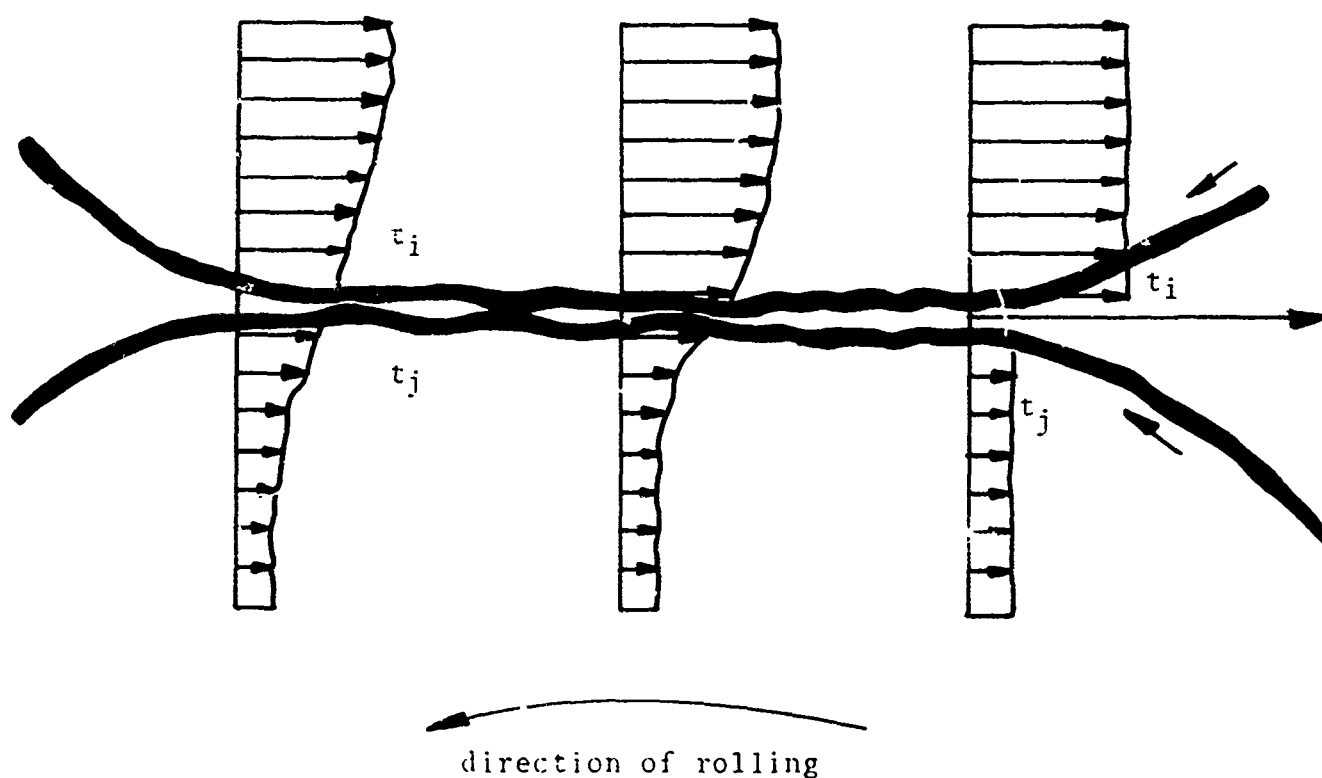
V = rolling speed

The resultant resistance is

$$\Omega_{res} = \Omega_1 + \Omega_2 \quad (3-39)$$



(a) Schematic Concentrated Contact



(b) Temperature Distribution at Rolling,
Concentrated Contact Surfaces

FIGURE 3-7

CONTACT GEOMETRY AND TEMPERATURES

There is one such resistance at each rolling element. They all act in parallel. The resultant resistance, Ω_{res} , is thus obtained from

$$\frac{1}{\Omega_{res}} = \sum_{i=1}^n \frac{1}{\Omega_{res,i}} \quad (3-40)$$

where n is the number of rolling elements

3.9 SOLUTION SCHEMES AND CONVERGENCE CRITERIA

As described in Section 2 the complete shaft-bearing system solution is achieved when four sets of conditions are simultaneously satisfied through numerical iteration schemes.

These schemes and the accuracy criteria invoked at each are discussed in this section. Certain aspects of the solution scheme discussed more qualitatively in Section 2 and 3.1 are reiterated herein in the context of solution accuracy discussions.

1. Temperature Equilibrium Calculations - these occur at two levels designated internal and external temperature equilibrium. Internal temperature equilibrium refers to the calculation of equilibrium temperatures for a specified set of heat generation rates. External temperature equilibrium is satisfied when the system temperatures are nearly equal in two successive calculations of bearing generated heats.
2. Diametral Clearance Change - satisfied when the change in bearing diametral clearance is sufficiently close to zero in two successive calculations of bearing load distribution.
3. Bearing Inner Ring Equilibrium - satisfied when shaft-inner ring loads are sufficiently close to equalling rolling element-inner ring loads.
4. Rolling Element and Cage Quasi-dynamic Equilibrium - satisfied when rolling element applied loads plus inertia forces sum to zero.

The information presented below is general in nature and is intended to give the user an appreciation of the four main aspects of the Computer Program.

3.9.1 Temperature Equilibrium Convergence Criteria

a) Internal Temperature Equilibrium

After each calculation of bearing generated heat, which results from a solution of the shaft-bearing system portion of the program, a set of system temperatures is determined which satisfy the system of equations:

$$q_i = q_{oi} + q_{gi} = 0 \text{ for all temperature nodes } i \quad (3-41)$$

where q_{oi} is the heat flow from all neighboring nodes to node i

q_{gi} is the heat generated at node i . These values may be input or calculated by the shaft bearing program as bearing frictional heat

This scheme is solved with a modified Newton-Raphson method which successfully terminates when either of two conditions are met:

$$\frac{\Delta t_i}{t_i} \leq EP2 \text{ for all nodes } i$$

where: Δt represents the Newton-Raphson correction to the temperature t at a given iteration such that, $t_{N+1} = t_N + \Delta t$ and $N + 1$, and N , refer to the next and current iteration respectively.

EP2 is a user specified constant. If EP2 is left blank or set to zero (0) a default value of 0.001 is used.

A second convergence criterion dependent upon EP2 is also used. In the system of equations, $q_{oi} + q_{gi} = 0$ for all nodes i , absolute convergence would be obtained if the right hand side (EQ) in fact reduced to zero (0). Usually a small residue remains at each node, such that $(q_{oi} + q_{gi}) = (EQ)_i$.

The second convergence criterion is satisfied if

$$\left\{ \sum_i^{NEQ} \left[\frac{(EQ)_i^2}{NEQ} \right] \right\}^{1/2} \leq 10 \times EP2 \quad (3-42)$$

where NEQ = number of equations in bearing solution

The two convergence criteria independently terminate the iteration scheme. The second criterion is an explicit test for an equilibrium condition. The first criterion is implicit. The first criterion tends to terminate the iteration scheme when convergence is extremely slow and the equilibrium condition is approached but not satisfied.

This solution is referred to as the internal steady state thermal solution. It applies for a specific set of heat generation rates. It is not a final solution inasmuch as the generated heats will generally vary with the steady state temperatures so that iteration is necessary to achieve a solution for which the temperatures and heat generation rates are mutually compatible.

b) External Temperature Equilibrium

The external steady state thermal solution is obtained when, after two successive calculations of ball bearing generated heats, the system temperatures remain numerically equal within prescribed limits. The system generated heats are then compatible with the system temperatures and system steady state equilibrium is satisfied.

The external solution is satisfied when

$$t_{N-1} - t_N \leq EP1 \text{ for all nodes } i \quad (3-43)$$

where N refers to the current set of system temperatures and $N-1$ refers to the system temperatures achieved for the previous iteration, with the previous set of bearing generated heats. $EP1$ is a user supplied convergence criteria. A value $EP1 = 0.001$ is acceptable.

3.9.2 Bearing Diametral Clearance Change Analysis

The program calculates the changes in bearing diametral clearances according to the analysis described in {26}, and expressed in generalized equation form as,

$$\Delta DCL = f[(Fits)_m, t_i, \Omega_m, (Q_r)_m], \quad m = 1, 2 \text{ for inner and outer rings} \quad (3-44)$$

respectively

$i = 1, 2, 3, 4, 5$ for shaft,
inner ring, outer ring,
housing and rolling
element respectively

where: ΔDCL is the change in bearing diametral clearance
 Fits are the cold mounted shaft and housing fits.
 t_i are the component temperatures
 Ω_m refers to the ring rotational speeds
 Q_r refers to the radial component of the minimum
 rolling element-race normal force.

A bearing clearance change criterion is satisfied when the change in bearing diametral clearance remains within a narrow, user specified range, for two successive iterations as follows:

$$\frac{|(\Delta DCL)_N - (\Delta DCL)_{N-1}|}{D} \leq EPSFIT \text{ for all bearings } (3-45)$$

where: N denotes the most recent iteration and
 $N-1$ denotes the previous iteration,
 D denotes the ball or roller diameter and
 EPSFIT is a user specified value, = .0001D

It should be noted that although ring rotational speeds, and initial, i.e. cold, shaft and housing fits are considered in the clearance change analysis, the two factors are fixed at input and remain constant through the entire solution. Although component temperatures may change as a consequence of the thermal solution, temperatures remain constant through a complete set of clearance change iterations as shown in the general logic diagram Fig. 2-2. As a result, only the change in bearing load distribution affects the change in bearing clearance within a set of clearance change iterations.

3.9.3 Bearing Inner Ring Equilibrium

The bearing inner ring equilibrium solution is obtained by solving the system:

$$(\vec{FM}_b)_i - (\vec{FM}_s)_i = 0 \text{ for all bearings, } i \quad (3-46)$$

where: \vec{FM}_b denotes a vector of bearing loads and moments resulting from rolling element/race forces and moments.

$$\vec{FM}_{bi} = \begin{bmatrix} F_{bxi} \\ F_{byi} \\ F_{bzi} \\ \hline M_{byi} \\ M_{bzi} \end{bmatrix} \quad \begin{array}{l} \text{Forces} \\ \\ \text{Moments} \end{array} \quad (3-47)$$

If the bearing solution considers friction, \vec{FM}_b is comprised of the ball race friction forces as well as the normal forces.

If the ball bearing solution is, at the user's option frictionless, \vec{FM}_b is comprised only of rolling element/race normal contact forces.

\vec{FM}_{si} denotes a similar vector of loads, exerted on the inner ring by the shaft.

$$\vec{FM}_{si} = \begin{bmatrix} F_{sxi} \\ F_{syi} \\ F_{szi} \\ \hline M_{syi} \\ M_{szi} \end{bmatrix} \quad \begin{array}{l} \text{Forces} \\ \\ \text{Moments} \end{array} \quad (3-48)$$

The variables in this system of equations are the bearing inner ring deflections Δ_b and the shaft displacements $\vec{\Delta}$ at all bearing locations. The bearing loads may be expressed as a function of the inner ring deflections.

$$\vec{FM}_b = \vec{FM}_b(\vec{\Delta}_b) \quad (3-49)$$

The deflection $\vec{\Delta}_b$ of a bearing is described by two radial deflections δ_y and δ_z , two angular deflections θ_y and θ_z and one axial deflection δ_x . The axial deflection is assumed to be the same for all bearings on a shaft, i.e.

$$\vec{\Delta b} = \begin{bmatrix} \delta x \\ \delta y \\ \delta z \\ \theta y \\ \theta z \end{bmatrix} \quad (3-50)$$

In the same manner for the shaft

$$\vec{FM}_s = \vec{FM}_s (\vec{\Delta}) \quad (3-51)$$

$$\vec{\Delta} = \begin{bmatrix} \delta y_1 \\ \delta z_1 \\ \theta y_1 \\ \theta z_1 \\ \hline \delta y_2 \\ \delta z_2 \\ \theta y_2 \\ \theta z_2 \\ \hline \vdots \\ \vdots \\ \vdots \\ \vdots \\ \delta x \end{bmatrix} \begin{matrix} \text{1st bearing} \\ \text{2nd bearing} \\ \text{Applicable} \\ \text{to all brg.} \\ \text{locations} \end{matrix} \quad (3-52)$$

A matrix of influence coefficients allows the shaft loads at each bearing location to be expressed in terms of shaft displacements at the bearing seat in question plus the displacements at the two adjacent bearing seats.

Using the Newton-Raphson solution scheme to solve the set of equations:

$$\vec{FM}_{bi} - \vec{FM}_{si} = 0 \quad (3-52)$$

produces a set of corrections $\delta(\vec{\Delta})$ which are added to the values of $\vec{\Delta}$ used in the previous iteration.

The solution scheme is ended when

$$\frac{\delta(\vec{\Delta})_{ij}}{(\vec{\Delta})_{ij}} \leq \begin{cases} \text{EPS1 (frictionless)} \\ \text{EPS2 (friction)} \end{cases} \quad (3-53)$$

$i = 1, \dots (\text{Number of bearings})$
 $j = 1, 5 - \text{for the 3 linear and two angular deflections at each bearing}$

If for some i or j , $(\vec{\Delta})_{ij} = 0$

$$\frac{\delta(\vec{\Delta})_{ij}}{(0.001 \times \text{NBRG})} < \begin{cases} \text{EPS1 (frictionless)} \\ \text{EPS2 (friction)} \end{cases} \quad (3-54)$$

wherein NBRG denotes the number of bearings in the system is substituted for the previous expression. EPS1 or EPS2 is used depending on whether the bearing solutions are frictionless or include friction, respectively. If the bearing deflections are extremely small, computer-generated numerical inaccuracies may prevent convergence according to the above criteria although a perfectly good solution has been obtained. To overcome this problem, the iteration is terminated if all angular deflections are less than 2×10^{-6} radians and all linear deflections are less than 5×10^{-8} inches. Any one of the above criteria imply that inner ring equilibrium is satisfied.

3.9.4 Bearing Quasi-Dynamic Solution

The bearing quasi-dynamic solution is obtained through a two step process:

- 1) Elastic Solution - considering rolling element centrifugal force.
- 2) Elastic and Quasi-dynamic Solution*

*Quasi-dynamic equilibrium is used to connote that the true dynamic equilibrium terms containing first derivatives of the ball rotational speed vectors and the second derivatives of rolling element position vectors with respect to time are replaced by numerical expressions which are position rather than time dependent.

The equations which define rolling element quasi-dynamic force equilibrium take the form

$$\sum_m \left[\int_{-a_m}^{a_m} (\vec{Q}_m + \vec{f}_m) ds + \vec{F}_m \right] + \vec{F} = 0 \quad m = 1-3 \text{ refers to the } (3-55)$$

outer, inner and cage
rolling element contacts
respectively

where: \vec{Q}_m is the vector normal load per unit length of the contact ellipse

\vec{f}_m is the vector of friction force per unit length of the contact ellipse

\vec{F} is the vector of inertia and drag forces
s is a coordinate along the contact perpendicular to the direction of rolling (usually the major axis)

a is half the contact length

\vec{F}_m is the vector sum of the hydrodynamic forces acting on the ball at the m-th contact

Rolling element moment equilibrium is defined by:

$$\sum_m \left[\int_{-a_m}^{a_m} \vec{r}_m \times (\vec{Q}_m + \vec{f}_m) ds \right] + \vec{r}_m \times \vec{F}_m + \vec{M}_I = 0 \quad (3-56)$$

$\vec{Q}_m, \vec{f}_m, \vec{F}_m, a_m$, and t are defined above, \vec{M}_I is a vector of inertia moments (cf. Eq. 3-9)

\vec{r}_m is a vector from the rolling element center to the point of contact.

In the frictionless elastic solution \vec{F}_m and $\vec{f}_m = 0$. Additionally the only rolling element inertia term considered in the frictionless solution is centrifugal force. As a consequence only the axial and radial force equilibrium equations are solved for each ball. For each roller the radial force equilibrium and the tilting moment about the Z axis of Fig. 3-1 is solved. A dummy equation for axial force equilibrium is included in the solution matrix which keeps the roller centered with respect to the outer race. The cylindrical roller bearing considered by the program cannot carry axial loading.

The friction solution determines ball quasi-dynamic equilibrium for six degrees of freedom. The ball variables in this solution are, x_1 , y_1 , ω_x , ω_y , ω_z , and ω_o .

where x_1 is the ball axial position relative to the outer race,
 y_1 is the ball radial position relative to the outer race,
 ω_x , ω_y , ω_z are orthogonal ball rotational speeds
relative to the cage speed, about the x, y and z
axes and ω_o is the ball orbital speed.

The variables x_1 and y_1 are the ball variables in the frictionless solution.

It is required to solve the set of equilibrium equations for each ball as well as the moment equilibrium equation for the cage, about the bearing X axis. (Refer to Section 10 of {6}.) See Fig. (3-1). This latter equation considers the ball cage pocket normal and friction forces plus the friction force developed between the bearing lands and the cage rail. The cage variable is the cage circumferential position relative to the ball at the first angular location $(z_c)_1$.

The ball bearing friction solution is thus obtained by solving a set of $6n + 1$ equations, where n is the number of rolling elements. The ball bearing frictionless solution contains $2n$ equations representing the ball center coordinates for each ball. The roller bearing frictionless solution contains $3n$ equations representing the tilt angle and roller center coordinates for each roller.

A modified Newton-Raphson scheme implemented in subroutine SOLVXX and described in Section 3-10 is used to solve the systems of equations. These modifications enhance convergence.

The iteration scheme is terminated by either of two criteria:

The first criterion involves the rate of convergence of each variable to its value at solution. It is:

$$\left| \frac{\Delta X_{Ni}}{X_{Ni}} \right| \leq \begin{cases} \text{EPS1 (frictionless)} \\ \text{EPS2 (friction)} \end{cases} \quad (3-57)$$

where X_{Ni} is the value of variable X_i at iteration N and
 ΔX_{Ni} the change in the value of variable X_i calculated
at iteration N .

If the solution scheme is to terminate on the basis of this criterion each of the variables must satisfy this condition, the number of variables being $6n + 1$, $2n$ or $3n$ depending upon whether the bearing is a ball or roller type and whether the solution does or does not consider friction.

The second criterion checks the root mean square of the equilibrium equation residue values (EQ_i). If the cage and each rolling element were in quasi-dynamic equilibrium, all of the residues would be zero. As a practical matter the equations may be considered to be solved when:

$$\left[\frac{\sum_{i=1}^{NEQ} EQ_i^2}{NEQ} \right]^{1/2} < 10X \begin{cases} EPS1 & (\text{frictionless}) \\ EPS2 & (\text{friction}) \end{cases} \quad (3-58)$$

Experience has shown this criterion is somewhat more readily achieved than the first criterion.

As with the internal steady state thermal solution, the two convergence criteria are independent. The first criterion causes termination when the convergence is extremely slow, i.e., when the changes in the variable values predicted by the solution scheme are extremely small compared to the actual variable values.

3.10 METHOD FOR SOLVING BEARING EQUILIBRIUM EQUATIONS

The bearing equilibrium equations {6} are non-linear and can only be solved by approximate methods. The method of modified quasilinearization due to Miele, et al {23} is employed in Program AT74Y001 and has been found to be very effective.

Consider a system described by the equation

$$f(x) = 0 \quad (3-59)$$

where f and x are n -vectors. Let the sum of the squares of the equation residues be designated the performance index P , which can be expressed by

$$\left[\sum_{i=1}^{NEQ} EQ_i^2 \right] = P = f^T(x) f(x) \quad (3-60)$$

where the superscript T denotes matrix transposition. For any vector x satisfying Eq. (3-59), $P = 0$. For all other vectors x ,

$P \neq 0$. For an approximate solution, it is required that

$$\frac{P}{\epsilon} \leq \frac{\epsilon}{100} \cdot \text{NEQ} \cdot \begin{cases} \text{EPS1}^2 \\ \text{EPS2}^2 \end{cases} \quad (3-61)$$

Consider two points X_k and X_{k+1} which are related by

$$X_{k+1} = X_k + \Delta X_k, \quad k = 0, 1, 2, \dots \quad (3-62)$$

The passage from the point X_k to the point X_{k+1} causes the performance index P to change. To the first order, i.e. for small values of the ΔX_k this change is

$$\delta P = 2f^T(x) \delta f(x) \quad (3-63)$$

where the symbol δ denotes the first variation.

Consider the system of variations defined by

$$\delta f(x) = -\alpha f(x) \quad (3-64)$$

where α is a positive scaling factor and is restricted to the range

$$0 \leq \alpha \leq 1 \quad (3-65)$$

From Eqs. (3-60), (3-63) and (3-64), one obtains

$$\delta P = -2\alpha P \quad (3-66)$$

Since both P and α are non-negative, one must have

$$\delta P < 0 \quad (3-67)$$

which establishes the basic descent property of the algorithm defined by Eq. (3-64) i.e. first order variations, or small changes in the x vector will cause a decrease in P .

The first order change in $f(x)$ can be written as

$$\delta f(x) = f_x^T(x) \Delta x \quad (3-68)$$

where $f_x^T(x)$ is the Jacobian matrix.

From Eqs. (3-64) and (3-68), it follows

$$f_x^T(x) \Delta x + \alpha f(x) = 0 \quad (3-69)$$

For a given value of α , Eq. (3-69) is equivalent to n scalar equations which are linear in the n components of the correction vector ΔX .

For $\alpha = 1$, Eq. (3-69) becomes identical with that of the well-known Newton-Raphson method, or ordinary quasilinearization.

Introduce the auxiliary variable

$$B = \Delta X / \alpha \quad (3-70)$$

Equation (3-69) can be written as

$$f_x^T(x) B + f(x) = 0 \quad (3-71)$$

Combining Eqs. (3-62) and (3-70), one obtains

$$X_{k+1} = X_k + \alpha B \quad (3-72)$$

Since X_k is known and B can be obtained from Eq. (3-71), Eq. (3-72) yields a one-parameter family of solutions, where α is the parameter. The appropriate value of α is obtained by starting with $\alpha = 1$ and testing inequality (3-67). If the value of the performance index P does not decrease, a smaller value of α , found by a repeated division by 2.0 is used.

The solution variables for bearing equilibrium must fall within certain limits or constraints i.e. the speed of an inner ring guided cage must not exceed the speed of the inner ring. These constraints are of the form

$$a \leq x \leq b$$

where the values of a and b depend upon the operating conditions and are calculated by the program. When a component of the correction vector ΔX places the component value outside a constrained range, this component is set equal to zero following the procedure set fourth in {24}.

As with all numerical procedures for solving systems of simultaneous nonlinear equations, the procedure described above is not foolproof although it is a substantial improvement over the ordinary Newton-Raphson technique.

Occasionally the technique has been found to stall when the assumed starting values fall in a region of the solution space wherein the values of P given by Eq. (3-60) are at a

local minimum. When this occurs the value of α is successively reduced to the point where it is vanishingly small and then by Eq. (3-72) the procedure never moves from the point of local minimum.

This condition will result in a message indicating convergence failure (cf. Section 6).

SECTION 4

MATHEMATICAL MODELS

4.1 SCOPE

This section contains a description of the mathematical models specifically adapted or developed for use in computer program AT74Y001 including, where appropriate, the expressions for curve fitted approximations to complex relationships.

4.2 LUBRICANT PROPERTY MODELS

Many of the calculations performed by computer program AT74Y001 require that the dynamic viscosity η and the pressure-viscosity coefficient α be known at a given temperature.

Accordingly the program employs subroutines which, when given lubricant kinematic viscosity ν at 100°F (37.78°C) and 210°F (98.89°C), density ρ at 60°F (15.56°C) and the thermal coefficient of expansion, determine the lubricant density, kinematic and dynamic viscosity, and the pressure-viscosity coefficient at any temperature required.

The kinematic viscosity ν (cs) at atmospheric pressure is calculated at a given temperature t (°F) from Walther's relation [3]

$$\log_{10} \log_{10} (\nu + 0.6) = A - B \log_{10} (t + 460) \quad (4-1)$$

where A and B are constants determined by substituting the known values of ν at $t = 100^\circ\text{F}$ and $t = 210^\circ\text{F}$ into Eq.(4-1) and solving the two equations which result for A and B.

Having calculated ν at a specific t , η is computed as

$$\eta = \nu \rho \quad (4-2)$$

where ρ the lubricant density at temperature t is given by,

$$\rho(t) = \rho(60^\circ\text{F}) - G(t - 60^\circ\text{F}) \quad (4-3)$$

where G is the lubricant coefficient of thermal expansion.

The pressure-viscosity index α is defined implicitly by the relation

$$\eta(p) = \eta(p = 0) \cdot e^{\alpha p} \quad (4-4)$$

where $\eta(p)$ denotes the dynamic viscosity at pressure p at an arbitrary temperature.

The value of α itself varies with pressure. The appropriate value of α to use in the film thickness prediction equations wherein it appears, is the value applicable at the inlet i.e. at atmospheric pressure.

The value of α at a given temperature and at atmospheric pressure is calculated by the relation developed by Fresco, (4)

$$\alpha = (2.303) \cdot 10^{-4} \left[C + D \log_{10} v + E (\log_{10} v)^2 \right] \frac{(560)}{(t+460)} \quad (\text{in.}^2/\text{lb}) \quad (4-5)$$

wherein v is evaluated at temperature t ($^{\circ}\text{F}$) and C , D and E are constants tabulated by Fresco as a function of $S \approx 0.2B$ where B is the coefficient in Walther's equation.

Another lubricant property that appears in the model for film thickness reduction due to inlet heating is the temperature viscosity coefficient β , that appears in Reynold's exponential temperature - viscosity relationship $\eta(t) = \eta_0 e^{-\beta t}$.

β is computed from the dynamic viscosity values at $t = 100^{\circ}\text{F}$ and 210°F as follows,

$$\beta = 0.00909 \ln \frac{\eta(t = 100^{\circ}\text{F})}{\eta(t = 210^{\circ}\text{F})} \quad (4-6)$$

Relevant lubricant properties for the oils whose properties have been preprogrammed in computer program AT74Y001, are listed in Table 4-1. These property values have been supplied by the manufacturers. Lubricants No. 2 and 4 in Table 4-1 have been used in the bearing testing described in Section 7.

4.3 LUBRICANT FILM THICKNESS

The elastohydrodynamic (EHD) film thickness h at each ball-race contact is computed as the product of the film thickness predicted by the Archard-Cowking formula {11} and two reduction factors ϕ_t and ϕ_s . The factors ϕ_t and ϕ_s account respectively for the reduction in film thickness due to heating in the contact inlet and the decrease in film due to lubricant starvation i.e. due to the finiteness of the distance between the contact zone and the inlet oil meniscus. In equation form,

$$h = \phi_t \cdot \phi_s \cdot h_{a.c.} \quad (4-7)$$

TABLE 4-1

LUBRICANT PROPERTIES OF FOUR OILS USED IN PROGRAM AT74Y001

Oil No.	Oil Type	Kinematic Viscosity, 100°F	(cs) 210°F	Walther Equation Constants A	B	Density @ 60°F gm/cm ³	Thermal Conductivity Kf Btu/Hr/Ft/°R	Thermal Coeff. of Expansion β (OR-1)	Temp. Viscosity Coeff.
1	Mineral Oil	64	8.0	10.349	3.673	0.8800	0.0671	3.52×10^{-4}	0.0193
2	MIL-L-7808G	12.8	3.2	10.215	3.698	0.9526	0.0879	3.94×10^{-4}	0.0132
3	C-Ether	25.4	4.13	11.452	4.113	1.201	0.0690	4.15×10^{-4}	0.0168
4	MIL-L-23699	28.0	5.1	10.207	3.655	1.010	0.0879	4.14×10^{-4}	0.0161

The Archard-Cowking film thickness formula takes the following form

$$h_{a.c.} = 2.04 \left[1 + \frac{2R_x}{3R_y} \right]^{-0.93} (\alpha n v)^{0.740} R^{0.407} (Q/E')^{-0.074} \quad (4-8)$$

where

R_x, R_y - effective radii of curvature parallel and transverse to the rolling direction respectively

α - pressure viscosity coefficient

V - lubricant entrainment velocity

$$R = \left[R_x^{-1} + R_y^{-1} \right]^{-1}$$

Q - load

$$E' = 2 \left(\frac{1 - \nu_1^2}{E_1} + \frac{1 - \nu_2^2}{E_2} \right)^{-1}$$

η = absolute viscosity

E_1, E_2 - Young's modulus for the contacting bodies

ν_1, ν_2 - Poisson's ratio for the contacting bodies

4.3.1 Inlet Heating Factor ϕ_t

A Grubin type inlet film thickness analysis considering full thermal effects was developed for line contact by Cheng {1}. Results presented in {1} covering wide ranges of loads, speeds and lubricant parameters were used to develop regression formulas for the thermal reduction factor ϕ_t .

Based on 28 sets of data, each containing 15 data points, from the analysis of Cheng, the regression formulas obtained take the following form:

$$\phi_t = e^{x_0} \quad (4-9)$$

where

$$1) \ x_0 = -0.3011 - 0.00432 \ln(p_0/E') - 0.03469 \ln(1+S) \\ - 0.16423 \ln Q_m - 0.01728 (\ln Q_m)^2 + 0.00389 \ln \alpha' \\ - 0.06316 \ln \beta' \\ \text{for } 0 < Q_m < 0.1, \beta' > 11.5 \text{ and } 0 < Q_m < 0.4, \beta' < 11.5$$

$$2) x_o = -1.119304 - 0.16192 \ln (p_o/E') - 0.0895 \ln (1+S) \\ - 0.29 \ln Q_m - 0.04572 (\ln Q_m)^2 + 0.13615 \ln \alpha' \\ - 0.31614 \ln \beta' \\ \text{for } 0.1 < Q_m < 1, \beta' > 11.5 \text{ and } 0.4 < Q_m \leq 1, \beta' < 11.5$$

$$3) \text{ and } x_o = -3.66426 - 0.48511 \ln (p_o/E') + 0.00568 \alpha' \\ - 0.05491 \beta' - 0.1678 \ln (1+S) - 0.19573 \ln Q_m \\ - 0.09392 \cdot (\ln Q_m)^2 + 0.20908 \cdot \ln \alpha' \\ \text{for } Q_m > 1$$

$$\text{where, } \alpha' = \frac{\pi}{2} \alpha p_o$$

$$\beta' \approx \beta t$$

$$S = (u_2 - u_1)/2V$$

$$Q_m = 2 V^2/K_f t_o$$

- α - pressure viscosity coefficient, in^2/lb
- b - half of Hertzian width in the rolling direction, in
- p_o - maximum Hertz pressure, lb/in^2
- β_o - temperature viscosity coefficient, $^{\circ}\text{R}^{-1}$ computed via Eq. (4-6)
- t - ambient temperature, $^{\circ}\text{R}$
- η - ambient viscosity, $(\text{lb} \cdot \text{sec}/\text{in}^2)$

u_1, u_2 - surface velocity of bodies No. 1 and 2, (relative to the contact) in/sec

K_f - conductivity of the film ($\text{lb}/^{\circ}\text{F} \cdot \text{sec}$)

V - $(u_1 + u_2)/2$, lubricant entrainment velocity (in/sec)

It is noted that for small values of Q_m , ϕ_t computed from Eq. (4-9) may be larger than unity. $\phi_t = 1.0$ is used whenever the value computed using Eq. (4-9) is larger than 1.0.

In evaluating ϕ_t for the elliptical point contacts in a ball bearing, p_o is taken to be the maximum of the Hertzian pressure ellipse.

The point contact is thus treated as if it were a line contact having a maximum contact pressure p_o along its entire length of contact. This is a conservative approximation inasmuch as it will tend to underestimate ϕ_t and hence underestimate film thickness. In any case the magnitude of the error is small as p_o is not a highly influential variable in ϕ_t .

4.3.2 Starvation Reduction Factor ϕ_s

A hydrodynamic analysis of an elliptical point contact having two equivalent principal radii of curvature R_x and R_y (parallel and transverse to the rolling direction, respectively) was conducted by considering finite thicknesses of half films ($h_{1,1}$ and $h_{1,2}$) upstream from the inlet and setting the flow rate in the center plane at the meniscus line equal to the incoming flow rate at the contact centerline. The complete analysis is given in {5} and {12}.

Figure 4-1 shows the geometry considered. h_s and r^* denote respectively the starved plateau film thickness and the meniscus distance from the contact center along the direction of rolling. u_1 and u_2 are the velocities with which the ambient film layers move toward the contact zone.

The analysis shows h_s and r^* to be related to h_1 , the sum of the upstream ambient film layer thicknesses, ($h_1 = h_{1,1} + h_{1,2}$) through the following two equations:

$$\frac{5.5V\eta\alpha R_x^{1/2}}{h_s^{3/2}(3+2k)} - \frac{12V\eta\alpha r^*}{(3+2k)(h_s + r^{*2}/2R_x)^2} = 1.0 \quad (4-10)$$

$$\text{and } h_1 = \frac{2(2+k)}{3+2k} \cdot (h_s) + \frac{kr^{*2}}{(3+2k)R_x} \quad (4-11)$$

where $k \equiv R_x/R_y$, η is the dynamic viscosity of oil at the contact inlet, α the pressure-viscosity coefficient and $V \equiv (\frac{u_1+u_2}{2})$

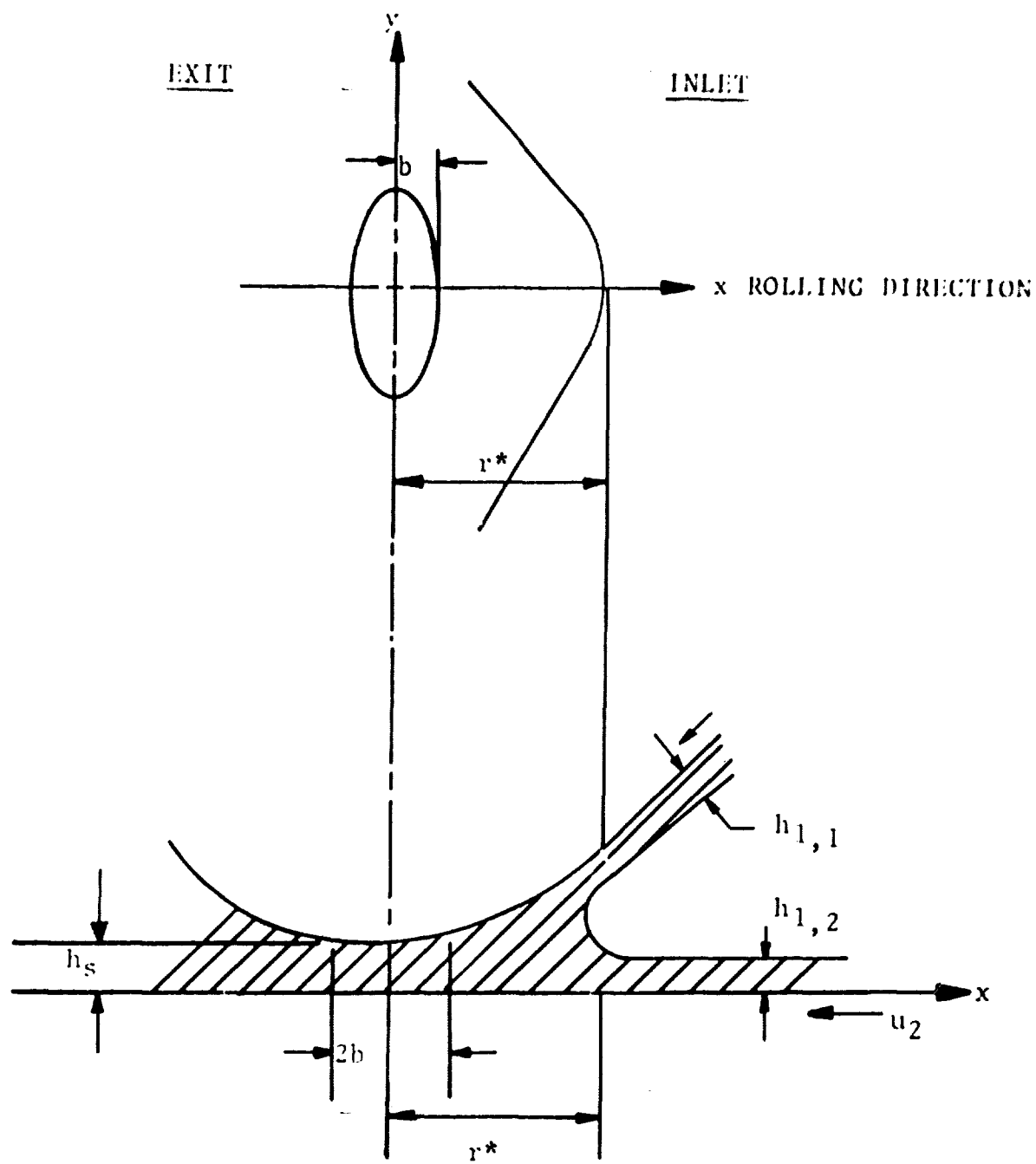
is the entrainment velocity in the x-direction.

The simultaneous solution of Eqs. (4-10) and (4-11) for given values of R_x , R_y , V , η , α and h_1 yields the associated values of h_s and r^* . Subroutine STARFC performs this calculation.

As the meniscus distance r^* increases, the film thickness h_s increases, asymptotically approaching a value h_f as $r^* \rightarrow \infty$. Therefore, h_f is the film thickness under fully flooded conditions.

On letting $r^* \rightarrow \infty$ and $h_s \rightarrow h_f$ in Eq. (4-10), the second term on the left hand side vanishes and one may solve for h_f as

$$h_f = \left[\frac{5.5V\eta\alpha(R_x)^{1/2}}{(3+2k)} \right]^{2/3} \quad (4-12)$$



$$h_1 = h_{1,1} + h_{1,2}$$

FIGURE 4-1
FILM GEOMETRY

Subroutine STARFC evaluates h_f from Eq. (4-12) and then calculates the ratio $\phi_s = h_s/h_f$. h_f as given by Eq. (4-12) does not indicate a dependence upon load. This is characteristic of film thickness formulas derived from a Grubin type assumption applied to rigid bodies (cf. (11)). It was considered preferable to use the Archard-Cowking formula for the unstarved case rather than h_f since the Archard-Cowking formula better describes the dependence of film thickness upon the influential physical variables. The only role played by h_f is to scale h_s to yield the ratio ϕ_s , which is applied as a multiplicative factor on the Archard-Cowking prediction of unstarved film thickness.

4.3.3 Film Replenishment

As noted above it is necessary to know the combined oil layer thickness h_l in order to calculate ϕ_s and r^* .

As a rolling element passes a point on the inner or outer raceway of a bearing, a very thin lubricant film remains on each of the components and is of the same order of magnitude as half the plateau film thickness in the EHD contact. Replenishment of the lubricant layer on the raceway is required in order to assure sufficient lubricant in the inlet region of the succeeding contact, so that the EHD film thickness will be the same as in the preceding contact. If replenishment fails to occur, each successive rolling element pass would have a thinner EHD film and steady state operation with EHD lubrication would not be possible.

Many mechanisms serve to replenish the lubricant in the track of a high speed bearing. Of prime concern is replenishment at the inner race in high speed ball bearings since centrifugal force tends to direct free fluid away from that surface. Seven replenishment mechanisms have been identified:

- 1) Centrifugal flinging of the lubricant from the ball
- 2) Centrifugal travel of oil along the surface
- 3) Random splashing of lubricant in the bearing cavity
- 4) Direct deposition from a jet
- 5) Back flow along the surface into the track, from its edges resulting from lubricant surface tension
- 6) Carrying into the contact, of lubricant adhering to the ball

Subroutine STARFC evaluates h_f from Eq. (4-12) and then calculates the ratio $\phi_s = h_s/h_f$. h_f as given by Eq. (4-12) does not indicate a dependence upon load. This is characteristic of film thickness formulas derived from a Grubin type assumption applied to rigid bodies (cf. (11)). It was considered preferable to use the Archard-Cowking formula for the unstarved case rather than h_f since the Archard-Cowking formula better describes the dependence of film thickness upon the influential physical variables. The only role played by h_f is to scale h_s to yield the ratio ϕ_s , which is applied as a multiplicative factor on the Archard-Cowking prediction of unstarved film thickness.

4.3.3 Film Replenishment

As noted above it is necessary to know the combined oil layer thickness h_l in order to calculate ϕ_s and r^* .

As a rolling element passes a point on the inner or outer raceway of a bearing, a very thin lubricant film remains on each of the components and is of the same order of magnitude as half the plateau film thickness in the EHD contact. Replenishment of the lubricant layer on the raceway is required in order to assure sufficient lubricant in the inlet region of the succeeding contact, so that the EHD film thickness will be the same as in the preceding contact. If replenishment fails to occur, each successive rolling element pass would have a thinner EHD film and steady state operation with EHD lubrication would not be possible.

Many mechanisms serve to replenish the lubricant in the track of a high speed bearing. Of prime concern is replenishment at the inner race in high speed ball bearings since centrifugal force tends to direct free fluid away from that surface. Seven replenishment mechanisms have been identified:

- 1) Centrifugal flinging of the lubricant from the ball
- 2) Centrifugal travel of oil along the surface
- 3) Random splashing of lubricant in the bearing cavity
- 4) Direct deposition from a jet
- 5) Back flow along the surface into the track, from its edges resulting from lubricant surface tension
- 6) Carrying into the contact, of lubricant adhering to the ball

- 7) Back flow into the gap behind the contact exit due to vacuum in the cavitated area.

A model has been constructed for item 5) above, in {5}, and {12} and a concept is advanced in Sect. 4.3.4 below for applying it to a full scale bearing. In view of the other, possibly more influential sources of replenishment enumerated above, this model has not been adopted in this program. Instead it is assumed that an externally supplied replenishment amount $\Delta\zeta$ adds to the plateau film thickness to yield h_1 .

As a simplification since $\Delta\zeta$ is usually much larger than h the approximation $h \sim h_s$ is used so that,

$$h_1 = h_s + \Delta\zeta \quad (4-13)$$

Subroutine STARFC uses Eq. (4-13) in solving Eqs. (4-10) and (4-11), with a user specified $\Delta\zeta$ value.

4.3.4 Film Replenishment Model for a Full Scale Bearing

As mentioned above a model has been developed as summarized in {5} and {12} to compute the increment $\Delta\zeta$ due to replenishment via the fluid's surface tension. The model postulates that the ambient oil layer away from the rolling track has a known thickness h_∞ .

Since h_∞ is itself generally unknown the approach has been adopted for the present, to use values of $\Delta\zeta$ directly as input in developing the computer program for predicting bearing performance.

A plausible procedure for applying the replenishment model to a full scale bearing has been conceived however and is outlined as follows:

Assume that due to oil flinging under a centrifugal force field, the bearing outer ring groove becomes full of oil and the inner ring groove becomes dry. In this case when a ball passes a given point on the outer ring the entire groove cavity not swept out by the ball, up to the edge of the flange, will be full of oil as shown below:

- 7) Back flow into the gap behind the contact exit due to vacuum in the cavitated area.

A model has been constructed for item 5) above, in {5}, and {12} and a concept is advanced in Sect. 4.3.4 below for applying it to a full scale bearing. In view of the other, possibly more influential sources of replenishment enumerated above, this model has not been adopted in this program. Instead it is assumed that an externally supplied replenishment amount $\Delta\zeta$ adds to the plateau film thickness to yield h_1 .

As a simplification since $\Delta\zeta$ is usually much larger than h the approximation $h \sim h_s$ is used so that,

$$h_1 = h_s + \Delta\zeta \quad (4-13)$$

Subroutine STARFC uses Eq. (4-13) in solving Eqs. (4-10) and (4-11), with a user specified $\Delta\zeta$ value.

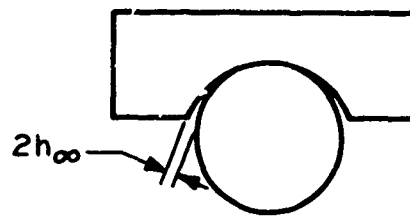
4.3.4 Film Replenishment Model for a Full Scale Bearing

As mentioned above a model has been developed as summarized in {5} and {12} to compute the increment $\Delta\zeta$ due to replenishment via the fluid's surface tension. The model postulates that the ambient oil layer away from the rolling track has a known thickness h_∞ .

Since h_∞ is itself generally unknown the approach has been adopted for the present, to use values of $\Delta\zeta$ directly as input in developing the computer program for predicting bearing performance.

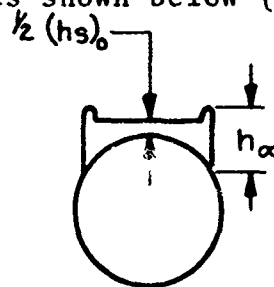
A plausible procedure for applying the replenishment model to a full scale bearing has been conceived however and is outlined as follows:

Assume that due to oil flinging under a centrifugal force field, the bearing outer ring groove becomes full of oil and the inner ring groove becomes dry. In this case when a ball passes a given point on the outer ring the entire groove cavity not swept out by the ball, up to the edge of the flange, will be full of oil as shown below:



h_∞ as thus defined may be readily calculated for a given bearing geometry and ball load.

It may be further assumed that as the ball rotates from the outer to inner ring contact, it has an oil layer clinging to it as shown below (exaggerated)



Using the same value of h_∞ as used for the outer ring, one may apply the replenishment model to determine the ball replenishment $(\Delta\zeta)_b$ during the time interval it takes the ball to rotate from the outer ring contact to the inner ring contact.

Since the oil replenishment on the inner ring groove is assumed negligible, h_1 at the inner ring contact will be simply $h_1 = \frac{1}{2}(h_s)_i + \frac{1}{2}(h_s)_o + (\Delta\zeta)_b$ from which the inner ring film thickness may be computed via the starvation model. The inlet layer thickness at the outer ring contact will be $h_1 = \frac{1}{2}(h_s)_i + (\Delta\zeta)_b + \frac{1}{2}(h_s)_o + (\Delta\zeta)_o$ from which the outer ring film thickness $(h_s)_o$ is calculated as previously described.

A computer program has been developed to perform the calculation outlined above and was applied and gave reasonable results for the conditions of one of the tests run with a 125mm bore bearing in the full scale test phase of this program. These results are discussed further in Sections 7 and 8.

4.4 TRACTION IN BALL-RACE CONTACTS

The traction model developed for use in program AT74Y001 is applicable to the partial EHD regime in which the lubricant film separating the contacting surfaces may be small enough to permit some degree of asperity contact. The model computes the traction coefficient as a function of the ratio h/σ of film thickness h to composite surface roughness σ . For small values of h/σ ($h/\sigma < 1$) the model reduces to a coulomb friction model, i.e. the traction coefficient becomes a constant μ_a , independent of sliding rate. For large values of h/σ ($h/\sigma > 3$) the model becomes a non-Newtonian semi-empirical fluid film

model in which the traction coefficient, μ_{EHD} , depends upon sliding rate, as well as the load, rolling speed and lubricant properties at operating temperature. For intermediate values of h/σ the model is a combination of coulomb and fluid film friction. Details of the model development are contained in {2}, {5} and {6}. Essential features of the model are described below.

4.4.1 Asperity Traction Model

If Q is the total load applied to a contact (or to a suitable subelement of a contact), a portion of this load, designated Q_a will be carried by elastically deformed asperities and the remaining, $Q - Q_a$, will be carried by the EHD film. The traction force T_s then is,

$$T_s = \mu_a Q_a + \mu_{EHD} (Q - Q_a) \quad (4-14)$$

Under the assumption that the rough surface consists of two-dimensional ridges of random height and slope angle, the average asperity borne load Q_a is the following function of the ratio h/σ .

$$Q_a = \frac{E'}{4\pi^2} A \sigma_\theta I(h/\sigma, \alpha) \quad (4-15)$$

where

$$E' = 2 \left(\frac{1-\nu_1^2}{E_1} + \frac{1-\nu_2^2}{E_2} \right)^{-1}$$

E_1, E_2 = Young's moduli of the contacting bodies
 A = contact area

σ_θ = RMS value of the distribution of asperity slope angles (radians)

$I(h/\sigma, \alpha)$ = A function defined in {'} of the film parameter h/σ and a statistical micro-geometry parameter σ defined in Nayak {13}.

It is shown in {6} that $\alpha = 2$ is a reasonable value to use for rolling bearing surfaces. The following polynomial fit to the function $I(h/\sigma, \alpha = 2.0)$ is used in computation:

$$I(h/\sigma, 2) = 2.31e^{-1.84 h/\sigma} + 0.1175(h/\sigma - 0.4)^{0.6}(2-h/\sigma)^2;$$

$$0.4 \leq h/\sigma \leq 2 \quad (4-16)$$

$$I(h/\sigma, 2) = 17e^{-2.84 h/\sigma} + 1.44 \times 10^{-4} (h/\sigma - 2)^{1.1} (4 - h/\sigma)^{7.8};$$

$$2 < h/\sigma$$

The value $\mu_a = 0.1$ was recommended in {6} as being consistent with values deduced in traction measurements in the partial EHD regime. Any other value of μ_a may be specified at input however (cf. Section 5).

4.4.2 Fluid Traction Coefficient μ_{EHD} ---

The general behavior of the fluid traction coefficient μ_{EHD} as a function of sliding rate is illustrated by the curves in Fig. (4-2). (Throughout Section 4.4.2 the subscript on μ_{EHD} will be omitted.)

In the curve in Fig. (4-2a) the traction coefficient increases linearly, at low sliding speeds, reaches a maximum $\mu = \mu^*$ at speed $u_s = u_s^*$, and decreases thereafter.

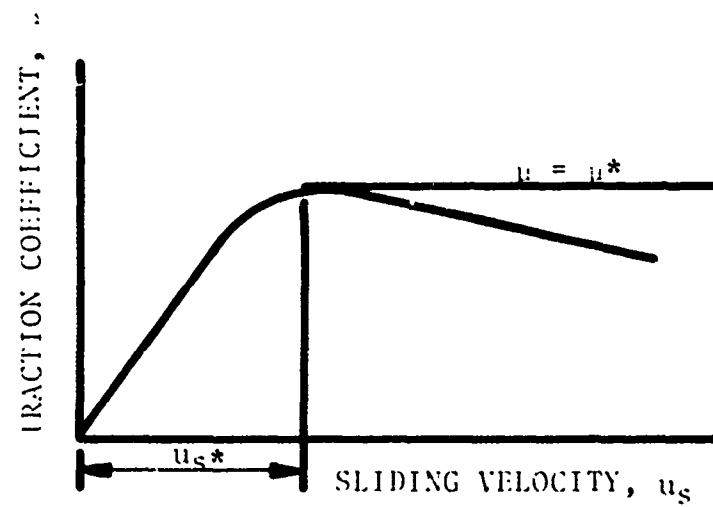
In the curve in Fig. (4-2b) the traction coefficient increases linearly at low sliding speeds and then approaches an asymptotic value μ^* .

Both types of traction curves have been experimentally observed. Both signify a departure from isothermal Newtonian fluid behavior since for this situation the traction coefficient increases linearly with sliding speed at all sliding speeds.

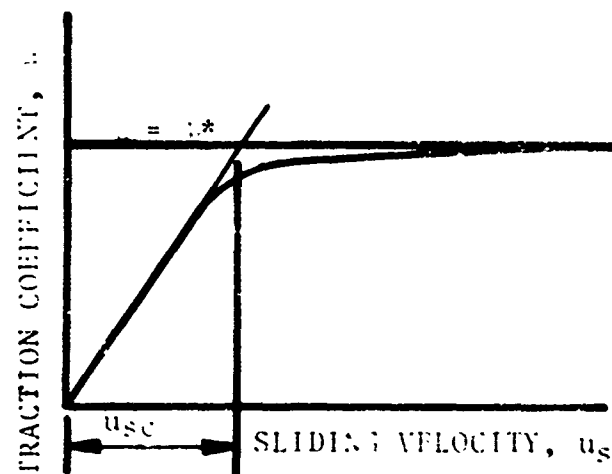
For the curve of Fig. (4-2b), μ^* denotes the asymptotic traction coefficient. Define $u_s^* = 3 \times u_{sc}$, where u_{sc} is the sliding speed at which the line $\mu = \mu^*$ intersects the extended linear portion of the curve μ vs. u_s .

It has been found that μ^* for either type of curve increases with the contact pressure and decreases with rolling velocity and lubricant viscosity (and hence ambient temperature); μ_s^* on the other hand decreases with pressure and increases with rolling velocity and viscosity. This joint variation has been found to result in a scale change in the two axes but not in a substantial change in the character of the traction curve.

This means that traction curves obtained under widely different conditions of pressure, rolling velocity and temperature when plotted on a grid with coordinates $\mu_r \equiv \mu/\mu^*$ and $x \equiv u_s/u_s^*$, yield substantially the same curve {5,6}.



a) A CURVE EXHIBITING A PEAK



b) A CURVE EXHIBITING ASYMPTOTIC BEHAVIOR

FIGURE 4-2
TYPICAL TRACTION CURVES

A characteristic of the curves of the type of Fig (4-2a) is that μ_r decreases indefinitely with large x . Curves of this type can cause convergence difficulties in a bearing dynamics computer program because there are two sliding speeds associated with each value of the traction coefficient. The computer may cycle between the two values in seeking to find an equilibrium condition.

An approach to avoiding this difficulty is to use a monotonically increasing curve that is a good match to the actual curve over the increasing portion of that curve. If the program then converges at a sliding speed that is within the range where the curves match, the solution is valid.

A useful monotonic functional form for fitting the ascending portion of traction curves has been devised. It is linear up to a certain sliding speed, after which it increases nonlinearly to an asymptotic value. In the present context i.e. using relative traction and sliding speed values μ_r and u_s the curve has the following form:

$$\mu_r = \frac{(\mu_r)_B}{X_B} \cdot X; \quad X \leq X_B$$

$$\mu_r = (\mu_r)_B + (\mu_r)_B \left[\frac{\{1 - (\mu_r)_B\} (X - X_B)}{\{1 - (\mu_r)_B\} X_B + (\mu_r)_B (X - X_B)} \right]; \quad X > X_B \quad (4-17)$$

The parameters $(\mu_r)_B$ and x_B are simply the coordinates of the point at which the curve becomes nonlinear. The fit is continuous and has a continuous first derivative at $x = x_B$. As $x \rightarrow \infty$, $\mu_r \rightarrow 1.0$. Fig. (4-3) illustrates the form of this approximation drawn for the case $(\mu_r)_B = 0.68$ and $x_B = 0.25$.

For a given oil, the maximum traction coefficient μ^* has been found (5) to vary with pressure, viscosity, rolling velocity, and film thickness in the following manner:

$$\mu^* = f(p_0)^{0.61} p_0^{-1.14} \eta^{0.59} \lambda^{0.48-0.61\lambda} h^{-0.45} \quad (4-18)$$

where

- p_0 = the maximum contact pressure (lb/in²)
- h = plateau EHD film thickness (in)
- $f(p_0)$ = a function governing the dependence of viscosity on pressure p_0 (oil parameter)
- λ = a visco-elastic constant (oil parameter)

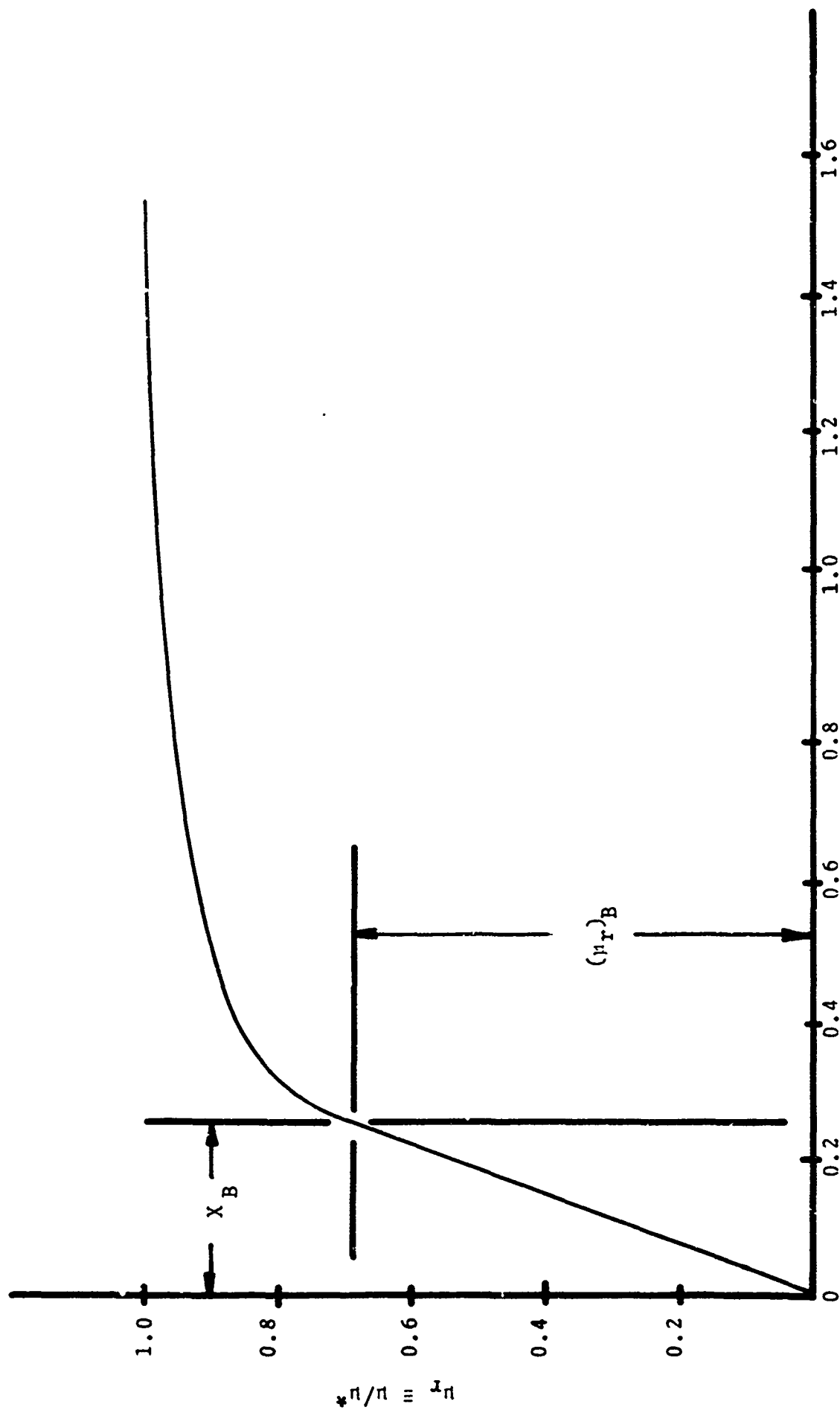


FIGURE 4-3
 $x \equiv u_s / u_s^*$

μ_r vs. x

$$*n/n \equiv I_n$$

Similarly u_s^* exhibits the following dependence on p_0, η_0, V and h .

$$u_s^* \sim p_0^{(-0.14)} f(p_0)^{(-0.40)} \eta^{(-1.1)} V^{(0.40\lambda - 0.09)} h^{(0.55)} \quad (4-19)$$

The quantities μ^*, μ_s^* and h can be measured experimentally for a set of given values of p_0, η , and V . For the oils thus far examined the function $f(p_0)$ has been found to follow a law of the form, {6,7}

$$\begin{aligned} f(p_0) &\sim (p_0/p_1)^{A_1} && \text{for } p_0 < p_1 \\ &\sim (p_0/p_1)^{A_2} && \text{for } p_0 > p_1 \end{aligned} \quad (4-20)$$

where A_1, A_2 and p_1 are lubricant dependent constants. Values of A_1, A_2 and p_1 for four oils are listed in Table 4-2. The procedure for determining these values for other oils is given in {6,7}.

Making use of Eq. (4-20), Eqs. (4-18) and (4-19) can be expressed in the following form on introducing C_1 and C_2 as proportionality constants.

$$\mu^* = C_1 p_0^{-1.14} \cdot (p_0/p_1)^{0.61A_i} \cdot \eta^{(0.59)} \cdot V^{(0.48-0.61\lambda)} \cdot h^{-0.45} \quad (4-21)$$

$$u_s^* = C_2 p_0^{-0.14} \cdot (p_1/p_0)^{0.4A_i} \cdot \eta^{(-1.1)} \cdot V^{(0.40\lambda-0.09)} \cdot h^{0.55} \quad (4-22)$$

$i = 1, 2$

The values of C_1 and C_2 are evaluated by substituting measured μ^*, u_s^* and h values for a specific test condition. Then knowing values of C_1, C_2, p_1, A_i and h (starved), it is possible to predict values of μ^* and u_s^* as functions of the operating parameters p_0, V , and η by Eqs. (4-21) and (4-22). Values for C_1 and C_2 thus calculated for four oils are tabulated in Table 4-2. The units in Eqs. (4-21) and (4-22) are V (in/sec), η (cp), p_0 (ksi) and h (microinches). Also shown in Table 4-2 are the values of $(\mu_T)_B$ and x_B used for the four oils. These data have been preprogrammed into program AT74Y001. For other lubricants a user may input the parameter values for a traction sliding speed curve of the general form of Eq. (4-17). (See Section 5.3.8.)

In summary, the calculation of μ_{EHD} at a given sliding velocity u_s and for a given pressure p_0 , film thickness h , rolling velocity V and temperature t , proceeds as follows:

1. Calculate viscosity η at temperature t .
2. Using appropriate constants from Table 4-2, calculate μ_s^* and μ^* for given p_0 , h , V and $\eta(t)$
3. Calculate $x = u_s / u_s^*$
4. Use Eq. (4-17) with values of $(\mu_r)_B$ and x_B from Table 4-2 to calculate μ_r associated with the value of x calculated in step 3.
5. Compute $\mu_{EHD} = \mu_r \cdot \mu^*$

4.4.3 Computing Traction Force for a Hertzian Contact

In computing the traction force acting at a ball-race contact, the elliptical Hertzian contact zone is divided into a large number (21) of slices parallel to the minor axis. The tractive force is computed for each slice and then summed to give the total traction.

Figure (4-4a) shows a Hertzian contact area with the semi-elliptical distribution of pressure due to elastic deformation (Effects of the lubricant on the pressure distribution are neglected) and a local coordinate system established at the contact center.

By considering sufficiently many slices (21 are used in the program) the variation of pressure in the x direction over a slice width may be neglected, i.e. each slice is regarded as the contact zone due to a cylindrical disk (without edge effects).

Sliding velocities at a typical slice are shown in Fig. (4-4b). A sliding velocity in the x direction results if the ball auto rotational vector has a component ω_z (cf. Fig. (3-1)). The sliding velocity u_{sx} is always equal for all slices.

Because of groove curvature the sliding velocity component u_{sy} will vary from slice to slice across the contact ellipse.

Fig. (4-4c) shows the traction components T_x and T_y on the slice, as computed individually using the partial EHD traction model of Eq. (4-1). i.e. T_x depends upon u_{sx} and the load, rolling velocity and film thickness to surface roughness ratio. T_y similarly depends on u_{sy} and the other variables. T indicates the resultant for the given slice. The forces T_x and T_y are computed for each slice and summed to give the components of the total traction force acting at the contact.

TABLE: 4-2

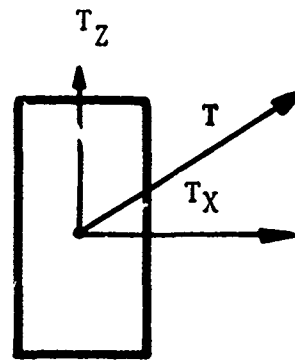
TABULATION OF CONSTANTS FOR FOUR OILS

Oil No.	Oil Type	λ	A_1	A_2	$P_1 \times 10^5$	C_1	C_2	$(\mu_r)B$	x_B
1	Mineral (1) Oil	0.3	3.42	2.14	1.5	1.8	115.9	0.65	0.10
2	MIL-L-7808(2)	0.94	4.08	1.48	1.7	17.6	39.0	0.68	0.25
3	SP4E (3)	0.70	3.29	1.50	1.7	26.2	6.6	0.65	0.15
4	MIL-L-23699(2)	0.93	6.88	3.44	2.2	10.4	47.3	0.68	0.25

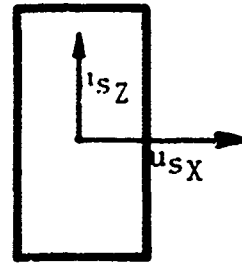
69

NOTES:

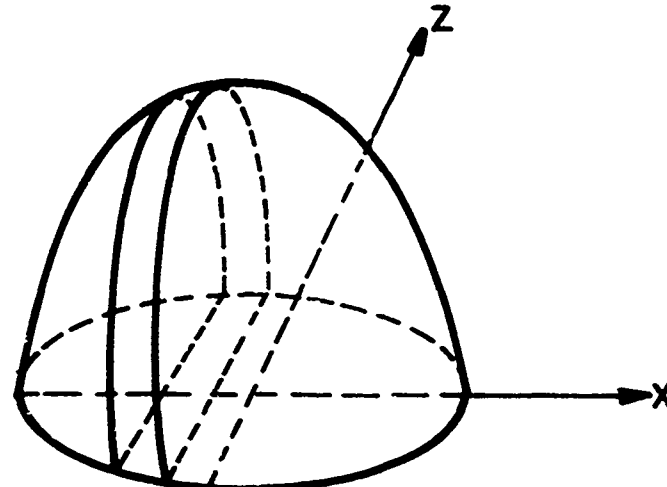
- (1) obtained from Traction Data reported by Johnson and Cameron (14)
 (2) S K F tests
 (3) obtained from Traction Data reported by Smith et al (15)



c. TRACTION COMPONENTS AND THEIR RESULTANTS AT A TYPICAL SLICE



b. SLIDING VELOCITIES ON TYPICAL SLICE



a. CONTACT ELLIPSE AND PRESSURE DISTRIBUTION

4.5 CALCULATION OF CAGE POCKET NORMAL FORCES

A means for calculating the cage driving forces due to the balls was developed in {6}. In this development, the normal force exerted by a ball on the cage pocket, is presumed to act in the plane of rotation through the cage pocket midpoint.

The analysis is applied to determine the normal forces acting at two diametrically opposite points on a ball; the points of nearest and furthest approach of the ball relative to the cage. The net normal force acting on the ball is the resultant of the two forces acting at the diametrically opposite points.

The ball pockets are assumed to be cylindrical cavities of radius r' , oriented radially such that the axis of each cylinder passes through the fixed origin of the bearing inertial frame (Fig. 3-1).

The geometry is shown in Fig. (4-5). z_c denotes the offset between the ball and cage pocket centers in the direction of rolling. ω_x and ω_y denote the components of the ball rotational velocity vector that cause relative slip between the ball and cage pocket at the point of closest approach. The magnitude of the closest approach is h_0 . h_0 is the minimum film thickness when the cage is lubricated.

In the bearing analysis program, AT74Y001, it is required at several points during the iterative solution procedure that the ball cage pocket eccentricity z_c be assumed and the associated cage pocket load Q_3 be calculated. When z_c is small the load is small and borne hydrodynamically by the lubricant film, which then has minimum thickness $h_0 = r' - r - z_c$. In this regime, the load for a given value of the ball and the cage pocket clearance is that supported by a point hydrodynamic contact of minimum thickness h_0 . Elastic deformation is negligible in this regime. As z_c increases, h_0 decreases until it reaches a critical value h_c , below which a further increase in z_c results in joint elastic deformation but no further decrease in film thickness. In this regime

$$h = h_c \quad (4-23)$$

and the elastic deformation is calculated from,

$$\delta_e = z_c + h_c - C_r \quad (4-24)$$

where C_r is the cage pocket radial clearance ($r' - r$).

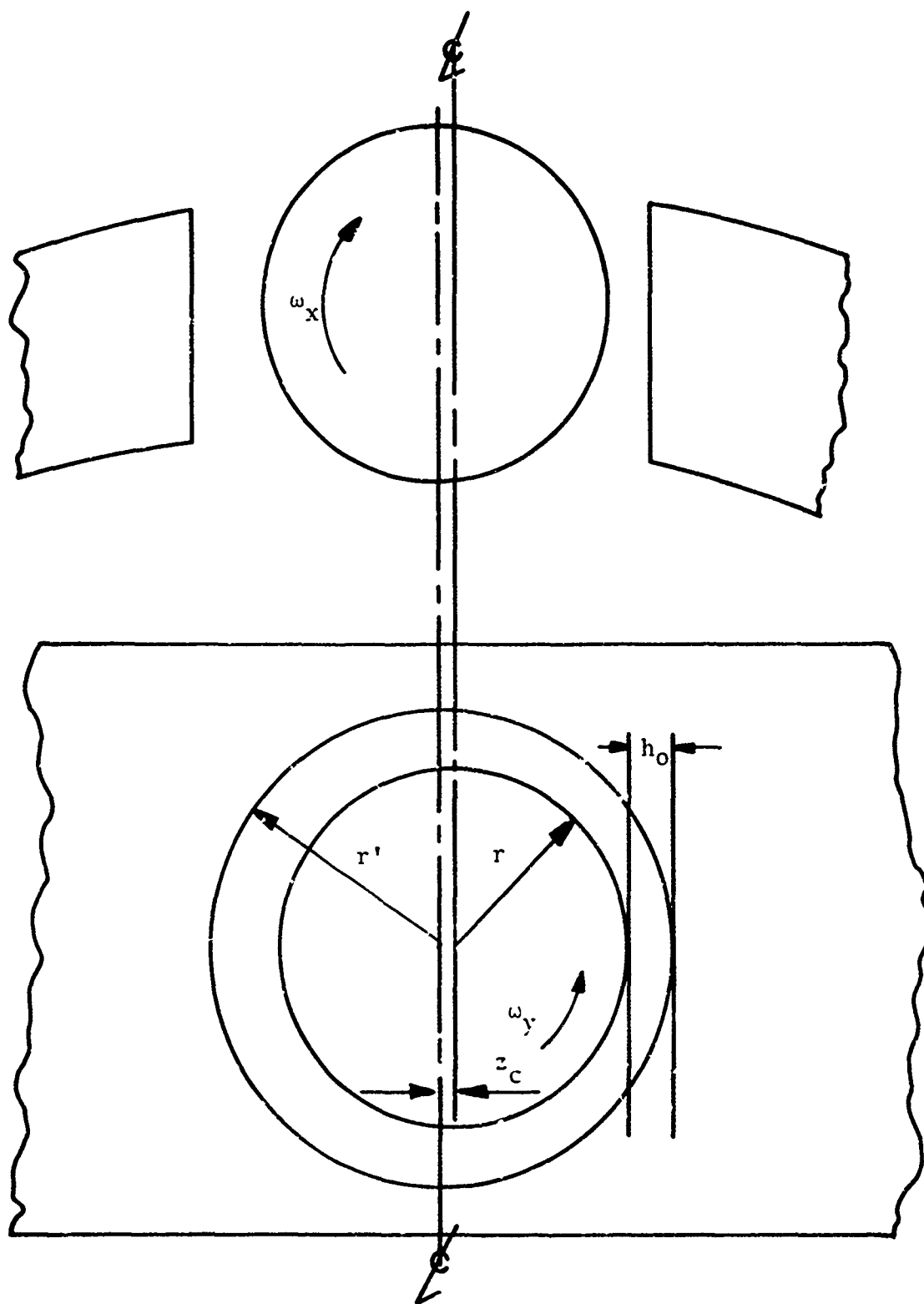


FIGURE 4-5
CAGE POCKET GEOMETRY

The load Q_3 in this case is assumed to be the sum of the load Q_c hydrodynamically related to the film thickness h_c , and an additional load Q_e associated with the elastic deformation through the Hertzian equations of contact elasticity.

An analysis was performed as described in { 6 }, of the relationship between normal load Q and minimum film thickness h_o in a lubricated point contact between two rigid bodies each having two principal radii of curvature, assuming that the lubricant viscosity increases exponentially with pressure. The analysis yielded a relationship between the nondimensional load parameter \bar{Q} and the nondimensional film thickness parameter \bar{H} , as shown by the solid curve in Figure 4-6. These nondimensional variables are defined as:

$$\bar{Q} = Q (\alpha R_y / C_o^2)^{1/3} (R_x R_y)^{-1/2} = Q \cdot D \quad (4-25)$$

$$\bar{H} = h_o R_x (C_o R_x^\alpha)^{-2/3} = \frac{h_o}{C_r} \cdot B \quad (4-26)$$

where:

$$C_o = \eta V_y (R_x R_y)^{1/2} k_1 \quad (4-27)$$

$$k_1 = \left[(3 + 2k)^{-2} + (3 + 2k^{-1})^{-2} k^{-1} \left(\frac{V_x}{V_y} \right)^2 \right]^{1/2} \quad (4-28)$$

$$k \equiv R_y / R_x \quad (4-29)$$

$$D \equiv (\alpha R_y / C_o^2)^{1/3} (R_x R_y)^{-1/2} \quad (4-30)$$

$$B \equiv C_r R_x (C_o R_x^\alpha)^{-2/3} \quad (4-31)$$

$$R_x = \left(\frac{1}{r} - \frac{1}{r'} \right)^{-1} \frac{r^2}{C_r} \quad (4-32)$$

$$R_y = r$$

$$C_r = r' - r, \text{ cage pocket radial clearance}$$

$$V_x = \frac{1}{2} \omega_y r$$

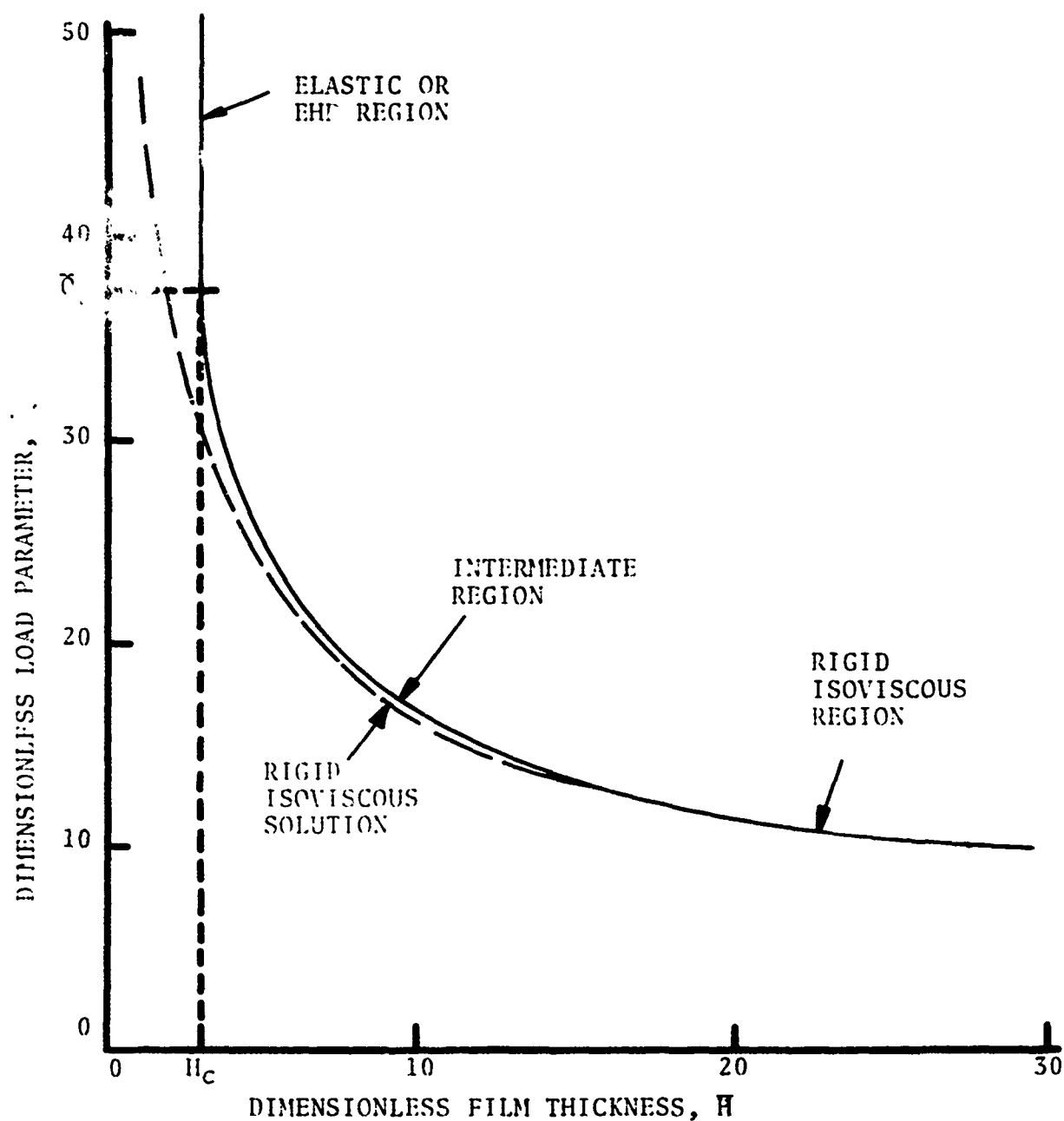


FIGURE 4-6

LOAD CAPACITY VS. FILM THICKNESS FOR
HYDRODYNAMIC AND ELASTOHYDRODYNAMIC OPERATING REGIMES

η = ambient dynamic viscosity

$$V_y = -\frac{1}{2} \omega \frac{r}{x}$$

It has been found that the relationship between \bar{Q} and \bar{H} for an unstarved point contact can be approximated by the following formula.

$$\bar{Q} = 53.3 (\bar{H})^{-\frac{1}{2}} + 163(\bar{H})^{-3} \quad (4-33)$$

provided that

$$\bar{Q} < \bar{Q}_c = 37.6$$

4.5.1 Elastohydrodynamic (EHD) Contact

For $\bar{Q} > 37.6$, the film thickness is independent of load and the nondimensional parameter H remains constant at H_c . Operation in this case is in the EHD region.

$$\bar{H} = \bar{H}_c = 3.122 \quad (4-34)$$

for EHD Contact

$$\bar{Q} \geq \bar{Q}_c = 37.6 \quad (4-35)$$

Equations (4-25) and (4-26) result in the following for the EHD region of operation,

$$Q = \bar{Q}_c/D = 37.6/D \quad (4-36)$$

$$h_o = h_c = 3.122 C_r/B \quad (4-37)$$

The elastic deformation δ_e is given by,

$$\delta_e = z_c + h_c - C_r \quad (4-38)$$

$Q_e (\delta_e)$ is calculated according to Hertz theory. In performing this calculation in Program AT74Y001 the axis ratio of the elliptical contact area is taken at a representative value of 9.0 corresponding to $C_r = 0.033 r$. The total ball-cage contact load Q_3 is thus:

$$Q_3 = Q_c + Q_e (\delta_e) \quad (4-39)$$

4.5.2 Hydrodynamic (HD) Contact

If the contact film thickness h_o is greater than the critical value h_c , the contact is assumed to be hydrodynamic:

$$\bar{H} \geq \bar{H}_c = 3.122 \text{ for HD contact}$$

The minimum film thickness for this case is given in terms of the ball cage clearance and eccentricity z_c , as:

$$h_o = C_r - z_c \quad (4-40)$$

The calculation procedure is,

- a) Calculate h_o as above
- b) Evaluate $\bar{H} = h_o R_x (C_o R_x \alpha)^{-2/3}$
- c) For H from (b) find $\bar{Q} = 53.3 (\bar{H})^{-1/2} + 163 (\bar{H})^{-3}$
- d) Calculate cage ball load Q_3 as \bar{Q}/D

The procedure for determining the ball race normal load is performed twice for each ball, for the points of nearest approach at both ends of the cage pocket (h_o min and h_o max). The net normal load acting on the ball is given by:

$$P_3 = Q_3 (h_o \text{ minimum}) - Q_3 (h_o \text{ maximum}) \quad (4-41)$$

4.6 CALCULATION OF HYDRODYNAMIC FRICTION FORCES IN POINT CONTACT

The contacts between ball and race and between ball and cage pockets are point contacts. Under lubricated conditions, the surfaces are separated by a fluid film and there is a pressure build-up around the contact caused by the sweeping-in motion of the surfaces. This pressure build-up contributes to the friction in rolling in two ways, i.e., (1) the tangential surface forces required to pump the oil into the high pressure zone and (2) the component F_n of the inlet pressure acting to oppose rolling.

The pumping forces (1) are of two kinds, i.e. that due to rolling, F_r , and that due to sliding F_s .

Expressions have been found for these forces in a starved point contact. The complete analytical development is contained in {5} and {16}.

Since these friction forces arise in the contact inlet region, elastic deformation is not considered to have a significant effect and the analysis invokes a rigid body assumption.

Fig. (4-7) shows the relevant geometry. Two rigid bodies are shown in nominal point contact but separated by an oil film and undergoing relative rolling and sliding. A local cartesian coordinate system is established with the x-y plane parallel to the tangent plane of the two bodies and with the origin coincident with the surface of body 2. The coordinate system remains fixed in the contact as the surfaces of the two bodies move. The principal radii of curvature of the two bodies are $(R_x)_i$ and $(R_y)_i$, $i = 1, 2$. The equivalent radii are

$$R_x = (1/R_{x1} + 1/R_{x2})^{-1}; R_y = (1/R_{y1} + 1/R_{y2})^{-1} \quad (4-42)$$

The normal separation of points on the two bodies near the origin is given by

$$h = h_0 + \frac{x^2}{2R_x} + \frac{y^2}{2R_y} \quad (4-43)$$

where h_0 is the minimum film thickness at the origin. This separation function is applicable if the width of the Hertzian flat region in the contact is negligible compared to the relevant x and y dimensions in the inlet and outlet.

The surfaces are assumed to be moving with velocities u_i and v_i ($i = 1, 2$) relative to the origin in the x and y directions. The rolling velocities in the x and y directions are defined respectively as $v_x = (u_1 + u_2)/2$ and $v_y = (v_1 + v_2)/2$ and sliding velocities in the respective directions are $u_{sx} = u_1 - u_2$ and $u_{sy} = v_1 - v_2$.

Q is the portion of the normal load that is being supported by hydrodynamic forces in the inlet. For elastic ball race contact Q is considered negligible when compared to the load supported over the Hertzian contact zone.

The forces F_R , F_S , and F_N are displayed in Fig. 4-8. For representational clarity the special case when the contact is between two disks is illustrated. In this case, R_y is infinite and the forces are directed along the x axis. In the general point contact case the forces have both x and y components.

The force F_T acts in the same direction on both contacting bodies and opposite to the direction of motion. F_S acts in opposite directions on the two bodies in such a way as to

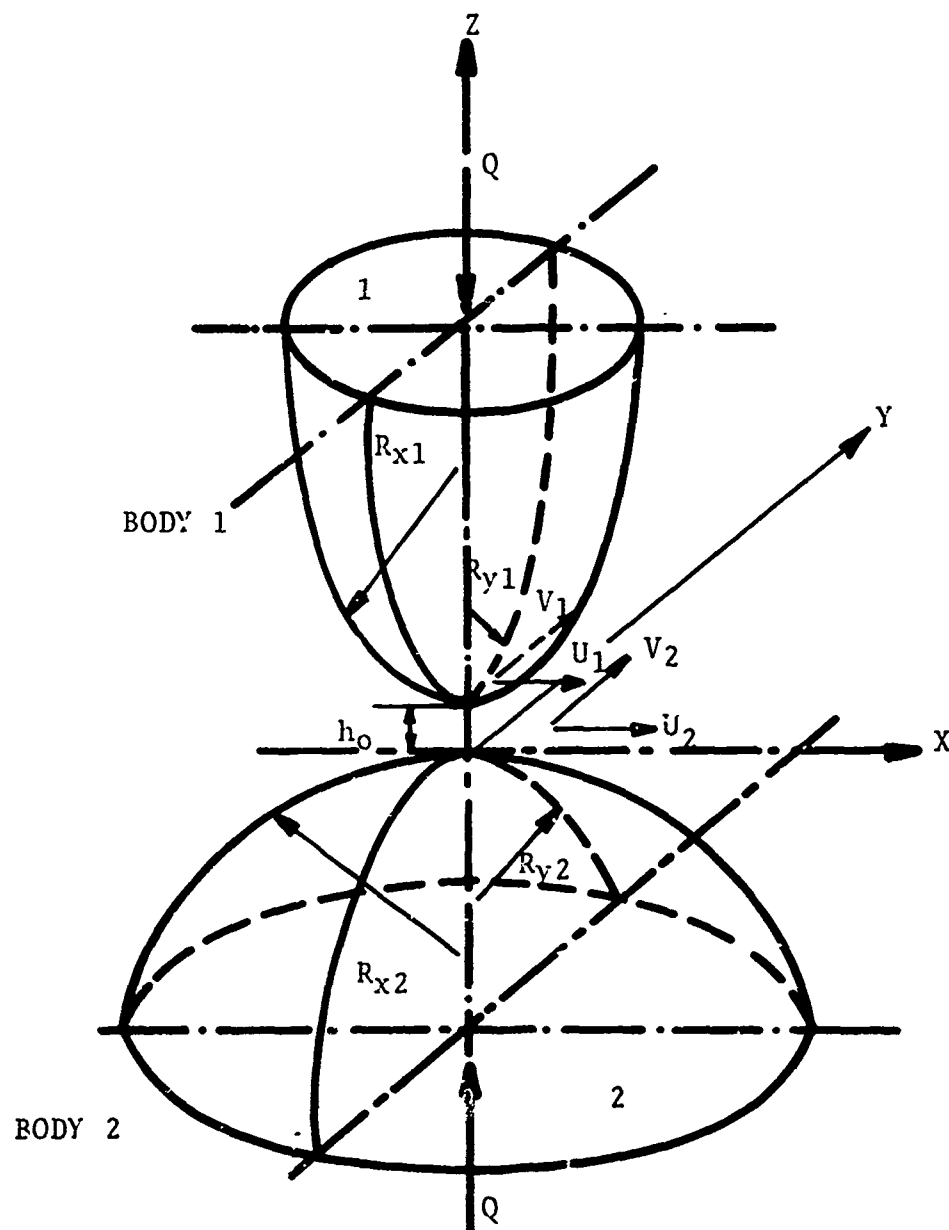
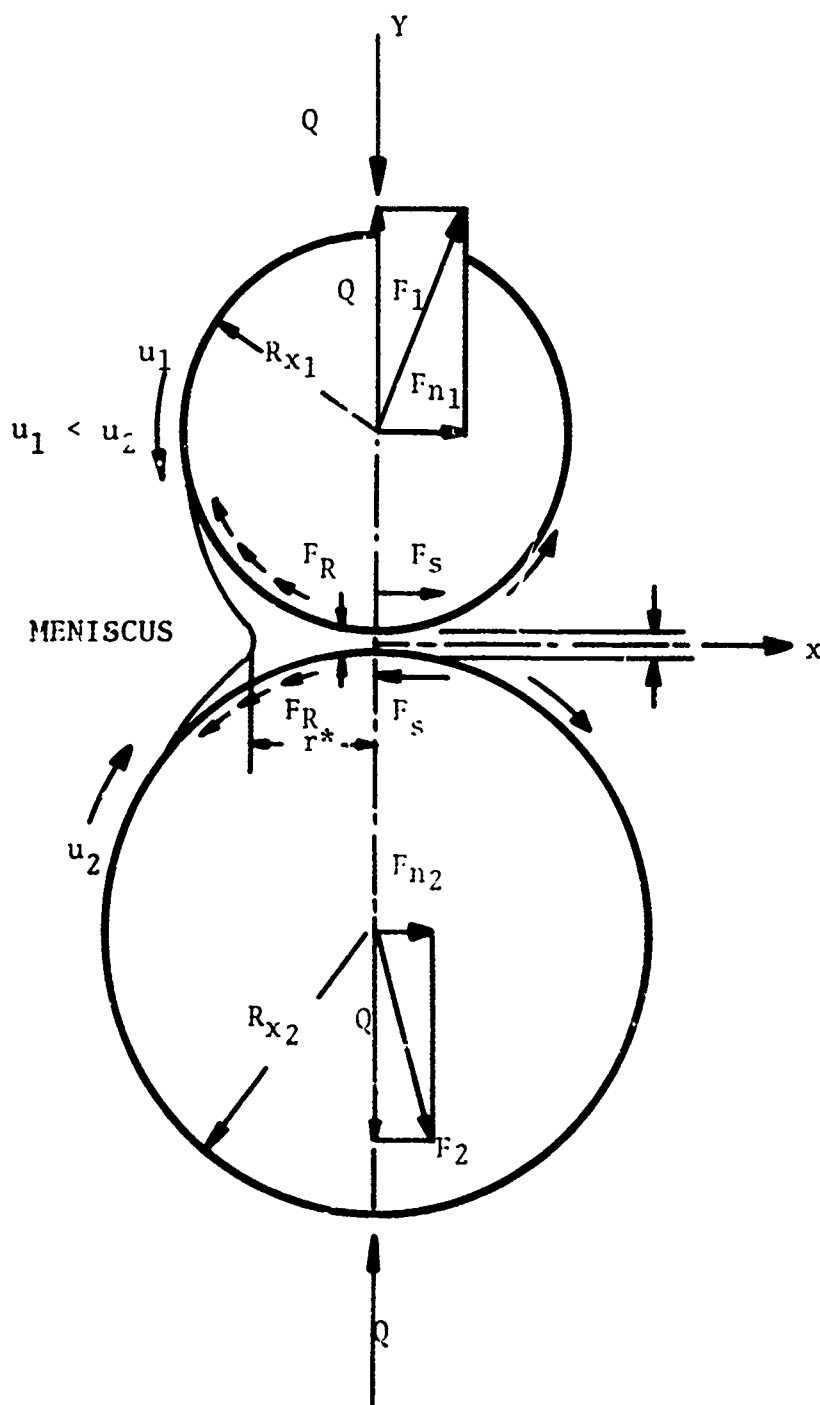


FIGURE 4-7

NOTATION FOR ROLLING SLIDING POINT CONTACT

FORCES ON SOLID BODIES



FORCES ON FLUID

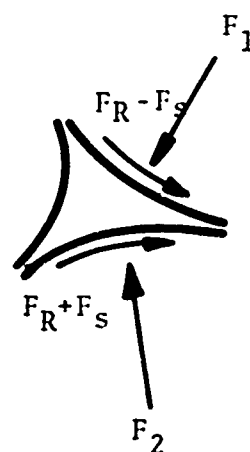


FIGURE 4-8

FRICTION FORCES ON SLIDING AND/OR ROLLING DISKS

tend to increase the speed of the slower body and to decrease the speed of the faster body.

The forces F_1 and F_2 are the resultants of the hydrodynamic pressure distribution in the inlet and act through the centers of the two bodies. The component of these forces in the y direction represents the (small) portion of the total load supported hydrodynamically. The components F_{n1} and F_{n2} acting in the x direction contribute to the force balance in the rolling direction.

The magnitude of the forces F_R , F_S and F_n depend upon the meniscus location r^* . The calculation of r^* for ball race contact was discussed in Section 4.3.2. For ball-cage contact an assumption regarding r^* is made as discussed later in this section.

Expressions for the x and y components of the forces F_R , F_S and F_n are given below in terms of the dimensionless quantities \bar{F}_R and \bar{F}_S .

Pumping Forces

$$F_{Rx} = \frac{1}{2} C_o \bar{F}_R \cos \gamma \quad (4-44)$$

Rolling component

$$F_{Ry} = \frac{1}{2} C_o \bar{F}_R (\sin \gamma) (R_x/R_y)^{1/2} \quad (4-45)$$

$$F_{Sx} = \bar{F}_S \eta u_{sx} (R_x R_y)^{1/2} \quad (4-46)$$

Sliding component

$$F_{Sy} = \bar{F}_S \eta u_{sy} (R_x R_y)^{1/2} \quad (4-47)$$

Normal Forces (on ball)

$$F_{nx} = C_o \bar{F}_R \frac{R_x}{r} \cdot \cos \gamma \quad (4-48)$$

$$F_{ny} = C_o \bar{F}_R \frac{R_y}{r} \cdot (\sin \gamma) (R_x/R_y)^{1/2} \quad (4-49)$$

(For a ring, r is replaced by the raceway radius)

where

$$C_o = \eta V_x (R_x R_y)^{1/2} \left[(3+2k)^{-2} + (V_y/V_x)^2 (3+2k^{-1})^{-2} k^{-1} \right]^{1/2} \quad (4-50)$$

$$\gamma = \tan^{-1} \left[\frac{3+2k}{k^{1/2}(3+2k^{-1})} \cdot \frac{V_y}{V_x} \right]$$

$$k \equiv R_x/R_y$$

η = absolute ambient viscosity

The quantities \overline{F}_R and \overline{F}_S are dimensionless and depend upon two further dimensionless parameters $\overline{\alpha}$ and ρ_1 . ρ_1 is a dimensionless meniscus distance defined as

$$\rho_1 \equiv r^*/(2h_0 R_x)^{1/2} (\cos^2 \gamma + 1/k \sin^2 \gamma)^{1/2} \quad (4-52)$$

h_0 for ball-race contact is taken as the plateau EHD film thickness given by Eq. (4-7).

For ball-cage contact h_0 is as calculated in Section 4.5.

r^* is the distance of the oil meniscus from the contact center along the rolling direction.

$\overline{\alpha}$ is the product of the pressure viscosity coefficient of the lubricant and the maximum fluid pressure q_{\max} that prevails if the lubricant is isoviscous.

$\overline{\alpha}$ assumes values between 0 and 1 with $\alpha = 0$ indicative of purely hydrodynamic and $\alpha = 1$ of purely elastohydrodynamic conditions. $\alpha = 1$ is taken for ball-race and $\alpha = 0$ for ball-cage pocket calculations.

Plots of \overline{F}_S and \overline{F}_R as a function of ζ_1 for various values of $\overline{\alpha}$ are given as Figs. (4-9) and (4-10) taken from [5].

For the EHD ball race contacts the following expressions have been fit to the \overline{F}_R vs ρ_1 curve in Figure 4-10 for $\overline{\alpha} = 1$.

$$\begin{aligned} \overline{F}_R &= 28.59 \ln \rho_1 - 10.1; \rho_1 \leq 5 \\ \overline{F}_R &= 36.57 \ln \rho_1 - 22.85; \rho_1 > 5 \end{aligned} \quad (4-53)$$

\overline{F}_S is not considered for a ball-race contact because the amount of sliding is so small.

For the predominantly hydrodynamic contacts, ($\overline{\alpha} = 0$) which arise between the ball and the cage web, both pumping and sliding friction are considered. The following equations were fit to the $\overline{\alpha} = 0$ curves in Figs. (4-9) and (4-10)

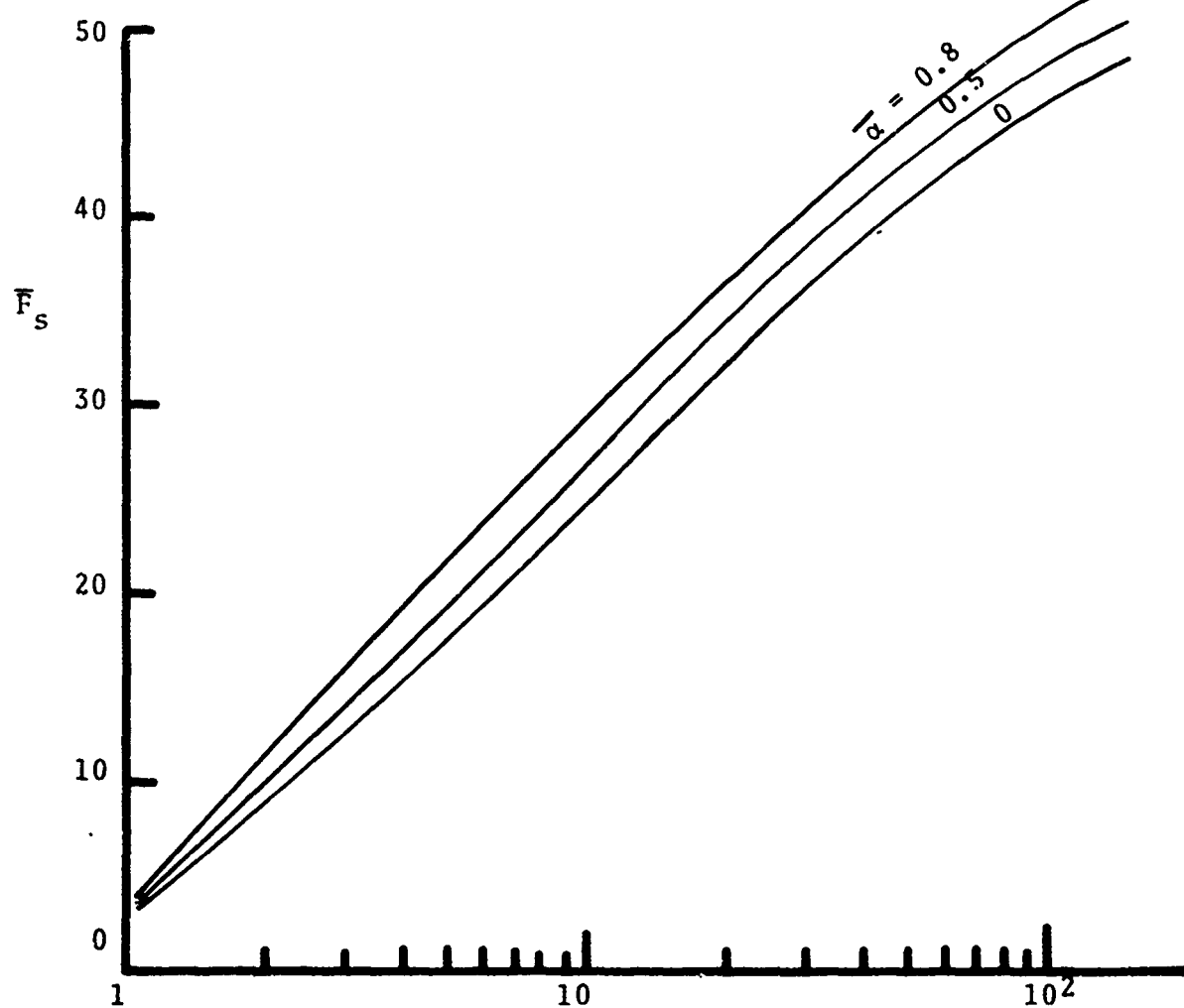


FIGURE 4-9
VARIATION OF F_s WITH ρ_1

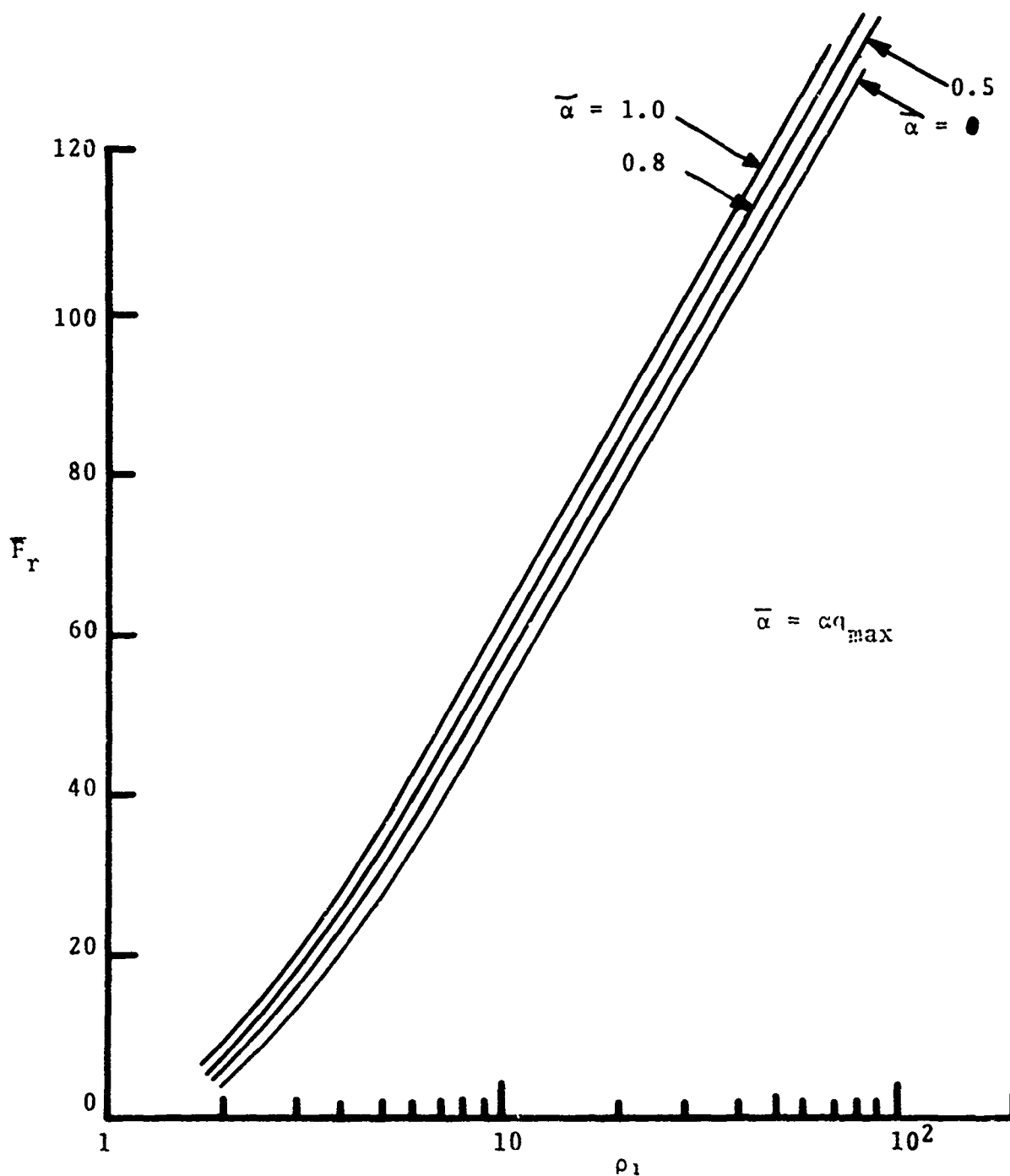


FIGURE 4-10
 VARIATION OF F_R WITH THE DIMENSIONLESS
 MENISCUS DISTANCE ρ_1

$$\overline{F}_R = 8.53 \times 10^{-14} [\ln(1000\rho_1)]^{15.570}; \rho_1 < 5.4 \quad (4-54)$$

$$\overline{F}_R = 36.576 \ln \rho_1 - 29.32; \rho_1 \geq 5.4$$

$$\overline{F}_S = 1.71 \times 10^{-9} \ln(1000\rho_1)^{11.01}; \rho_1 < 2 \quad (4-55)$$

$$\overline{F}_S = 10.115 (\ln \rho_1)^{.965} + 1.5; \rho_1 \geq 2$$

In applying the above results to ball-cage web and ball-race contacts it is necessary to interpret the geometrical parameters of the general configuration of Fig. 4-7 in terms of the appropriate bearing dimensions.

Fig. 4-11 shows the relevant geometry for the two contact types as well as the direction of the various force components.

In this Figure r denotes the ball radius, r' the cage pocket radius, r_g the outer ring groove radius, R the radius to the center of the contact ellipse and α the outer ring contact angle.

The value of the meniscus distance r^* to use for a ball-cage contact must be selected. It will vary with the efficiency of the lubricant supply and the size of the ball. A relation of the following form has been assumed.

$$r^* = k_1(XCAV) r \quad (4-56)$$

where

r = ball radius

$XCAV$ = fraction of oil in the oil air mixture present in the bearing

k_1 = a constant of proportionality

The form of Eq. (4-56) follows from the rather simple considerations that 1) r^* should increase with ball radius if lubricant supply is plentiful and 2) it should increase with the total amount of oil available, a quantity that is reflected in the term $XCAV$. Eq. (4-56) simply combines these two factors multiplicatively with k_1 as a constant of proportionality.

Experience in fitting experimental and calculated heat generation rates indicates that $XCAV = 0.10$ represents a relatively large amount of lubricant.

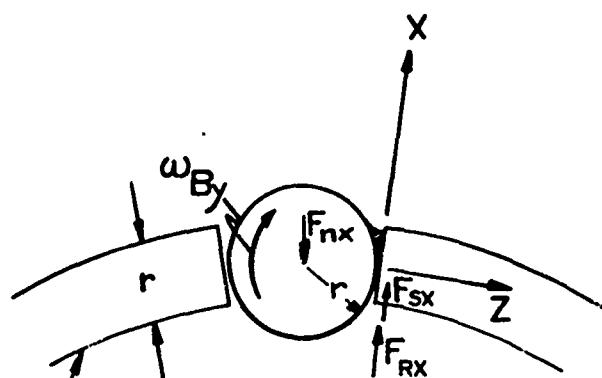
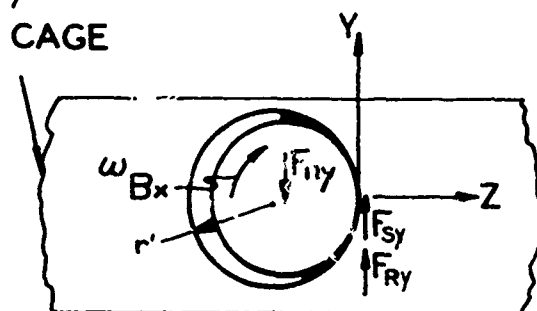


FIGURE A



$$R_x = r, \quad R_y = (1/r - 1/r')^{-1}$$

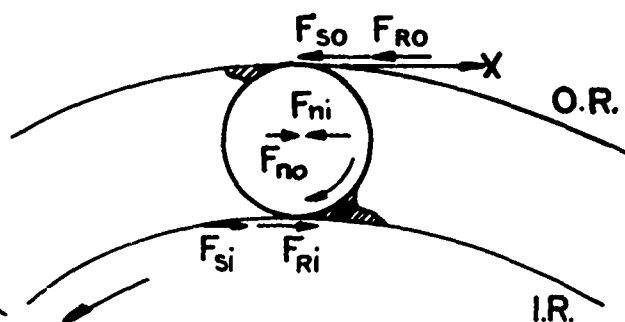
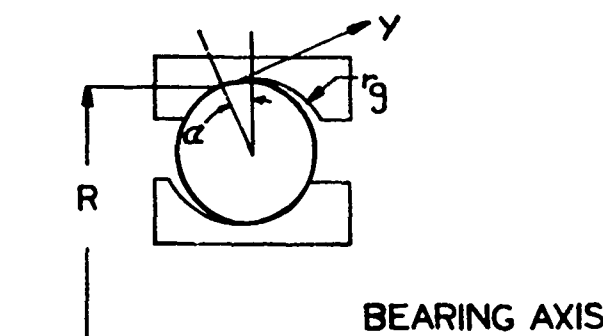


FIGURE B



$$R_y = (1/r - 1/r_g)^{-1}$$

$$R_x = (1/r - \cos \alpha / R)^{-1}$$

FIGURE 4-11

CONFIGURATION OF CONTACTS

(A) BALL-CAGE CONTACT

(B) BALL-RACE CONTACT (OUTER RING)

Reasoning that for values of XCAV approaching 0.10 the lubricant will tend to fill the cage pocket and, assuming a pocket height of half the ball diameter r (see Fig. (4-5)), then $r^* = 0.5r$ for $XCAV = 0.10$.

This gives

$$k_1 = \frac{r^*}{(XCAV)r} = \frac{0.5r}{0.10r} = 5.0 \quad (4-57)$$

Accordingly, $k_1 = 5.0$ has been used in Program AT74Y001 for calculating the meniscus location for ball-cage pocket contacts.

4.7 BALL DRAG FORCE IN AMBIENT LUBRICANT

In [17] the following form of "churning friction force" is cited, to account for all friction losses on the ball other than EHD sliding traction in the ball/race contacts:

$$F_w = \frac{\rho A_v C_v (d_m \omega_o)^2}{8 g} \quad (4-58)$$

where F_w is the drag force

A_v : the ball frontal area

C_v : a drag coefficient given in (17) as a function of the Reynolds number

d_m : the bearing pitch diameter

ω_o : the ball orbital angular velocity

g : the gravitational constant

ζ : the density of the air-oil mixture in the bearing cavity

$$\zeta = XCAV \cdot \rho_o \quad (4-59)$$

XCAV: the fractional amount of lubricant assumed to be in the bearing cavity

ρ_o : the density of the oil

Three hydrodynamic force components at each point contact on a ball have been defined and are identified in Section 4.6.

These components tend to retard ball motion as would F_w . Since two race contacts and a cage contact exist for each ball, 15 force components have been made explicit. After accounting for all contact friction forces, there is left a residual loss due to "windage" or "drag" acting on a ball as it moves through the air-oil mixture in the bearing cavity. Eq (4-58) has been used to model this windage force.

The value $XCAV = 0.025$ was adopted in using Program AT74Y001 to predict the bearing performance under full scale test conditions (cf. Section 7) after comparing experimental and computed heat generation rates for various values of $XCAV$ using the data in {20}. As discussed in Section 7, $XCAV$ in actuality is a function of lubricant supply rate, method of supply, speed and bearing and bearing cavity geometry. Additional insight into the influence of $XCAV$ on bearing performance variables is contained in Section 8.

4.8 BEARING LIFE REDUCTION DUE TO ASPERITY INTERACTION

In {5} and {18} the form of a reduction factor accounting for the effect of surface asperity interaction was deduced and its parameters were set to best fit to a large body of rolling contact life test data.

As employed in Program AT74Y001 the reduced tenth percentile life L_{10} is calculated as follows,

$$L_{10} = \left[1 + \frac{\psi(h/\sigma)}{\psi(1.5)} \right]^{-1/\beta} \cdot (L_{10})_{\infty} \quad (4-60)$$

where

$$\psi(h/\sigma) = \frac{\phi^2(h/\sigma)}{1 - \phi(h/\sigma)} \quad (4-61)$$

$\phi(\cdot)$ = density function of standard normal distribution

$\Phi(\cdot)$ = cumulative distribution function of standard normal distribution

h/σ = ratio of plateau film thickness to surface roughness for most heavily loaded ball

$(L_{10})_{\infty}$ = the full film life

The term $(L_{10})_{\infty}$ is calculated using the principles of Lundberg-Palmgren and multiplying by the user supplied product of two factors which represent by Industry practice the life improvement due to the type of material from which the bearing is fabricated and the life improvement due to full EHD film conditions. $(L_{10})_{\infty}$ is then down-rated to actual film conditions by Eq. (4-60). This point is discussed further in Sections 5 and 6.

SECTION 5

INPUT DATA PREPARATION

5.1 TYPES OF INPUT DATA

A complete set of input data comprises data of four distinct categories. Within these categories cards which convey specific kinds of information are referred to as card types. Depending on the complexity of the problem the input data set may contain one or several cards of a given type. The categories are listed below.

- I. A Title Card plus a second card which provides the program control information for the shaft-bearing solution.
- II. A set of up to sixteen (16) card types each set describing one bearing in the assembly. All bearings must be so described. The card sets must be input sequentially in order of increasing distance from a selected end of the shaft.
- III. A set of up to nine (9) card types to describe the thermal model of the assembly.
- IV. A set of three (3) card types to describe the shaft geometry, bearing locations on the shaft and shaft loading.

If the program is being used to predict the performance of a bearing assembly, cards from all four sets must be included in the runstream. If the program is being used to thermally model a mechanical system wherein no bearing heat generation rates are required, and therefore no bearing calculations need be performed, the cards from sets II and IV are omitted.

The review of required input information which follows is broken into the four sets of data categories given above, with special emphasis on program control data.

The input data instructions are given in Appendix B, and are for the most part, self explanatory. They are laid out in the format of an eighty column data card. A description of the variables is given in the input instruction forms. Also included in Appendix B is a sample set of completed forms for the special case wherein a single thrust loaded ball bearing is to be analyzed.

The units used for input data are as follows:

- Linear Dimensions - (mm)
- Area - (mm^2)
- Angles - (degrees)
- Bearing Angular Mounting Errors - (radians)
- Rotational Speeds - (RPM)
- Linear Speeds - (m/sec)
- Force - (Newtons) (N)
- Moments - (N-mm)
- Pressure, Elastic Modulus - (N/mm^2)
- Density - (Kg/m^3)
- Kinematic Viscosity - (m^2/sec)
- Temperature - (degrees centigrade) ($^{\circ}\text{C}$)
- Coefficient of Thermal Expansion ($^{\circ}\text{C}^{-1}$)
- Thermal Conductivity - ($\text{Watts/m}^2/^{\circ}\text{C}$)

5.2 DATA SET I - TITLE CARDS

5.2.1 Title Card 1

This card should contain the computer run title and any information which might prove useful for future identification. The full eighty (80) columns are available for this purpose. The title will appear at the top of each page of Program output.

5.2.2 Title Card 2

This card provides the control information for the shaft bearing solution.

Item 1: Shaft Speed in rpm, GOV (1), helps identify the card as bearing related.

Item 2: Number of Bearings on the shaft (NBRG), a minimum of zero is permitted if no bearing solution is being sought. A maximum of five is permitted.

Item 3: Print Flag (NPRINT), NPRINT equal to zero is normal and will result in no intermediate or debug output. With a value of one, a low level intermediate print is obtained at the end of each shaft bearing iteration. The values of the variables, the inner ring displacements, and the equation residues are printed. At the end of each bearing iteration, wherein the rolling element and cage equilibrium equations are solved, an error parameter is printed which has the value:

$$\text{Error Parameter} = \Delta X_N / \Delta X_{N-1}$$

ΔX_N is the change in the variable X specified at iteration N.

ΔX_{N-1} is the change in the variable specified at the previous iteration.

The Error Parameter is calculated for each of the bearing variables, but only the largest one is printed.

Additionally, at the end of each Clearance Change iteration, the clearance change error parameter is printed. This error is defined:

$$\text{Error Parameter} = \frac{\Delta \text{DCL}_N - \Delta \text{DCL}_{N-1}}{\text{Rolling Element Diameter}}$$

where ΔDCL_N and ΔDCL_{N-1} denote the clearance changes calculated at the current and previous iterations respectively.

If NPRINT is set to 2 all of the above information is printed. Additionally the variable values and residue values are printed for each iteration of the rolling element elastic (frictionless) equilibrium solution. For a ball bearing, these variables are x_1 and y_1 , the ball center coordinates for each ball.

An NPRINT value of 3 is the same as NPRINT = 2 except that variable and residue values are printed during the frictional equilibrium solution and omitted during the elastic solution. For a ball bearing these variables are, for each ball, x_1 , y_1 , ω_0 , ω_x , ω_y , ω_z and additionally, z_c , the displacement between the cage pocket and ball centers for a reference ball.

Item 4: ITFIT controls the number of iterations allowed to satisfy the bearing clearance change iteration scheme. If ITFIT is set to zero (0), or left blank, the clearance change portion of the program is not executed. If a positive integer is input, the clearance change scheme is utilized with a maximum iteration limit of five (5). If a negative integer is input, the scheme is used with a maximum iteration limit equal to the absolute value of the negative integer.

Item 5: ITMAIN limits the number of iterations attempted during the solution of the shaft and bearing inner ring equilibrium problems, i.e. establishing the equilibrium of bearing

reactions and applied shaft loads. If ITMAIN is left blank, set to zero, or to a positive integer, then (15) iterations are permitted. If ITMAIN is set to a negative integer the number of iterations is limited to the absolute value of that integer.

Item 6: GOV(2) or EPSFIT is the convergence criterion for the diametral clearance change portion of the analysis. As mentioned under item 3 above, this error parameter is defined to be

$$\text{Error Parameter} = \frac{(\Delta\text{DCL})_N - (\Delta\text{DCL})_{N-1}}{\text{Rolling Element Diameter}}$$

The iteration scheme is terminated when the error parameter is less than the input value of EPSFIT. If EPSFIT is left blank or is set to zero (0), the program default value of 0.0001 is used.

Items 7 & 8: Main loop accuracy for frictionless elastic (EPS1) and friction solution (EPS2). These accuracy values control the accuracy of the shaft bearing deflection solution as well as the quasi-dynamic solution of the component dynamics (cf. Sect. 3). If EPS1 and EPS2 are left blank or set to zero (0), default values of 0.001 and 0.0001 respectively are used.

Item 9: NPASS controls the level of the bearing solution

NPASS = blank or zero results in a frictionless solution

NPASS = 1 results in bearing dynamic solutions based on ring displacements which produced inner ring equilibrium in the frictionless solution. Inner ring displacements are not then recalculated with friction forces included and therefore inner ring equilibrium is not guaranteed.

NPASS = 2 results in bearing dynamic solutions and inner ring equilibrium.

5.3 DATA SET II - BEARING DATA

Most of the input instructions are self-explanatory. Where certain items are deemed to require more explanation

than given in the input data format instructions they are treated on an individual basis by card type and item number.

Most of the bearing input data is read into a two dimensional array named "BD", which has the dimensions (1580, 5). For each of the five bearings permitted on a shaft, a total of 1580 pieces of data may be stored. Denoting $BD(I, J)$, I represents a specific piece of bearing data, J represents the bearing number. The bearing input data of Data Set II occupies the first 85 locations of the 1580 allotted. On the input data format sheets the designation $BD(I)$ where $I = 1...85$, denotes the location within the BD array where each piece of input data is stored.

5.3.1 Card Type 1

Item 1: Bearing type columns 1-10 must be specified, left justified, i.e., "B" or "C" in column 1. This format must be followed since the Program recognition of bearing type, (ball bearing or cylindrical roller bearing), is derived from reading the "B" or "C" in the first column of this card.

Items 2 & 3: Columns 11-30 and 31-50, "Steel designations", inner and outer rings respectively. The alphameric-literal description of the steel types such as "M-50" or "AISI 52100" is input.

Items 4 & 5: Columns 51-60 and 61-70, the numbers input for items 4 and 5 are used to account for improved materials and multiply the raceway fatigue lives as determined by Lundberg-Palmgren methods. Typical life factor values for modern steels are in the neighborhood of 2.0 to 3.0. If the ASME Publication Life Adjustment Factors for Ball and Roller Bearings, is referenced by the user, the Material Factor D and the Material Process Factor E should be used multiplicatively as inputs for items 4 and 5.

Item 6: Columns 71-78, "Orientation angle of the first rolling element". (ϕ_1) (degrees). Refer to Fig. (3-1). The quasi-dynamic rolling element bearing problem has an infinite number of solutions which fall within a narrow envelope having a periodic shape. The solution obtained is a function of the rolling element positions relative to the bearing system coordinate axes. $\phi_1 = 0$, places a rolling element on the Y axis and is the choice customarily made. ϕ_1 can be designated as any value $0 \leq \phi_1 < \frac{2\pi}{n}$ where n is the number of rolling elements. For each different value assigned to ϕ_1 a different, although similar, bearing solution will be attained.

Item 7: Column 80, a signal, termed the crown drop flag, which specifies for a cylindrical roller bearing, whether the roller-race crown drops will be calculated, or read directly. If item 7 is blank or zero, the crown drops are calculated based on the roller-race crown radius, effective and flat length input information. If the crown drop flag is other than zero or blank the race to roller crown drop for a non-uniform race or roller profile must be specified at up to 20 uniformly spaced positions along the roller-race effective contact length using Bearing Data Card Types 5 and 6 (see below).

5.3.2 Card Type 2

Card Type 2 data are self-explanatory.

5.3.3 Card Type 3

5.3.3.1 Ball Bearing Geometry Input - The Program can analyze three types of ball bearings:

- 1) Split Inner Ring
- 2) Angular Contact (mounted in sets of two or more)
- 3) Deep Groove

However, the input is structured from the point of view of split inner ring ball bearings. For this bearing Figs. 5-1 and 5-2 define the input variables. Recognizing that the user might not have all of the data readily on hand and in fact might like to have the variables calculated, he must input only two of the first six variables. He must input either Items 3 or 6. Item 3 is the contact angle under an axial gage load, as shown in Fig. 5-1(a). Item 6 is the bearing diametral clearance PD, i.e., that clearance measured with the shim in place with the inner and outer ring groove centers axially aligned. PD is shown in Fig. 5-2(a). The user must also specify one of the four variables, Items 1, 2, 4 or 5. viz, shim width, W, shim angle, α_s (degrees), diametral play (Sd), or axial play without the shim, (PE), respectively. All of these variables are shown on Fig. 5-2. The unspecified variables will be calculated and printed.

In order that the angular contact and deep groove ball bearings be treated properly, care must be taken with the input specifications of bearing contact angle and diametral clearance. Within the Program the deep-groove and angular contact bearings are distinguished from each other by the

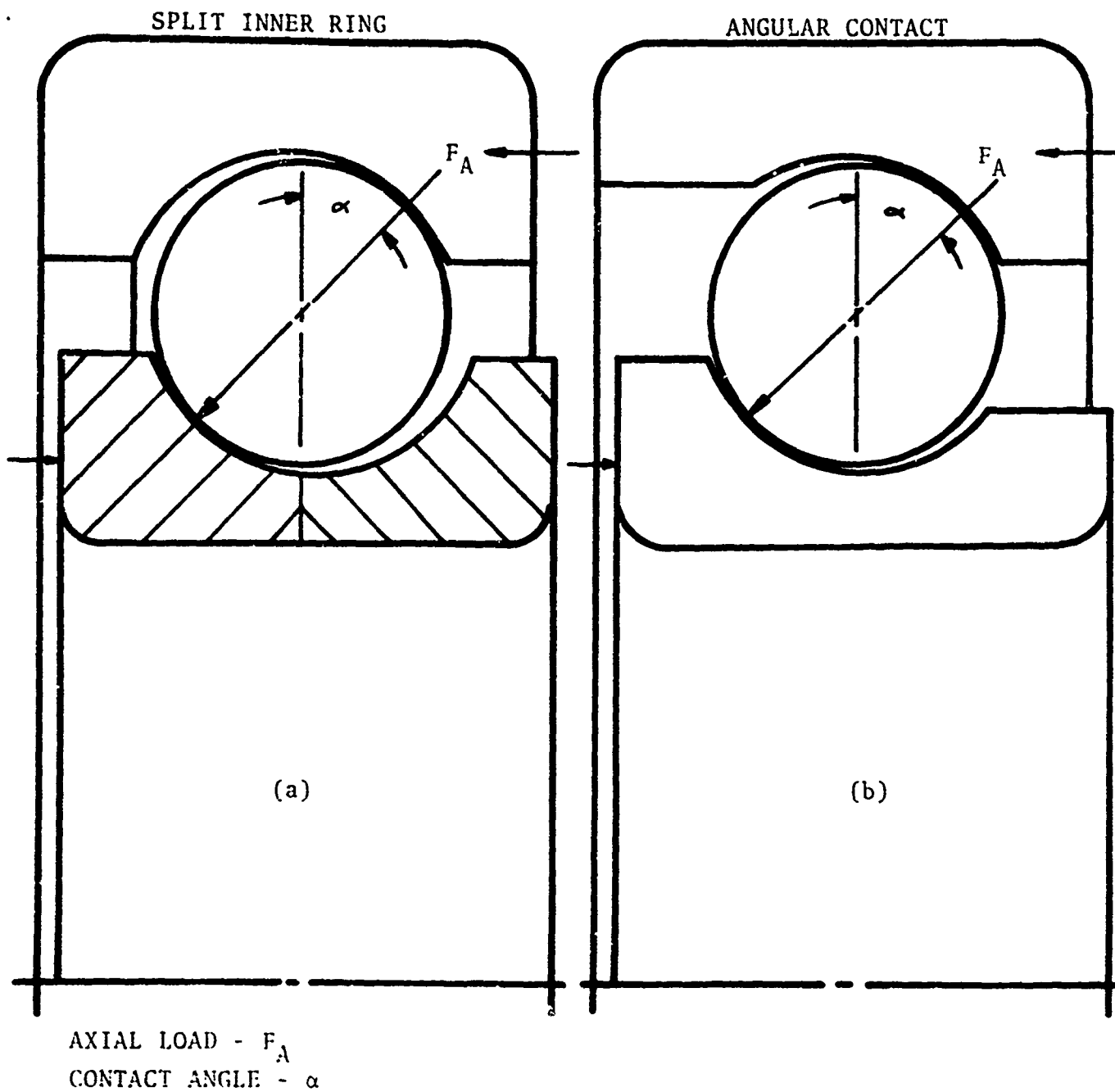


FIGURE 5-1
SPLIT INNER RING AND ANGULAR CONTACT BALL BEARINGS
UNDER AXIAL LOAD

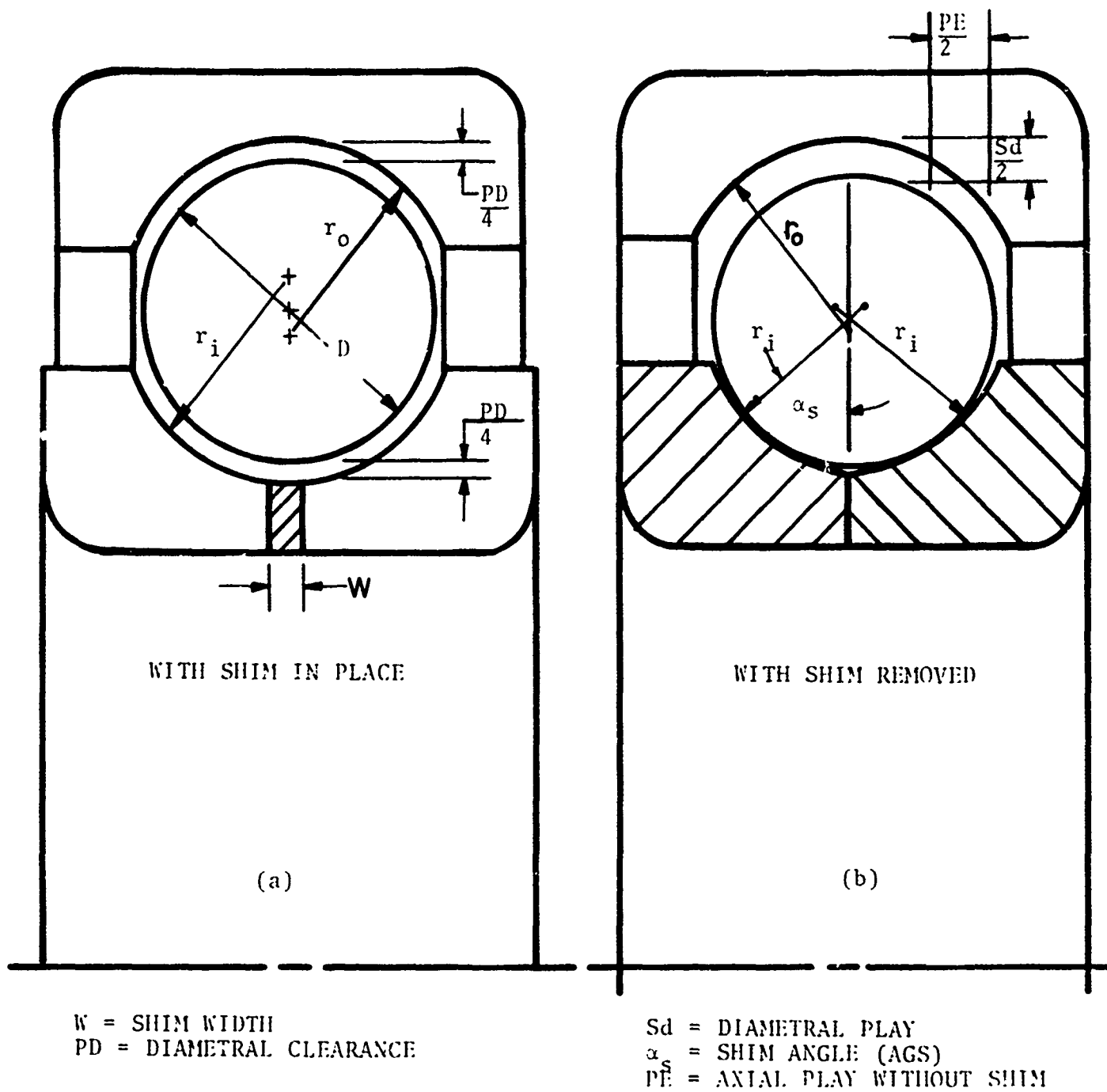


FIGURE 5-2
SPLIT INNER RING BALL BEARING

ability of the inner ring groove of deep-groove ball bearings to axially align and move freely with respect to the outer ring groove. Angular contact bearings are usually mounted in pairs such that the inner and outer ring grooves of a single bearing are offset under a no-load condition. This offset is fixed and is maintained despite changes which might occur in ring and ball diameters during operation.

If the bearing is a deep-groove ball bearing with the inner ring free to move axially such that a positive or negative contact angle can be obtained under respective positive or negative axial loads then the initial contact angle, (ANG, Item 3), should be set to zero degrees at input and the bearing diametral clearance PD is then input as the value measured with the curvature centers of the inner and outer rings in the same plane.

When defining the input to Item 3 for an angular contact ball bearing, the user should input the actual contact angle as defined in Fig. 5-1(b) only if the bearing has no initial operating clearance. If there is some clearance, S_d , the angle α_0 , as defined in Fig. 5-3(b) should be input, as Item 3.

5.3.3.2 Cylindrical Roller Bearing Contact Geometry Data -
All items are used to define the roller-race contact geometry. "Flat length" and "Crown Radius" are used to calculate roller-race separation along the roller profile if this information is not specifically input. See Item 7 of the Bearing Data title card and Bearing Data Cards 5 & 6.

Items 1 and 3 "Effective Contact Length" refer to the longest possible length which can obtain at a roller-race contact. Typically this is the roller total length less the corner radii. If, however, the raceway undercuts are exceptionally large so that the track width is smaller than the effective roller length then the track width should be input.

5.3.4 Card Type 4

Items 1 through 6 define the statistical surface microgeometry parameters of the rollers and raceways. Items 1 through 3 require the input of root mean square (RMS) surface roughness. If the user's source data specifies surface roughnesses in arithmetic average values (AA) these values must be converted to RMS by multiplying by 0.9.

Items 4 through 6 are RMS values of the slopes measured in degrees of the surface asperities as measured in a traverse

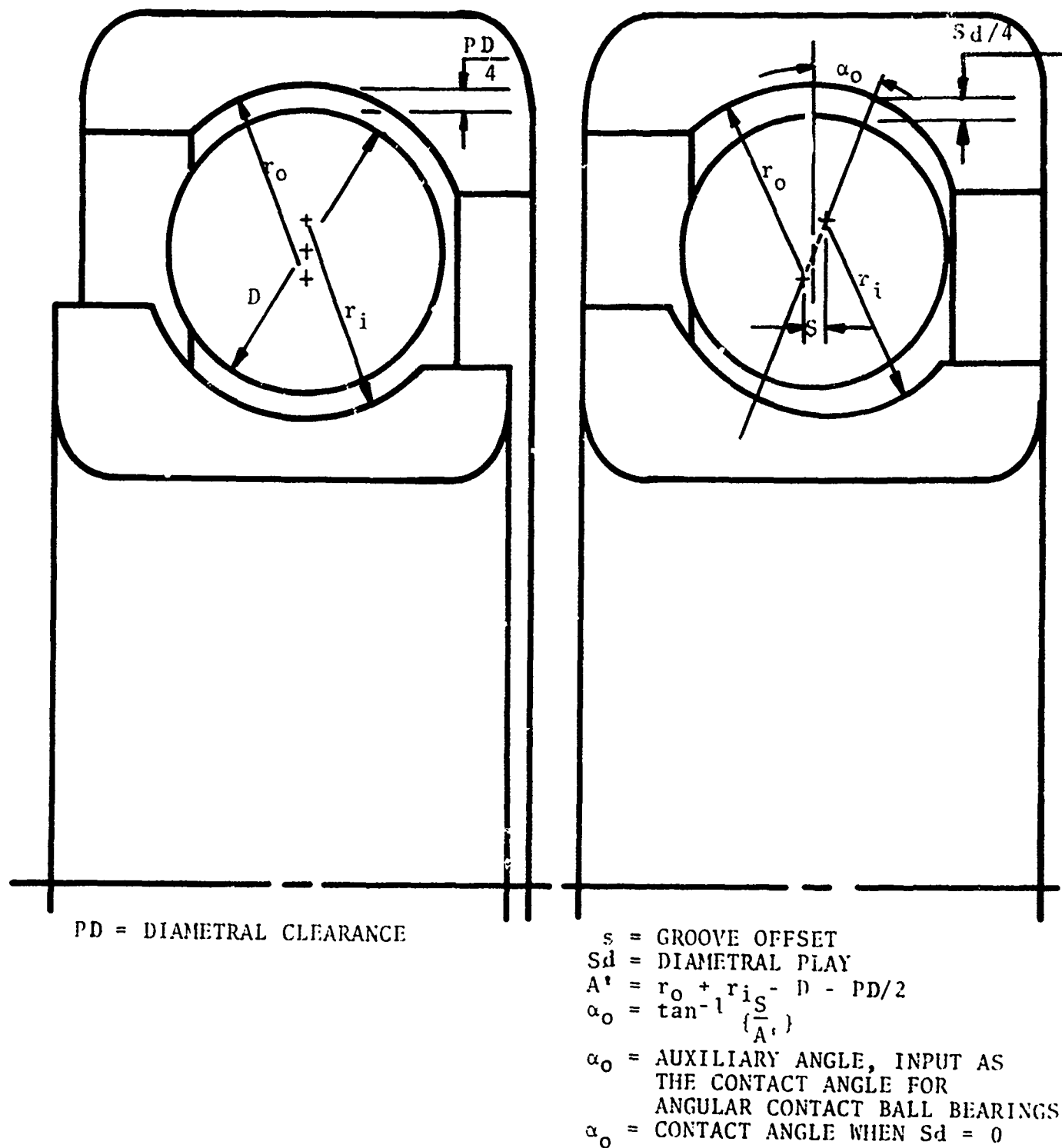


FIGURE 5-3
ANGULAR CONTACT BALL BEARING

across the groove for rings, longitudinally for rollers and in any arbitrary direction for balls. Typical values for raceway and rolling element surfaces are 1 to 2 degrees.

Item 7 is the coefficient of coulomb friction applicable for the contact of asperities. Unless specific information indicates otherwise, a value of 0.1 is recommended.

5.3.5 Card Types 5 & 6

These cards are used to input the outer and inner race roller-race separation along the roller profile. These cards must be omitted if item 7 of the Bearing Data Title card is zero or blank.

5.3.6 Card Type 7

Item 1: Column 1-10, this item (XCAV) is used to describe the percentage of the bearing cavity, estimated by the user, to be occupied by lubricant, $0 < \text{XCAV} < 100$. A value $\text{XCAV} = 2.5$ has been used in conjunction with predicting the full scale bearing test results in Section 7. Additional discussion on the influence of XCAV is given in Section 8.

The fluid drag acting on each rolling element is directly proportional to XCAV. Of the factors considered it has been found that fluid drag has the most significant influence upon cage slip. The drag effect also makes a substantial contribution to bearing heat generation.

Items 2-6: These items describe the cage design information which allows the application of Petroff's Equation to model cage-rail-ring-land friction.

5.3.7 Card Types 8, 9, 10, 11, 12

These cards are to be included only if the change in bearing diametral clearance with operating conditions is to be calculated, i.e. if item 4 ITFIT on the Bearing Title Card is non-zero. On Card Type 8, tight interference fits bear a positive sign and loose fits, a negative sign.

Items 3 and 6 on Card No. 8 are termed the shaft and housing effective widths respectively. The value specified for these effective widths may be as great as twice the ring width.

Use of an effective width is an attempt to account for the greater radial rigidity of a shaft than the ring that is

pressed on to it, owing to the fact that the shaft deflects over a distance that extends beyond the ring width. In the program the calculated internal pressure on the ring due to its interference fit with the shaft, is distributed over the shaft effective width and this (lower) pressure is used in computing the shaft deflection. Using double the actual width as the effective width is customary.

5.3.8 Card Type 13

This card specifies the lubricant type. If Item 1, NCODE is 1, 2, 3 or 4 the Program uses preprogrammed lubricant properties for the lubricants discussed in Sect. 4.

<u>NCODE</u>	<u>Lubricant</u>
1	A specific mineral oil
2	A MIL-L-7808 G
3	C-Ether
4	A MIL-L-23699

No further information is required on Card 13.

If zero is input for Item 1 the lubricant information and properties corresponding to Items 2 and 7 must be specified.

5.3.9 Card Type 14

Items 1 and 2. These items are the amounts $\Delta\zeta$ by which the combined thickness of the lubricant film on the rolling track and rolling element is increased during the time interval between the passage of successive rolling elements, from whatever replenishment mechanisms are operative. Item 1 applies to the outer and Item 2 to the inner race-rolling contacts respectively. The question of selecting appropriate values of $\Delta\zeta$ is discussed in Section 4.3 and in Section 8.

Items 3 through 6 are to be non-zero only if the user specifies a lubricant other than one of the four previously listed, in which case Items 3 through 6 define the concentrated contact friction model according to Fig. (5-4). The equation of this curve is the same as Eq. (4-7) of Section 4-4, with appropriate changes in the notation.

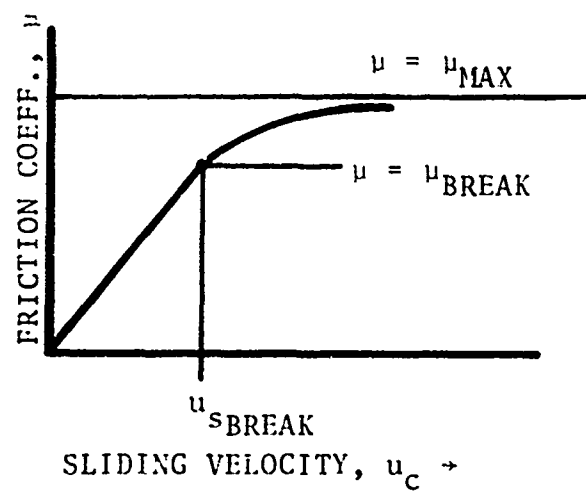


FIGURE 5-4

FRICTION COEFFICIENT VERSUS SLIDING VELOCITY

For the four lubricants noted the above curve is calculated as a function of sliding and entrainment velocities, local contact pressure and film thickness as described in Section 4.

5.4 DATA SET III - THERMAL MODEL DATA

Appendix A has been included to aid the user in his data preparation and calculation of heat transfer coefficients required at input.

5.4.1 Card Type 1

Card type 1 is a control card. If no temperature map is to be calculated, this card is to be included as a blank card followed by a Type 2 card for each bearing on the shaft. Card Type 1 contains control input for both steady state and transient thermal analyses. It is not intended however, that both analyses be executed with the same run.

Item 1: The highest node number (M). The temperature nodes must be numbered consecutively from one (1) to the highest node number. The highest node number must not exceed one hundred (100).

Item 2: Node Number of the Highest Unknown Temperature Node (N). This number should equal the total number of unknown node temperatures. It is required that all nodes with unknown temperatures be assigned the lowest node numbers. The nodes which have known temperatures are assigned the highest numbers.

Item 3: Common Initial Temperature (TEMP)^{°F}: The temperature solution iteration scheme requires a starting point, i.e., guesses of the equilibrium temperatures. Card Type 3 allows the user to input guesses of individual node temperatures. When a node is not given a specific initial temperature, the temperature specified as Item 3 of Card Type 1 is assigned.

Item 4: Punch Flag (IPUNCH): If the Punch Flag is not zero (0) or blank, the system equilibrium temperatures along with the respective node numbers will be punched according to the format of Card T3. This option is useful if, for instance, the user makes a steady state run with lubrication, and then wishes to use the resultant temperature as the initiation point for a transient dry friction run in order to assess the consequence of lubricant flow termination.

Item 5: "Output Flag" (IUB). If the "Output Flag" is not zero the bearing program output and a temperature map will be printed after each call to the shaft bearing solution scheme. This printout will allow the user to observe the flow of the solution and to note the interactive effects of system temperatures and bearing heat generation rates. Since the temperature solution is not mathematically coupled to the bearing solution the possibility exists that the solution may diverge or oscillate. In such a case, study of the intermediate output produced by the "Output Flag" option may provide the user with better initial temperature guesses that will effect a steady state solution.

Item 6: "Maximum Number of Calls to the Shaft Bearing Program" (IT1). IT1 is the limit on the number of Thermal-Shaft-Bearing iterations, i.e., the external temperature equilibrium calculation. The user must input a non-zero integer such as 5 or 10 in order for the Program to iterate to an equilibrium condition. If IT1 is left blank or set to zero (0) or 1, shaft bearing performance will be based on the initially guessed temperatures of the system. The temperatures printed out will be based on the bearing generated heats. It is unlikely that an acceptable equilibrium condition will be achieved. However, the temperatures which result may provide better initial guesses, for a subsequent run, than those specified by the user.

IT1 also serves as a limit on the transient temperature solution scheme, by limiting the number of times the shaft-bearing solution scheme is called. Each call to the shaft-bearing scheme will input a new set of bearing heats to the transient temperature scheme until a steady state condition is approached or until the transient solution time up limit is reached.

Item 7: "Absolute Accuracy of Temperatures for the External Thermal Solution" (EP1). In the steady state thermal solution scheme, each calculation of system temperatures occurs after a call to the shaft-bearing scheme which produces bearing generated heats. After the system temperatures have been calculated for each iteration, using the internal temperature solution scheme, each node temperature is checked against the nodal temperature at the previous iteration.

If $\{t_{(N)}\}_i - t_{(N-1)}\}_i < EP1$ for all nodes i then equilibrium has been achieved and the iteration process stops.

Item 8: "Iteration Limit for the Internal Thermal Solution" (IT2). After each call to the shaft bearing program, the internal temperature calculation scheme is used to determine the steady state equilibrium temperatures based on the calculated set of bearing heat generation rates. If the program is used to calculate the temperature distribution of a non bearing system it is the internal temperature scheme which is employed. If IT2 is left blank or set to zero, the number of internal iterations is limited to twenty (20).

Item 9: "Accuracy for Internal Thermal Solution" (EP2). The use of EP2 is explained in Section 3.6. If EP2 is left blank or set to zero (0), a default value of 0.001 is used.

Item 10: "Starting Time" (START) is a time T_s at which the transient solution begins; usually set to zero (0).

Item 11: "Stopping Time" (STOP) is the time in seconds at which the transient solution terminates, T_f . The transient solution will generate a history of the system performance which will encompass a total elapsed time of

$$(T_f - T_s) \text{ seconds}$$

Item 12: "Calculation Time Step" (STEPIN). The transient internal solution scheme solves the system of equations

$$t_{k+1} = t_k + \frac{q_k}{\rho C_p V} \Delta T$$

$$\Delta T = \text{STEPIN}$$

The user may specify STEPIN. If left blank or set to zero (0), the Program calculates an appropriate value for STEPIN using the procedure described in Section 3.6.

Item 13: "Time Interval Between Printed Temperature Maps" (TTIME) seconds. The user must specify the length of time which will elapse between each printing of the temperature map. The interval will always be at least as large as the "calculation timestep" (STEPIN).

Item 14: "Time Interval Between Calls of the Shaft Bearing Portion of the Program" (BTIME). BTIME will always have a value larger than or equal to (STEPIN) even if the user inadvertently inputs a shorter interval. Computational time savings result if BTIME is greater than STEPIN, however, accuracy might be lost.

5.4.2 Card Type 2

Card Type T2 is required, one card for each bearing if no thermal analysis is being performed. The temperature data is used within the shaft-bearing analysis portion of the program to fix temperature dependent properties of the lubricant in which case the inner race, outer race and lubricant bulk cavity temperatures are used. The assembly component temperatures at each bearing location are used in the analysis which calculates the change in bearing diametral clearance from "off the shelf" to operating conditions.

Item 9: "Flange" temperature is not currently used in the analysis. It simply provides for future consideration of tapered roller bearings.

5.4.3 Card Type 3

In the steady state analysis this card is used to input initial guesses of individual nodal temperatures for unknown nodes as well as the constant temperatures for known nodes, such as ambient air and/or an oil sump.

In the transient analysis, Card Type T3 is used to input the nodal temperatures of all nodes at (START) = T_s i.e. at the initiation of the transient solution.

5.4.4 Card Type 4

With this card, node numbers are assigned to the components of each bearing, one card per bearing. With this information the proper system temperatures are carried into each respective bearing analysis. The inner race and inner ring node numbers may or may not be the same at the user's discretion. Similarly the outer race and outer ring node numbers may or may not be the same.

5.4.5 Card Type 5

The shaft bearing system analysis accounts for frictional heat generated at four locations in the bearing, i.e. at the inner race, the outer race, between the cage rail and ring land, and in the bulk lubricant due to drag. The heat generated at the hydrodynamic cage-rolling element contact is added to the bulk lubricant. Heat generated at the flange is not presently considered. This card allows the heat generated to be distributed equally to two nodes. For instance the heat generated at the inner race-rolling element contact should be

distributed half to the rolling element and half to the inner race. The heat developed between the cage and inner ring land may be distributed half to the inner ring and half to the cage if a cage node has been defined, otherwise, half to the bulk lubricant.

5.4.6 Card Type 6

This card specifies the node numbers and the heat generation rate for those nodes where heat is generated at a constant rate such as at rubbing seals or gear contacts.

5.4.7 Card Type 7

This card type is used to input the numerical values of the various heat transfer coefficients which appear in the equations for heat transfer by conductivity, free convection, forced convection, radiation and fluid flow. Up to ten coefficients of each type may be used. Separate values of each type of coefficient are assigned an index number via card T7 and in describing heat flow paths (Card Type T8 below) it is necessary only to list the index number by which heat transfers between node pairs.

Indices 1-10 are reserved for the conduction coefficient λ , 11-20 for the free convection parameters, 21-30 for forced convection, 31-40 for emissivity and 41-50 for fluid flow (product of specific heat, density and volume flow rate).

As an example, for heat transfer by conduction with coefficient λ of 53.7 watts/M°C one could prepare a card type T7 with the digit 1 punched in column 10 and the value 53.7 punched in the field corresponding to card columns 11-20. If a conduction coefficient of 46.7 were applicable for certain other nodes in the system one could punch an additional card assigning index No. 2 to the value $\lambda = 46.7$ by punching a "2" in card column 10 and 46.7 anywhere within card columns 11-20.

Rather than inputting constant forced convection coefficients optionally these coefficients can be calculated by the program in one of three ways. If the calculation option is exercised a pair of cards is used in place of a single card containing a fixed value of α . The contents of the pair of cards depend upon which of the three optional methods are used.

Option 1) α is independent of temperature but is calculated as a function of the Nusselt number which in turn is a function of the Reynolds number Re , the Prandtl number Pr as follows, (cf. {10})

$$\alpha = \lambda_{oil} / L N_u$$

$$N_u = a R_e^b P_r^c$$

where λ_{oil} is the lubricant conductivity, L is a characteristic length (with a unit of meters) and K , a and b are constants.

Option 2) α is a function only of fluid dynamic viscosity and viscosity is temperature dependent.

$$\alpha = c \eta^d$$

Option 3) α is a function of the Nusselt, Reynolds and Prandtl numbers and viscosity is temperature dependent.

5.4.3 Card Type 8

This card defines the heat flow paths between pairs of nodes. Every node must be connected to at least one other node, i.e., two or more independent node systems may not be solved with a single Program execution.

The calculation of heat transfer areas is based on lengths, L_1 and L_2 (per page 194) input using Card Type T8. Additionally, the type of surface for which the area is being calculated is indicated by the sign assigned to the heat transfer coefficient index. If the surface is cylindrical or circular the index should be positive, if the surface is rectangular the index should be input as a negative integer.

In the case of radiation between concentric axially symmetric bodies, L_3 is the radius of the larger body. For radiation between two parallel flat surfaces or for conduction between nodes, L_3 is the distance between them.

Fluid flow heat transfer accounts for the energy which the fluid transports across a node boundary. Along a fluid node at which convection is taking place, the temperature varies. The nodal temperature which is output is the average of the fluid temperature at the output and input boundaries. If the emergence temperature of the fluid is of interest, it is necessary to have a fluid node at the fluid outlet. At this auxiliary node only fluid flow heat transfer occurs and the fluid temperature would be constant throughout the node. Thus the true fluid outlet temperature will be obtained.

Conduction of heat through a bearing is controlled by index 51. The actual heat transfer coefficient which contains a conductivity, area and a path length term is calculated in the bearing portion of the program. The term is based upon an average outer race and inner race rolling element contact.

5.4.9 Card Type 9

This card inputs data required to calculate the heat capacity of each node in the system. This card type is required only for a transient analysis.

5.5 DATA SET IV - SHAFT INPUT DATA

The shaft-bearing analysis requires all loading to be applied to the shaft. The loads applied to each bearing are a product of the shaft-bearing solution. There is no need for the user to solve the statically determinant or indeterminate system for bearing loads. Even if a single bearing is being analyzed with the applied load acting through the center of the bearing, data for a dummy shaft must be supplied.

In the analysis the housing is assumed to be rigid. Provision has been allowed to input data for housing radial and angular spring characteristics. However, this has been done for future consideration of an elastic housing and is not used.

The shaft input data consists of three card types:

- 1) Shaft Geometry and Elastic Modulus Data
- 2) Bearing Position and Mounting Error Data
- 3) Shaft Load Data

5.5.1 Card Type 1

This card type is used to describe shaft geometry at up to twenty locations along the shaft. The user must place his shaft in a cartesian coordinate system with the end of the shaft at the origin and with the shaft lying along the X-axis.

The shaft may have stepwise and linear diameter variations. The stepwise variations require a single card which specifies different diameters immediately to the left and right of the relevant X shaft coordinate. The shaft analysis assumes a linear diameter variation if on two successive cards, i.e. two successive X coordinates, the diameters to the right of the location differ from the diameters to the left of the location

of the following card. Complex shaft geometries may be approximated with a set of linear diameter variations spaced at close intervals.

If an Elastic Modulus is not specified at the designated input location, the modulus of steel is assumed.

5.5.2 Card Type 2

This card type locates the bearing inner ring on the shaft in the X-Y and X-Z planes. For a ball bearing, the X coordinate specified locates the inner ring center of curvature. For cylindrical roller bearings the X coordinate locates the center of the inner race roller path.

In addition to specifying bearing location, the Type 2 card is also used to specify housing radial and angular mounting errors. As mentioned previously, space has been reserved for inputting housing radial and angular spring characteristics, however, these characteristics are not used in the system analysis.

Two sets of Type 2 cards may be required. The first set is always required and defines housing alignment errors in the shaft X-Y plane. The second set defines the housing alignment errors in the shaft X-Z plane and is required only if non zero errors exist for the particular bearing in question.

The first set of Type 2 cards must contain a card for each bearing.

5.5.3 Card Type 3

Type 3 cards are used to specify shaft loadings at a given X coordinate. Loading may be applied in the x-y and x-z planes, thus requiring two distinct sets of Type 3 cards. Applied loads may have the form of concentrated radial forces, concentrated moments, linearly distributed radial forces and concentrated axial loads which may be eccentrically applied. If an axial load is eccentrically applied, the moment which results must not be separately calculated and input as a concentrated moment.

Variations in distributed radial loads are handled at input just as shaft linear diameter variations are handled.

Note that each set of Type 3 cards must be followed by a blank card.

SECTION 6

COMPUTER PROGRAM OUTPUT

6.1 INTRODUCTION

The Program Output is intended to provide the engineer or designer with a complete picture of a shaft-bearing system's performance.

In addition to the calculated output data, the input data is listed, thus producing a complete record of the computer run.

A sample set of program output is included for reference as Appendix C and represents the solution for a single 125 mm bore angular contact ball bearing operating at 25,000 rpm under a thrust load of 3,280 lbs. (14,679 Newtons) with MIL-L-7808G lubricant.

The first seven pages of output essentially consists of a summary of the input data categorized into bearing, cage, steel, lubricant, fit temperature, and shaft geometry and loading data.

Included in the list of input data pertinent to the bearing are the results of bearing geometry calculations which pertain only to the split inner ring ball bearing. Typically the split inner ring cold, free contact angle and shim width are specified by the user at input. The program calculates the shim angle, diametral play, diametral clearance as measured with the shim in place between the two inner ring halves, and the bearing end play. The input need not be limited to the specification of shim width and contact angle. The input instructions are made explicit in Section 5. Regardless of the specific geometry data which is input, all of the geometry information listed above is calculated and printed.

For four specific lubricants evaluated under U. S. A. F. Contract F33615-72-C-1467 the relevant lubricant data has been coded into the Program. In this case the lubricant input information consists only of a single number which designates the particular lubricant but the relevant information for the lubricant is printed in the input data list.

Except as just noted the actual results of calculations are printed under the headings "Bearing Output" and "Rolling Element Output".

Key output items are discussed briefly below.

6.2 BEARING OUTPUT

6.2.1 Linear and Angular Deflections

These deflections refer to the bearing inner ring relative to the outer ring and are defined in the inertial coordinate system of Fig. 3-1. The bearing deflections are not necessarily equal to the shaft displacements since the bearing outer ring radial or angular mounting errors may be specified as nonzero input.

6.2.2 Forces and Moments

These values reflect bearing reactions to shaft applied loading and outer ring mounting errors.

When the bearing inner ring has achieved an equilibrium position, the summation of all bearing reaction loads should numerically equal the shaft applied loading. When the level of solution indicated by "NPASS" = 1 is employed, as discussed in Section 5, differences between shaft applied and bearing reaction loads will exist but will typically be less than 10%.

6.2.3 Friction Heat Generation Rate (watts)

The various sources of frictional heat generated within the bearing are listed. The values printed for "OUTER, INNER, CAGE-ROLLING ELEMENT" and BALLDRAG represent the sum of the generated heats for all rolling elements. Additionally the heats printed for the first three items reflect the friction developed outside the concentrated contacts i.e. the HD friction as well as the EHD friction developed within the concentrated contacts. Items 1 and 2 also include any heat generated as a consequence of asperity contacts. Asperity friction is neglected in the cage-rolling element contacts. "BALL DRAG" should be interpreted as the heat resulting from lubricant churning as the rolling elements plow through the air-oil mixture.

6.2.4 Torque

The torque value is calculated as a function of the total generated heat and the sum of the inner and outer ring rotational speeds. The intent is to present a realistic value of the torque required to drive the bearings. Under conditions of inner ring rotation the torque value reflects the torque required to drive the inner since the inner ring torque also includes that fraction of torque required to impart an angular velocity to the lubri-

cant in the test bearing. A considerable portion of the lubricant will come to rest within the housing and not at the outer ring.

6.2.5 Fatigue Life (Hours)

The L_{10} fatigue life of the outer and inner raceways as well as the bearing are presented. The bearing life represents the statistical combination of the two raceway lives. These lives reflect the combined effects of the lubricant film thickness and material life factors. The lubricant film thickness life factor is described in detail in Section 4.

6.2.6 h/σ

h/σ , commonly referred to as Λ , is printed for the most heavily loaded rolling element. h represents the EHD plateau film thickness with thermal and starvation effects considered. σ represents the composite root mean square surface roughness of the rolling element and the relevant raceway.

6.2.7 Life Multipliers

6.2.7.1 Lubrication - This life multiplier is a function of h/σ at each concentrated contact and is in the form of derating factor. Its value ranges from 0.479 for $h/\sigma = 0$ to 1.0 at $h/\sigma = 4$. Since the lubricant life multiplier is decremental the normal multiple of 3 used for thick film lubrication must be multiplied by the material life factor normally used and this product should be specified at input. This subject is covered in more detail in Section 5.

6.2.7.2 Material - This output simply reflects the input value. Again, it is covered in Section 5.

6.2.8 EHD Film Data for the Most Heavily Loaded Rolling Element

6.2.8.1 Friction Coefficient - These values are the arithmetic average, over the 21 slices into which the contact ellipse is divided, of the fluid EHD friction coefficient for inner and outer race contacts. The actual friction coefficient varies throughout the contact, dependent upon pressure, and rolling element/race sliding and rolling speeds.

The effective friction coefficient i.e. the total tractive force at the contact divided by the normal load is different from and generally higher than this value as it includes a contribution from the asperity borne portion of the normal load as explained in Section 4.

6.2.8.2 Corrected Film - These values refer to the calculated EHD plateau film thickness at both contacts and include the effects of the thermal and starvation reduction factors.

6.2.8.3 Thermal Reduction Factor - These factors pertain to the EHD film thickness for both the inner and outer race contacts of the most heavily loaded rolling elements, but are applied to the respective inner and outer race film thickness for each rolling element in the bearing.

6.2.8.4 Starvation Reduction Factor - These factors give for the inner and outer ring contacts, the reduction in EHD film thickness ascribable to lubricant film starvation using the model described in Section 4.

6.2.8.5 Meniscus Distance (mm) - These quantities are the distance in mm from the contact center to the point in the inlet along the rolling direction at which the lubricant pressure rises above ambient.

6.2.9 Lubricant Temperatures and Physical Properties

The lubricant properties, particularly the dynamic viscosity and to a lesser degree the pressure viscosity coefficient, are heavily temperature dependent. These factors enter the EHD film thickness calculation and the HD and EHD friction models. The lubricant is assumed to be at the same temperature as the relevant raceway. As noted elsewhere these temperatures may be either input directly or calculated by the Program.

The physical properties printed are self explanatory. The units are enumerated.

6.2.10 Ring Speeds

The input values for the outer and inner ring speeds are printed both in revolutions per minute and radians per second.

6.2.11 Calculated Cage Speed

The calculated cage speed will differ from the epicyclic speed (see below) only when the friction solution is employed. The calculated cage speed reflects a steady state speed considering all of the friction forces which develop within the bearing.

6.2.12 Epicyclic Cage Speed

Epicyclic cage speed is the average ball orbital speed as calculated under the assumption that the balls move with the speed dictated by the outer race control assumption.

6.2.13 Percent Difference

This value reflects the difference between the calculated cage speed and the speed obtained from the outer race control assumption.

6.2.14 Fit Pressures

These data refer to the pressures built up as a consequence of interference fits between shaft and inner ring and housing and outer ring. Pressures are presented both for the standard cold-static condition (15.667°C) and at operating conditions.

6.2.15 Clearances

"Original" refers to cold unmounted clearance which is specified at input if the diametral clearance change analysis is executed. "Change" refers to the change in diametral clearance at operating conditions relative to the cold unmounted condition. A minus sign indicates a decrease in clearance. "Operating" refers to the clearance at operating conditions. For all types of ball bearings the decrease in clearance can be combined with the initial diametral clearance, and the free operating contact angle at operating conditions may be calculated. Note that the change in clearance should be compared against the diametral play of the split inner ring ball bearing in order to determine if the possibility for three point contact exists. The Program does not account for three point contacts even though the change in clearance might suggest that three point contact is obtained.

6.2.16 Speed Giving Zero Fit Pressure (Between the shaft and inner ring)

This is a calculated value based upon operating conditions and provides a measure of the adequacy of the initial shaft fit.

6.3 ROLLING ELEMENT OUTPUT

This output is printed for each ball azimuth position.

6.3.1 Ball Speeds

All of the ball speeds tend to vary from position to position when the bearing is subjected to combined loading.

The total absolute ball speed is with reference to a fixed frame and represents the vector sum of the four components. The component ω_x and orbital speed ω_o are additive but opposite in sign.

6.3.2 Speed Vector Angles

The ball speed vector angles, $\text{Arctan}(\omega_y / \omega_x)$ and $\text{Arctan}(\omega_z / \omega_x)$ are presented in order to show a clearer picture of the predicted ball kinematics. The ball speed vector tends to become parallel with the bearing X axis with increasing shaft speed and decreasing contact friction.

6.3.3 Normal Forces

The normal forces acting on each ball are printed. The ball race normal forces are self explanatory. The cage force is calculated only when the friction solution is employed. It is always directed along the rolling element Z axis. If the rolling element orbital speed is positive, a positive cage force indicates that the cage is pushing the rolling element, tending to accelerate it. Cage force is a function of rolling element position within the cage pocket. Its magnitude is derived using hydrodynamic lubrication assumptions, when the distance between the ball and cage web is large, and EHD assumptions when the separation is of the order of the EHD film thickness or when ball cage web interference exists (Section 4).

6.3.4 Hertz Stress

The stress printed represents the maximum normal stress at the center of each ball race contact.

6.3.5 Load Ratio Q_{asp}/Q_{tot}

If the EHD film thickness is small compared to the RMS composite ball-race surface roughness, the ball-race normal load will be shared by the EHD film and asperity contacts. The load ratio reflects the portion of the total load carried by the asperities.

6.3.6 Contact Angles

A ball bearing, subject to axial loading, misalignment or mounted such that the inner ring is always displaced axially relative to the outer ring, (i.e. a duplex set of angular contact ball bearings) will have non-zero contact angles. At low ball orbital speeds the inner and outer race angles will be substantially the same. At high speeds ball centrifugal force will cause the outer race contact angle to be less than the inner race angle.

6.4 THERMAL DATA

Appendix D contains a sample set of thermal output data for the steady state analysis of the helicopter gearbox depicted in Fig. 2-1 and using the node assignment shown in that figure. As in the case for bearing output, all of the input data is printed. The calculated output data is presented in the form of a temperature map in which a node number and the respective node temperature appear. The appearance of the steady state and transient temperature maps are identical. The transient temperature map also includes the time (T) at which the temperature calculations were made.

6.5 PROGRAM ERROR MESSAGES

6.5.1 From Subroutine ALLT

"Steady State Solution with (EP1) degrees accuracy was not obtained after (IT1) Iterations".

This message pertains to the external temperature iteration scheme in which system temperatures and bearing generated heats are being solved for an equilibrium condition.

6.5.2 From Subroutine SHABE

"It was not possible to obtain the change of clearance with an accuracy of (ERFIT) times the rolling element diameter in (ITFIT) iterations".

This message pertains to the bearing diametral clearance change iteration scheme. The solution may be converging in which case the number of iterations (ITFIT) should be increased. This can be checked with an NPRINT = 1 intermediate printout. The intermediate print may indicate that the solution is oscillating. The most likely cause of oscillation is the

alternate prediction of bearing preload with all rolling elements loaded, and then in the next iteration, only a subset of the rolling elements loaded. This problem can usually be overcome by either of two methods.

- 1) In subroutine FIT remove the GO TO 20 statement. This will cause the inner ring load distribution to have no effect on the change in diametral clearance.
- 2) The solution can be damped by redefining the solution damping factor FA, such that it would take on a value $0 < FA < 1$. FA is presently set to 1 in subroutine SHABE. If this damping technique is used, the number of FIT iterations should be increased as the value of FA is decreased. An upper limit of 10 iterations is recommended.

6.5.3 From Subroutine SOLVXX

- 1) "SINGULAR SET OF EQUATIONS"

This message might occur when the thermal input data is not input properly.

- 2) "THE LIMIT FOR NUMBER OF ITERATIONS IS REACHED"

This message might occur either during an internal thermal solution or bearing solution. Before increasing the number of iterations check the equation residue values. If they are low, the solution may be good enough.

- 3) "THIS IS THE BEST WE CAN DO. IT MAY BE USEABLE."

This message reflects the fact that the next iteration will result in divergence. The iteration procedure is thus terminated. The equation residue values should be checked, if they are low, the solution may be useable.

As noted above the occurrence of messages 2) and 3), do not necessarily mean that the solution is not good. Generally the messages indicate that the solution has not converged as tightly as the user has requested.

Note: SOLVXX Subroutine is used to solve the internal thermal solution scheme and the rolling element and cage quasi-dynamic equilibrium scheme. The XX suffix on SOLV specifies the version of SOLV contained in the user's program. As of this writing the current version is SOLV12. The suffix is changed each time improvements are made which require a change in the SOLVXX calling sequence.

6.5.4 From Subroutine INTFIT

"Singular matrix on tight shaft fit"
"Singular matrix on loose shaft fit"

These messages reflect an error in the input data usually as a consequence of inconsistent component diameters, such as the shaft inside diameter being greater than the outside diameter.

6.6 GUIDES TO PROGRAM USE

The Computer Program is a tool. As with any tool the results obtained are at least partially dependent upon the skill of the user. Certainly the economics of the Program usage are highly dependent upon the user's technical need and discriminate use of Program options.

Some general guides for efficient use of the Program are listed below:

1. Attempt to use the lowest level of solution possible. For instance if the prime object of a given run is to obtain bearing fatigue lives, execute only the elastic solution (NPASS = 0). If an estimate of bearing frictional heat is required, execute the low level friction solution (NPASS = 1). Execute the higher level friction solution only if the bearing reaction loads deviate substantially from the shaft applied loading, i.e. a deviation greater than ten percent.
2. Attempt to input bearing operating diametral clearance rather than calculate it. Or, execute the diametral clearance change analysis once for a group of similar runs and use the output from the first run as input to the subsequent runs omitting the clearance change analysis.
3. Attempt to input accurate operating temperatures rather than calculate them.
4. The more nonlinear the problem the more computer time required to solve it. In the bearing friction solution large coefficients of friction seem to increase the degree of nonlinearity. In the thermal solutions, if possible, eliminate nonlinearities by omitting radiation terms and by using constant rather than temperature dependent free and forced convection coefficients.

5. In the transient thermal solution, space the calls to the shaft-bearing solution (BTIME) to as large an interval as prudently possible.
6. In the steady state thermal analysis attempt to estimate nodal temperatures on a node by node basis. Nodes which are heat sources should have higher temperatures than the surrounding nodes.

The above suggestions are intended to encourage the use of the Program on a cost effective basis. The intent is not to discourage the use of important program capabilities but to emphasize how the program should be most effectively used.

It is suggested that the user take a simple, axially loaded ball bearing problem and execute the program through the full range of options beginning with a frictionless solution proceeding to the low and high level friction solution with a low (0.01) and high (0.1) friction coefficient. The diametral clearance change analysis and the thermal solutions should also be executed on an experimental basis. This exercise will provide the user with some insight into economics of the Program usage on his computer as well as the results obtained from various levels of solution of the same problem.

It is also suggested that a constant user of the program should study the hierarchical Program flow chart (Fig. 2-4) along with the Program listing to gain an appreciation of the program complexity and the flow of the problem solution. The Program is comprised of many small functional subroutines. Knowledge of these small elements may allow the user to more easily piece together the philosophy of the total problem solution.

SECTION 7

DISCUSSION OF PREDICTIVE ACCURACY

In order to evaluate the predictive accuracy of computer program AT74Y001 a series of full scale bearing tests were run using a rig capable of simulating the thermal, speed and loading environment of a high speed aircraft turbine engine. Heat generation rate, cage and ball rotational velocity and a measure of the lubricant film thickness were monitored at many combinations of load and speeds with the speeds ranging up to 3.1×10^6 DN.

This section contains a description of the test rig, the methods used to measure heat generation rate, cage and ball speeds, the quantitative interpretation of conductivity data and a comparison of the measured and predicted results.

7.1 TEST RIG DESCRIPTION

A layout drawing of the rig is presented in Fig. 7-1. A description of the major rig components follows.

7.1.1 Rig Structural Components

The rig is designed to simulate a single aircraft turbine engine mainshaft thrust bearing installation utilizing a 125 mm bore - 190 mm O.D. bearing. To this end it avoids thick sections in the shaft and bearing housing and uses flexible bearing housing supporting sections. This flexibility is intended to simulate the self-aligning ability of current aircraft engine bearing mounts.

The rig proper consists of a 12" diameter cylindrical housing of Inconel X-750 in which a hollow shaft of the same material and approximately 5" in outside diameter is supported by the test bearing at one end and by a 7019 size (95 mm bore - 145 mm O.D.) angular contact ball bearing (referred to in this report as the "rig" bearing) at the other end. The housing itself is mounted in a horizontal position on a table by means of a special support system which maintains centerline height and parallelism with the table while freely permitting both radial and axial thermal expansion of the rig.

7.1.2 Thrust Application and Measurement System

The test bearing outer ring housing is not attached directly to the outer rig housing but rather is supported within a "load plug" assembly which itself is supported within the main rig housing by two angular contact bearings (referred to as

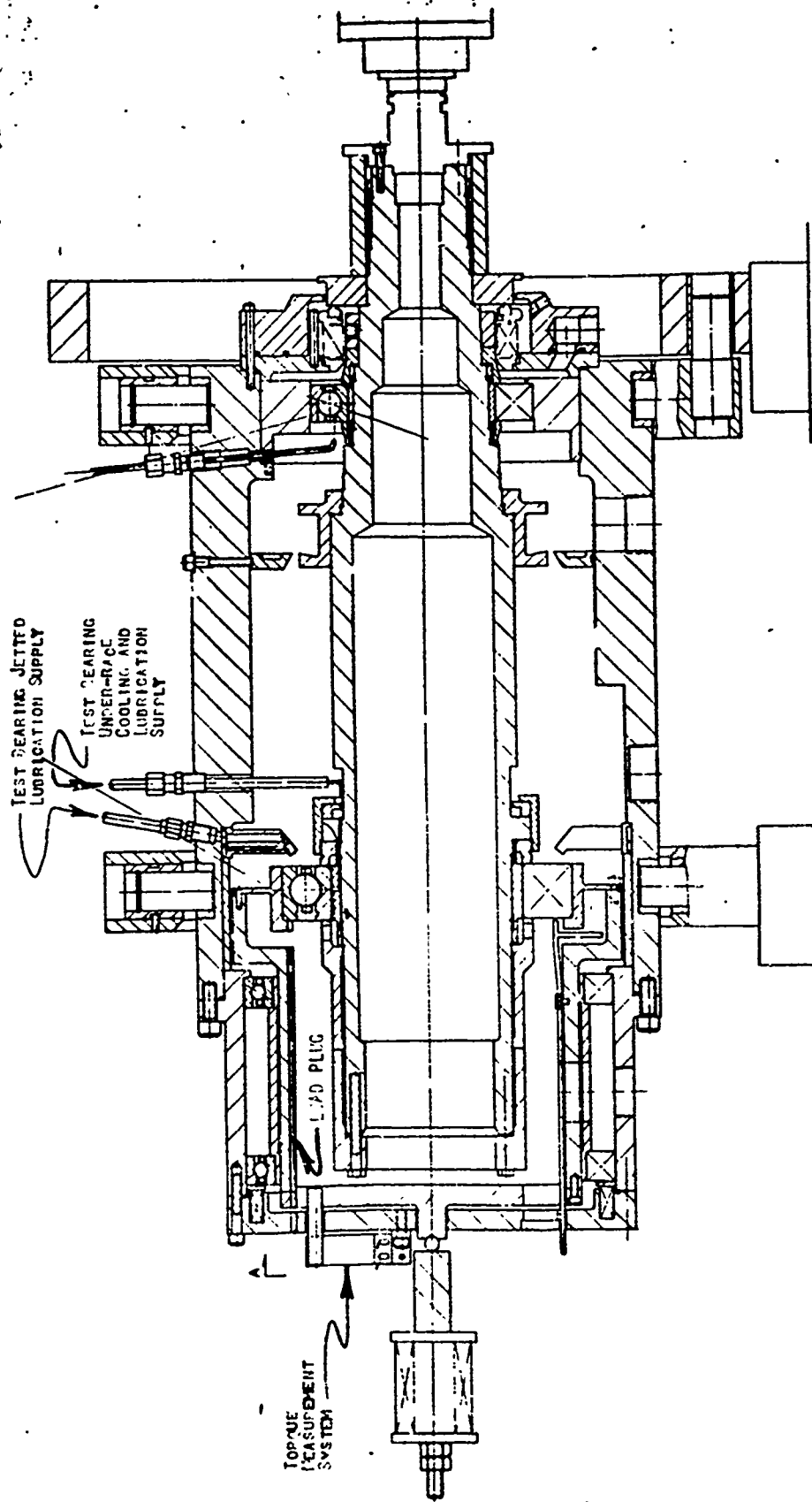


FIGURE 7-1
TEST RIG FOR FULL-SCALE BEARING TESTS

the "load plug" bearings) mounted in a face to face arrangement. A sliding fit is provided between the inner ring mounting sleeve for these angular contact bearings and the O.D. of the load plug. The axial and rotational movement capability which is attendant to this method of supporting the load plug provides a means of applying thrust to the test bearing and of measuring the bearing's torque. Thrust load is applied directly to an extension of the load plug which projects through a hole in the rig end plate. A spring loaded beam, reacting against the rig end plate, exerts thrust on this load plug extension through a ball to flat contact. The load beam is equipped with a temperature compensated strain gage system to provide thrust measurement capability. The thrust load, imparted in this manner to the rig shaft through the test bearing, is reacted by the previously mentioned 7019 angular contact bearing on the other end of the shaft.

7.1.3 Torque Measurement System

Test bearing torque measurement is permitted by the fact that the load plug assembly is free to rotate in its supporting angular contact bearings and at the ball to flat thrust application point. During operation of the rig the load plug assembly is restrained from rotating by a flexible "torque arm" attached to the end plate of the rig. The torque arm is provided with a temperature compensated strain gage system to allow continuous recording of test bearing torque during testing.

7.1.4 Rig Drive System

The rig drive system is shown diagrammatically in Fig. 7-2. A constant speed 75 HP motor drives the test rig through an eddy-current clutch to provide variable speed.

The motor and clutch combination, mounted on an adjustable base bolted to the rig table, drives a jackshaft through a flat belt drive. The jackshaft unit consists of a hollow shaft mounted in matched pairs of preloaded angular-contact bearings with a 3" diameter removable slightly crowned pulley at its center. The bearings are supported in steel pillow blocks welded to a rigid base and are lubricated by a separate circulating cold mineral oil supply fed to the top cap of each bearing. An oil drain running horizontally across the width of the pillow block returns the oil to the scavenge lines.

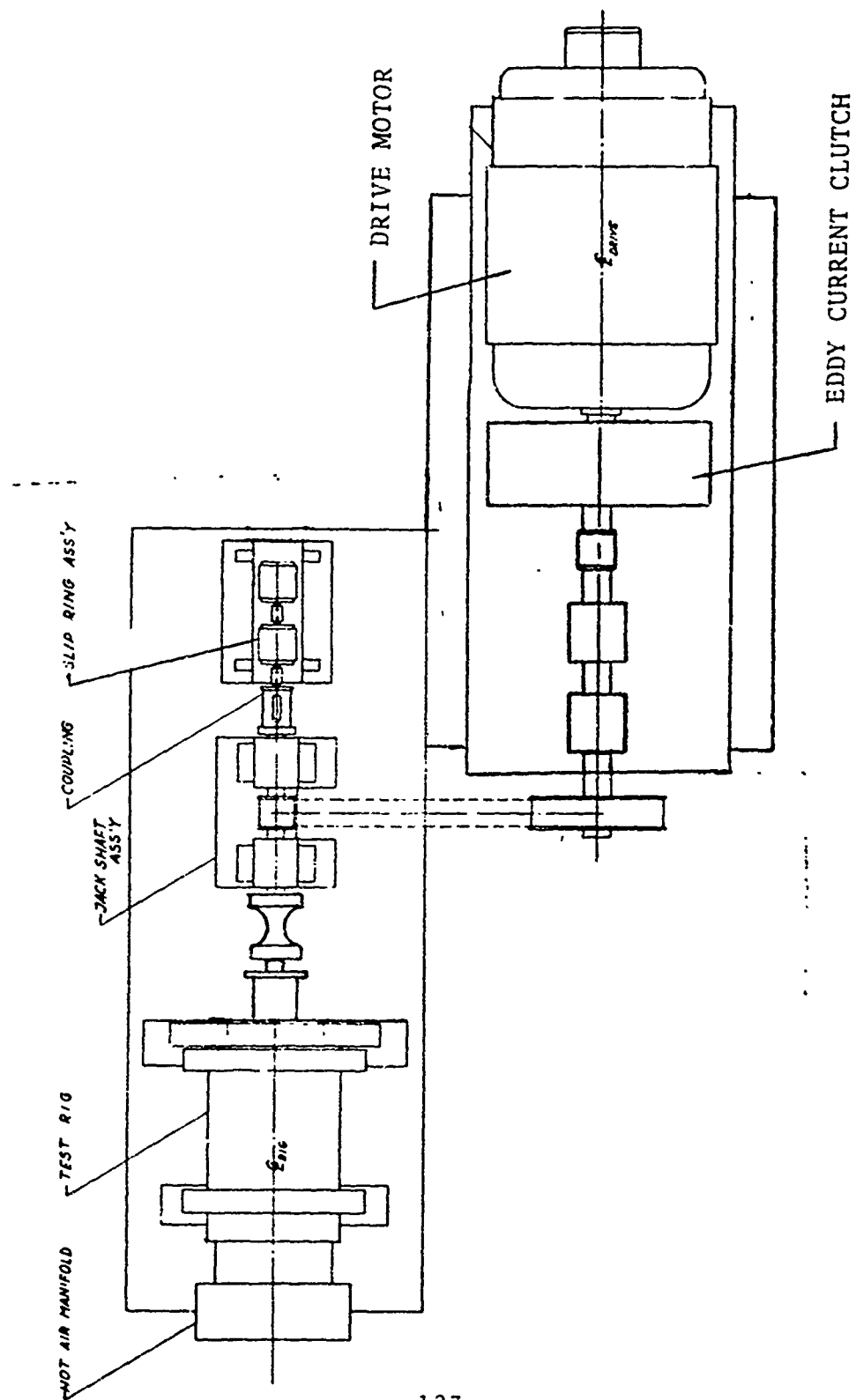


FIGURE 7-2
 TEST RIG - GENERAL PLAN VIEW

The rig shaft is connected to the jackshaft by a Koppers gear coupling. The other end of the jackshaft drives the slip ring and tachometer assemblies through a rotating electrical connector and a small flexible coupling. The jackshaft is hollow to carry the wiring from transducers in the test rig to the slip rings. Shear pins are provided in the base of the motor pulley to permit rapid stoppage of the rig in the event of seizure of a rotating component within the rig. A plain bearing is fitted to the motor shaft to prevent damage to the surfaces in the event of shear pin breakage.

7.1.5 Test Oil Recirculating and Conditioning System

Oil circulation proceeds from an internal-gear-type pump, a filter unit accepting fiberglass elements, through a flowmeter to the rig. The elements have a specified pore size of 20 microns and deliberately have excess flow capacity, by a factor of approximately $2\frac{1}{2}$, in order to secure low pressure drop and long life, even with oil that is suffering some thermal degradation.

The system oil tank is also designed to act as a defoamer. Oil from the rig drain manifold enters the top of the tank, which is below rig level, in a direction tangential to the cylindrical inside surface of the tank. The swirling motion set up in this way allows time for entrained air to separate from the oil. The oil then collects in the bottom of the tank where it is drawn out by the supply pump, either through an oil cooler or through a cooler by-pass line. The air passes on to the test cell exhaust system. A certain amount of residual oil vapor is carried away by the departing air. The air is therefore passed through a water-cooled condenser to remove as much of this entrained oil as possible.

Both the condenser and the rig's oil cooler are cooled with water from a central recirculating water system. The oil-inlet temperature to the rig is maintained at specified limits by controlling the water flowrate to the cooler.

The oil tank and defoamer unit will accommodate six gallons of lubricant which, together with the capacity of the pipes, pump, filter and inlet manifold, gives a maximum rig oil capacity of approximately $6\frac{1}{2}$ gallons.

To keep the system oil capacity to a minimum the rig's oil heating system is integral with the oil tank. Heat is supplied to the oil through the cylindrical inside surface of

the oil tank by surrounding it with an oil heater. To preclude the possible occurrence of local "hot-spots" in the heater, which could lead to premature coking of the oil on the tank surfaces, liquid metal is used as a heat transfer medium. The metal selected for this purpose is a lead-bismuth-tin eutectic which has a melting point of 158°F. This is directly heated by a 230V 12kw electric immersion heater. Corrosion problems with this liquid are minimized by the use of carbon steel for the outer container and heat sheath and by using hard chromium plating on the surfaces of the oil tank which are exposed to the liquid metal.

After performing its function in lubricating and cooling the test and rig bearings, the oil is returned to the oil tank by the drainage system. This system contains a scavenge pump with gravity feed providing suction head.

All components of the overall lubrication system, including the oil tank, the heat exchanger, and the condenser, are designed for ready disassembly and cleaning. To this end the system is provided with a number of extra flanged joints. Threaded connections are avoided wherever possible.

7.1.6 Bearing Inner Ring Mounting Sleeves

The bearing inner ring mounting on the test rig shaft must restrain the ring from rotation on the shaft and at the same time not induce excessive mounting stresses or deflections affecting the internal clearance in the bearing. The ring materials selected for the test and rig bearings, M-50 and 52100 respectively, both have lower coefficients of thermal expansion than the shaft material, Inconel X-750. If the normal practice of fitting the bearing inner rings directly onto the shaft with a slight interference fit were employed, excessive tensile hoop stress would be generated at operating temperature due to the unequal thermal expansions of the two materials. This could lead to ring fracture or a significant reduction in internal bearing clearance. M-1 steel sleeves are therefore interposed between the shaft and inner rings of the test and rig bearings. These are of the form shown in Figure 7-3 and have a gap at room temperature between the shaft and the inside surface of the sleeve under the bearing. Rotation of the sleeve on the shaft is prevented by an interference fit between the shaft and the thinned-down ends of the sleeve. Radial location of the bearings at low temperatures is achieved by the bending stiffness of the sleeves. As the temperature rises during the heat-up period and the shaft expands it

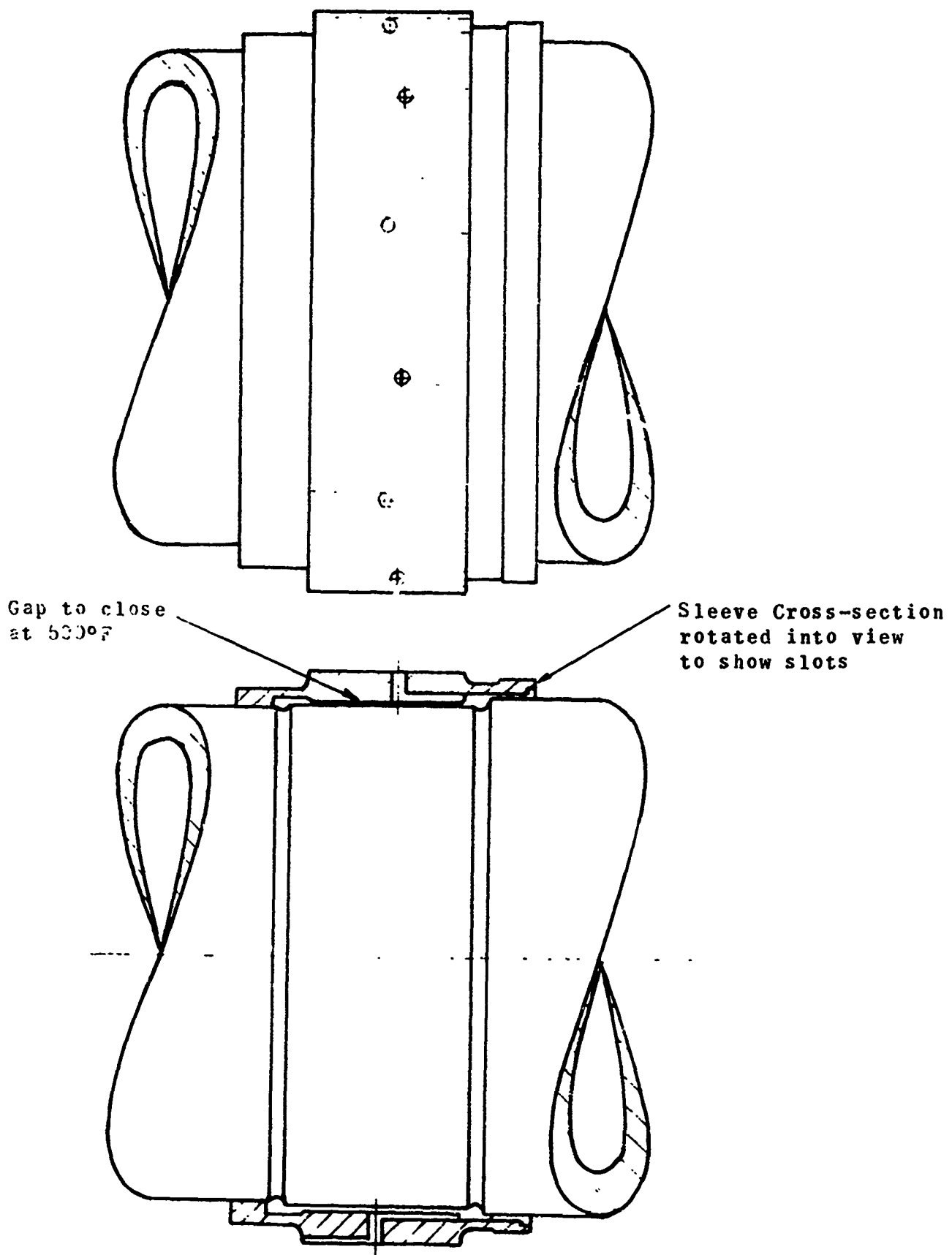


FIGURE 7-3

BEARING INNER RACE MOUNTING SLEEVE

progressively closes the gap under the sleeve until contact occurs at a temperature of 500°F. It should be noted that the under-race cooling and lubrication flow holes shown in the sleeve in Figure 7-3 are present only in the sleeve used with the split inner race test bearing. The rig angular contact bearing on the other end of the shaft utilizes a similar mounting sleeve without these holes.

7.1.7 Instrumentation Used in Full Scale Bearing Testing

The output of transducers located at various points in the test rig are recorded on two recorders. One of these is a continuous recording Honeywell two-pen strip chart recorder and the other is a commutated multipoint recorder with a forty-eight point capacity. The use of the two-pen strip chart recorder permits bearing inner and outer ring temperatures to be continuously monitored during testing. This allows evaluation of any excursion in these parameters which might occur. Any of the parameters recorded discretely on the multipoint recorder may also be plugged into the two-pen recorder at any time for continuous monitoring.

The multipoint recorder records the value of each parameter every 70 seconds. The following are recorded, in duplicate in most cases:

- oil outlet temperature
- oil tank heater temperature
- test bearing chamber temperature
- rig housing temperature, test bearing end
- rig housing temperature, rig bearing end
- drive system jackshaft pillow block temperature
- rig bearing outer ring temperature
- test bearing outer ring temperature
- test bearing inner ring temperature

In addition the following data is collected manually:

- rig running time
- shaft speed
- motor current
- motor voltage
- current to all rig heaters
- test bearing oil flow rate
- applied thrust load
- oil pump outlet pressure
- oil inlet temperature

7.2 EXPERIMENTAL EVALUATION OF CAGE AND BALL ANGULAR VELOCITIES

In all eleven tests performed on this program both ball and cage speeds of the test bearing were experimentally determined by the use of dual differential induction coils (search coils) wound concentric with the bearing axis and placed on the inboard side of the test bearing from the bearing face. A cutaway view of the search coil is shown in Figure 7-4. As described in [5] the dual differential coil design was conceived as a means of deducing the ball rotational axis position as well as the ball and cage rotational speeds. Use in this mode however requires a series of calibration tests which could not economically be fit into the test schedule without displacing work judged to be more urgently needed. The search coil was therefore used in the single element mode.

One of the bearing balls was permanently magnetized as a dipole to obtain approximately 28 Gauss maximum residual flux density at the ball surface. As the magnetized ball rotates about its own axis the magnetic flux is cut by the coil producing a variable voltage proportional to the flux being cut.

The amplitude of the search coil voltage depends on the angle between the magnetic axis of the magnetized ball and the axis of ball rotation. The induced voltage is at its maximum when the magnetic axis is perpendicular to the ball rotational axis and at a minimum when the magnetic axis of the ball is parallel to the rotational axis of the ball. Thus a change in the sensed voltage at constant operating speed, indicates a change in axial position of the ball spin axis. Variations of the frequency of the induced voltage indicate changes in ball rotational speed produced by sliding, changes in contact or pitch angle, or a change in the shaft speed.

The search coil axis was assembled at a slight angle with respect to the bearing producing a uniformly varying gap between the face of the bearing and the coil. This gap which results in a change in the reluctance of the magnetic path at different azimuth positions of the bearing produces a modulation in the sensed voltage which is equal to the mean ball orbiting velocity or cage angular velocity.

The induced voltage/time traces were recorded at specific conditions during each test while visually observing the signal presentation on an oscilloscope. The ball and cage angular velocities were then established by analyzing the tape recorded data.

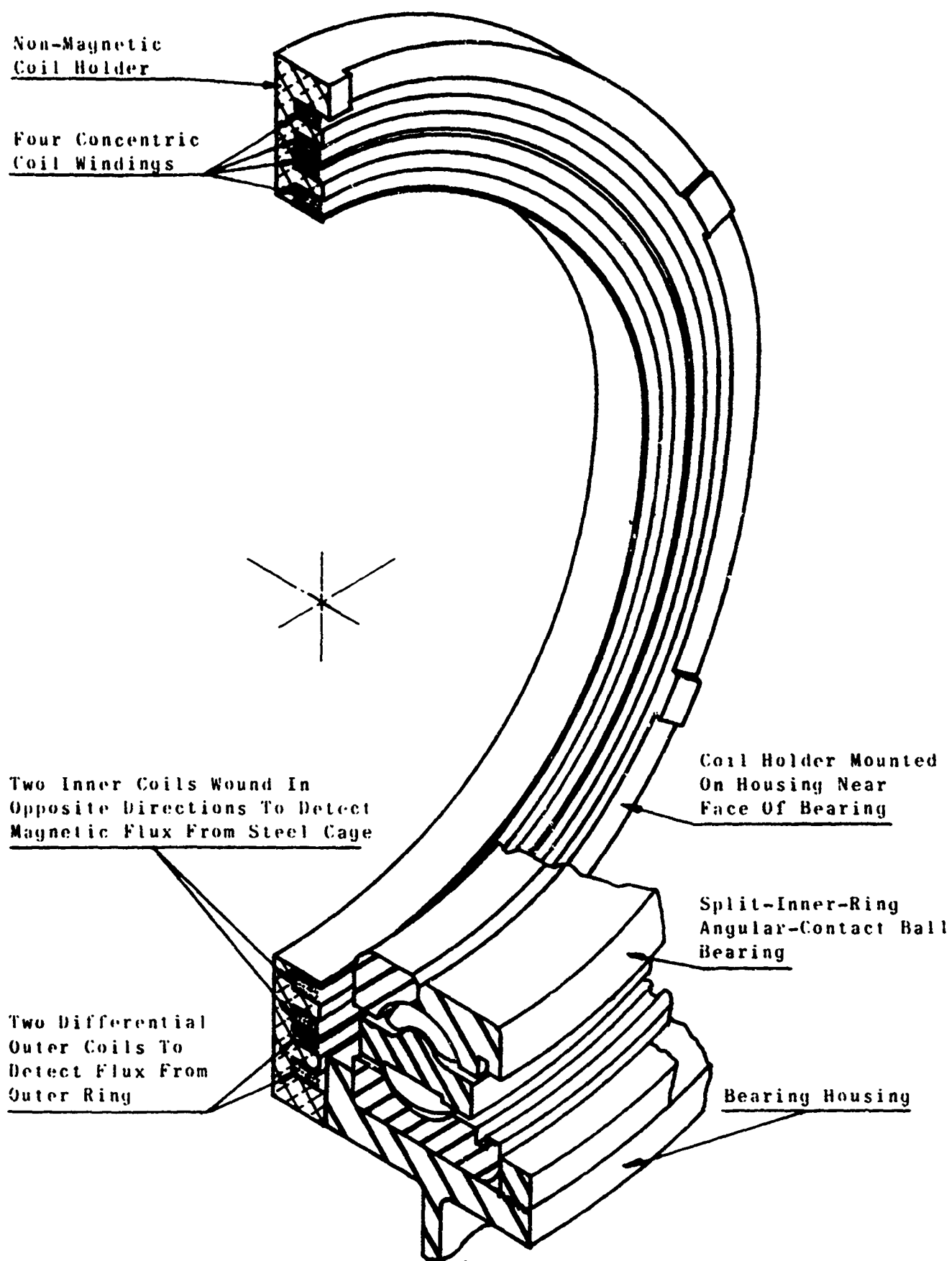


FIGURE 7-4

SEARCH COIL DESIGN

It was found that the modulation of the signal was insufficient to determine the cage velocity by electronic counting. Therefore, the signal was presented on a high speed writing oscillograph while replaying at a reduced recorder speed. A known frequency signal was also recorded on the visicorder paper at the same time. By utilizing the ratio of recording to playback speed and the ratio of the known signal frequency to cage frequency as presented on the visicorder paper the cage speed was determined. To minimize evaluation error the data was analyzed over several cage cycles for each test condition.

The amplitude of the ball frequency signal was sufficient in magnitude to permit evaluation by feeding a clipped signal directly into a counter. During this analysis the tape was played back at the recorded speed permitting direct frequency evaluation. A ten second gate was used during this evaluation with a fixed display time between counts. Four to six counts were recorded for each test condition. If appreciable variation was noted, the maximum, minimum and average frequencies were recorded. To minimize possible evaluation error, the ball frequencies were also periodically checked on the visicorder traces.

7.3 DESIGN OF THE TESTS

The test bearing used in these tests was a 125 mm bore split inner ring angular contact aircraft quality bearing (S K F No. 456939) having an inner land riding cage. The test variables were axial load, inner ring rotational speed and lubricant type. Two lubricants were used corresponding to MIL-L-7808G and MIL-L-23699 specifications.

Table 7-1, shows the bearing test matrix. Three loads 1,000, 2,000 and 3,280 pounds are shown as the columns of Table 1. The two lubricants represent the major row divisions. For each load and lubricant, data was recorded at speeds in the range from 4,000 to 25,000 rpm. The numbers shown in the body of Table 7-1 indicate which of eleven test series were conducted at the given conditions. A total of three ball bearings were tested. One bearing was used in Test Series No. 1, another in Series 2-10 and a third in Series 11. In Test No. 5 the bearing was brought to a temperature of approximately 460°F and allowed to soak at that temperature for a period of time sufficient to cause a varnish to be deposited on the bearing from lubricant degradation products. (This was confirmed in post test inspection.) This bearing was then used in Test Series 6 through 10. In Series 11 a fresh bearing was used and run at speeds from 8,000 to 25,000 rpm at the highest load.

	p = 1000 lbs.	p = 2000 lbs.	p = 3280 lbs.
MIL-L-23699	2 2 2 2 2 2 2 2	2 2 2 2 2 2 2 2	2 2 2 2 2 2 2 2
	3 3 3 3 3 3 3 3		
	c c c c c c c c	c c c c	
MIL-L-78086	1 1 1 1	4 4 4 4 4 4 4 4	4 4 4 4 4 4 4 4
	(6) (6) (6) (6)	5 5 5 5 5 5 5 5	(8) (8) (8) (8) (8) (8) (8) (8)
	c c c c		
	4 6 8 10 12.5 15 17.5 20.0 22.5 25		
		11 11 11 11 11 11 11 11	11 11 11 11 11 11 11 11
		c c c c c c c c	c c c c c c c c
			(9) (9) (9) (9) (9) (9) (9) (9)

() Bearing Varnished
c indicates a computer solution has been obtained for that set of conditions

Table 7-1
Bearing Test Matrix

The test number for those tests in which the bearing was in a varnished condition is shown parenthesized in Table 7-1. The letter C in Table 1 indicates that a computer solution has been obtained for that set of conditions.

Table 7-2 shows the conditions of a special test series conducted at 10,000 rpm in which the load was varied from 200 to 2,000 pounds in order to examine whether skidding occurred. For the unvarnished bearing these tests were conducted as part of Test Series No. 4. With the varnished bearing they were conducted as Test Series No. 7.

7.4 TEST BEARING HEAT GENERATION RATES

Two methods were designed into the test rig to establish the thermal energy expended in the test bearing namely 1) direct measurement of the test bearing torque, and 2) measurement of the recirculating oil temperature entering and leaving the test rig bearing and the oil flow rate supplied to the test bearing. The accuracy of the bearing torque measuring device depended upon the freedom of rotational motion of the load plug. As described in Section 7.1.3 the load plug was supported on two torque tube bearings to provide the desired rotational freedom. It was noted during the test series that at speeds above 8,000 rpm, the friction in the torque tube bearing became excessively high, thus preventing accurate test bearing drag torque measurements. This condition was attributed to change in the radial loading of the torque tube bearing resulting from differential thermal expansion between the torque tube shaft (load plug) and housing. Therefore the differential temperature between oil in and oil out was utilized in all bearing heat generation calculations.

Experimental bearing heat generation rates thus determined were established from the recorded data for all tests except 1, 5 and 10 where insufficient information was recorded to perform the necessary thermal calculation.

At speeds up to about 6,000 rpm it was found that due to the loss of heat from the bearing and from the oil to the test rig housing the temperature of the oil leaving the rig was lower than that entering the rig. To compensate for this loss the difference in the measured values, (temperature in minus temperature out) was added to the measured oil out temperatures along with the temperature change corresponding to the thermal energy value equivalent of the measured bearing torque at a speed of 4,000 rpm. The measured torque was considered accurate at a shaft speed of 4,000 rpm as only minimal thermally applied

p = 200	p = 400	p = 600	p = 800	p = 1000	p = 1500	p = 2000
4 c (7)	4 c (7)	4 c (7)	4 c (7)	4 c (7)	4 (7)	4 c (7)

TABLE 7-2

SKIDDING TESTS, MIL-L-7808G, 10,000 RPM

radial loading of the torque tube bearing should exist at that speed. The total correction thus determined was 29°F.

It is reasonable to assume that a larger magnitude of heat would be transferred from the bearing and exhausting oil directly into and through the rig housing at the higher shaft speeds. However, no accurate method of establishing this value could be effected.

Table 7-3 presents the experimental bearing heat generation rates for all tests evaluated. Tests 2 and 3 were performed with MIL-L-23699 lubricant with applied thrust loads of 3280 and 1000 lbs. respectively. These experimental values indicate only minor changes in the bearing heat generation rates with changes in applied loads. The remaining tests were performed with MIL-L-7808G lubricant.

Tests 4 and 7 were performed at a constant speed of 10,000 rpm with variable applied thrust loads in order to evaluate the ability of the computer program to predict skidding of the rolling elements i.e. cage slip. It is noted that the values are higher in Test 7 which was performed after oil was coked and a layer of varnish applied to the test bearing during Test 5.

Test 6 was performed with an applied thrust load of 1000 lbs, Test 8 with 2000 lbs, and Test 9 with 3280 lbs. Test 6 data shows a higher bearing heat generation rate than obtained with the greater applied loads in Tests 8 and 9. This condition could be the result of the varnish formed on the bearing during Test 5. The operating period required to remove the varnish from the ball and race contact areas is not known. The heat generation rates in Test 9 performed with the greater load are slightly higher than those obtained in Test 8.

Test 11 was performed with a new bearing and shaft speeds up to 25,000 rpm (3.1×10^6 DN) are investigated. The heat generation rate values in this test agree quite well with those in Test 9 where the same thrust load (3280 lbs) was applied. Figure 7-5 is a graphical presentation of the measured test bearing outer ring and oil in temperature and the corrected oil out temperature.

Table 7-3

Experimental Bearing Heat Generation Rates

Test No.	Lubricant (MIL-Spec)	Applied Thrust Load (lb)	Shaft Speed (krpm)	Test Bearing Heat Generation Rate	
				(Btu/hr)	(Watts)
2	MIL-L-23699	3280	4	4600	1350
	MIL-L-23699	3280	6	8800	2580
	MIL-L-23699	3280	~	12,900	3780
	MIL-L-23699	3280	10	16,000	4700
	MIL-L-23699	3280	12.5	18,600	5440
	MIL-L-23699	3280	15	27,500	8060
	MIL-L-23699	3280	17.5	33,800	9910
3	MIL-L-23699	1000	4	4100	1200
	MIL-L-23699	1000	6	8300	2430
	MIL-L-23699	1000	8	12,000	3520
	MIL-L-23699	1000	10	16,200	4750
4	MIL-L-7808G	2000	10	15,500	4550
	MIL-L-7808G	1500	10	16,100	4720
	MIL-L-7808G	1000	10	15,500	4550
	MIL-L-7808G	800	10	14,400	4220
	MIL-L-7808G	600	10	13,900	4060
	MIL-L-7808G	400	10	13,300	3900
	MIL-L-7808G	200	10	11,650	3410
6	MIL-L-7808G	1000	4	10,600	3100
	MIL-L-7808G	1000	6	13,000	3810
	MIL-L-7808G	1000	8	15,800	4620
	MIL-L-7808G	1000	10	18,000	5270
7	MIL-L-7808G	1500	10	22,100	6470
	MIL-L-7808G	1000	10	19,500	5710
	MIL-L-7808G	800	10	19,500	5710
	MIL-L-7808G	600	10	18,500	5420
	MIL-L-7808G	400	10	17,000	4960
	MIL-L-7808G	200	10	12,900	3780
8	MIL-L-7808G	2000	4	7,800	2280
	MIL-L-7808G	2000	6	10,400	3040
	MIL-L-7808G	2000	8	13,000	3810
	MIL-L-7808G	2000	10	15,500	4550
	MIL-L-7808G	2000	12.5	19,000	5560
	MIL-L-7808G	2000	15	22,000	6450

Table 7-3 (Continued)

Experimental Bearing Heat Generation Rates

Test No.	Lubricant (MIL-Spec)	Applied Thrust Load (lb)	Shaft Speed (krpm)	Test Bearing Heat Generation Rate	
				(Btu/hr)	- (Watts)
9	MIL-L-7808G	3280	4	7,200	2,110
	MIL-L-7808G	3280	6	10,700	3,140
	MIL-L-7808G	3280	8	14,000	4,100
	MIL-L-7808G	3280	10	17,400	5,100
	MIL-L-7808G	3280	12.5	21,500	6,300
	MIL-L-7808G	3280	15	25,900	5,790
	MIL-L-7808G	3280	17.5	30,200	8,850
11	MIL-L-7808G	3280	8	14,000	3,805
	MIL-L-7808G	3280	10	17,300	5,460
	MIL-L-7808G	3280	12.5	21,900	7,960
	MIL-L-7808G	3280	15	56,500	16,570
	MIL-L-7808G	3280	17.5	30,600	9,731
	MIL-L-7808G	3280	20	35,000	11,450
	MIL-L-7808G	3280	22	38,300	10,800
	MIL-L-7808G	3280	25	43,500	11,830

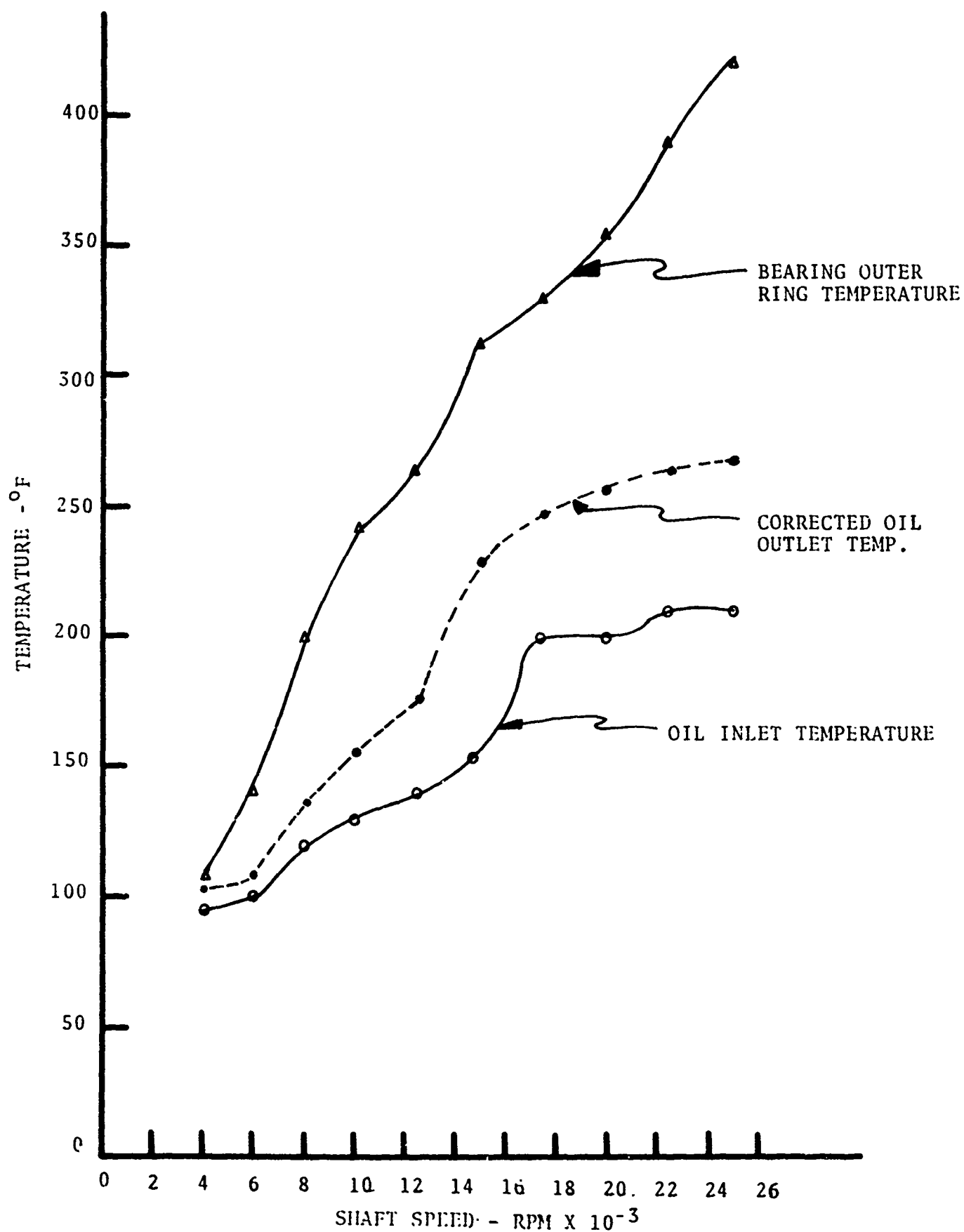


FIGURE 7-5

BEARING AND LUBRICATION TEMPERATURE (TEST 11)

7.5 COMPUTER PREDICTIONS FOR FULL SCALE TESTS

7.5.1 Input Parameter Values

7.5.1.1 Geometry Data - In preparing the input data for the full scale test runs the following geometrical values were used.

Rolling Element Diameter	20.6375 mm
Bearing Pitch Diameter	159.4885 mm
No. of Rolling Elements	21.
Shim Width	0.178 mm
Free Contact Angle	26°
Outer Race Radius/Ball Diameter	0.521
Inner Race Radius/Ball Diameter	0.516
Cage Rail Land Area	2615 mm ²
Cage Rail Diameter	151 mm
Rail-Land Dia. Clearance	0.53 mm
Cage Pocket Tangential Clearance	0.3937 mm
Shaft Interference Fit	0.0762 mm
Bearing Inner Ring Width	18. mm
Bearing Outer Ring Width	32.4 mm
Shaft Inner Diameter	112 mm
Bearing Bore Diameter	125 mm
Bearing Inner Ring Mean O. D.	142.5 mm
Bearing Outer Ring Mean I. D.	176.6 mm
Bearing O. D.	190 mm
Housing O. D.	220 mm

The shaft and housing effective length and widths respectively were taken as 35.0 mm.

Additionally the following surface roughness values were measured on a representative bearing.

RMS Surface Roughness - Outer	6.0×10^{-5} mm
RMS Surface Roughness - Inner	16.0×10^{-5} mm
RMS Surface Roughness-Rolling Element	4.0×10^{-5} mm
RMS Asperity Slope Angle Outer	2.4°
RMS Asperity Slope Angle Inner	2.0°
RMS Asperity Slope Angle - Rolling Element	2.0°

7.5.1.2 Temperature Data - In preparing the input data for the computer runs the various system temperatures were calculated in terms of the outer ring and inner ring bulk temperatures t_{OR} and t_{IR} using the following empirically determined rules:

Outer Ring Raceway/Ball Contact Temperature = $t_{OR} + 10^{\circ}\text{F}$

Bulk Oil Temp = $t_{OR} - 75^{\circ}$ or
Oil Inlet Temp + 5° (whichever is larger)

Housing = t_{OR}

Bearing Inner Ring/Ball Contact Temperature = $t_{IR} + 10^{\circ}\text{F}$

Rolling Element Temperature = $t_{IR} + 15^{\circ}\text{F}$

Shaft Temperature = $t_{IR} - 10^{\circ}\text{F}$

The inner ring bulk temperature t_{IR} was measured directly and found to be reasonably well related to the outer ring bulk temperature at various speeds as follows:

$$t_{IR} = t_{OR} + 6^{\circ}\text{F} + 1.2 \times \text{RPM}/1000$$

This relation was used in preparing the input temperature data.

7.5.1.3 Other Input Parameter Values - The coefficient of coulomb friction was taken to be 0.1 based on the experimental work reported in {6}.

The percentage of lubricant in the air-oil mixture (XCAV) was taken as 2.5% based on a comparison of measured and calculated heat generation rates with various XCAV values using data reported in {20}.

The lubricant replenishment amount $\Delta\zeta$ was taken as 0.01 mm at both rings for all conditions. A calculation of $\Delta\zeta$ using the model described conceptually in Section 4.3.4 was performed for the MIL-L-7808G test at 10,000 RPM and 1,000 lbs. load. The equivalent value of $\Delta\zeta$ was found to be 0.00016 mm and the film thickness starvation reduction factor ϕ_s was calculated as 0.78. The choice $\Delta\zeta = 0.01$ therefore represented an essentially unstarved condition. As discussed subsequently in this section, the film thickness results did not contradict this choice.

Further discussion of the influence of XCAV and $\Delta\zeta$ on the predicted values of bearing performance criteria are given in Section 2.

7.5.2 Comparison of Predicted and Measured Values - MIL-L-7808G Lubricant

Table 7-4 gives the program predicted values of heat generation rate, film thickness at the inner and outer ring contacts, (h_i and h_o), cage speed ω_c and ball speed ω_b for the 7808G tests of Series Nos. 1, 4, and 11.

Also shown in Table 7-4 are the measured values of the no-contact time fraction, T/T_o , heat generation rate q , cage speed, ball speed and outer ring bulk temperature T_{OR} .

7.5.2.1 Heat Generation Rate Prediction - MIL-L-7808G Lubricant - Figure 7-6 is a plot of the experimental heat generation rate computed for Test Nos. 2, 9 and 11 as a function of bearing speed. Except for a high heat generation rate at 15,000 rpm for Test No. 11 the trend of the data is for heat generation to increase with speed and then level off. The data points calculated by Computer Program AT74Y001 increase uniformly with speed. For comparison, plots are also shown of heat generation rate measured in tests conducted at Pratt & Whitney Aircraft under NASA sponsorship {20}. These heat generation rates, obtained with two different values of lubricant mass flow rate in an under-race lubrication supply system, show heat generation rate increasing uniformly with speed. The computer calculated heat generation rates are quite consistent with the Pratt & Whitney data particularly when it is observed that the mass flow rate used in the present tests was 0.167 kg per second. The computer predicted heat generation rates appear to extrapolate well at low speeds to the experimental heat generation rate. One explanation for the goodness of the low speed fit might be that in the lubricant supply system used in the present tests the amount of oil effectively entering the bearing decreases with speed, i.e., a greater proportion is deflected by windage at the higher rotational speeds. Thus at low speeds the effective value of the flow rate \dot{m} may be close to the supply value 0.167 kg per second, while at high speeds the effective flow rate may be closer to the value in the Pratt & Whitney tests with $\dot{m} = 0.045$ kg/sec. There is also, as discussed previously, appreciable room for error in the experimental heat generation rate inasmuch as the corrections applied to the data to compensate for rig cooling were as determined at low speeds, and different corrections may well be applicable at high speeds.

TABLE 7-4

MIL-I-7808G TLST A-3D PROGRAM COMPARISON

Test No.	Speed (rpm)	Load (lbs)	Computer Prediction				(T/To)	Measured				TOR (OF)
			q (watts)	h ₀ (in)	h ₁ (in)	ω_c (rad/sec)		ω_b (rad/sec)	q (watts)	ω_b (rad/sec)	ω_b (rad/sec)	
1	4000	1000	567	18.5	14.7	187	0.86	1686	189	2325	2325	110
1	6000	1000	1159	15.5	12.2	286	0.76	2601	283	2827	2827	145
1	8000	1000	2118	14.1	11.2	387	0.57	3484	377	3544	3544	170
1	10000	1000	3468	11.9	9.1	478	0.25	4247	478	4606	4606	194
1	10000	3280	4898	6.1	5.0	474	0.015	4240	-	-	-	300
1	12500	3280	7450	5.5	4.2	602	0.045	5394	660	5504	5504	335
1	15000	3280	10520	5.5	4.5	735	0.18	6558	754	7012	7012	345
1	17500	3280	13950	5.6	4.5	859	0.12	7658	-	7728	7728	355
11	12500	3280	7787	7.5	6.1	604	0.40	5394	7960	5504	5504	275
11	15000	3280	10610	6.5	5.2	735	0.84	6576	16570	7012	7012	315
11	17500	3280	14180	6.4	5.1	860	0.87	7685	9731	7550	7550	330
11	20000	3280	17970	5.9	4.6	984	0.85	8740	11450	8545	8545	355
11	25000	3280	26530	4.2	2.9	1217	0.65	10734	11830	9048	9048	420
1	10000	200	2982	11.2	9.0	316	0.88	2803	3410	2890	2890	120
1	10000	400	3191	10.0	8.4	376	0.98	3339	3900	3770	3770	160
1	10000	600	3482	12.1	9.7	436	0.94	3918	4060	4273	4273	180
1	10000	800	3610	13.7	11.0	488	0.93	4886	4220	4398	4398	185
1	10000	1000	3613	13.8	11.6	487	0.90	4353	4550	4524	4524	200
1	10000	1500	5307	15.5	13.7	447	0.95	3929	4720	5424	5424	215
1	10000	2000	4052	22.5	20.5	482	0.90	4364	4550	4524	4524	205

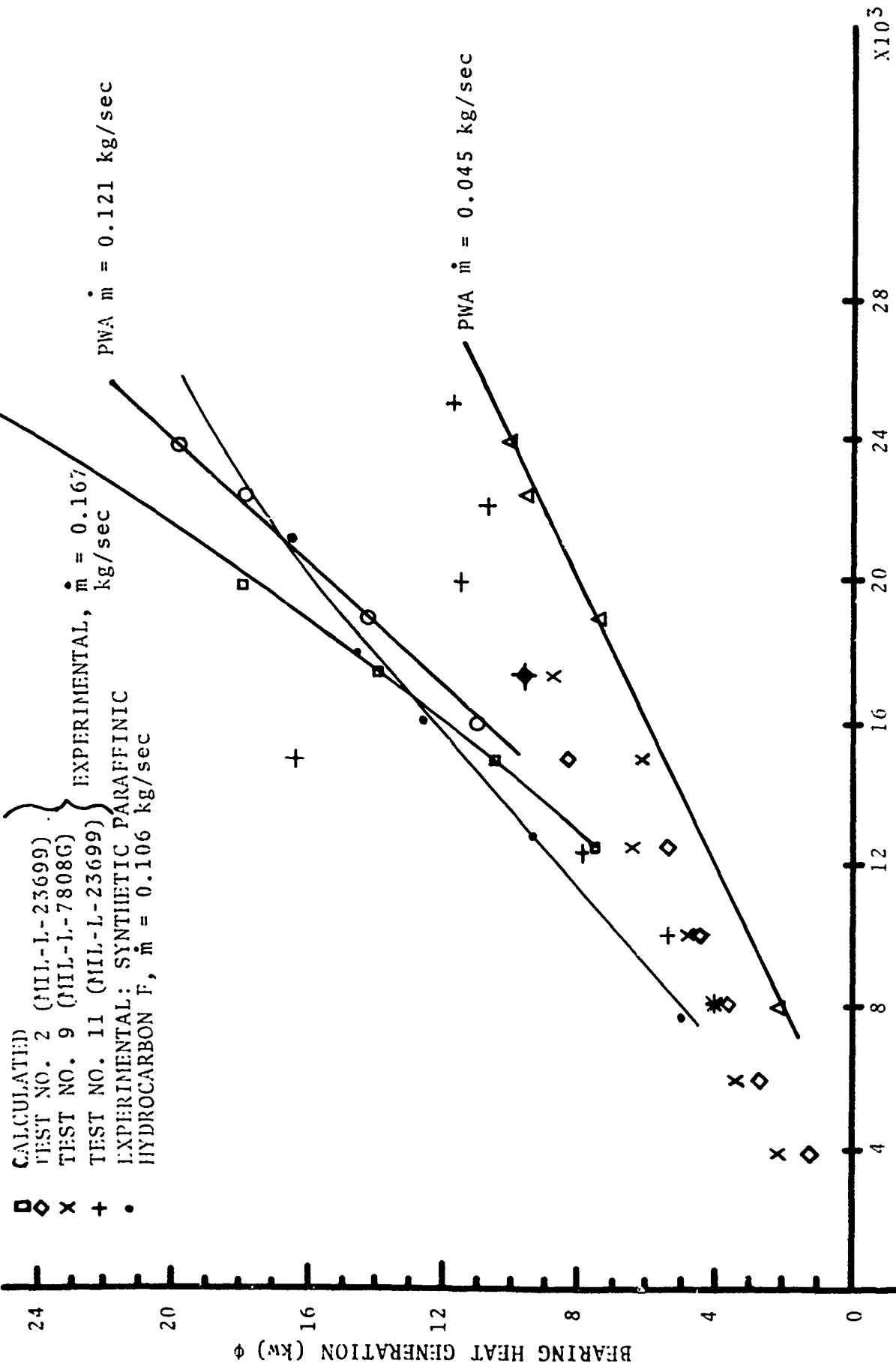


FIGURE 7-6

This theory is substantiated by data from a subsequent test performed by S K F on the same rig with a similar test bearing (125 mm bore, split inner ring, angular contact bearing with an outer-ring land riding cage). During the test, which was performed in a similar manner, to those with an applied thrust load of 3280 lbs., special emphasis was placed on obtaining good bearing torque data. This was accomplished by determining and accounting for the hysteresis friction on drag friction in the torque tube bearings supporting the load plug at each operating speed. The bearing heat generation rates calculated from the drag torque data is also plotted on Figure 7-6 and labelled synthetic paraffinic hydrocarbon. Although the lubricant differed from those tested on this program, the bearing heat generation rate is more nearly linear with speed and consistent with both the Pratt & Whitney data and computer calculated data.

Figure 7-7 shows the experimental and calculated heat generation rates as a function of load for the tests conducted at 10,000 rpm. It is clear that the computer program correctly follows the trend of the experimental data but it seems to be systematically too low by about a $\frac{1}{2}$ kw corresponding to a percentage error of roughly 12 to 15%. This discrepancy may be due in part to an overestimation of contact temperatures according to the rules in Section 7.5.1.2 at the low bearing loads used in this test series.

7.5.2.2 Ball and Cage Kinematic Predictions - MIL-L-7808G Lubricant - From Table 7-4 both the cage and ball rotational speeds are seen to be well predicted by the computer program. The same values were also calculated under the assumption of outer race control typically invoked in the earliest bearing dynamics prediction programs. The ball speeds predicted under this assumption are lower than those predicted using program AT74Y001.

It is believed that the discrepancies between measured and calculated ball speeds cannot wholly be explained by measurement error.

An attempt was made to use the measured values of ω_c and ω_B to deduce possible errors in the program's prediction of the rolling velocity vector pitch and yaw angles.

In terms of the orthogonal components ω_x , ω_y and ω_z of the ball autorotational velocity vector ω_B , the pitch angle β is defined as

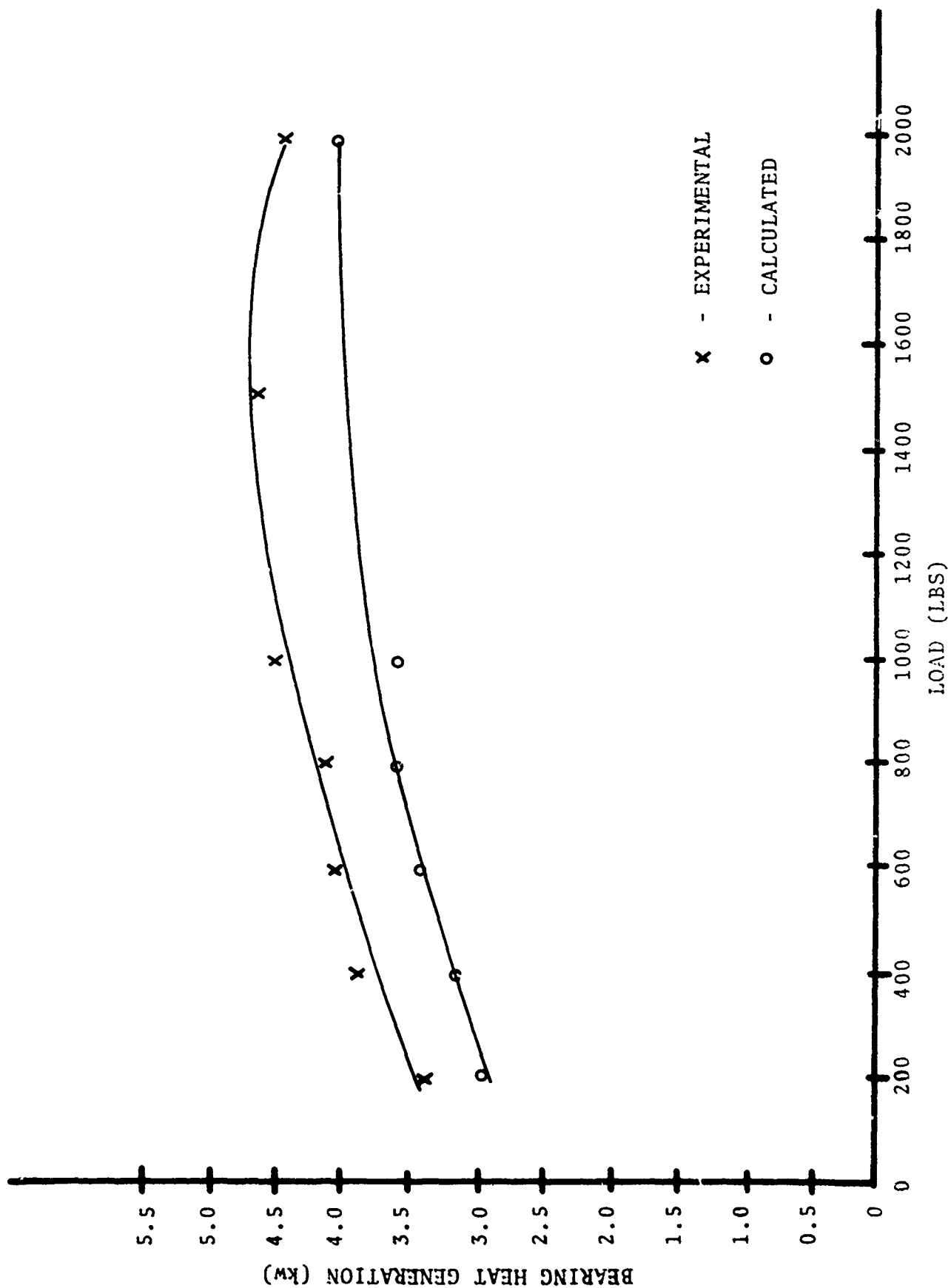


FIGURE 7-7
SKIDDING TEST NO. 4 MIL-L-7808G LUBRICANT 10000 RPM

$$\beta \equiv \tan^{-1}(\omega_y/\omega_x)$$

and the yaw angle δ is

$$\delta \equiv \tan^{-1}(\omega_z/\omega_x)$$

Using the computer predicted contact angles it was found in most cases that negative values of β or very large values of δ (20° - 30°) were required to bring the computer predictions into coincidence with the measured values of ω_c and ω_B .

Although it cannot be ruled out that such values actually occurred due to unaccounted for constraints on the ball motion such values of β and δ are generally regarded as unlikely.

Figure 7-6 shows the comparison of predicted and observed cage rotational velocity as a function of load for the skidding test conducted at 10,000 rpm. It shows that the trend toward lower cage speed at low loads, indicative of slipping has been successfully followed by the program.

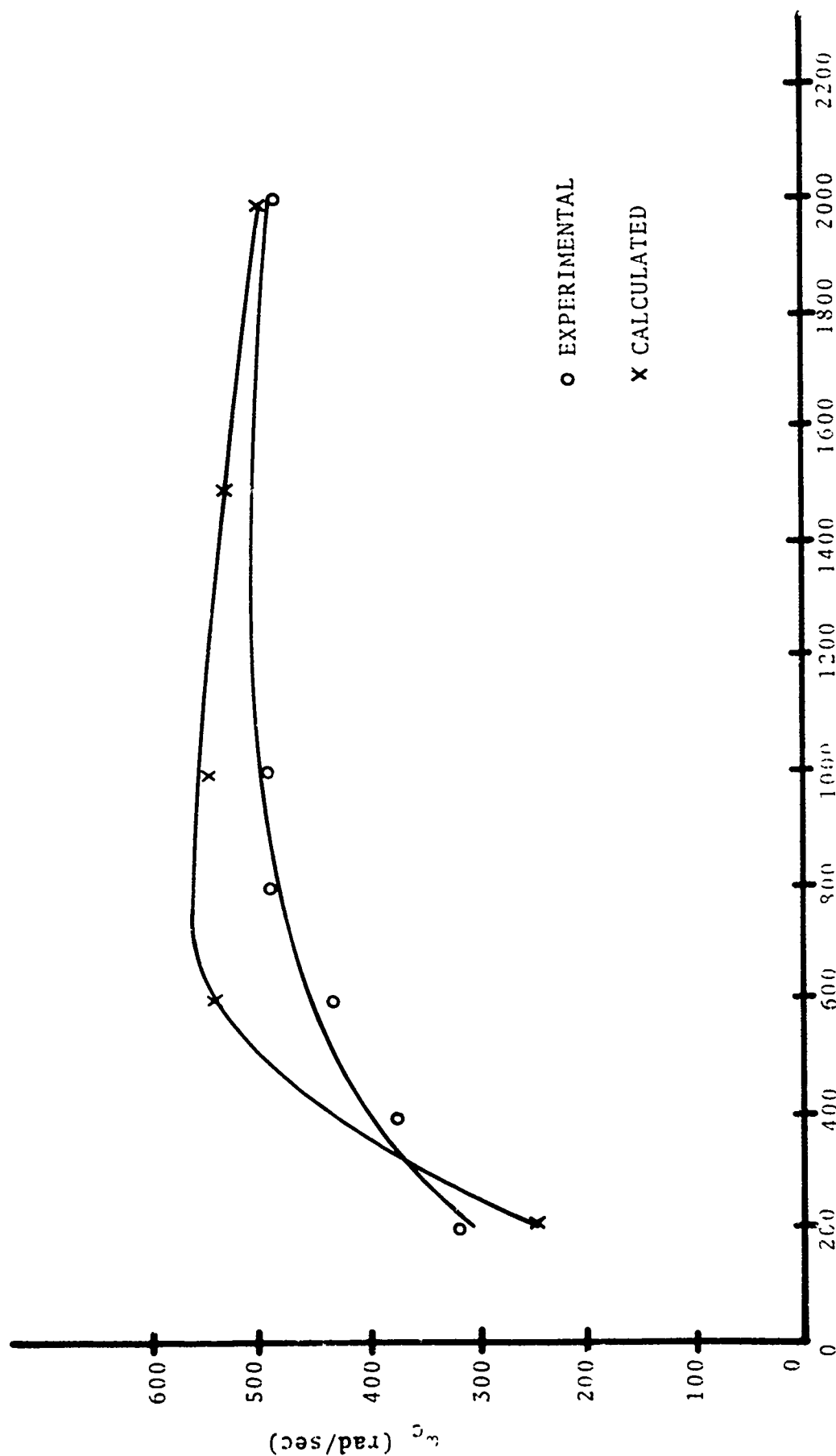
7.5.2.3 Film Thickness Predictions - MIL-L-7808G Lubricant - When a voltage is applied across the rings of an operating bearing, current will flow if there is a conducting path between the rings. During a long period of operation T_0 , the time T during which such a conducting path presents itself will depend upon how well the rings are insulated by the EHD film that forms at the inner and outer ring contacts. T will vary with the insulating ability of the film over the range ($0 < T < T_0$) and the ratio T/T_0 will vary over the range ($0 < T/T_0 < 1.0$).

In practice the ratio T/T_0 is reasonably well approximated by the ratio V/V_0 of the measured voltage drop V across the bearing rings and the applied voltage V_0 . The value of T/T_0 measured may be used as a qualitative indicator of the thickness of the EHD film.

By making certain assumptions it is also possible to interpret T/T_0 quantitatively to predict film thickness.

Two models are considered which tend to bracket the actual situation. In the first model it is assumed that the cage is non-conductive and that therefore a conducting path between the inner and outer rings will exist if there is contact at both rings at the same time for at least one ball.

In the second model the cage/ball contacts are assumed perfectly conductive and a conducting path between the rings



LOAD (LBS)

FIGURE 7-8

MIL L-7834C 11.5% 4 10000 RPM

will arise if any ball makes contact at the outer and any ball makes contact at the inner. Under the first model the no-contact time fraction across the rings is related to the no-contact time fraction at individual inner and outer ring contacts as follows

$$(T/T_o)_{\text{rings}} = \left\{ 1 - \left[1 - (T/T_o)_i \right] \cdot \left[1 - (T/T_o)_o \right] \right\}^n \quad (7-1)$$

where subscripts i and o denote individual inner and outer ring contacts and n is the number of rolling elements. (A thrust loaded bearing is assumed i.e. all contacts at a given ring are of the same size.)

For the second model the relationship is,

$$(T/T_o)_{\text{rings}} = 1 - \left\{ \left[1 - (T/T_o)_i^n \right] \cdot \left[1 - (T/T_o)_o^n \right] \right\} \quad (7-2)$$

Following Johnson et al [21], the no-contact time fraction at an individual contact may be expressed with good approximations by the relation,

$$(T/T_o)_{\text{single contact}} = e^{-m} \quad (7-3)$$

where

$$m = N A \left[1 - \phi(h/\sigma) \right] \quad (7-4)$$

and

N = no. of asperity peaks/unit area

A = contact area

h/σ = ratio of EHD film thickness to composite surface roughness (RMS)

$\phi(.)$ = the Gaussian cumulative distribution function

Following Nayak [13] the number of asperity peaks per unit area is related to m_2 and m_4 , the second and fourth moments of the surface roughness spectrum, as follows:

$$N = (1.2) \left(\frac{1}{2\pi} \right)^2 \left[\frac{m_4}{m_2} \right] \quad (7-5)$$

Introducing the parameter $\alpha = \frac{m_0 m_4}{m_2^2}$ and using the fact

that the zero order spectral moment m_0 is the mean square roughness σ^2 and the second order spectral moment m_2 is the mean square, σ_θ^2 , of the slope θ of the surface profile, gives

$$N = 1.2 \left(\frac{1}{2\pi} \right)^2 \left[\alpha \frac{\sigma_\theta^2}{\sigma^2} \right] \quad (7-6)$$

Using the value $\alpha = 2$ as deduced for bearing surfaces in {5}, and values of $\sigma = 6.5 \mu\text{in}$, $\sigma_\theta = 3.0 \mu\text{in}$, $(\sigma_\theta)_i = 0.035 \text{ rad.}$, $(\sigma_\theta)_o = 0.042 \text{ rad}$, gives the values $N_i = 1.87 \times 10^6/\text{in}^2$ and $N_o = 17.1 \times 10^6/\text{in}^2$ using Eq. (7-6).

Using the contact area values of A_i and A_o output by computer program AT74Y001 it was possible to evaluate $(T/T_o)_{\text{rings}}$ as a function of h using Eqs. (7-1) and (7-3) for both the non-conducting and conducting cage models. It was found that because the inner ring roughness exceeded the outer ring roughness by more than a factor of two, the conducting cage and non-conducting cage models gave indistinguishable results. The reason is the following. If h is small enough for $(T/T_o)_0$ to be less than 1.0, then $(T/T_o)_i \rightarrow 0$. Thus Eq. (7-1) reduce to

$$(T/T_o)_{\text{rings}} = \left\{ 1 - [1 - (T/T_o)_o] \right\}^n = (T/T_o)_o^n \quad (7-7)$$

and Eq. (7-2) likewise becomes,

$$(T/T_o)_{\text{rings}} = 1 - \left\{ 1 - \left(\frac{T}{T_o} \right)_o^n \right\} = (T/T_o)_o^n \quad (7-8)$$

Figure (7-9) is a plot of T/T_o vs. h constructed for the case where the thrust load was 1000 lbs and the inner ring speed was 4000 rpm. (Note the suppressed areas on the abscissa.)

In principle one can locate a measured value of T/T_o on the ordinate of Figure 7-9 and read the associated film thickness on the abscissa. The film thickness thus determined is an "effective" film thickness in the sense that it is the value of a common inner and outer ring film thickness that

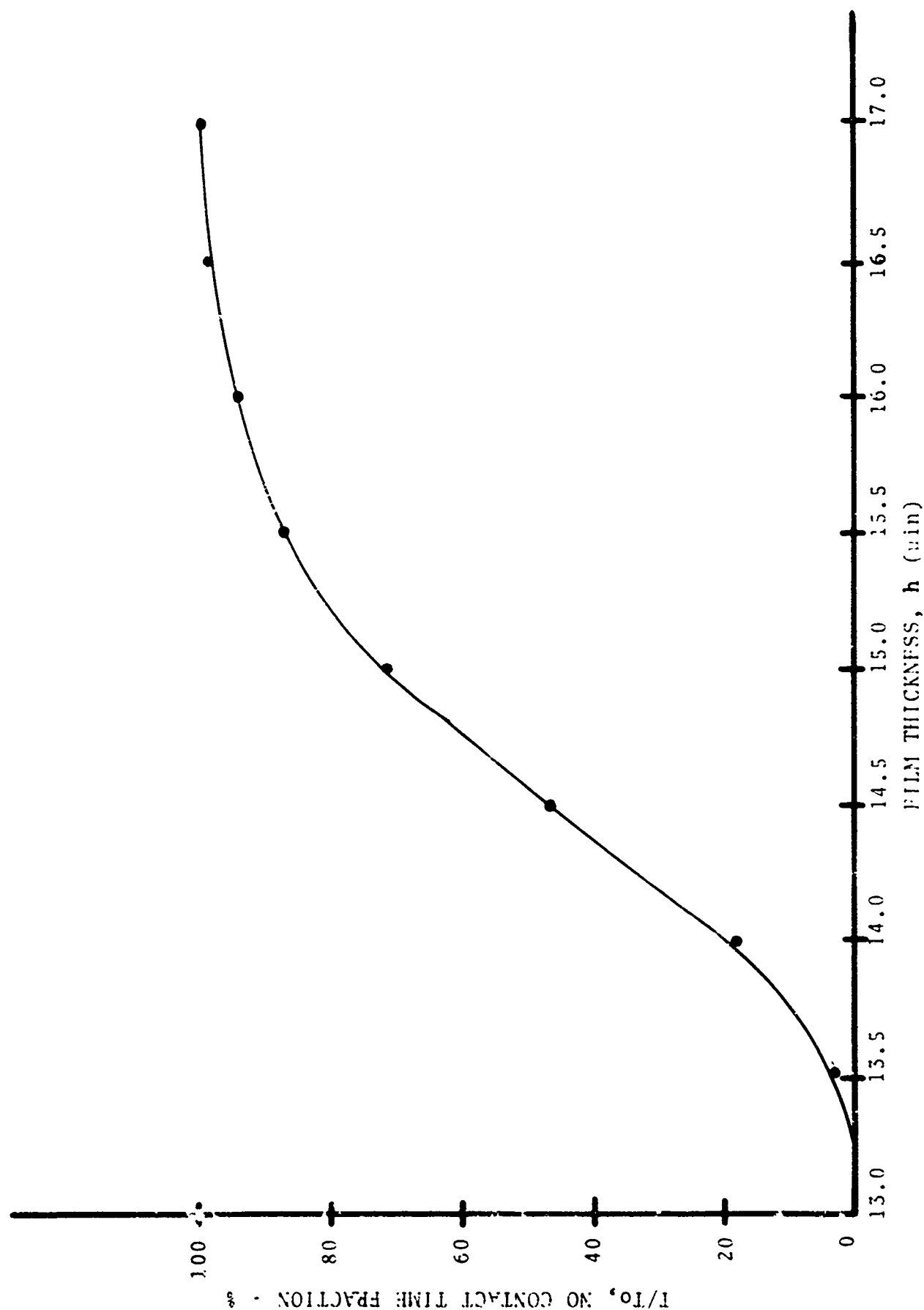


FIGURE 7-9

THEORETICAL RELATION BETWEEN T/T_o AND FILM THICKNESS FOR 1000 LBS. THRUST LOAD AT 4000 RPM

gives the same measured T/T_0 value as the somewhat unequal film thicknesses which actually prevail at the inner and outer ring contacts.

It is seen from Fig. 7-7 that the resolving power of T/T_0 is not great i.e. effective film thickness values lower than 13.0 μin , result in $T/T_0 \rightarrow 0$ and above 17.0 μin . in $T/T_0 \rightarrow 1.0$.

The location of the curve of Fig. 7-7 did not differ substantially at the other test loads and speeds.

Referring to Table (7-4) we see that for Test No. 1 the measured T/T_0 values are quite compatible with the predicted film thickness values. Moderate to high values of T/T_0 are associated with predicted outer ring film thicknesses in the range of 14-18 μin . Low values are associated with film thickness predictions in the range 5-6 μin .

Figure 7-10 shows a plot of the measured values of T/T_0 and predicted outer ring film thickness for the 7808G test series.

For Test Series No. 1 the curve has a shape and location quite comparable to the theoretical curve of Fig. 7-9. The finite values of T/T_0 measured at the predicted film thickness of 5-6 μin could reasonably have been due to noise or random contact due to wear debris.

The data from Test No. 4 yielded uniformly high values of T/T_0 with corresponding predicted film thicknesses in the range of 10-22 μin .

According to Fig. 7-10 low values of T/T_0 should result for film thicknesses at the low end of this range. It is quite conceivable however that the roughnesses of the bearing in Test No. 4 were less than those in Test No. 1 (or became so in running), so that the film thickness values of 10 μin . could have resulted in high T/T_0 values.

A post test roughness determination for the bearing used in Tests 2-10 confirmed a lower value of the inner ring roughness (3.5 μin .) than the value (6.3 μin .) measured on a representative bearing prior to test.

The data from Test No. 11 show no discernible pattern. However, post test inspection of the bearing used in Test No. 11 indicated that the balls had acquired a coating of lubricant degradation products (varnish) which is known as an

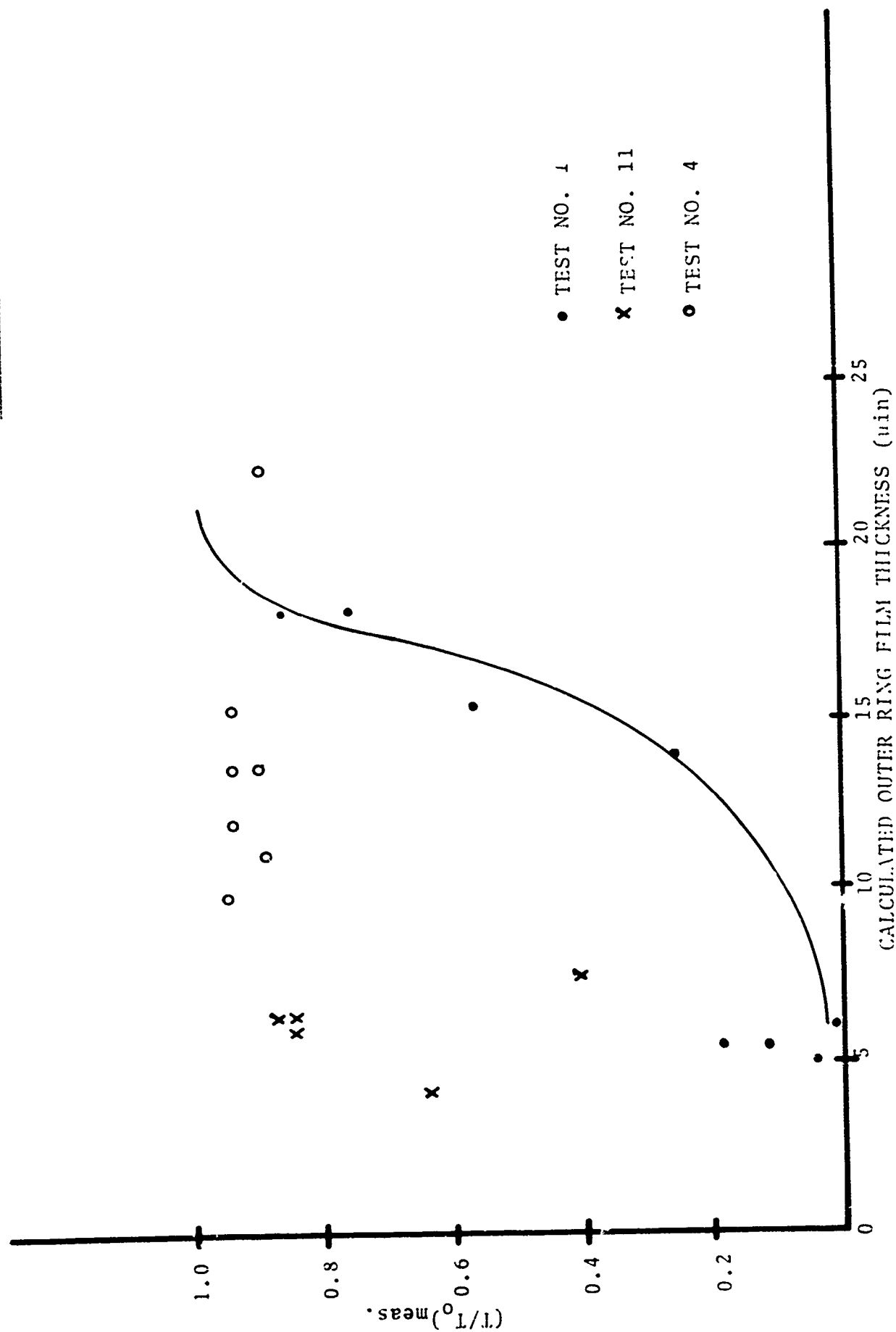


FIGURE 7-10

MEASURED T/T_0 vs. CALCULATED OUTER RING FILM THICKNESS - NIL-L-7808G

insulator, giving uniformly high T/T_0 .

Table 7-5 shows comparative T/T_0 values from tests in which the bearing was unvarnished and varnished. The tendency for the measured no contact time fraction to be high in the tests with the varnish is quite clear. The data for Test No. 11 when contrasted with the data from Test No. 1 supports the hypothesis that varnish deposits acted to give thick film indications for Test No. 11.

7.5.3 Comparison of Predicted and Measured Values - MIL-L-23699 Lubricant

Table 7-6 shows for the MIL-L-23699 tests the computer predicted values of heat generation rate, film thickness and cage and ball rotational velocities. The corresponding measured values of the no-contact time fraction, heat generation rates, cage and ball velocities and outer ring bulk temperature are also shown. The measured heat generation rates for the tests at 2,000 lbs load were unavailable. As with the 7808 oil results it is seen that the calculated heat increases more rapidly with speed than the measured values.

At 10,000 rpm the calculated heat generation rate for the tests of 3280 lbs load is smaller than measured by 17% and at 17,500 rpm it is larger than the measured value by 36%.

At the highest load (3280 lbs) the measured and predicted cage speeds are in substantial agreement while at the two lowest loads the cage speeds are underpredicted by as much as 40%. The ball speed predictions behave similarly. The program is thus predicting skidding conditions at low loads which the experiments do not substantiate.

Figure 7-11 is a plot of the measured no-contact time fraction values T/T_0 against calculated outer ring film thickness. The various points are identified by the value of the bearing axial loads used in the test.

Also shown is the theoretical curve of Fig. 7-9 redrawn to the scale of Fig. 7-11. The points for the 1000 lb load test fall to the right of the theoretical curve. Accepting the theoretical curve as correct this would indicate a systematic overestimate of film thickness by the computer program of 1.5 to 2 μ in. For the 3280 lb tests the points lie to the left of the theoretical curve. This is consistent with an overestimate of film thickness only if the bearing roughness process has changed i.e. become smoother. Inasmuch as the tests were run sequentially in increasing order of load this explanation is plausible.

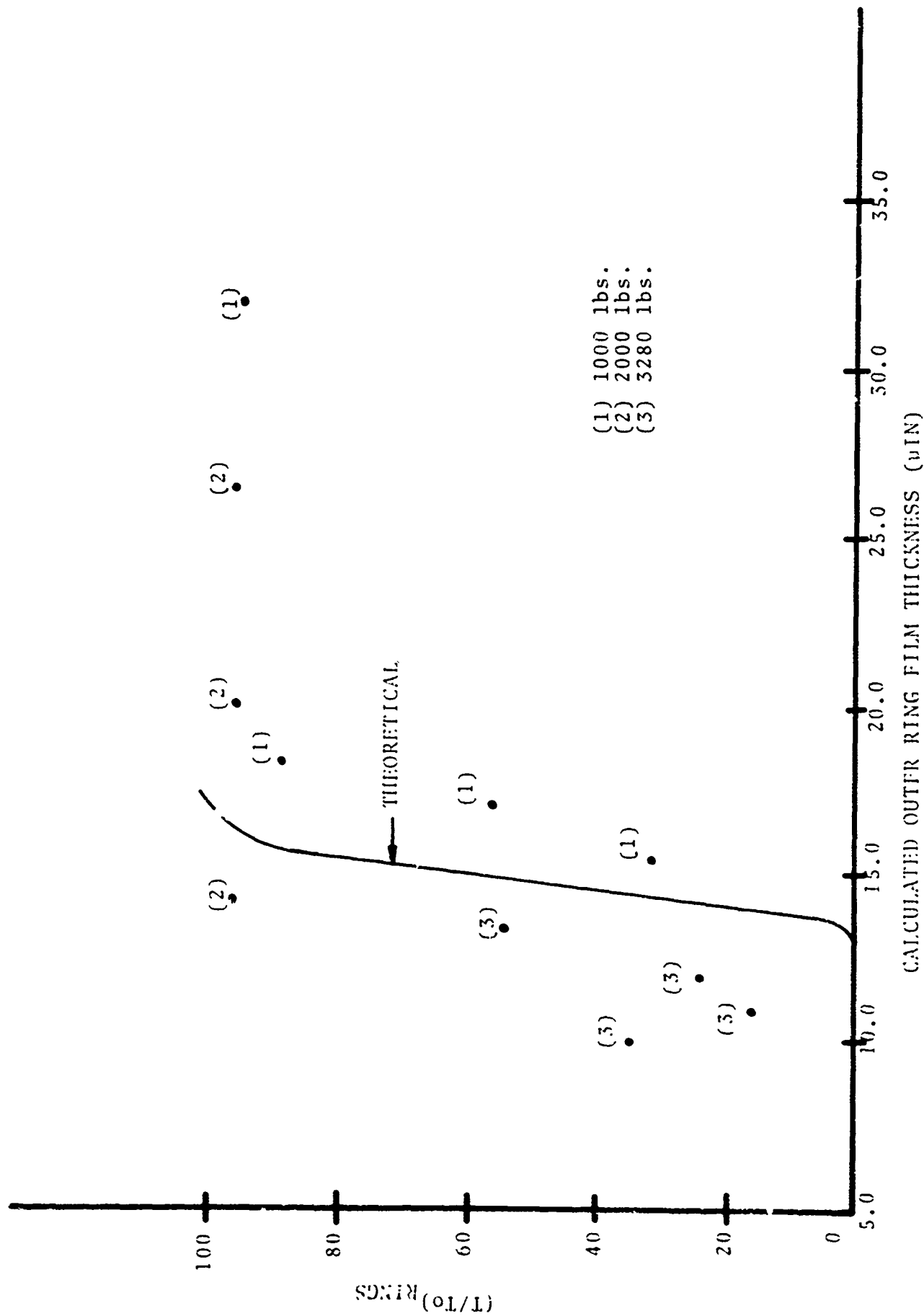
TABLE 7-5
MEASURED T/To - VARNISHED AND UNVARNISHED BEARINGS

Load	Speed	T/To (Test No.)	
		Unvarnished	Varnished
1000	4000	0.86 (1)	0.99 (6)
	6000	0.76 (1)	0.97 (6)
	8000	0.57 (1)	0.97 (6)
	10000	0.25 (1)	0.97 (6)
2000	4000	0.97 (4)	0.94 (8)
	6000	0.83 (4)	0.88 (8)
	8000	0.96 (4)	0.95 (8)
	10000	1.00 (4)	1.00 (8)
	12500	0.77 (4)	1.00 (8)
	15000	0.45 (4)	1.00 (8)
3280	4000	1.00 (4)	0.99 (9)
	6000	-	0.64 (9)
	8000	0.54 (4)	0.90 (9)
	10000	0.95 (4)	1.00 (9)
	12500	0.09 (1)	1.00 (9)
	15000	0.18 (1)	0.97 (9)
	17500	0.12 (1)	0.99 (9)
		0.40 (11)	
		0.84 (11)	
		0.87 (11)	

TABLE 7-6

MIL-L-25699 TEST AND PROGRAM COMPARISON

Speed RPM	Load (lbs)	Computer Prediction					Measured				TOR (°F)
		h _o (min)	h _i	ω _c (rad/sec)	ω _b	(T/T _o)	q Watts	ω _c (rad/sec)	ω _b (rad/sec)		
4000	1000	31.9	26.6	175	1486	0.950	1200	238	2148	110	
6000	1000	18.3	16.9	279	1656	0.880	2430	345	2895	160	
8000	1000	17.0	14.7	320	2530	0.570	3520	-	3617	190	
10000	1000	15.4	13.5	415	3764	0.320	4250	534	4364	220	
4000	2000	26.4	21.0	186	1729	0.96		232	1809	125	
6000	2000	20.0	16.6	261	2298	0.97		320	2687	160	
8000	2000	14.2	13.6	252	2335	0.97		414	3542	195	
10000	3280	15.2	10.6	475	4384	.540	4700	574	4515	240	
12500	3280	11.9	9.7	597	5466	.240	5440	590	5570	270	
15000	3280	10.8	8.6	722	6549	.160	8060	741	6393	300	
17500	3280	9.7	7.4	842	7559	.350	9910	872	7240	330	



The data thus viewed offers no serious inconsistency with the hypothesis that the program is very nearly correctly predicting film thickness.

7.5.4 Summary of Program Accuracy Assessment

1. The computer program has been found for both oils tested to give good predictions of heat generation rate measured in S K F tests in the vicinity of 10000 rpm but to overestimate the heat generation rate by progressively greater amounts at higher speeds. The program is capable of at least partially compensating for this discrepancy by using more realistic input estimates of EHD film replenishment ($\Delta\zeta$). The program has been found however to give good predictions when compared to test results obtained using a different method of lubricant supply. Inasmuch as the heat generation models do not account for the method of lubricant supply it is recommended that future efforts be directed at developing models to account for the distribution of and energy transfer to lubricant as a function of supply method.

The program has been found to correctly predict the trend of heat generation rate with applied axial load.

2. Cage and ball speed predictions for MIL-L-7808G are quite accurate, correctly predicting cage slip when it has been found experimentally to occur and predicting near epicyclic conditions when no cage slip was observed. For MIL-L-23699 lubricant cage slip was predicted under 1000 lbs and 2000 lbs load but was not observed to occur.

3. Considering the effects of run-in on surface finish, the approximation in the theoretical relationships between no-contact time fraction and film thickness and the insulating effect of varnish films, the computer predictions of EHD film thickness have been found compatible with experimental findings, i.e. there is no reason to reject the film thickness predictions as erroneous on the strength of the experimentally observed values of no-contact time fractions. This is not to say that the film thickness predictions are perfectly correct. They could well be off by as much as 10-20% and still be compatible with the experiments.

SECTION 8

PARAMETRIC STUDIES AND DISCUSSION OF PROGRAM BEHAVIOR

8.1 INTRODUCTION

The previous section demonstrated the correlation between experimental results and the predictions made by the computer program. The information on computer program results discussed in that section was limited to the parameters measured in the test program. In this section additional aspects of the computed data are examined to demonstrate the capabilities of the program and, more importantly, to provide additional insight into the various models which comprise the program. An expanded list of the program output relevant to the full scale test runs is given as Table 8-1.

Two additional sets of computer output data will be presented and reviewed. One set, given in Table 8-2, comprises the results of a brief parametric study performed with the test bearing at a fixed load and speed condition. This study is intended to help the user identify reasonable values for two of the less familiar program input variables namely, XCAV, the percentage of bearing cavity occupied by the lubricant, and $\Delta\zeta$, the thickness of the layer of lubricant which replenishes the ball and raceway surfaces between each contact pass. Although the $\Delta\zeta$ values may be input independently for both the inner and outer raceways, common values were selected at both races for this study. The bearing initial, unmounted, contact angle was also varied in a systematic fashion as a simple demonstration of how the user might employ the program to help design a bearing for a given application.

The third data set, given in Table 8-3, was generated as part of another study in which the heat generation rates and the distribution of frictional heat was being examined for 45 mm bore size angular contact bearings operating within the load-speed spectrum of most industrial applications.

The three sets of data, Tables 8-1, 8-2, and 8-3, will first be examined on a set by set basis. Then some general observations will be made based on an overview of all the data.

The following variables are listed for each data set.

- q outer - heat generation rate at the outer ring (watts)
- q inner - heat generation rate at the inner ring (watts)
- q cage-ball - heat generated at the cage-ball contact (watts)

TABLE 2-1

EXPANDED DUMPLIST III SCW TEST PROGRAM

Run No.	Test No.	Speed	Load	q outer	q inner	q Cap- Ball	q Cap- Land	q mean	q Tot	SHRDL qTot	b ₀	b ₁	b ₀ , e	b ₁ , e	ω_x rad/sec	ω_y rad/sec	ω_z rad/sec
1	1	1000	1000	100	100	20.1	14.2	100	307	0.192	10.3	11.7	0.30	2.25	-1076.4	145.3	-16.0
2	1	1000	1000	275	307	10.7	9.5	113	1139	0.363	15.5	12.2	3.32	1.86	-600.0	49.3	-12.6
3	1	1000	1000	500	500	10.1	10.1	100	2100	0.710	14.1	11.2	4.83	1.71	-3483.0	33.6	-12.6
4	1	1000	1000	100	100	6.9	1.2	224	3400	0.611	11.9	9.1	4.10	1.39	-4247.0	24.3	-16.7
5	1	1000	1000	100	100	23.3	10.3	200	4800	0.425	6.1	5.0	2.08	0.76	-4500.2	39.8	-74.7
6	1	1000	1000	100	100	26.9	13.1	2249	7250	0.436	5.3	4.2	1.81	0.65	-5375.0	41.5	-74.7
7	1	1000	1000	100	100	37.1	20.6	2500	10520	0.495	5.5	4.3	1.89	0.66	-6350.4	29.5	-67.2
8	1	1000	1000	100	100	17.6	10.5	7571	13950	0.533	5.6	4.3	1.91	0.67	-7654.2	216.0	-62.8
9	11	1000	1000	100	100	16.7	10.6	1150	7707	0.531	7.5	6.1	2.59	0.93	-5454.7	249.3	-60.7
10	11	1000	1000	100	100	16.7	10.6	1150	7707	0.531	7.5	6.1	2.59	0.93	-5454.7	249.3	-60.7
11	11	1000	1000	100	100	16.7	10.6	1150	7707	0.531	7.5	6.1	2.59	0.93	-5454.7	249.3	-60.7
12	11	1000	1000	100	100	16.7	10.6	1150	7707	0.531	7.5	6.1	2.59	0.93	-5454.7	249.3	-60.7
13	11	1000	1000	100	100	16.7	10.6	1150	7707	0.531	7.5	6.1	2.59	0.93	-5454.7	249.3	-60.7
14	11	1000	1000	100	100	16.7	10.6	1150	7707	0.531	7.5	6.1	2.59	0.93	-5454.7	249.3	-60.7
15	11	1000	1000	100	100	16.7	10.6	1150	7707	0.531	7.5	6.1	2.59	0.93	-5454.7	249.3	-60.7
16	11	1000	1000	100	100	16.7	10.6	1150	7707	0.531	7.5	6.1	2.59	0.93	-5454.7	249.3	-60.7
17	11	1000	1000	100	100	16.7	10.6	1150	7707	0.531	7.5	6.1	2.59	0.93	-5454.7	249.3	-60.7
18	11	1000	1000	100	100	16.7	10.6	1150	7707	0.531	7.5	6.1	2.59	0.93	-5454.7	249.3	-60.7
19	11	1000	1000	100	100	16.7	10.6	1150	7707	0.531	7.5	6.1	2.59	0.93	-5454.7	249.3	-60.7
20	11	1000	1000	100	100	16.7	10.6	1150	7707	0.531	7.5	6.1	2.59	0.93	-5454.7	249.3	-60.7
21	11	1000	1000	100	100	16.7	10.6	1150	7707	0.531	7.5	6.1	2.59	0.93	-5454.7	249.3	-60.7
22	11	1000	1000	100	100	16.7	10.6	1150	7707	0.531	7.5	6.1	2.59	0.93	-5454.7	249.3	-60.7
23	11	1000	1000	100	100	16.7	10.6	1150	7707	0.531	7.5	6.1	2.59	0.93	-5454.7	249.3	-60.7
24	11	1000	1000	100	100	16.7	10.6	1150	7707	0.531	7.5	6.1	2.59	0.93	-5454.7	249.3	-60.7
25	11	1000	1000	100	100	16.7	10.6	1150	7707	0.531	7.5	6.1	2.59	0.93	-5454.7	249.3	-60.7
26	11	1000	1000	100	100	16.7	10.6	1150	7707	0.531	7.5	6.1	2.59	0.93	-5454.7	249.3	-60.7
27	11	1000	1000	100	100	16.7	10.6	1150	7707	0.531	7.5	6.1	2.59	0.93	-5454.7	249.3	-60.7
28	11	1000	1000	100	100	16.7	10.6	1150	7707	0.531	7.5	6.1	2.59	0.93	-5454.7	249.3	-60.7
29	11	1000	1000	100	100	16.7	10.6	1150	7707	0.531	7.5	6.1	2.59	0.93	-5454.7	249.3	-60.7
30	11	1000	1000	100	100	16.7	10.6	1150	7707	0.531	7.5	6.1	2.59	0.93	-5454.7	249.3	-60.7
31	11	1000	1000	100	100	16.7	10.6	1150	7707	0.531	7.5	6.1	2.59	0.93	-5454.7	249.3	-60.7

TABLE 8-1 (CONT.)

Run No.	ω_R rad/sec	ω_C rad/sec	α_1 Deg	α_2 Deg	Pitch Angle Deg	Yaw Angle Deg	$\frac{QASP}{QTOT}$	ϕ_{TOT} Newtons	$\frac{QASP}{QTOT}$	ϕ_{TOT} Newtons	μ_0	μ_1	A_{EFF1}	A_{EFF10}	MAX EOL
1	1689	186.9	23.14	21.03	5.0	0	0.020	501.4	0.	593.4	0.0044	0.0063	0.0082	0.0044	-
2	2601	283.7	27.20	18.38	1.1	0	0.019	475.9	0.	692.0	0.0033	0.0049	0.0096	0.0033	-
3	3484	386.7	28.63	15.06	0.6	0	0.072	465.9	0.	866.0	0.0022	0.0029	0.0092	0.0022	-
4	4247	477.8	25.43	11.07	0.7	0	0.141	503.0	0.	1129.6	0.0074	0.0031	0.0168	0.0034	-
5	4240	474.1	29.41	20.71	7.3	1.0	0.303	1406.0	0.022	1986.2	0.0017	0.0075	0.0355	0.0068	-
6	5394	602.3	30.63	17.84	4.5	0	0.363	1389.5	0.040	2339.2	0.0042	0.0070	0.0408	0.0080	-
7	6558	732.6	31.44	15.05	2.1	0	0.355	1390.9	0.031	2014.9	0.0042	0.0055	0.0390	0.0072	-
8	7638	859.4	31.53	12.51	1.6	0	0.351	1400.7	0.026	3394.4	0.0040	0.0041	0.0378	0.0067	-
9	5394	604.0	30.72	17.63	2.6	0	0.231	1405.6	0.005	2362.2	0.0034	0.0076	0.0289	0.0059	-
10	6576	732.5	31.26	15.01	1.8	0	0.269	1406.4	0.014	2631.1	0.0046	0.0058	0.0329	0.0059	-
11	7685	860.4	31.53	12.51	1.2	0	0.296	1411.2	0.014	3401.3	0.0043	0.0041	0.0325	0.0056	-
12	8740	983.5	30.90	16.91	1.1	0	0.332	1430.7	0.021	4060.9	0.0039	0.0035	0.0355	0.0059	-
13	10734	1217.4	26.77	6.94	1.5	0	0.404	1417.8	0.066	5524.3	0.0031	0.0046	0.0508	0.0095	-
14	2003	315.7	27.87	11.46	0.2	0	0.002	201.1	0.	472.9	0.0017	0.0069	0.0071	0.0017	0.187
15	3516	376.0	26.65	16.63	0.2	0	0.036	236.9	0.	633.9	0.0016	0.0067	0.0101	0.0016	0.360
16	3918	435.6	29.59	10.20	0.2	0	0.072	292.2	0.	813.1	0.0030	0.0065	0.0132	0.0030	1.12
17	4006	460.2	30.21	10.47	0.3	0	0.063	367.4	0.	1017.2	0.0024	0.0029	0.0110	0.0024	-
18	4353	467.1	29.65	11.96	0.4	0	0.119	459.6	0.	1103.0	0.0037	0.0033	0.0148	0.0027	-
19	3929	447.3	29.13	15.37	0.3	0	0.158	646.7	0.	1177.9	0.0063	0.0091	0.0235	0.0093	1.94
20	4364	482.7	29.56	17.03	1.6	0	0.122	892.3	0.	1507.2	0.0031	0.0065	0.0179	0.0031	-
21	1486	172.8	24.96	21.35	0.7	0	0.	494.3	0.	572.9	0.0014	0.0020	0.0020	0.0014	0.11
22	1656	214.2	23.44	19.48	0.1	0	0.008	424.1	0.	545.4	0.0012	0.0013	0.0021	0.0012	0.10
23	2530	320.1	27.50	15.62	0	0	0.021	392.0	0.	664.9	0.0011	0.0009	0.0030	0.0011	0.21
24	3764	413.1	26.86	12.58	0	0	0.037	380.4	0.	842.4	0.0002	0.0008	0.0073	0.0002	0.071
25	1729	186.5	26.08	23.50	0.7	0	0.001	963.8	0.	1054.2	0.0008	0.0017	0.0018	0.0008	0.027
26	2298	260.6	26.69	22.12	0.3	0	0.007	931.9	0.	1108.7	0.0021	0.0016	0.0023	0.0021	0.467
27	2335	272.0	25.91	21.41	0.2	0	0.025	848.2	0.	1014.5	0.0004	0.0022	0.0046	0.0004	0.989
28	4361	474.5	26.20	19.77	0.6	0	0.060	1476.0	0.	2068.8	0.0006	0.0016	0.0073	0.0006	0.0001
29	5460	597.1	26.86	17.05	0.1	0	0.084	1456.1	0.	2401.4	0.0013	0.0013	0.0096	0.0013	-
30	5719	722.3	29.47	14.49	0.1	0	0.114	1436.7	0.	3436.2	0.0013	0.0009	0.0122	0.0013	0.0002
31	7556	841.6	26.02	11.91	0.4	0	0.160	1500.9	0.	3426.8	0.0014	0.0008	0.0167	0.0014	-

FOR THE UNITED STATES OF AMERICA

PERMISSION TO REPRODUCE THIS

[illegible]

TABLE 3-2 (CONT.)

Run No.	ω_n	ϕ_i	α_i	Pitch Angle	Yaw Angle	$\frac{\partial \Delta E}{\partial \theta_{TOT}}$	ϕ_{TOT}	$\frac{\partial \Delta E}{\partial \theta_{TOT}}$	Newton's	μ_0	μ_1	$(\mu_{EFF})_1$	$(\mu_{EFF})_0$	MAX EQ
	rad/sec	rad/sec	Deg	Deg	Deg		Newton's		Newton's					
1	12.17	17.6	11.07	0.7	0.2	0.141	504.0	0	1129.6	0.0031	0.0031	0.0168	0.0034	-
2	12.59	17.6	11.06	0.7	0.2	0.142	504.3	0	1131.5	0.0029	0.0029	0.0159	0.0024	-
3	12.97	17.6	11.04	0.7	0.1	0.142	504.3	0	1139.2	0.0024	0.0019	0.0158	0.0024	0.018
4	13.40	17.6	11.11	0.6	0.1	0.140	493.6	0	1057.3	0.0080	0.0078	0.0216	0.0080	1.859
5	14.16	22.0	11.17	0.4	0.2	0.139	467.6	0.001	223.6	0.0060	0.0036	0.0189	0.0061	0.710
6	14.51	20.1	12.11	0.2	0.2	0.134	400.1	0	1072.4	0.0027	0.0035	0.0184	0.0027	0.366
7	14.19	16.4	6.15	1.0	0.2	0.133	690.1	0	1292.1	0.0025	0.0030	0.0159	0.0025	0.027
8	10.79	16.1	0.90	1.3	0.2	0.141	771.6	0	1372.3	0.0025	0.0030	0.0157	0.0025	-
9	12.51	17.6	11.08	0.6	0.2	0.142	503.0	0	1129.2	0.0026	0.0024	0.0163	0.0026	-
10	12.52	17.6	11.08	0.6	0.2	0.142	503.4	0	1129.7	0.0026	0.0023	0.0162	0.0026	-
11	12.42	17.6	11.07	1.1	0.3	0.202	503.4	0.005	1129.0	0.0038	0.0027	0.0224	0.0043	0.006

TABLE B-3
PARAMETRIC RUNS - 45 mm BORE ANGULAR CONTACT BALL BEARING
WIL-L-7600G LUBRICANT

Run No.	Solution Type	Speed	Load	q Outer	q Inner	q Cage-Ball	q Cage-Land	q Drag	q Tot	Watts	μ -in	h_0	h_1	h_0/σ	h_1/σ	ω_x rad/sec	ω_y rad/sec	ω_z rad/sec
1	full	1725	700	9.15	3.10	0.0020	0.123	0.100	13.1	0.008	3.6	3.2	0.543	0.479	0.479	-225.7	293.6	-0.02
2	full	3450	700	12.5	14.4	0.0166	1.69	0.823	29.5	0.020	6.1	5.4	0.903	0.803	0.803	-518.7	512.6	-2.16
3	full	6900	700	31.0	64.9	0.233	6.38	7.64	160.0	0.049	10.5	8.9	1.56	1.33	1.33	-1614.6	405.9	-32.2
4	full	13800	700	190.0	226.0	1.01	55.8	2.72	476.0	0.006	13.9	17.0	2.08	2.54	2.54	-3294.	2.39	-4.1
5	full	1725	1700	6.41	43.2	0.0062	0.424	0.108	50.1	0.002	3.4	3.0	0.508	0.449	0.449	-303.6	202.3	-1.45
6	full	3450	1700	19.1	40.2	0.0191	1.69	0.831	61.0	0.013	5.7	5.0	0.851	0.752	0.752	-545.5	481.8	-1.45
7	full	5175	1700	45.9	30.7	0.0334	3.80	2.81	91.3	0.031	7.7	6.8	1.15	1.02	1.02	-747.8	804.2	-4.44
8	full	6900	1700	69.2	82.1	0.0622	6.74	6.94	165.0	0.042	9.5	8.4	1.42	1.26	1.26	-1032.7	1037.4	-16.3
9	full	13800	1700	359.	582.	0.976	24.2	77.3	1044.	0.074	15.3	12.9	2.28	1.93	1.93	-3299.9	799.4	-85.3
10	full	1725	2700	77.2	24.9	0.002	0.421	0.109	103	0.001	3.3	2.9	0.493	0.435	0.435	-193.0	330.8	-0.52
11	full	3450	2700	36.9	36.8	0.015	1.68	0.834	113	0.007	5.5	4.9	0.823	0.727	0.727	-495.4	539.0	-0.42
12	full	5175	2700	80.5	58.8	0.033	3.79	2.83	146.0	0.019	7.4	6.6	1.11	0.983	0.983	-744.8	807.8	-2.58
13	full	6900	2700	107.0	96.0	0.060	6.73	6.98	217.0	0.032	9.2	8.2	1.37	1.22	1.22	-1003.6	1068.7	-8.91
14	full	13800	2700	518.0	873.0	0.850	25.4	69.6	1407.	0.047	14.6	12.7	2.18	1.89	1.89	-3131.7	971.4	-105.8
15	partial	1725	700	8.56	15.1	0.0063	0.423	0.108	24.2	0.004	3.6	3.2	0.541	0.477	0.477	-303.9	198.0	-3.63
16	partial	3450	700	15.3	29.4	0.026	1.69	0.826	47.2	0.018	6.1	5.4	0.905	0.799	0.799	-611.8	392.9	-7.27
17	partial	5175	700	23.1	46.9	0.060	3.79	2.82	76.7	0.037	8.2	7.2	1.22	1.08	1.08	-928.4	581.2	-10.95
18	partial	6900	700	33.2	68.9	0.111	6.69	7.06	116.0	0.061	10.2	9.0	1.52	1.35	1.35	-1260.0	759.0	-14.7
19	partial	13800	700	119.	199.	0.662	24.1	77.4	420.	0.184	16.4	14.2	2.45	2.12	2.12	-2925.9	1312.0	-32.1
20	partial	1725	1700	18.4	45.4	0.006	0.422	0.109	64.3	0.002	3.4	3.0	0.507	0.447	0.447	-302.0	201.1	-3.63
21	partial	3450	1700	31.5	82.1	0.025	1.69	0.828	116	0.007	5.7	5.0	0.817	0.748	0.748	-605.7	400.9	-7.26
22	partial	5175	1700	44.1	117.	0.057	3.79	2.81	168.	0.017	7.6	6.8	1.14	1.01	1.01	-912.8	593.0	-10.91
23	partial	6900	1700	57.8	155.	0.102	6.73	6.97	226.	0.031	9.5	8.4	1.42	1.25	1.25	-1225.3	791.0	-14.6
24	partial	13800	1700	148.	372.	0.477	26.3	64.8	611.	0.106	14.9	13.2	2.23	1.97	1.97	-2588.2	1495.8	-29.9
25	partial	1725	2700	29.3	84.3	0.006	0.421	0.109	114.	0.001	3.3	2.9	0.490	0.433	0.433	-300.7	203.3	-3.63
26	partial	3450	2700	50.4	148.	0.024	1.69	0.832	201.	0.004	5.5	4.9	0.819	0.724	0.724	-602.4	405.8	-7.26
27	partial	5175	2700	69.4	203.	0.055	3.79	2.82	279.	0.010	7.4	6.6	1.11	0.978	0.978	-906.3	606.6	-10.9
28	partial	6900	2700	88.0	257.	0.099	6.73	6.98	360.	0.019	9.2	8.1	1.37	1.21	1.21	-1213.7	804.8	-14.6
29	partial	13800	2700	202.	537.	0.436	26.6	63.1	928.	0.076	14.3	12.7	2.14	1.90	1.90	-2508.4	1554.9	-29.5

TABLE B-3 (CONT.)

Run No.	ω_B	ω_C	α_1	α_0	Pitch Angle	Yaw Angle	$\frac{Q_{ASP}}{Q_{TOT}}$	$(Q_{TOT})_i$	$\frac{Q_{ASP}}{Q_{TOT}}$	Newton's	$(Q_{TOT})_0$	R_0	μ_1	$(\mu_{EFF})_i$	$(\mu_{EFF})_0$	MAX EQ
	rad/sec	rad/sec	Deg.	Deg.	Deg.	Deg.		Newton's		Newton's						
1	370.	73.97	40.90	40.68	52.1	0.0	0.600	395.0	0.579	398.2	0.0047	0.00087	0.030	0.032	0.057	
2	726.	147.8	41.77	40.20	44.7	0.0	0.371	300.9	0.329	401.6	0.0030	0.0019	0.020	0.018	0.075	
3	1665.	308.1	45.16	38.06	14.1	1.1	0.150	377.0	0.094	433.3	0.0003	0.0147	0.020	0.012	-	
4	3204.	219.8	52.10	31.68	0	0.1	0.016	52.8	0.050	82.7	0.0069	0.0053	0.006	0.009	0.392	
5	365.	73.0	41.90	41.05	33.7	0.3	0.466	953.7	0.155	955.5	0.0037	0.023	0.036	0.025	2.13	
6	720.	148.2	41.93	41.08	41.4	0.2	0.299	945.6	0.270	958.5	0.0061	0.0109	0.023	0.018	0.37	
7	1098.	222.1	42.29	40.86	34.3	0.3	0.195	934.3	0.163	963.4	0.0102	0.0086	0.017	0.017	-	
8	1464.	296.4	43.00	40.37	47.1	0.9	0.126	921.4	0.097	972.6	0.0116	0.0098	0.015	0.015	-	
9	3396.	638.7	49.22	36.34	13.6	1.5	0.0299	928.7	0.0125	1161.7	0.016	0.013	0.014	0.017	1.71	
10	383.	74.2	41.80	41.90	39.7	0.2	0.408	1497.4	0.490	1501.0	0.020	0.013	0.028	0.037	0.85	
11	732.	148.4	42.12	41.71	47.4	0.0	0.267	1491.5	0.243	1504.5	0.015	0.014	0.024	0.024	-	
12	1099.	222.6	42.44	41.52	47.3	0.2	0.177	1481.3	0.150	1510.4	0.014	0.014	0.020	0.019	-	
13	1466.	296.9	42.92	41.22	46.8	0.3	0.118	1467.6	0.092	1519.0	0.014	0.015	0.019	0.017	-	
14	3281.	618.5	46.83	30.74	17.2	1.9	0.028	1417.1	0.014	1636.1	0.017	0.020	0.021	0.017	-	
15	363.	73.9	41.01	40.64	33.1	0.7	0.602	395.1	0.581	398.4	0.0049	0.010	0.034	0.031	-	
16	727.	147.9	41.81	40.18	32.7	0.7	0.373	309.2	0.330	402.1	0.0045	0.010	0.025	0.020	-	
17	1095.	222.4	43.00	39.39	32.	0.7	0.236	379.9	0.189	408.9	0.0043	0.010	0.019	0.013	-	
18	1471.	298.0	41.86	38.24	31.1	0.7	0.147	367.9	0.104	419.2	0.0042	0.0068	0.013	0.009	-	
19	3207.	638.8	53.46	29.81	24.2	0.6	0.028	315.0	0.010	522.0	0.0049	0.0099	0.011	0.005	-	
20	363.	74.0	41.50	41.33	33.7	0.7	0.167	950.9	0.456	954.2	0.015	0.0247	0.037	0.029	-	
21	726.	148.1	41.82	41.14	33.5	0.7	0.301	945.0	0.271	957.8	0.0105	0.0211	0.030	0.021	-	
22	1091.	222.3	42.36	40.82	33.2	0.7	0.197	935.2	0.164	964.1	0.0100	0.0100	0.018	0.017	-	
23	1459.	296.8	43.11	40.35	32.8	0.7	0.129	922.1	0.097	973.2	0.0097	0.0109	0.016	0.017	-	
24	3489.	663.8	48.18	36.95	30.	0.7	0.028	845.5	0.015	1048.4	0.0096	0.0156	0.017	0.010	-	
25	363.	74.1	41.93	41.82	34.1	0.7	0.409	1497.6	0.401	1500.8	0.0150	0.0138	0.029	0.028	-	
26	726.	148.3	42.14	41.70	34.	0.7	0.268	1491.7	0.244	1504.4	0.0138	0.0112	0.022	0.023	-	
27	1091.	222.5	42.42	41.49	33.8	0.7	0.179	1481.9	0.151	1510.6	0.0132	0.0097	0.017	0.019	-	
28	1456.	296.9	42.96	41.20	33.6	0.7	0.119	1468.5	0.092	1519.4	0.0127	0.0150	0.019	0.016	-	
29	2931.	598.9	46.25	39.88	31.8	0.7	0.028	1385.5	0.016	1587.4	0.0125	0.0172	0.018	0.013	-	

$q_{\text{cage-land}}$ - heat generated at the cage-land contact (watts)
 q_{drag} - heat generated by fluid resistance (drag) (watts)
 q_{tot} - total heat generation rate (watts)
 $q_{\text{drag}}/q_{\text{TOT}}$ - fraction of total heat generated due to fluid resistance
 h_o, h_i - EHD film thicknesses at the outer and inner ring contacts (μ in.)
 $h_o/\sigma, h_i/\sigma$ - EHD film thickness to composite surface roughness ratio
 $\omega_x, \omega_y, \omega_z$ - orthogonal components of ball autorotational velocity vector (rad/sec)
 ω_B - resultant of ball autorotational velocity vector (rad/sec)
 ω_C - cage rotational velocity (rad/sec)
 α_i, α_o - inner and outer ring contact angles
pitch angle $\tan^{-1}(\omega_y/\omega_x)$ (deg)
yaw angle $\tan^{-1}(\omega_z/\omega_x)$ (deg)
 $(Q_{\text{ASP}}/Q_{\text{TOT}})_i, (Q_{\text{ASP}}/Q_{\text{TOT}})_o$ - fraction of contact load carried by asperities of the inner and outer rings respectively
 $(Q_{\text{TOT}})_i, (Q_{\text{TOT}})_o$ - contact load at inner and outer ring contacts (Newtons)
 μ_i, μ_o - average fluid friction coefficient at the inner and outer contacts
 $(\mu_{\text{eff}})_i, (\mu_{\text{eff}})_o$ - effective friction coefficient at the inner and outer contacts
 $|\text{MAXEQ}|$ - the largest residual of the equilibrium equations

The μ_{eff} values are not computer output but have been calculated based on computer output data, with the following equation

$$\mu_{\text{eff}} = \mu \left(1 - \frac{Q_{\text{ASP}}}{Q_{\text{TOT}}}\right) + \mu_a \frac{Q_{\text{ASP}}}{Q_{\text{TOT}}} \quad (8-1)$$

where: μ represents the average coefficient of fluid friction computed at each slice in a given contact

$Q_{\text{ASP}}/Q_{\text{TOT}}$ is the ratio of the load carried by the asperities, Q_{ASP} , to the total contact load q_{TX}

μ_a is the coefficient of Coulomb friction assumed valid for asperity contact. A value of 0.1 was assumed for μ_a for data sets I and II, and 0.05 for data set III.

The value of μ_{eff} given by Eq. 8.1 is an effective friction coefficient only inasmuch as it is the average

magnitude of the friction coefficient acting at each of the slices into which the contact ellipse is divided in computing the total traction. It does not give the total traction force acting at a contact when multiplied by the normal force because it does not account for the direction of slip across the contact ellipse. Its primary use is as a gauge of the degree to which asperity contact participates in the determination of traction.

The value labeled $|MAXEQ|$, is related to program performance, not bearing performance. When a value of $|MAXEQ|$ is listed this indicates that the program has not converged to a solution as accurate as requested. The $|MAXEQ|$ value shown is the largest of the seven residues from the six ball and one cage equilibrium equations. Recall that ball equilibrium is satisfied considering six degrees of freedom and cage equilibrium is satisfied in the circumferential direction. For instance, a $|MAXEQ|$ value of 0.2 indicates that the largest unbalanced force or moment associated with the system is 0.2 pounds or inchpounds respectively. Experience has shown that $|MAXEQ|$ values less than 0.1 usually indicate the solution is good and certainly useable for the size bearings examined in this study. With $|MAXEQ|$ values greater than 0.1 the data may or may not be useable. Its useability can best be judged through examination of data from neighboring points which have solved completely.

8.2 DATA SET 1 - COMPUTER PREDICTIONS FOR FULL SCALE TEST CONDITIONS

The more important portions of the data of Table 8-1 will be examined and where applicable, experimental or analytical findings of other workers in the field will be related to it.

8.2.1 Film Thickness

The first three blocks of data, representing experimental tests 1, (run nos. 1-8) 11, (run nos. 9-13) and 4, (run nos. 14-20) reflect the use of a MIL-L-7808G lubricant. The test 2 data block (run nos. 21-31) reflects a MIL-L-23699 lubricant. Observe that film thickness tends to decrease with increasing shaft speed. This is not always the case, but certainly is the trend and is of course contrary to isothermal film thickness equation. That equation would have the film thickness increasing in proportion to the 0.7 power of shaft speed. With other things remaining constant, film thickness should increase with shaft speed. Obviously, other things are not remaining constant. Both the lubricant viscosity and the pressure

viscosity coefficient decrease as the operating temperature rises with increasing speed. The changes in temperature can be seen in Tables 7.6 and 7.8. Examination of the operating viscosity, film thermal reduction factor ϕ_T and the starvation reduction factor ϕ_S (not shown in Table 8.1) indicates that the loss of viscosity with increasing temperature rather than starvation or inlet heating is primarily responsible for the decrease in film thickness. The film replenishment layer $\Delta\zeta$ assumed for these runs was sufficiently thick that the starvation reduction factor never took on a value less than unity, i.e. starvation was never predicted.

In passing, note that in the computer runs made to compare against NASA test data, (see {20}), the same shaft speed temperature effect on film thickness, was observed.

While no general conclusions can be drawn from only two sets of data, it is instructive to note that it is not axiomatic that thick EHD films will result at high operating speeds and that they will become yet thicker with increasing speed.

8.2.2 Asperity Friction

In Section 7 the raceway surface roughness and asperity slopes used as input to the computer program were actual measured values on a representative bearing. The slopes were 2.4 degrees and 2.0 degrees for the outer and inner races respectively. The roughnesses were 0.060 and 0.160 micrometers for the outer and inner races. The ball surface characteristics used were, RMS slope, 20° , and a surface roughness of 0.040 microns. These roughness values are well within the tolerance range for M-50 aircraft quality bearings.

The calculated values of the ratio of the inner race film thickness to surface roughness h/σ , were always close to unity during operation with the 14590 Newton (3280 pound) axial load. Under these conditions the partial EHD theory embodied in the program predicted that roughly one third of the ball-race contact load would be carried by the asperities rather than the EHD film. A friction coefficient of 0.1 has been assumed for the purpose of calculating the friction force which results from the asperity portion of the normal load. In those contacts where the h/σ value is less than one, the effective friction coefficient is from five to ten times the value which can be derived from lubricant shear. The higher friction coefficient affects both the generation of frictional heat and ball kinematics.

First, regarding the frictional heat generation rate, examine the heat prediction for three different series of tests within which the bearing was subject to the same load and speed conditions. In Table 8-1, note the last four data points under test number 1, (run nos. 5-8) the first three points under test number 11 (run nos. 9-11) and the last four points under test number 2, (run nos. 28-31). In all cases the load was (3280 pounds) 14590 Newtons, and the shaft speeds ranged from 10,000 to 17,500 RPM. However, the lubricant was MIL-L-23699 in test no. 2 and MIL-L-7808G in the other five tests.

For all cases the total heat generation at a particular speed is fairly constant. However, the heat at the inner ring contact shows substantial variation from test to test. The variation can be attributed primarily to the degree of asperity contact. The more viscous and cooler MIL-L-23699 lubricated bearing, runs with greater drag and hydrodynamic losses. However, the losses at the inner ring concentrated contact are several times less than those in the corresponding bearing lubricated with the MIL-L-7808 lubricant.

The effect of the greater asperity contact for the MIL-L-7808G runs is a higher effective friction coefficient and consequently a higher ball speed vector pitch angle.

The pitch angles for runs 28-31 are seen to be quite small.

Figures 8-1, 8-2 and 8-3 are presented to demonstrate the distribution of the generated heat predicted by the various models in the program. The contribution made by the asperity interaction at the inner raceway is very apparent and significant.

For Test Nos. 1 and 11, the heat generated at the inner ring varies from 31 to 42% of the total generated heat. In Test No. 2 it varies from 17 to 23%.

8.2.3 Cage Slip, Test No. 4

Figure 8-4 is a plot of the distribution of bearing heat which was predicted by the program for the experimental test where shaft speed was maintained at 10,000 RPM while applied load was systematically reduced in an attempt to induce cage slip. As noted in Section 7, the degree of correlation between the experimental and computed data is exceptionally good both for total generated heat and cage to shaft speed ratio. The total frictional heat decreases with decreasing load, and

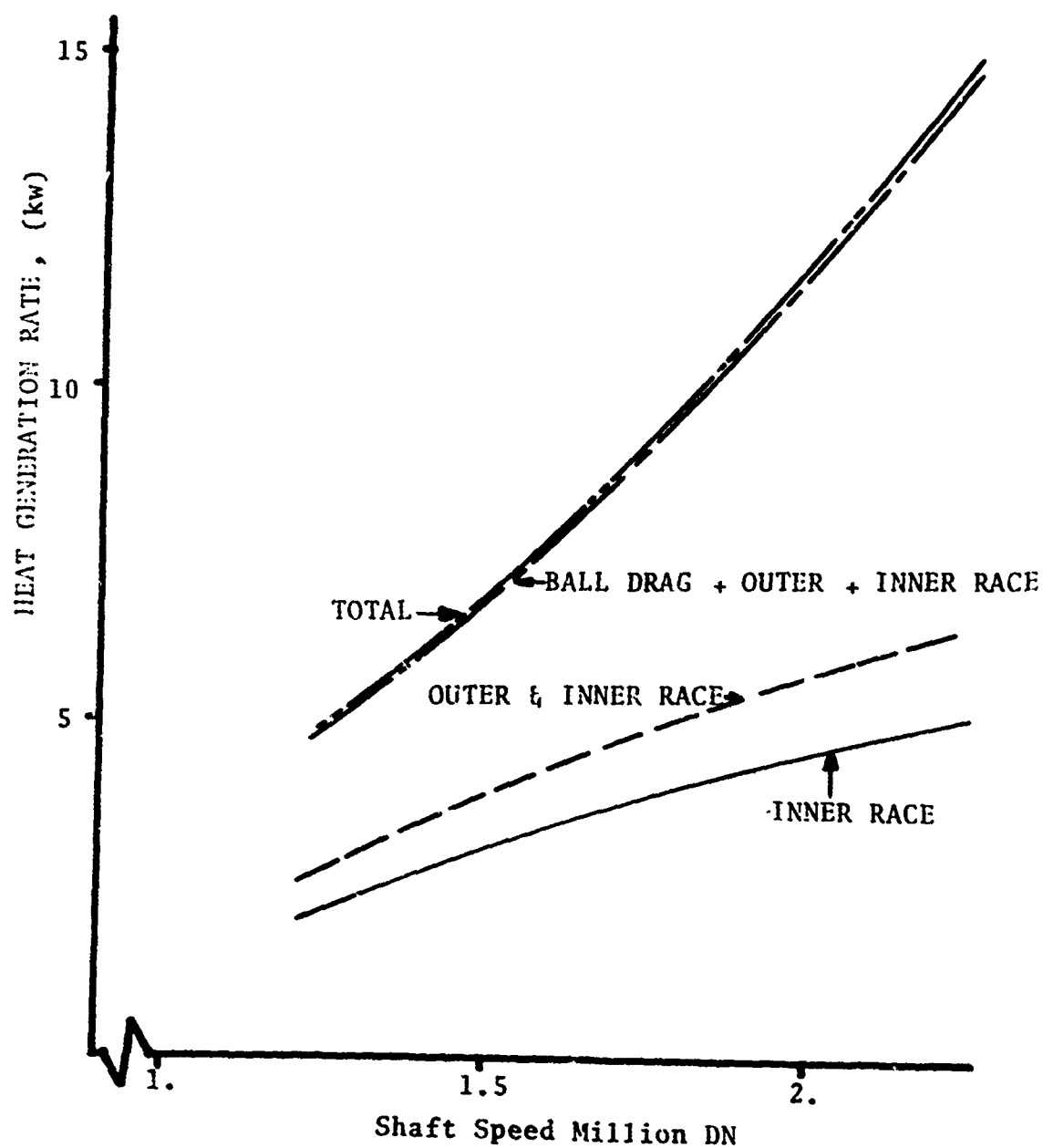


FIGURE 8-1

PROGRAM PREDICTED HEAT GENERATION RATES FOR EXPERIMENTAL TEST NO. 1
 VERSUS SHAFT SPEED (AXIAL LOAD 14590 N (3280 lb) MIL-L-7808G)

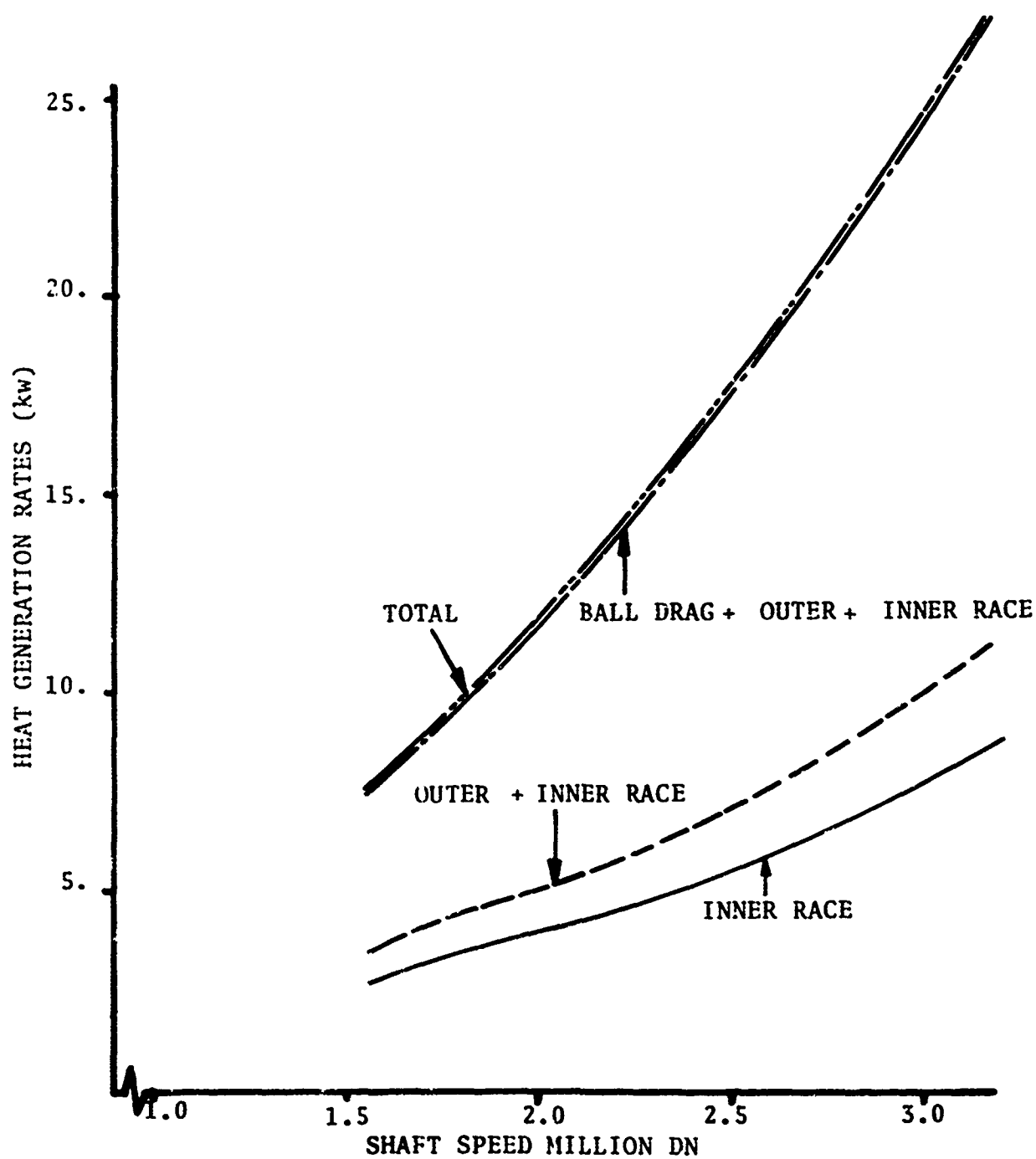


FIGURE 8-2

PROGRAM PREDICTED HEAT GENERATION RATES FOR EXPERIMENTAL TEST NO. 11
VERSUS SHAFT SPEED (AXIAL LOAD 14590 N (3280 Lb) MIL-L-7808G)

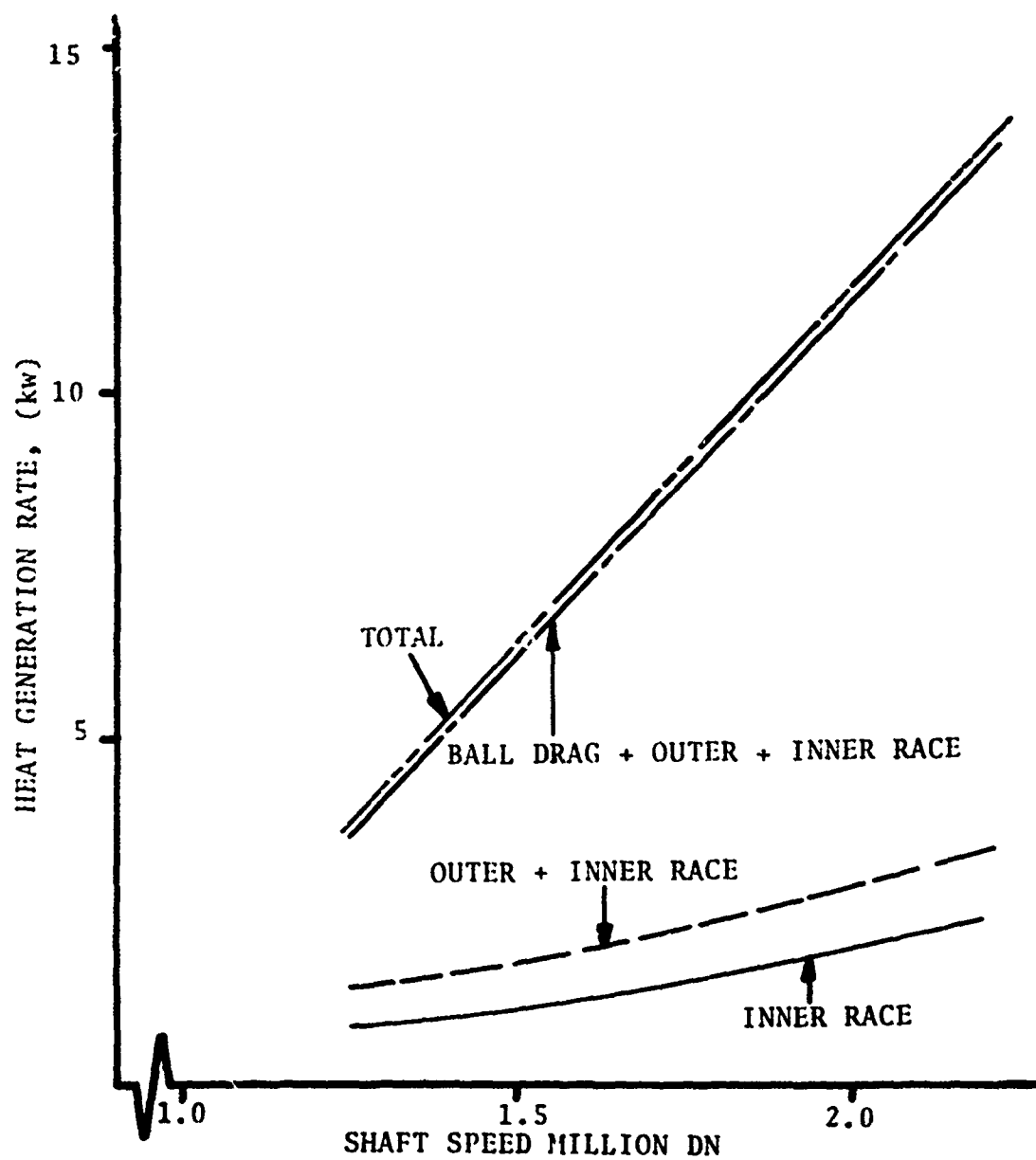


FIGURE 8-3

PROGRAM PREDICTED HEAT GENERATION RATES FOR EXPERIMENTAL TEST NO. 2
 VERSUS SHAFT SPEED (AXIAL LOAD 14590 N (3280 Lb) MIL-L-23699)

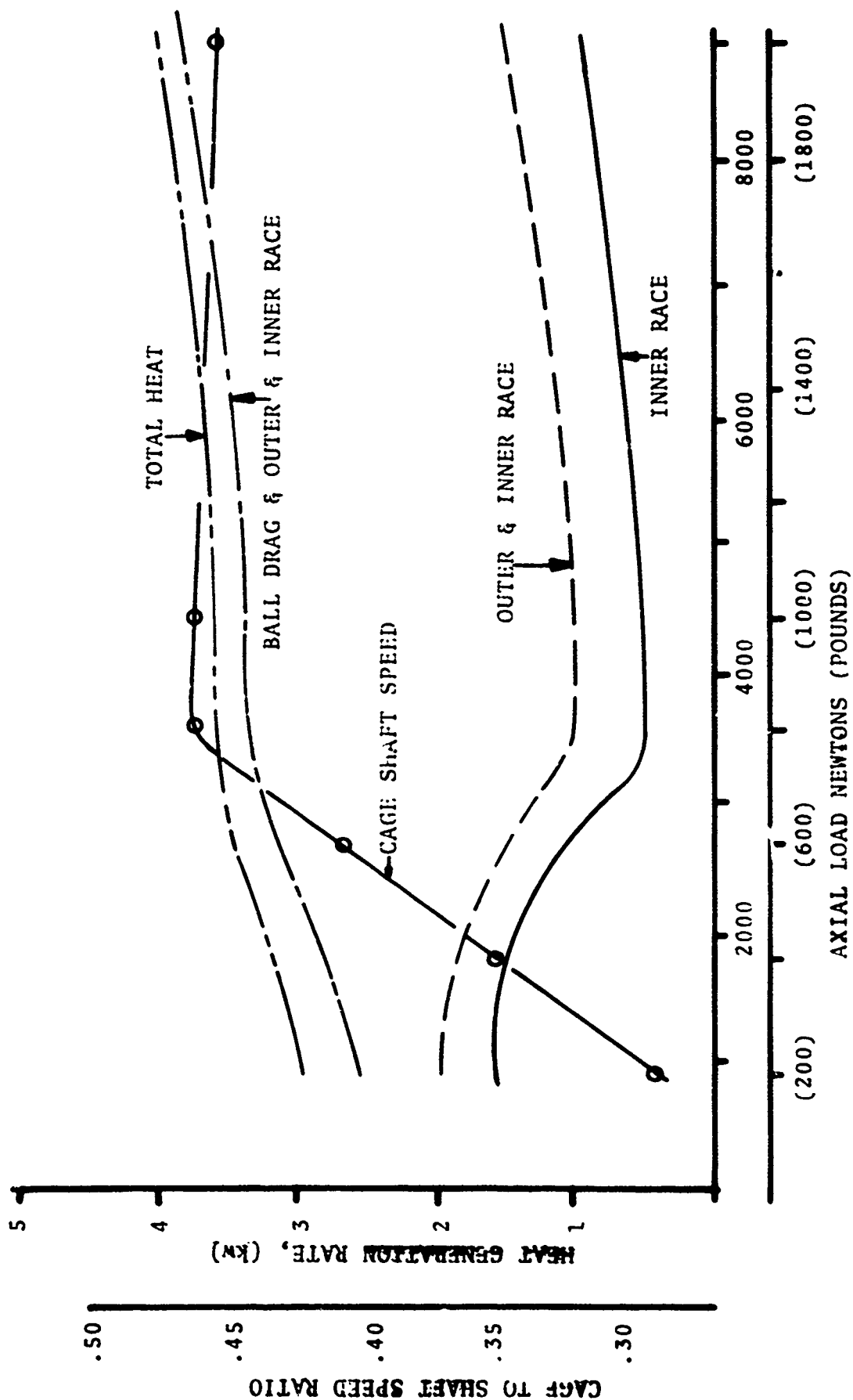


FIGURE 8-4

PROGRAM PREDICTED. CAGE TO SHAFT SPEED RATIO AND HEAT GENERATION RATES FOR
EXPERIMENTAL TEST NO. 4 VERSUS APPLIED AXIAL LOAD (SHAFT SPEED 10000 RPM MIL-L-7808G)

continues to decrease, but more drastically once substantial cage slip occurs. With increasing slip the inner ring frictional heat generation rate increases while the outer ring frictional heat generation rate remains relatively constant.

Figure 8-4 allows one to speculate upon the series of events which has been commonly referred to as a heat imbalance failure. For instance, the sudden increase in the rate at which heat is generated at the races under the conditions where the cage speed has dropped might lead to a large thermal gradient across the bearing and a loss of clearance and thus a reduction in contact angles. This might then progress to a thermal lockup situation where the contact angles approach zero and substantial contact loads develop. Provision of an adequate supply of inner race coolant, could circumvent thermal lockup. If this were done, the associated cage slip would be detrimental only if high loads are suddenly applied which cause the rolling elements and cage to accelerate rapidly. The thick films which were stable under the light load conditions might then collapse and significant amounts of microsmearing could take place. This is known as skid marking. If it becomes too severe, the surface of the ball and track is destroyed and the bearing fails from spalling.

It should be pointed out that the computer program has the capability to examine the transient thermal behavior of the bearing system while operating under either of the transient modes suggested above.

8.2.4 Raceway Control

Another observation that can be made from the data of Table 8-1 is that the ball pitch angle predictions are substantially less (i.e. the ball axis tends to be more nearly parallel to the bearing axis) than predicted by the outer race control theory.

For instance, under the highest shaft speed condition, 25,000 RPM, with outer race control (O. R. C.) the calculated pitch angle is 11.1 degrees, versus 1.5 degrees predicted by the program. Additionally, the yaw angle approaches but is not zero. The zero yaw condition is required by the O. R. C. analysis. In our analysis the small yaw angle is a consequence of the small gyro moment which is a function of the sine of the pitch angle.

8.3 DATA SET II - PARAMETRIC STUDIES OF FLUID RESISTANCE, FILM REPLENISHMENT AND CONTACT ANGLE

As noted earlier, parametric studies were performed to examine the sensitivity of the analysis to two program input variables which relate to the amount of lubricant within the bearing. The two variables are 1) XCAV, the percent of the bearing cavity filled with the fluid lubricant and 2) Δz , the thickness of the layer of lubricant which replenishes the ball and race surfaces between each pass of the contact.

8.3.1 Lubricant Medium Density Study

From experimental evidence, the density of the air lubricant mixture in the bearing, as measured by the variable XCAV appears to be associated not only with the lubricant flow rate but also the method of lubrication. For instance as noted in Section 7 there appears to be more churning type friction with through race lubrication than with jet lubrication given the same flow rates. It is speculated that not all of the jetted lubricant enters the bearing cavity.

There also appears to be an inverse relationship between the experimental value for XCAV and shaft speed when jet lubrication is being used. It is again speculated that the greater windage encountered with increasing speed tends to keep increasing amounts of the jetted lubricant away from the bearing. Note that the discussion in Section 7 concludes that there is a need to reduce the XCAV value as shaft speed increases.

The runs 1-3 in Table 8-2 show the effects of a reduction of the XCAV factor from 2.5% to 0.10%. (The data for the XCAV value of 0.01% (Run 4) is tabulated but this last run exhibited convergence problems and the data is suspect.)

The data behaves very predictably. The value Q_{DRAG} decreases approximately in the same proportion as the value of XCAV and this is the major change in the predicted operating parameters. The subtle changes in the ball and cage speeds as well as the effective friction coefficients can go almost unnoticed since they are so slight. However these small changes in ball and cage speed alter the distribution of sliding velocity across the contact ellipse sufficiently to change the tractive force, permitting it to resist the drag force for each value of XCAV. This occurs as the data show with negligible changes in the heat generation rates Q_{OUTER} and Q_{INNER} or in the degree of asperity participation as reflected in μ_{eff} .

8.3.2 $\Delta\zeta$ Variation

Next consider the consequences of changes in Δr at both the inner and outer race contacts. These data can be observed as runs 1, 9, 10, and 11 of Table 8-2.

Figure 8-5 shows a plot of the frictional heat generated at the ball race contacts as a function of $\Delta\zeta$. The inner and outer race heat generation rates include heat due to EHD friction, the asperity friction as well as the hydrodynamic losses around the contact. The hydrodynamic friction is being substantially reduced at both contacts with decreasing $\Delta\zeta$. The decrease is more apparent at the outer race for two reasons. The first is that the lubricant temperature is lower at the outer than at the inner and the viscosity is thus greater, producing greater hydrodynamic losses. The second reason is that at the inner race the EHD film is rather thin compared to the surface roughness and substantial asperity interaction is occurring. Starvation becomes apparent at the reduction of $\Delta\zeta$ from 0.0005 to 0.0001 mm. The 140 watt reduction in outer race heat generation rate from 215 to 75 watts is not observed at the inner race since the decrease in hydrodynamic friction is to a large part offset by an increase in asperity friction. The net decrease in inner race frictional heat is only 52 watts.

Figures 8-6 and 8-7 show plots of the outer race and inner race EHD film starvation factor and frictional heat generation rate as a function of $\Delta\zeta$. It is interesting to note that the films are not starved until the film replenishment layer is only 1/100 of the value used to generate all of the experimental data comparisons. The computed data indicates that a reduction in the amount of lubricant available to the EHD contacts can result in significant decreases in friction without resulting in starved films.

Experience shows that only a small amount of oil is needed to lubricate a conventional ball bearing. In a high speed and high viscosity situation, oil may have difficulty entering into the rolling track and the inlet of the contact, thus making EHD film starvation possible. An increase of oil supply into the inlet increases the meniscus distance which can effectively prevent the contact from starvation, but it also causes a persistent increase in rolling friction (F_R , F_N) (even if the meniscus distance grows considerable upstream of the contact, wherein the contact is almost unstarved). The degree of variation of starvation in high speed ball bearing contacts with the method of oil supply and the centrifugal force field acting on the lubricant requires further investigation.

Optimally it would be desirable to operate a bearing with as low a value of $\Delta\zeta$ as possible to avoid starvation while minimizing heat generation rates.

8.3.3 Contact Angle Variations

Runs 5-8 of Table 8-2 present the computed data obtained as the bearing initial, free, unmounted, contact angle was varied from 17 through 35 degrees. This data is interesting for two reasons. The first is that contact angle is one of the major bearing design variables over which the design engineer has control. The second interesting aspect of this data is

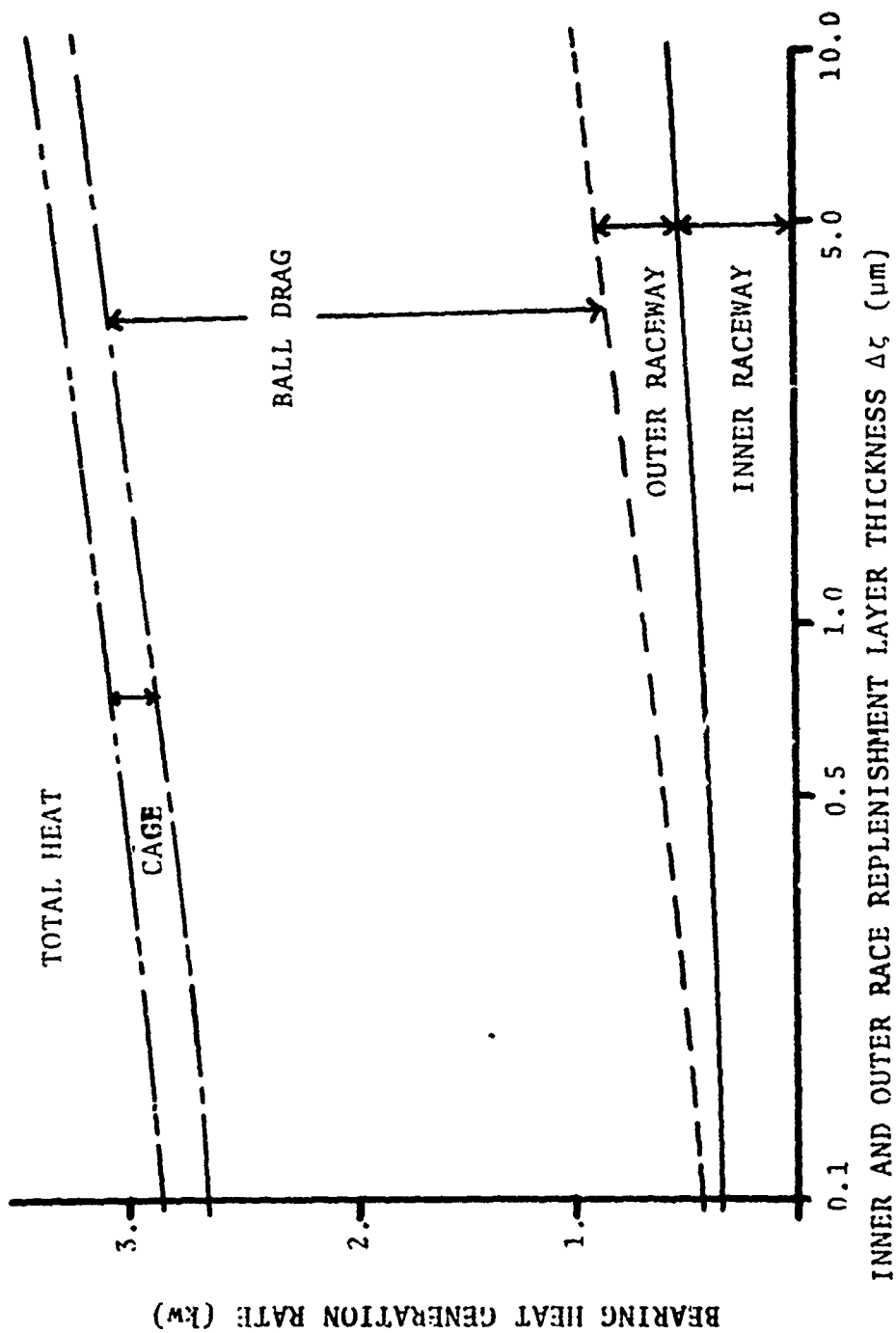


FIGURE 8-5

PROGRAM PREDICTED HEAT GENERATION RATE VERSUS
 $\Delta\zeta$ (AT AN AXIAL LOAD OF 4448.2 N (1000 lb))
 SHAFT SPEED 1000 RPM
 MIL-L-7808G

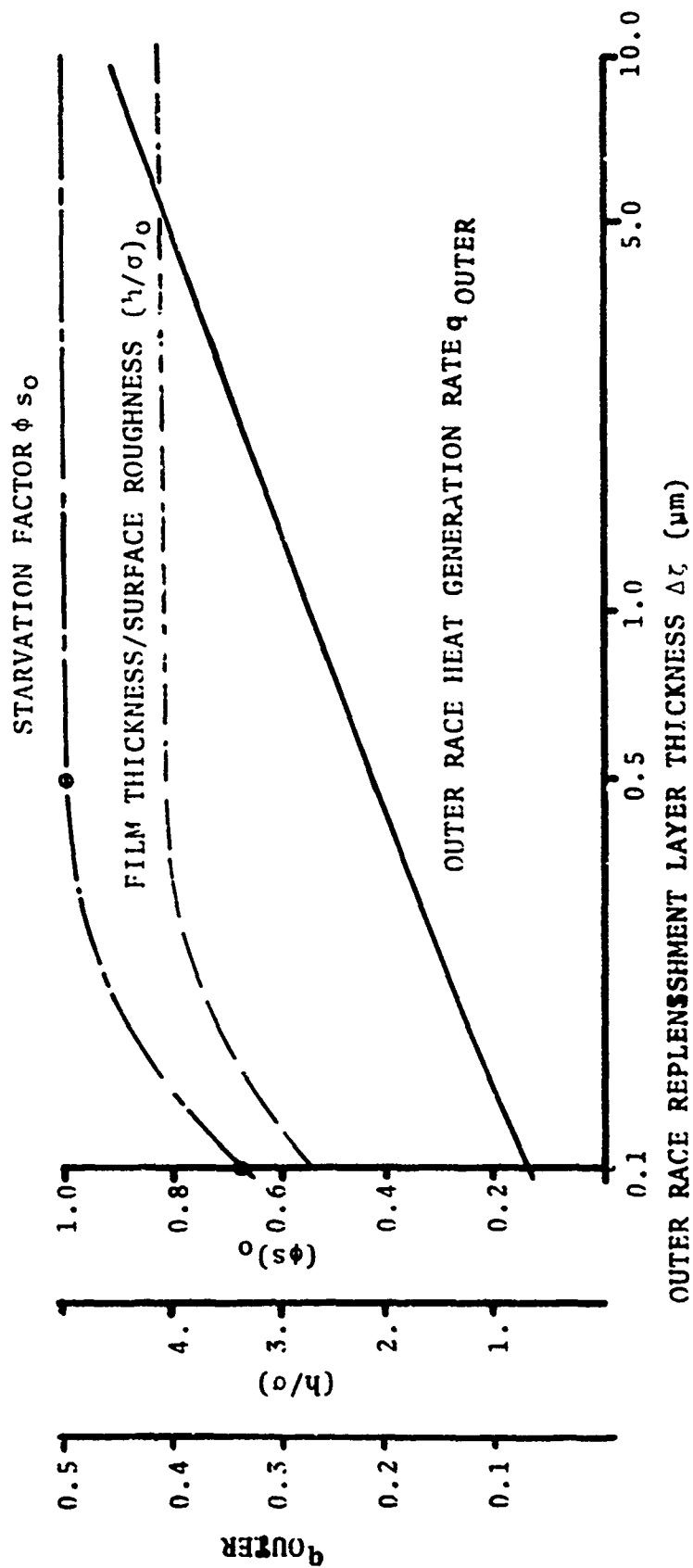


FIGURE 8-6

PROGRAM PREDICTED OUTER RACE DATA (HEAT GENERATION RATE, q_{OUTER} , FILM THICKNESS/
SURFACE ROUGHNESS $(h/\sigma)_0$; STARVATION FACTOR $(\phi s)_0$ VS. Δz)
AXIAL LOAD 4448.2 N (1000 LB), SHAFT SPEED 10000 RPM
MIL-L-7808G

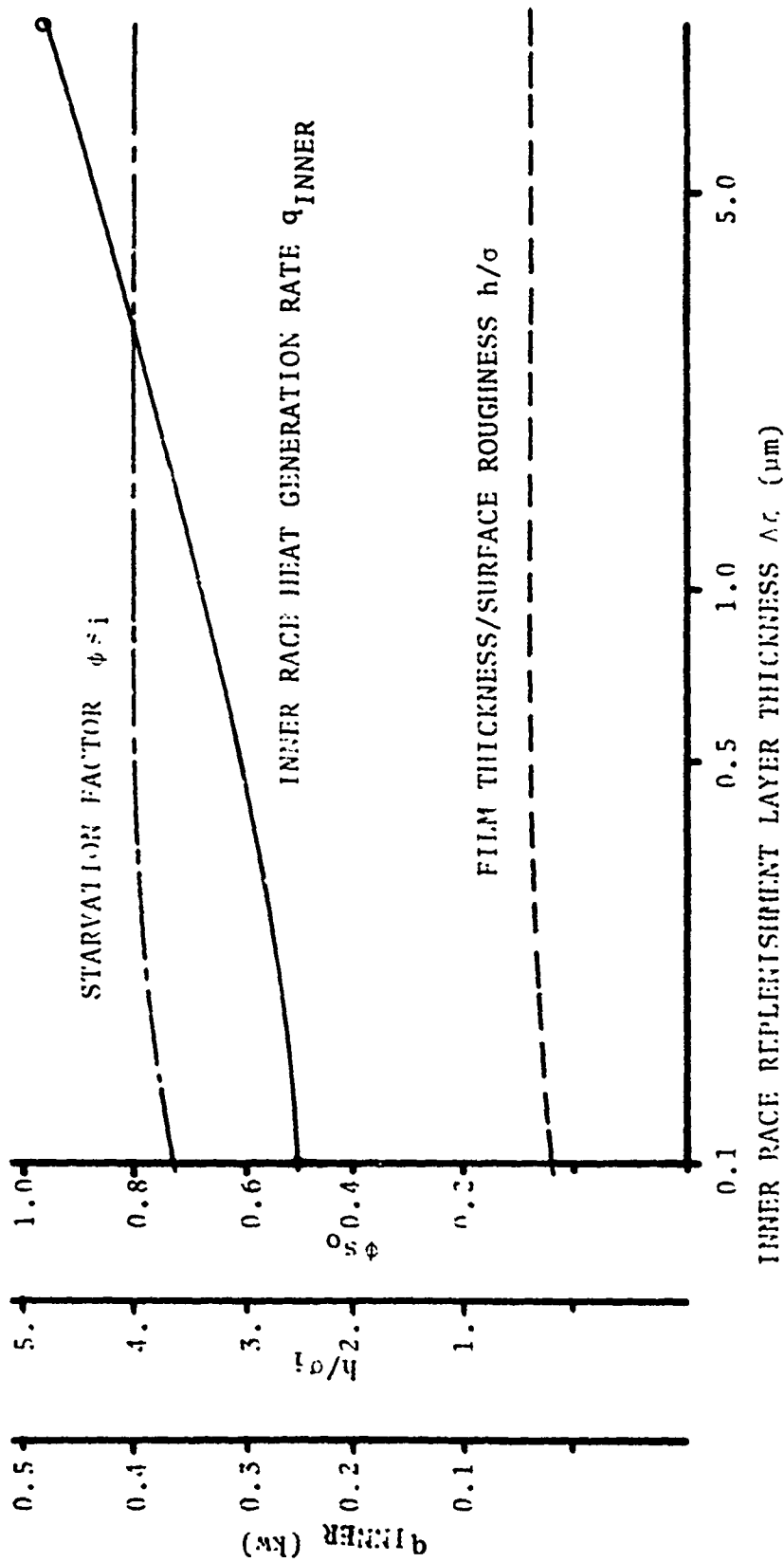


FIGURE 8-7

PROGRAM PREDICTED INNER RACE DATA, HEAT GENERATION RATE q_{INNER}
 FILM THICKNESS/SURFACE ROUGHNESS h/σ , STARVATION FACTOR $\phi_{s i}$ VS. Δc
 AXIAL LOAD 4448.2 N (1000 LB), SHAFT SPEED 10000 RPM
 MJL-1-7808G

that as a consequence of the relatively light applied load, we observe the tendency for cage slip to occur as the contact angle increases above 30° . The predictions of generated heat as shown in Fig. 8-8 are consistent with the set of cage slip data discussed earlier in Section 8.2.3. When slip occurs, the ball drag and the total heat decrease but inner race heat increases substantially.

The raceway and bearing fatigue lives as plotted against free unmounted contact angle in Fig. 8-9 show expected trends. As contact angle increases the ball-raceway contact loads decrease and thus fatigue life increases. Since the fatigue life is specified in hours and since the number of stress cycles per unit time decreases as cage slip is encountered, predicted fatigue life shows a dramatic increase. An additional factor contributing to the increased fatigue life resulting from cage slip is the reduction in ball centrifugal force and thus the reduction in outer raceway contact load.

It can also be seen from the values of MAXEQ in Table 8-2 that when slip occurs, the accuracy of the solution is often not as good as desired. This lack of stability of the program in the high slip regime seems to reflect a lack of kinematic stability in the bearing performance.

8.4 DATA SET III - PARAMETRIC STUDIES OF THE RACEWAY CONTROL ASSUMPTION

Table 8-3, presents a set of data generated for a 45 mm bore angular contact ball bearing to determine the consequences of using outer race control theory rather than quasidynamic equilibrium to predict bearing behavior under low speed and high load operating conditions. This data, although not relevant to high speed turbine bearings, does provide additional insight into the nature of the friction models contained in the computer program.

The first column of Table 8-3 refers to the solution type. "FULL" denotes that a full quasidynamic solution was obtained. "PARTIAL" indicates that the outer race control assumption was employed for determining ball kinematics. Friction forces were then evaluated using the velocities implicit in the outer race control assumption.

All of the computer runs were made assuming a constant bearing operating temperature of 150°F for all locations within the bearing. This is distinct from the data tabled in

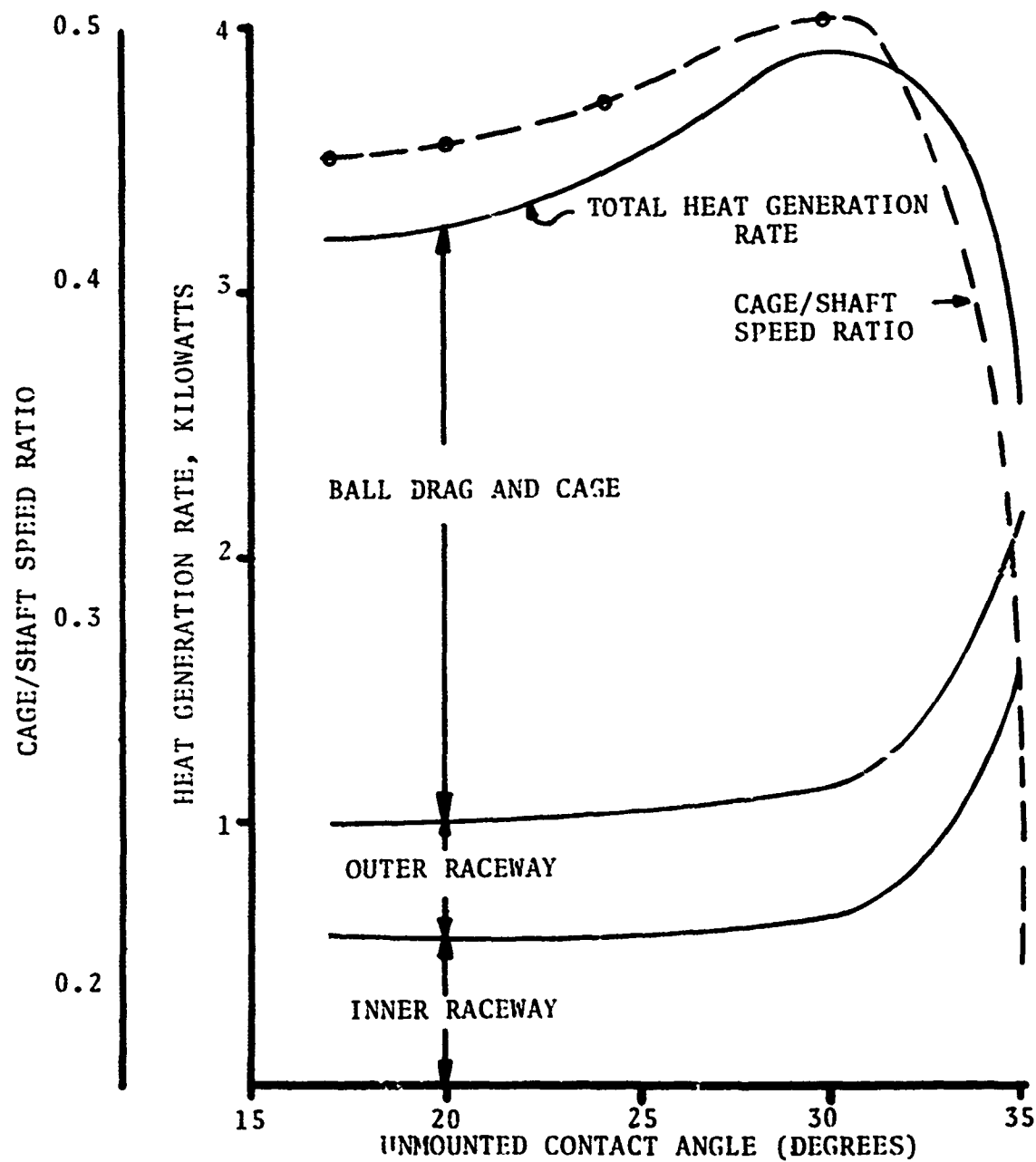


FIGURE 8-8

BEARING HEAT GENERATION RATES AND CAGE TO SHAFT SPEED RATIO VERSUS UNMOUNTED CONTACT (ANGLE SHAFT SPEED 10000 RPM APPLIED AXIAL LOAD 4448.2 N (1000 Lb) MIL-L-7808G)

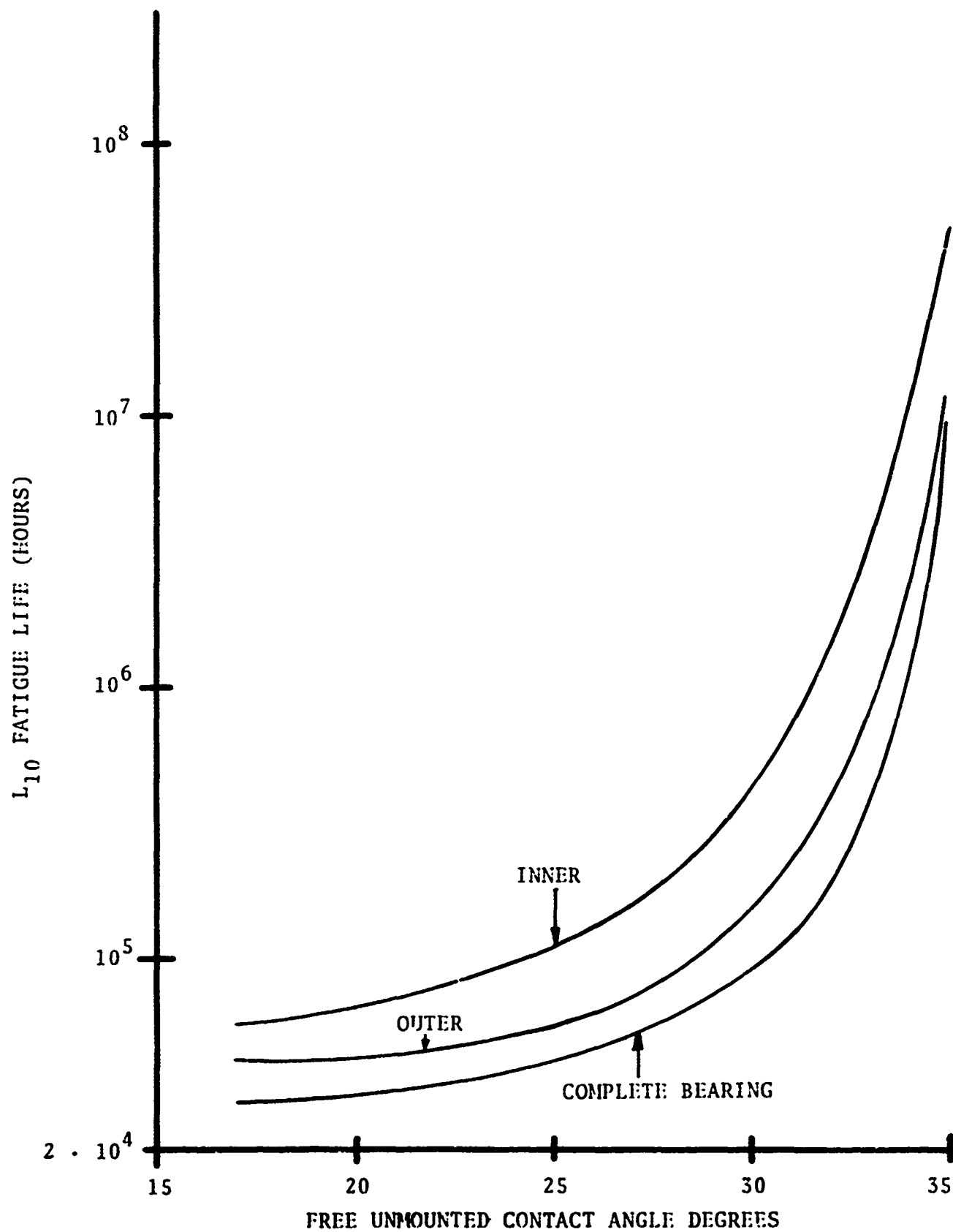


FIGURE 8-9

BEARING AND RACEWAY L_{10} FATIGUE LIFE VERSUS UNMOUNTED CONTACT
 ANGLE (SHAFT SPEED 10000 RPM APPLIED AXIAL LOAD 4448.2 N (1000 lb))
 MIL-L-7808G 180

8-1 and 8-2 in which the bearing operating temperatures increased with speed. A second significant distinction with this set of data is that an asperity friction coefficient of 0.05 was used rather than 0.10. Because film thickness increased with increasing speed in this set of runs, the asperity friction tended to become less influential with increasing speed.

Interesting inferences can be drawn regarding raceway control theory. Figures 8-10 and 8-11 show the ball speed vector pitch angle as a function of speed as calculated with inner race control, (I. R. C.), outer race control, (O. R. C.), and as predicted by the computer program for the 3310 N (700 lb) and 12010 N (2200 lb) applied axial loads. Obviously, the raceway control solutions do not even serve as bounds for the program solution over the full range of loads and speeds. Figure 8.11 does indicate that a state of ball kinematics lying in the range between I. R. C. and O. R. C. is maintained over a large part of the high load, low speed range. However, at the light load the ball kinematics fall inside this range.

Although raceway control does not any longer appear to be a universally valid concept, many ball bearing analyses are based upon it so it seems worthwhile to look for systematic errors which the race control theory might produce. Our data limits our examination to O. R. C. only. Examining the heat generation rates for the highest shaft speed, 13,800 RPM, and the two higher loads, 1,700 and 2,700 pounds, it is seen that the heat generated at both raceways is greater for the full solution data. In the light load case, since substantial cage slip is predicted outer race control certainly cannot match this prediction. Since the cage speeds and thus the drag heat is very similar for the respective full and partial solutions the overall heat generation calculated by the two solution routines may be reasonably well predicted, particularly when responsible for a large share of the total. Thus the outer race control solution may produce reasonable results for high speed operation with a plentiful supply of lubricant.

At first sight, a puzzling set of circumstances arises as one considers only the full and partial solution data in the table. The partial solution heat generation rates suggest, that at the set of ball and cage speeds predicted by outer race control, the bearing operates at lower losses than the full solution predicts. This of course is physically impossible. The reason for the anomalous result is that outer race control does not require the ball to be in the state of equilibrium, i.e., the gyroscopic moment which acts on the ball is assumed

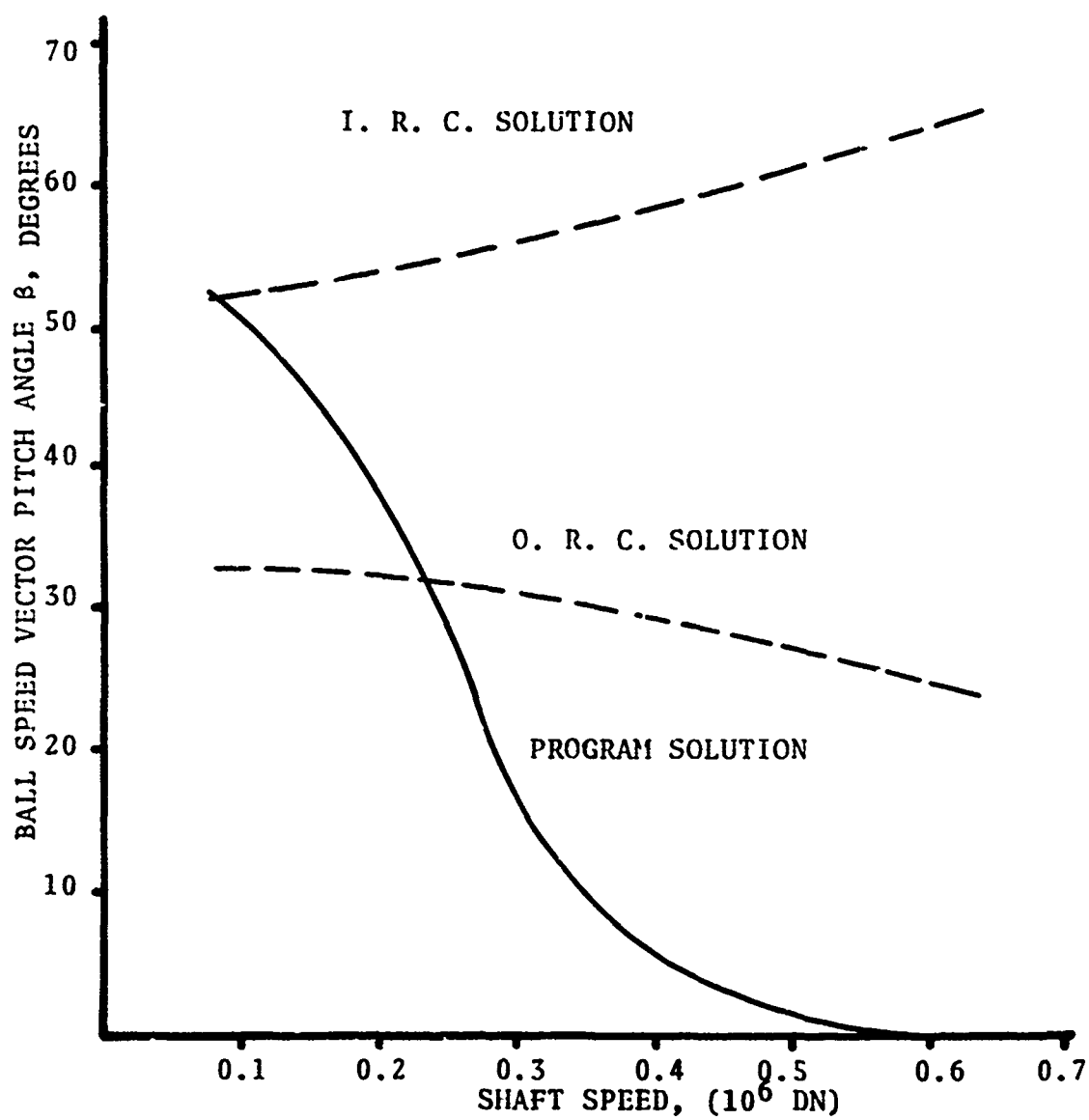


FIGURE 8-10

BALL SPEED VECTOR PITCH ANGLE VERSUS SHAFT SPEED (7309 ANGULAR CONTACT BEARING AXIAL LOAD 3114N, (700 lb))

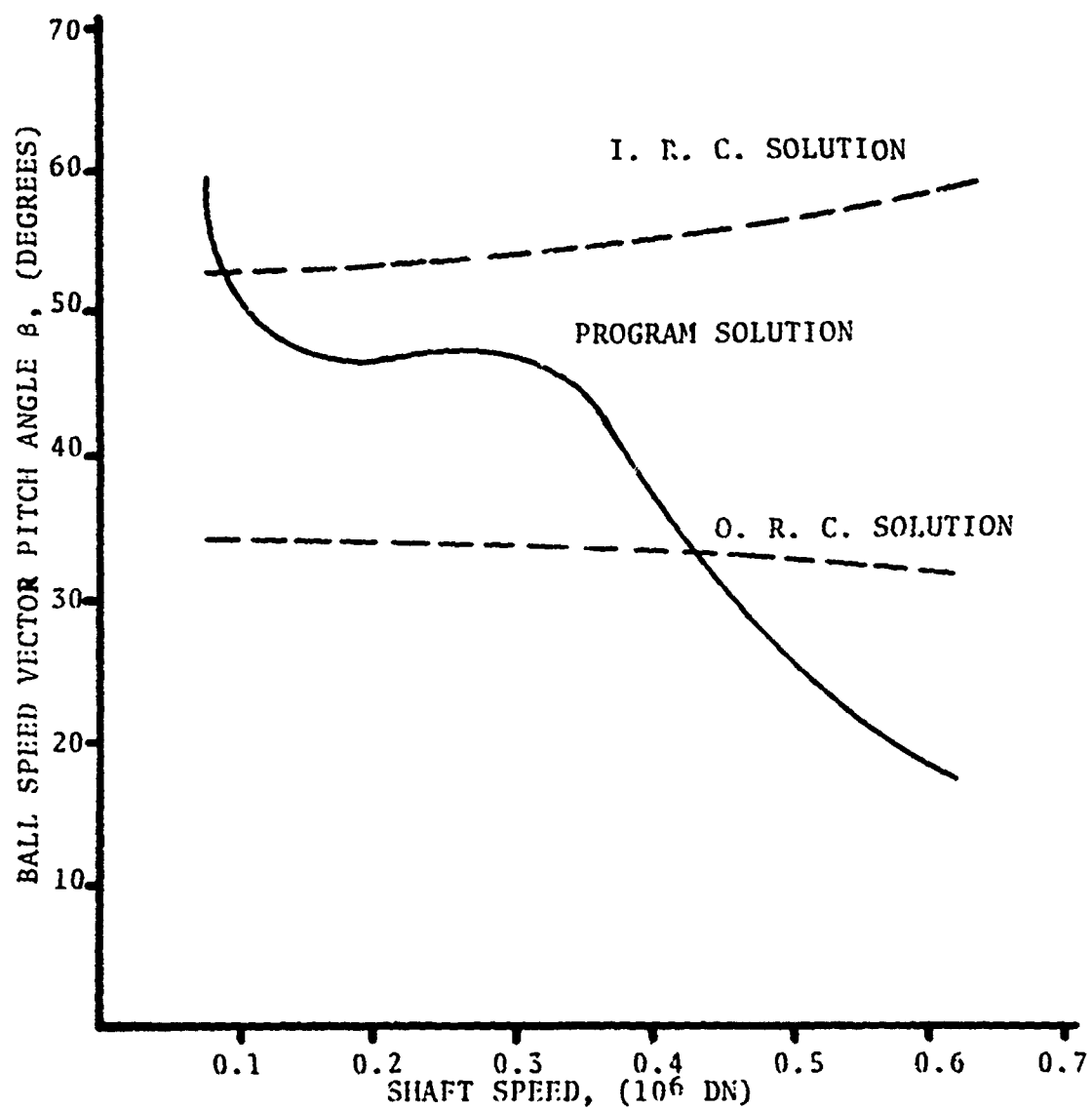


FIGURE 8-11

BALL SPEED VECTOR PITCH ANGLE VERSUS SHAFT SPEED
 7309 ANGULAR CONTACT BALL BEARING AXIAL LOAD 12010 N (2700 Lb)
 MIL-L-7808G

to be reacted by the friction force at the controlling ball race contact. However, the ball rotation is not allowed to change in reaction to the gyro moment, and there is no requirement that ball equilibrium be satisfied.

8.5 OVERVIEW OF THE DATA

The following principal observations emerge from the above discussion.

- 1) The partial EHD model which accounts separately for lubricant shear and asperity friction appears to be a necessity for the evaluation of bearings under general operating conditions. The asperity model is of major importance when the film thickness/surface roughness ratio is in the neighborhood of two or less. At a film parameter value, h/σ , of two, the effective friction coefficient in the raceway contacts may be more than twice the value which could be calculated considering lubricant shear alone, assuming an asperity friction coefficient of 0.1. As h/σ approaches 0.5 the effective friction coefficient may be as high as ten times the corresponding coefficient derived from the lubricant shear alone.
- 2) The tendency for the lubricant film thickness to increase with increasing speed can be more than offset by the tendency toward higher operating temperature and lower viscosity at the higher speed. This occurred consistently throughout the experiments run in this project as well as in similar NASA sponsored experiments conducted at Pratt & Whitney Aircraft {20}. The tendency for film thickness to decrease with increasing shaft speed exists even if there are no starvation effects.
- 3) The lubricant starvation effect tends to reduce the contact hydrodynamic friction before the EHD film thickness begins to be reduced. There is, then, a maximum oil supply which minimizes friction.
- 4) The model used to describe churning losses must be adjusted by the user to reflect decreasing proportions of lubricant within the bearing cavity as shaft speed increases. Put another way, the present churning loss model if used with constant XCAV yields heat generation rates that are too highly speed dependent when compared to experimental data.

- 5) The raceway control theory is not generally valid for the speed and load ranges considered. However, under conditions of moderate to heavy loading at low speeds, a state of ball kinematical behavior between outer and inner race control is achieved.

REFERENCES

1. Cheng, H. S., "Calculation of EHD Film Thickness in High Speed Rolling and Sliding Contacts", MTI Report 67-TR-24 (1967).
2. Dusinberre, G. M., "Numerical Analysis of Heat Flow", McGraw-Hill Book Company, Inc. (1949).
3. Tallian, T. E., "The Theory of Partial Elastohydrodynamic Contacts", Wear, 21, pp 49-101, (1972).
4. McGrew, J. M., et al, "Elastohydrodynamic Lubrication Preliminary Design Manual", Technical Report AFAPL-TR-70-27, pp 20-21, November 1970.
5. Fresco, G. P., et al, "Measurement and Prediction of Viscosity-Pressure Characteristics of Liquids". A Thesis in Chemical Engineering Report No. PRL-3-66, Department of Chemical Engineering College of Engineering The Pennsylvania State University, University Park Pennsylvania.
6. McCool, J. I., et al, "Interim Technical Report on Influence of Elastohydrodynamic Lubrication on the Life and Operation of Turbine Engine Ball Bearings," S K F Report No. AL73PO14, submitted to AFAPL and NAPTC under AF Contract No. F33615-72-C-1467, Navy MIPR No. M62376-3-000007, October 1973.
7. McCool, J. I., et al, "Interim Technical Report on Influence of Elastohydrodynamic Lubrication on the Life and Operation of Turbine Engine Ball Bearings," S K F Report No. AL74PO12, submitted to AFAPL and NAPTC under AF Contract No. F33615-72-C-1467, Navy MIPR No. M62376-3-000007, July 1974.
8. Kellstrom, M., "A Computer Program for Elastic and Thermal Analysis of Shaft Bearing Systems", S K F Report No. AL74PO04, submitted to Vulnerability Laboratory, U. S. Army Ballistic Research Laboratories, Aberdeen Proving Ground, MD, under Army Contract DAAD05-73-C-0011.
9. Burton, R. A., and Staph, H. E., "Thermally Activated Seizure of Angular Contact Bearings," ASLE Trans. 10, pp 408-417 (1967).
10. Jakob, M. and Hawkins, G. A., "Elements of Heat Transfer", 3rd ed., John Wiley & Sons, Inc. 1957.

11. Archard, J., and Cowking, E., "Elastohydrodynamic Lubrication at Point Contacts", Proc. Inst. Mech. Eng., Vol. 180, Part 3B, pp 47-56 (1965-1966).
12. Chiu, Y. P., "An Analysis and Prediction of Lubricant Film Starvation in Rolling Contact Systems", ASLE Transactions, 17, pp 22-35 (1974).
13. Nayak, P. R., "Random Process Model of Rough Surfaces", Journal of Lubrication Technology, 93, pp 398-407 (1971).
14. Johnson, K. L., and Cameron, R., "Shear Behavior of EHD Oil Film at High Rolling Contact Pressure", The Institution of Mech. Engr. Tribology Group, Westminster, London Vol 1 (1968).
15. Smith, R., et al, "Research on Elastohydrodynamic Lubrication of High Speed Rolling-Sliding Contacts", Air Force Aero Propulsion Laboratory, Wright-Patterson AFB, Ohio, Technical Report AFAPL-TR-71-54 (1971).
16. Chiu, Y. P., "A Theory of Hydrodynamic Friction Forces in Starved Point Contact Considering Cavitation", ASME Transactions, J. of Lub. Tech., 96, Series F, pp 237-246 (1974).
17. Harris, T. A., "An Analytical Method to Predict Skidding in Thrust Loaded Angular Contact Ball Bearings", Journal of Lubrication Technology, Trans. ASME, Series F, Vol. 93, No. 1, 1971, pp 17-24.
18. Liu, J. Y., Tallian, T. E., McCool, J. I., "Dependence of Bearing Fatigue Life on Film Thickness to Surface Roughness Ratio", ASLE Preprint 74AM-7B-1 (1974).
19. Lundberg, G. and Palmgren, A., "Dynamic Capacity of Roller Bearings", Proceedings of the Royal Swedish Academy of Engineering, Vol. 2, No. 4, 1952.
20. Holmes, P. W. "Evaluation of Drilled-Ball Bearings at DN Values to Three Million I-Variable Oil Flow Tests," NASA Contractor Report NASA CR2004.
21. Johnson, K. L., Greenwood, J. A., and Poon, S. Y., "A Simple Theory of Asperity Contact in Elastohydrodynamic Lubrication", Wear, 19, pp 91-108 (1972).

22. Tallian, T. E., et al, "Lubricant Films in Rolling Contact of Rough Surfaces," ASLE Trans. 7, pp 109-126 (1962).
23. Miele, A., et al, "Modified Quasilinearization Method for Solving Non-linear Equations," Rice University, Houston, Texas, Aero-Astronautics Rep. 78, 1970.
24. Wingo, D. R., "Maximum Likelihood Estimation of the Parameters of the Weibull Distribution by Modified Quasilinearization," IEEE Transactions on Reliability, Vol. R-21, No. 2, May 1972, pp 89-93.
25. Kent's Mechanical Engineering Handbook-Power Volume, John Wiley & Sons, Inc., 12th Ed., 1960, Chapter 3, p. 20.
26. Crecelius, W. J. and Milke, D., "Dynamic and Thermal Analysis of High Speed Tapered Roller Bearings Under Combined Loading," Technical Report NASA CR-121207.

APPENDIX A

HEAT TRANSFER INFORMATION

A.1 BACKGROUND

The temperature portion of Program AT74Y001 is designed to produce temperature maps for an axisymmetric mechanical system of any geometrical shape. The mechanical system is first approximated by an equivalent system comprising a number of elements of simple geometries. Each element is then represented by a node point having either a known or an unknown temperature. The environment surrounding the system is also represented by one or more nodes. With the node points properly selected, the heat balance equations can be set up accordingly for the nodes of unknown temperature. These equations become non-linear when there is convection and/or radiation between two or more of the node points considered. The problem is therefore reduced to solving a set of linear and/or non-linear equations for the same number of unknown nodal temperatures. It is obvious that the success of the approach depends largely on the physical subdivision of the system. If the subdivision is too fine, there will be a large number of equations to be solved; on the other hand, if the subdivision is too crude, the results may not be reliable. (In a system consisting of rolling bearings, for the sake of simplicity, the elements considered are usually axially symmetrical, e.g., each of the bearing rings can be taken as an element of uniform temperature. For an element which is not axially symmetrical, its temperature is also assumed to be uniform and its presence is assumed not to distort the uniformity in temperature of a neighboring element which is axially symmetrical. That is, the non-symmetrical element is represented by an equivalent axially symmetrical element with approximately the same surface area and material volume. This kind of approximation may seem to be somewhat unrealistic, but with properly devised equivalent systems, it can be used to solve complicated problems with results satisfying some of the important engineering requirements.)

The computer program can solve the heat-balance equations for either the steady state or the transient state conditions and produce temperature maps for the mechanical system when the input data are properly prepared.

A.2 BASIC EQUATIONS

A.2.1 Heat Conduction

The rate of heat flow that is conducted from node i to node j may be expressed by,

$$q_{ci,j} = \frac{\lambda_{ij} A_{ij}}{L_{ij}} (t_i - t_j)$$

t_i and t_j are the temperatures at i and j , respectively, $A_{i,j}$ the area normal to the heat flow, (m^2) L_{ij} the distance (m) and λ_{ij} the thermal conductivity between i and j , ($W/m^\circ C$).

Assuming that the structure between point i and j is composed of different materials, an equivalent heat conductivity may be calculated as follows:

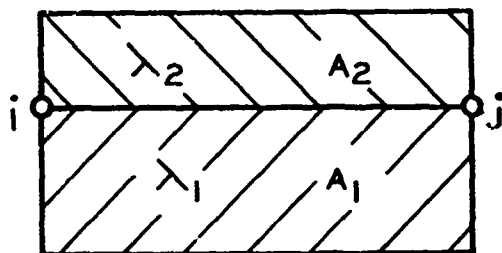


Fig. A-1

$$\lambda_{ij} = \frac{\lambda_1 A_1 + \lambda_2 A_2}{A_{ij}}$$

$$A_{ij} = A_1 + A_2$$

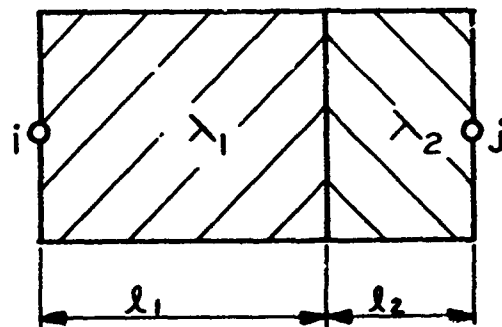


Fig. A-2

$$\lambda_{ij} = \frac{l_{ij}}{l_1/\lambda_1 + l_2/\lambda_2}$$

$$l_{ij} = l_1 + l_2$$

The calculation of the areas will be discussed in Section A.2.5.

A.2.2 CONVECTION

The rate of heat flow that is transferred between a solid structure and air by free convection may be expressed by

$$q_{vi,j} = \alpha_{i,j} A_{i,j} |t_i - t_j|^{1.25} \cdot \text{SIGN}(t_i - t_j)$$

where

$$\text{sign}(t_j - t_i) = \begin{cases} 1, & \text{if } t_i - t_j \geq 0 \\ -1, & \text{if } t_j - t_i < 0 \end{cases}$$

in which

$$\alpha_{ij} = \begin{cases} 2.5 \cdot 10^{-2} \text{ W/m}^2 \cdot (\text{degC})^{1.25} & \text{for hot surfaces facing upward} \\ & \text{and cold surfaces facing downward} \\ 1.4 \cdot 10^{-2} \text{ W/m}^2 \cdot (\text{degC})^{1.25} & \text{for hot surfaces facing downward} \\ & \text{and cold surfaces facing upward} \\ 1.8 \cdot 10^{-2} \text{ W/m}^2 \cdot (\text{degC})^{1.25} & \text{for vertical surfaces} \end{cases}$$

For other special conditions, α_{ij} must be estimated by referring to heat transfer texts.

The rate of heat flow that is transferred between a solid structure and a fluid by forced convection may be expressed by

$$q_{ni,j} = \alpha_{i,j} A_{i,j} (t_i - t_j)$$

in which α_{ij} is the heat transfer coefficient.

Now, with $\alpha = \alpha_{ij}$, introduce the Nusselt number

$$N_u = \frac{\alpha L}{\lambda}$$

the Reynolds number

$$R_e = \frac{UL}{\nu}$$

and the Prandtl number

$$P_r = \frac{\rho \nu c_p}{\lambda}$$

where

L is a characteristic length which is equal to the diameter in the case of a cylindrical surface and is equal to the plate length in case of a flat surface (m)

U is a characteristic velocity which is equal to the difference between the fluid velocity at some distance from the surface and the surface velocity (m/sec)

λ is the fluid thermal conductivity (W/M°C)

ν is the fluid kinematic viscosity (M²/sec)

ρ is the fluid density (kg/m³)

c_p is the fluid specific heat (W/kg°C)

For given values of R_e and P_r the Nusselt number N_u and thus the heat transfer coefficient may be estimated from one of the following expressions:

Laminar flow along a flat plate: $R_e < 2300$

$$N_u = 0.323 \sqrt{R_e} \cdot \sqrt[3]{P_r}$$

Laminar flow of a liquid in a pipe:

$$N_u = 1.36 \sqrt[3]{R_e} \cdot P_r \left(\frac{D}{L}\right)$$

where D is the pipe diameter and L the pipe length

Turbulent flow of a liquid in a pipe:

$$N_u = 0.027 \cdot R_e^{0.8} \cdot \sqrt[3]{P_r}$$

Gas flow inside and outside a tube:

$$N_u = 0.3 R_e^{0.57}$$

Liquid flow outside a tube:

$$N_u = 0.6 R_e^{0.5} \cdot P_r^{0.31}$$

Forced free convection from the outer surface of a rotating shaft

$$N_u = 0.11 \left[0.5 R_e^2 \cdot P_r \right]^{0.35}$$

where the Reynolds number R_e is developed by the shaft rotation.

$$R_e = \frac{\omega \pi D^2}{\nu}$$

in which ω is the angular velocity (rad/sec)
 D is the roll diameter (m)

The average coefficient of forced convection to the lubricating oil within a rolling contact bearing may be approximated by,

$$\alpha = 0.0986 \left\{ \frac{N}{v} \left[1 + \frac{D \cos(\beta)}{d_m} \right] \right\}^{\frac{1}{2}} \lambda (P_r)^{1/3}$$

using + for outer ring rotation
 - for inner ring rotation

in which N is the bearing operating speed (rpm)
 D is the diameter of the rolling elements (mm)
 d_m is the bearing pitch diameter (mm)
 α is the bearing contact angle (degrees)

A.2.3 FLUID FLOW

The rate of heat flow that is transferred from fluid node i to fluid j by fluid flow is

$$q_{fi,j} = \rho \dot{V}_{ij} C_p (t_i - t_j)$$

\dot{V}_{ij} is the volume rate of flow from i to j . It must be observed that the continuity of mass requires the following equation to be satisfied

$$\sum \dot{V}_{ij} = 0$$

provided the fluid density is constant. The summation should be extended over all nodes i within the fluid which have heat exchange with node j by fluid flow.

A.2.4 HEAT RADIATION

The rate of heat flow that is radiated to node j from node i is expressed by

$$q_{Ri,j} = \delta_{i,j} \left\{ \left(\frac{T_i}{1000} \right)^4 - \left(\frac{T_j}{100} \right)^4 \right\}$$

where

$$T_j = t_j + 273.16$$

$$T_i = t_i + 273.16$$

and the value of the coefficient $\delta_{i,j}$ depends on the geometry and the emissivity or the absorptivity of the bodies involved.

For radiation between large, parallel and adjacent surfaces of equal area, $A_{i,j}$ and emissivity, $\epsilon_{i,j}$, $\delta_{i,j}$ is obtained from the equation

$$\delta_{i,j} = \epsilon_{i,j} \sigma A_{i,j}$$

where σ , the Stefan-Boltzmann constant, is

$$\sigma = 5.76 \cdot 10^{-8} \text{ W/m}^2 / (\text{degK})^4$$

For radiation between concentric spheres and coaxial cylinders of equal emissivity, $\epsilon_{i,j}$, $\delta_{i,j}$ is given by the equation

$$\delta_{ij} = \frac{\epsilon_{i,j} \sigma A_{i,j}}{1 + (1 - \epsilon_{i,j}) \frac{A_{i,j}}{A_{i,j}^*}}$$

where σ is as above $A_{i,j}$ is the area of the enclosed body and $A_{i,j}^*$ is the area of the surrounding body, i.e. $A_{i,j} < A_{i,j}^*$.

Expressions for $\delta_{i,j}$ that are valid for more complicated geometries or for different emissivities may be found in textbooks.

A.2.5 CALCULATION OF AREAS

In the case of heat transfer in the axial direction $A_{i,j}$ is given by the equation (Fig. A-3)

$$A_{i,j} = 2\pi r_m \cdot \Delta r$$

Referring to the input instructions, Section V, but recalling L must be input in mm not m.

$$L_1 = r_m = \frac{r_1 + r_2}{2}$$

$$L_2 = \Delta r = r_2 - r_1$$

In the case of heat transfer in the radial direction, $A_{i,j}$ is obtained from the expression

$$A_{i,j} = 2\pi r_m \cdot H; L_1 = r_m; L_2 = H$$

and similarly for the radiation term above

$$A^*_{i,j} = 2\pi r_m^* H$$

$$L_3 = r_m^*$$

$$L_2 = 2H$$

in which H is the length of the cylindrical surface; where heat is conducted between i and j , r_m is given by the same equation as above (Fig. A-4 (a)); where heat is convected between i and j , r_m is the radius of the cylindrical surface (Fig. A-4(b)); where heat is radiated between i and j , r_m is the radius of the enclosed cylindrical surface and r_m^* the radius of the surrounding cylindrical surface (Fig. A-4(c))

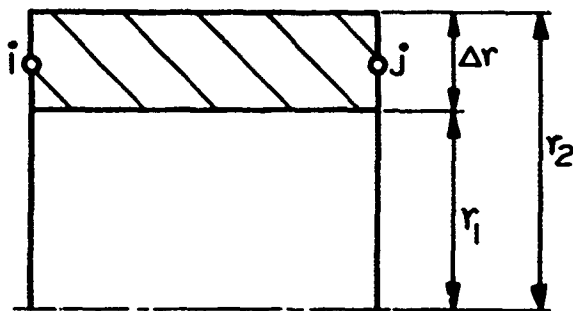


Fig. A-3

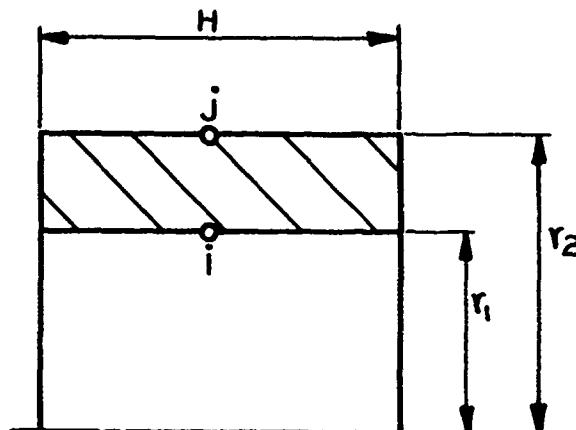


Fig. A-4(a)

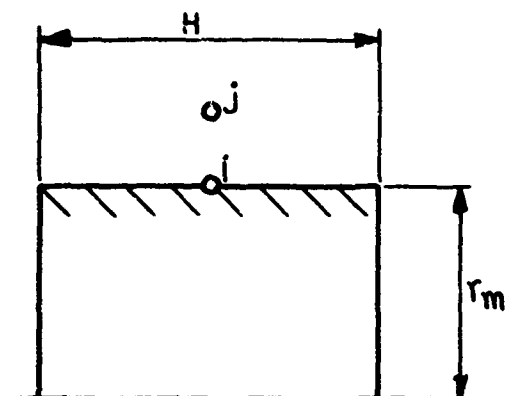


Fig. A-4(b)

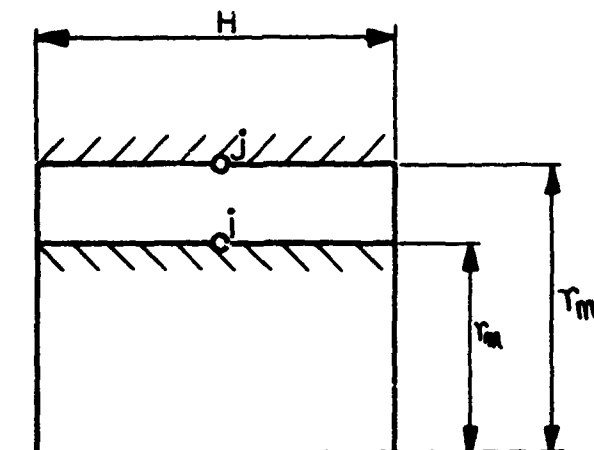


Fig. A-4(c)

A.3.1 TRANSIENT ANALYSIS

For the transient analysis all of the data pertaining to the node to node heat transfer coefficients must be input. Additionally, the volume and the specific heat at each node is required. For metal nodes this input is straightforward. However, when fluid flow is being considered there is no easy way to approximate the fluid nodal volume in a free space such as the bearing cavity. However, through use of the Program, the user's ability to make appropriate estimates should improve.

APPENDIX B

INPUT DATA PREPARATION FORMS

AND EXAMPLE

017,31

EX. 43. OF
GALLS

198

Title Card	Card 1	One Card
1	2	3
4	5	6
7	8	9
10	11	12
13	14	15
16	17	18
19	20	21
22	23	24
25	26	27
28	29	30
31	32	33
34	35	36
37	38	39
40	41	42
43	44	45
46	47	48
49	50	51
52	53	54
55	56	57
58	59	60
61	62	63
64	65	66
67	68	69
70	71	72
73	74	75
76	77	78
79	80	81
82	83	84
85	86	87
88	89	90
91	92	93
94	95	96
97	98	99
100	101	102
103	104	105
106	107	108
109	110	111
112	113	114
115	116	117
118	119	120
121	122	123
124	125	126
127	128	129
130	131	132
133	134	135
136	137	138
139	140	141
142	143	144
145	146	147
148	149	150
151	152	153
154	155	156
157	158	159
160	161	162
163	164	165
166	167	168
169	170	171
172	173	174
175	176	177
178	179	180
181	182	183
184	185	186
187	188	189
190	191	192
193	194	195
196	197	198
199	200	201
202	203	204
205	206	207
208	209	210
211	212	213
214	215	216
217	218	219
220	221	222
223	224	225
226	227	228
229	230	231
232	233	234
235	236	237
238	239	240
241	242	243
244	245	246
247	248	249
250	251	252
253	254	255
256	257	258
259	260	261
262	263	264
265	266	267
268	269	270
271	272	273
274	275	276
277	278	279
280	281	282
283	284	285
286	287	288
289	290	291
292	293	294
295	296	297
298	299	300
301	302	303
304	305	306
307	308	309
310	311	312
313	314	315
316	317	318
319	320	321
322	323	324
325	326	327
328	329	330
331	332	333
334	335	336
337	338	339
340	341	342
343	344	345
346	347	348
349	350	351
352	353	354
355	356	357
358	359	360
361	362	363
364	365	366
367</		

Title(20): 29

[illegible]

Title to be printed on each page.

Print Case
Case 2, end case

Case 1

Case 1

Case 1

Case 1

Case 1

Case 1

Case 1

Case 1

Case 1

Case 1

Case 1

Case 1

Case 1

Case 1

Case 1

Case 1

Case 1

Case 1

Case 1

Case 1

Case 1

Case 1

Case 1

Case 1

Case 1

Case 1

Case 1

Case 1

Case 1

Case 1

Case 1

Case 1

Case 1

Case 1

Case 1

Case 1

Case 1

Case 1

Case 1

Case 1

Case 1

Case 1

Case 1

Case 1

Case 1

Case 1

Case 1

Case 1

Case 1

Case 1

Case 1

Case 1

Case 1

Case 1

Case 1

Bearing Data
Card 2, One Card

										(5)										(6)										(17)										(BALL BEARING)																																							
Rolling Element Diameter										Bearing Pitch (Mean) Diameter										Number of Rolling Elements in the Row										Outer Ring Speed (RPM)																																																	
1	2	3	4	5	6	7	8	9	10	11	12	13	14	15	16	17	18	19	20	21	22	23	24	25	26	27	28	29	30	31	32	33	34	35	36	37	38	39	40	41	42	43	44	45	46	47	48	49	50	51	52	53	54	55	56	57	58	59	60	61	62	63	64	65	66	67	68	69	70	71	72	73	74	75	76	77	78	79	80

										BD (4)										BD (11)										BD (5)										BD (7)										UD (6)										BD (17)										(ROLLER BEARING)									
Rolling Element Diameter										Roller Length End to End										Bearing Pitch (Mean) Diameter										Diametral Clearance										Number of Rolling Elements										Outer Ring Speed (RPM)																													
1	2	3	4	5	6	7	8	9	10	11	12	13	14	15	16	17	18	19	20	21	22	23	24	25	26	27	28	29	30	31	32	33	34	35	36	37	38	39	40	41	42	43	44	45	46	47	48	49	50	51	52	53	54	55	56	57	58	59	60	61	62	63	64	65	66	67	68	69	70	71	72	73	74	75	76	77	78	79	80

[illegible]

If the bearing is a ball bearing give any two of the first six pieces of data. Zero is a valid entry:							
Shim Width	Shim Angle	Free Contact Angle	Diametral Play Measured With Inner and Outer Ring Grooves Offset	End Play	Diametral Clearance Measured With Inner and Outer Ring Grooves Aligned.	Outer Race Curvature RO/D Outer Race Radius Divided by the ball diameter	Inner Race Curvature RI/D Inner Race Radius Divided by the ball diameter

(18)										(19)										(20)										(21)										(22)										(23)																																																	
1	2	3	4	5	6	7	8	9	10	11	12	13	14	15	16	17	18	19	20	21	22	23	24	25	26	27	28	29	30	31	32	33	34	35	36	37	38	39	40	41	42	43	44	45	46	47	48	49	50	51	52	53	54	55	56	57	58	59	60	61	62	63	64	65	66	67	68	69	70	71	72	73	74	75	76	77	78	79	80	81	82	83	84	85	86	87	88	89	90	91	92	93	94	95	96	97	98	99	100

Cylindrical Roller Bearings:						
Outer Race Effective Contact Length	Flat Length	Crown Radius	Effective Contact Length	Inner Race Flat Length	Crown Radius	Number of Laminæ (20 max) if left blank it is set to 10

Bearing Data
Card 4, One Card

RUS Surface Roughness (mm)		Asperity Slope Degrees		Asperity Friction Coefficient																																																																																															
Outer	Inner	Rolling Element	Outer	Inner	Rolling Element																																																																																														
1	2	3	4	5	6	7	8	9	10	11	12	13	14	15	16	17	18	19	20	21	22	23	24	25	26	27	28	29	30	31	32	33	34	35	36	37	38	39	40	41	42	43	44	45	46	47	48	49	50	51	52	53	54	55	56	57	58	59	60	61	62	63	64	65	66	67	68	69	70	71	72	73	74	75	76	77	78	79	80	81	82	83	84	85	86	87	88	89	90	91	92	93	94	95	96	97	98	99	100

Onlt Cards 5 and 6 if crown drop play is 0

Bearing Data

Card Type 5, as many as needed, maximum of 3, for the inner race.

(2, 5)										(5, 5)										(6, 5)										(7, 5)																																																																																																																																																																																																																																																																																																																																																																																																																																																																																																																																																																																																																																																																																																																																																																																																																																																																																																																																																																																																																																																																																																																																																																																																																																																																																																																																																																																																																																																																																																																																																																																																																																																																																																																																																																																																																																																																																																																																																																																																																																																																																																																																																																																																																																																																																																																																																																																																																																																																																																																																																																																																																																																																																																																																																																																																																																																																																																																																																																																																																																																																																																																																																																																																																																																																																																																																																																																																																																																																																																																																																																																																																																																																																																																																																																																																																																																																																																																																																																																																																																																																																																																																																																																																																																																																																																																																																																																																																																																																																																																																																																																																																																																																																																																																																																																																																																																																																																																																																																																																																																																																																																																																																					
1	2	3	4	5	6	7	8	9	10	11	12	13	14	15	16	17	18	19	20	21	22	23	24	25	26	27	28	29	30	31	32	33	34	35	36	37	38	39	40	41	42	43	44	45	46	47	48	49	50	51	52	53	54	55	56	57	58	59	60	61	62	63	64	65	66	67	68	69	70	71	72	73	74	75	76	77	78	79	80	81	82	83	84	85	86	87	88	89	90	91	92	93	94	95	96	97	98	99	00																																																																																																																																																																																																																																																																																																																																																																																																																																																																																																																																																																																																																																																																																																																																																																																																																																																																																																																																																																																																																																																																																																																																																																																																																																																																																																																																																																																																																																																																																																																																																																																																																																																																																																																																																																																																																																																																																																																																																																																																																																																																																																																																																																																																																																																																																																																																																																																																																																																																																																																																																																																																																																																																																																																																																																																																																																																																																																																																																																																																																																																																																																																																																																																																																																																																																																																																																																																																																																																																																																																																																																																																																																																																																																																																																																																																																																																																																																																																																																																																																																																																																																																																																																																																																																																																																																																																																																																																																																																																																																																																																																																																																																																																																																																																																																																																																																																																																																																																																																																																																																																																																
Crown Drop at Laminum 1										Crown Drop at Laminum 2										... and so on, use more than one card if no. of laminas is greater than 7.																																																																																																																																																																																																																																																																																																																																																																																																																																																																																																																																																																																																																																																																																																																																																																																																																																																																																																																																																																																																																																																																																																																																																																																																																																																																																																																																																																																																																																																																																																																																																																																																																																																																																																																																																																																																																																																																																																																																																																																																																																																																																																																																																																																																																																																																																																																																																																																																																																																																																																																																																																																																																																																																																																																																																																																																																																																																																																																																																																																																																																																																																																																																																																																																																																																																																																																																																																																																																																																																																																																																																																																																																																																																																																																																																																																																																																																																																																																																																																																																																																																																																																																																																																																																																																																																																																																																																																																																																																																																																																																																																																																																																																																																																																																																																																																																																																																																																																																																																																																																																																																																																																																																																															

Bearing Date
Card Type, one card
DD(25) XCV 26

DLAN 27 28 29 30 31

ALAN

GAP

CPC

IDE

31

26

27

28

29

30

31

32

33

34

35

36

37

38

39

40

41

42

43

44

45

46

47

48

49

50

51

52

53

54

55

56

57

58

59

60

61

62

63

64

65

66

67

68

69

70

71

72

73

74

75

76

77

78

79

80

81

82

83

84

85

86

87

88

89

90

91

92

93

94

95

96

97

98

99

100

101

102

103

104

105

106

107

108

109

110

111

112

113

114

115

116

117

118

119

120

121

122

123

124

125

126

127

128

129

130

131

132

133

134

135

136

137

138

139

140

141

142

143

144

145

146

147

148

149

150

151

152

153

154

155

156

157

158

159

160

161

162

163

164

165

166

167

168

169

170

Percent Lube
in Bearing
Cavity

Rail Land Area

Rail Diameter

Rail-Land
Diameter
Clearance

Cage Data

Type of Cage -1 =
Outer Ring Land
Riding
1 = inner ring
land riding

Cage Pocket
End-to-End
Tangential
Clearance

Card 10. One Card.										(47)										(48)										(49)										(50)										(51)										(52)																			
Shaft										Inner Ring										Outer Ring										Housing										Shaft										Inner Ring																													
1	2	3	4	5	6	7	8	9	10	11	12	13	14	15	16	17	18	19	20	21	22	23	24	25	26	27	28	29	30	31	32	33	34	35	36	37	38	39	40	41	42	43	44	45	46	47	48	49	50	51	52	53	54	55	56	57	58	59	60	61	62	63	64	65	66	67	68	69	70	71	72	73	74	75	76	77	78	79	80
Young's Modulus, if left blank, steel is assumed.																																																																															
Poisson's Ratio, if left blank, steel is assumed.																																																																															

[illegible][illegible]

Lubricant Properties

440 (71)

[illegible]

Lubricant N Code 1-4 right justified NCODE

If NCODE is zero read this data

Lubricant Parameters

Bearing Data
Card 14, One Card

Bearing Data				Lubricant Parameters																																																																																															
Card 14, One Card																																																																																																			
Bearing Data				(11) US MAX				(12) US MAX				(13) US MAX				(14) US MAX				(15) US MAX																																																																															
Bearing Data				Inner Race				Sliding Rate				Maximum EHD				Maximum EHD																																																																																			
Bearing Data				Lubricant				at which the				friction				coefficient																																																																																			
Bearing Data				Replenishment				coefficient				coefficient				coefficient																																																																																			
Bearing Data				Layer Thickness				reaches a				maximum				maximum																																																																																			
Bearing Data				mm				maximum				maximum				maximum																																																																																			
1	2	3	4	5	6	7	8	9	10	11	12	13	14	15	16	17	18	19	20	21	22	23	24	25	26	27	28	29	30	31	32	33	34	35	36	37	38	39	40	41	42	43	44	45	46	47	48	49	50	51	52	53	54	55	56	57	58	59	60	61	62	63	64	65	66	67	68	69	70	71	72	73	74	75	76	77	78	79	80	81	82	83	84	85	86	87	88	89	90	91	92	93	94	95	96	97	98	99	100

These values should be non zero only
if the lubricant code, card 13,
item 1, is zero. These data define
the friction model.

Card Type 1

OUR CONTRIBUTIONS ARE. IF NO TOP, CALCULATION IS DESIRED, THEN CLAVE THE LAST TWO DIGITS OF THE

TRANSIENT ONLY

GENERAL

Card Type 2

72. Use only if no temperature calc. is desired, and then give no more thermal data.

[illegible]

Card Type 3
Thermal Data - Individual Initial Temperatures
T3. As many cards as needed, followed by a blank card

Node Number	Initial Temperature	Etc.	Node Number	Initial Temperature
1			71	
2			72	
3			73	
4			74	
5			75	
6			76	
7			77	
8			78	
9			79	
10			80	
11			81	
12			82	
13			83	
14			84	
15			85	
16			86	
17			87	
18			88	
19			89	
20			90	
21			91	
22			92	
23			93	
24			94	
25			95	
26			96	
27			97	
28			98	
29			99	
30			100	
31				
32				
33				
34				
35				
36				
37				
38				
39				
40				
41				
42				
43				
44				
45				
46				
47				
48				
49				
50				
51				
52				
53				
54				
55				
56				
57				
58				
59				
60				
61				
62				
63				
64				
65				
66				
67				
68				
69				
70				

三

T4, One card/btg.

214

T5, one card/box.

215

T6, as many cards as needed, followed by a blank card

Serial Number	Power
1	100
2	100
3	100
4	100
5	100
6	100
7	100
8	100
9	100
10	100
11	100
12	100
13	100
14	100
15	100
16	100
17	100
18	100
19	100
20	100
21	100
22	100
23	100
24	100
25	100
26	100
27	100
28	100
29	100
30	100
31	100
32	100
33	100
34	100
35	100
36	100
37	100
38	100
39	100
40	100
41	100
42	100
43	100
44	100
45	100
46	100
47	100
48	100
49	100
50	100
51	100
52	100
53	100
54	100
55	100
56	100
57	100
58	100
59	100
60	100
61	100
62	100
63	100
64	100
65	100
66	100
67	100
68	100
69	100
70	100
71	100
72	100
73	100
74	100
75	100
76	100
77	100
78	100
79	100
80	100
81	100
82	100
83	100
84	100
85	100
86	100
87	100
88	100
89	100
90	100
91	100
92	100
93	100
94	100
95	100
96	100
97	100
98	100
99	100
100	100

TABLE 1. COEFFICIENTS

44. ONE OF THE ALGEBRAIC CORRECTIONS IS WAY AS NIDCO, FOLLOWED BY A SLINK CAPD,

	9	3	V Velocity (m/sec)
Velocity (m/sec)			
M/sec			
V Velocity (m/sec)			

[illegible][illegible]

Principles of Microbiology (M/2020)

1941
FEDERAL BUREAU OF INVESTIGATION
U.S. DEPARTMENT OF JUSTICE
WASHINGTON, D.C.

[illegible]

11

Card Type 9
Thermal Data - Node heat capacities, only for transient calculations

TP, One Card/Node

Node Number If it is given without a sign, rotational symmetry is assumed and the volume is multiplied by 27 if it is negative the volume is not changed.	Volume at Node= $L_1 \cdot L_2 \cdot L_3$			Density (KG/M ³)	Specific Heat KS/KG°C	
	L_1 mm	L_2 mm	L_3 mm			
1	2	3	4	5	6	7
8	9	10	11	12	13	14
15	16	17	18	19	20	21
22	23	24	25	26	27	28
29	30	31	32	33	34	35
36	37	38	39	40	41	42
43	44	45	46	47	48	49
50	51	52	53	54	55	56
57	58	59	60	61	62	63
64	65	66	67	68	69	70
71	72	73	74	75	76	77
78	79	80	81	82	83	84
85	86	87	88	89	90	91
92	93	94	95	96	97	98
99	100	101	102	103	104	105
106	107	108	109	110	111	112
113	114	115	116	117	118	119
120	121	122	123	124	125	126
127	128	129	130	131	132	133
134	135	136	137	138	139	140
141	142	143	144	145	146	147
148	149	150	151	152	153	154
155	156	157	158	159	160	161
162	163	164	165	166	167	168
169	170	171	172	173	174	175
176	177	178	179	180	181	182
183	184	185	186	187	188	189
190	191	192	193	194	195	196
197	198	199	200	201	202	203
204	205	206	207	208	209	210
211	212	213	214	215	216	217
218	219	220	221	222	223	224
225	226	227	228	229	230	231
232	233	234	235	236	237	238
239	240	241	242	243	244	245
246	247	248	249	250	251	252
253	254	255	256	257	258	259
260	261	262	263	264	265	266
267	268	269	270	271	272	273
274	275	276	277	278	279	280
281	282	283	284	285	286	287
288	289	290	291	292	293	294
295	296	297	298	299	300	301
302	303	304	305	306	307	308
309	310	311	312	313	314	315
316	317	318	319	320	321	322
323	324	325	326	327	328	329
330	331	332	333	334	335	336
337	338	339	340	341	342	343
344	345	346	347	348	349	350
351	352	353	354	355	356	357
358	359	360	361	362	363	364
365	366	367	368	369	370	371
372	373	374	375	376	377	378
379	380	381	382	383	384	385
386	387	388	389	390	391	392
393	394	395	396	397	398	399
400	401	402	403	404	405	406
407	408	409	410	411	412	413
414	415	416	417	418	419	420
421	422	423	424	425	426	427
428	429	430	431	432	433	434
435	436	437	438	439	440	441
442	443	444	445	446	447	448
449	450	451	452	453	454	455
456	457	458	459	460	461	462
463	464	465	466	467	468	469
470	471	472	473	474	475	476
477	478	479	480	481	482	483
484	485	486	487	488	489	490
491	492	493	494	495	496	497
498	499	500	501	502	503	504
505	506	507	508	509	510	511
512	513	514	515	516	517	518
519	520	521	522	523	524	525
526	527	528	529	530	531	532
533	534	535	536	537	538	539
540	541	542	543	544	545	546
547	548	549	550	551	552	553
554	555	556	557	558	559	560
561	562	563	564	565	566	567
568	569	570	571	572	573	574
575	576	577	578	579	580	581
582	583	584	585	586	587	588
589	590	591	592	593	594	595
596	597	598	599	600	601	602
603	604	605	606	607	608	609
610	611	612	613	614	615	616
617	618	619	620	621	622	623
624	625	626	627	628	629	630
631	632	633	634	635	636	637
638	639	640	641	642	643	644
645	646	647	648	649	650	651
652	653	654	655	656	657	658
659	660	661	662	663	664	665
666	667	668	669	670	671	672
673	674	675	676	677	678	679
680	681	682	683	684	685	686
687	688	689	690	691	692	693
694	695	696	697	698	699	700
701	702	703	704	705	706	707
708	709	710	711	712	713	714
715	716	717	718	719	720	721
722	723	724	725	726	727	728
729	730	731	732	733	734	735
736	737	738	739	740	741	742
743	744	745	746	747	748	749
750	751	752	753	754	755	756
757	758	759	760	761	762	763
764	765	766	767	768	769	770
771	772	773	774	775	776	777
778	779	780	781	782	783	784
785	786	787	788	789	790	791
792	793	794	795	796	797	798
799	800	801	802	803	804	805
806	807	808	809	810	811	812
813	814	815	816	817	818	819
820	821	822	823	824	825	826
827	828	829	830	831	832	833
834	835	836	837	838	839	840
841	842	843	844	845	846	847
848	849	850	851	852	853	854
855	856	857	858	859	860	861
862	863	864	865	866	867	868
869	870	871	872	873	874	875
876	877	878	879	880	881	882
883	884	885	886	887	888	889
890	891	892	893	894	895	896
897	898	899	900	901	902	903
904	905	906	907	908	909	910
911	912	913	914	915	916	917
918	919	920	921	922	923	924
925	926	927	928	929	930	931
932	933	934	935	936	937	938
939	940	941	942	943	944	945
946	947	948	949	950	951	952
953	954	955	956	957	958	959
960	961	962	963	964	965	966
967	968	969	970	971	972	973
974	975	976	977	978	979	980
981	982	983	984	985	986	987
988	989	990	991	992	993	994
995	996	997	998	999	1000	1001

Shaft Data - Shaft Geometry
Omit all shaft data cards if there are no bearings

Type of Shaft card.		Blank	X-coordinate of shaft section	Shaft inner diameter immediately before the section.	Shaft inner diameter immediately after the section.	Shaft outer diameter immediately before the section.	Shaft outer diameter immediately after the section.	Shaft Modulus of elasticity.
1	2	3	4	5	6	7	8	9
10	11	12	13	14	15	16	17	18
19	20	21	22	23	24	25	26	27
28	29	30	31	32	33	34	35	36
37	38	39	40	41	42	43	44	45
46	47	48	49	50	51	52	53	54
55	56	57	58	59	60	61	62	63
64	65	66	67	68	69	70	71	72
73	74	75	76	77	78	79	80	81
82	83	84	85	86	87	88	89	90
91	92	93	94	95	96	97	98	99
100	101	102	103	104	105	106	107	108
109	110	111	112	113	114	115	116	117
118	119	120	121	122	123	124	125	126
127	128	129	130	131	132	133	134	135
136	137	138	139	140	141	142	143	144
145	146	147	148	149	150	151	152	153
154	155	156	157	158	159	160	161	162
163	164	165	166	167	168	169	170	171
172	173	174	175	176	177	178	179	180
181	182	183	184	185	186	187	188	189
190	191	192	193	194	195	196	197	198
199	200	201	202	203	204	205	206	207
208	209	210	211	212	213	214	215	216
217	218	219	220	221	222	223	224	225
226	227	228	229	230	231	232	233	234
235	236	237	238	239	240	241	242	243
244	245	246	247	248	249	250	251	252
253	254	255	256	257	258	259	260	261
262	263	264	265	266	267	268	269	270
271	272	273	274	275	276	277	278	279
280	281	282	283	284	285	286	287	288
289	290	291	292	293	294	295	296	297
298	299	300	301	302	303	304	305	306
307	308	309	310	311	312	313	314	315
316	317	318	319	320	321	322	323	324
325	326	327	328	329	330	331	332	333
334	335	336	337	338	339	340	341	342
343	344	345	346	347	348	349	350	351
352	353	354	355	356	357	358	359	360
361	362	363	364	365	366	367	368	369
370	371	372	373	374	375	376	377	378
379	380	381	382	383	384	385	386	387
388	389	390	391	392	393	394	395	396
397	398	399	400	401	402	403	404	405
406	407	408	409	410	411	412	413	414
415	416	417	418	419	420	421	422	423
424	425	426	427	428	429	430	431	432
433	434	435	436	437	438	439	440	441
442	443	444	445	446	447	448	449	450
451	452	453	454	455	456	457	458	459
460	461	462	463	464	465	466	467	468
469	470	471	472	473	474	475	476	477
478	479	480	481	482	483	484	485	486
487	488	489	490	491	492	493	494	495
496	497	498	499	500	501	502	503	504
505	506	507	508	509	510	511	512	513
514	515	516	517	518	519	520	521	522
523	524	525	526	527	528	529	530	531
532	533	534	535	536	537	538	539	540
541	542	543	544	545	546	547	548	549
550	551	552	553	554	555	556	557	558
559	560	561	562	563	564	565	566	567
568	569	570	571	572	573	574	575	576
577	578	579	580	581	582	583	584	585
586	587	588	589	590	591	592	593	594
595	596	597	598	599	600	601	602	603
604	605	606	607	608	609	610	611	612
613	614	615	616	617	618	619	620	621
622	623	624	625	626	627	628	629	630
631	632	633	634	635	636	637	638	639
640	641	642	643	644	645	646	647	648
649	650	651	652	653	654	655	656	657
658	659	660	661	662	663	664	665	666
667	668	669	670	671	672	673	674	675
676	677	678	679	680	681	682	683	684
685	686	687	688	689	690	691	692	693
694	695	696	697	698	699	700	701	702
703	704	705	706	707	708	709	710	711
712	713	714	715	716	717	718	719	720
721	722	723	724	725	726	727	728	729
730	731	732	733	734	735	736	737	738
739	740	741	742	743	744	745	746	747
748	749	750	751	752	753	754	755	756
757	758	759	760	761	762	763	764	765
766	767	768	769	770	771	772	773	774
775	776	777	778	779	780	781	782	783
784	785	786	787	788	789	790	791	792
793	794	795	796	797	798	799	800	801
802	803	804	805	806	807	808	809	810
811	812	813	814	815	816	817	818	819
820	821	822	823	824	825	826	827	828
829	830	831	832	833	834	835	836	837
838	839	840	841	842	843	844	845	846
847	848	849	850	851	852	853	854	855
856	857	858	859	860	861	862	863	864
865	866	867	868	869	870	871	872	873
874	875	876	877	878	879	880	881	882
883	884	885	886	887	888	889	890	891
892	893	894	895	896	897	898	899	900
901	902	903	904	905	906	907	908	909
910	911	912	913	914	915	916	917	918
919	920	921	922	923	924	925	926	927
928	929	930	931	932	933	934	935	936
937	938	939	940	941	942	943	944	945
946	947	948	949	950	951	952	953	954
955	956	957	958	959	960	961	962	963
964	965	966	967	968	969	970	971	972
973	974	975	976	977	978	979	980	981
982	983	984	985	986	987	988	989	990
991	992	993	994	995	996	997	998	999
1000	1001	1002	1003	1004	1005	1006	1007	1008
1009	1010	1011	1012	1013	1014	1015	1016	1017
1018	1019	1020	1021	1022	1023	1024	1025	1026
1027	1028	1029	1030	1031	1032	1033	1034	1035
1036	1037	1038	1039	1040	1041	1042	1043	1044
1045	1046	1047	1048	1049	1050	1051	1052	1053
1054	1055	1056	1057	1058	1059	1060	1061	1062
1063	1064	1065	1066	1067	1068	1069	1070	1071
1072	1073	1074	1075	1076	1077	1078	1079	1080
1081	1082	1083	1084	1085	1086	1087	1088	1089
1090	1091	1092	1093	1094	1095	1096	1097	1098
1099	1100	1101	1102	1103	1104	1105	1106	1107
1108	1109	1110	1111	1112	1113	1114	1115	1116
1117	1118	1119	1120	1121	1122	1123	1124	1125
1126	1127	1128	1129	1130	1131	1132	1133	1134
1135	1136	1137	1138	1139	1140	1141	1142	1143
1144	1145	1146	1147	1148	1149	1150	1151	1152
1153	1154	1155	1156	1157	1158	1159	1160	1161
1162	1163	1164	1165	1166	1167	1168	1169	1170
1171	1172	1173	1174	1175	1176	1177	1178	1179
1180	1181	1182	1183	1184	1185	1186	1187	1188
1189	1190	1191	1192	1193	1194	1195	1196	1197
1198	1199	1200	1201	1202	1203	1204	1205	1206
1207	1208	1209	1210	1211	1212	1213	1214	1215
1216	1217	1218	1219	1220	1221	1222	1223	1224
1225	1226	1227	1228	1229	1230	1231	1232	1233

22. AS MANY CAMPS AS THE NUMBER OF SCANNINGS. APPROX IN ORDER OF INCREASING X-COORDINATE.

22. As many camps as the number of trainees. Approved in order of increasing X-COMMUNITAT.

221

53. as many cards as needed, followed by a blank card.

222

as many cards as needed. Card needed only if any data is different from X-Y plane

[illegible]

S.S. as many cards as needed, followed by a blank card.

S.S. as many cards as needed, followed by a blank card.

Type of shaft card. This card is type 3

Title Card
(Card 1 One Card)

Title(28)	29	30	31	32	33	34	35	36	37	38	39	40	41	42	43	44	45	46	47
1	2	3	4	5	6	7	8	9	10	11	12	13	14	15	16	17	18	19	20
21	22	23	24	25	26	27	28	29	30	31	32	33	34	35	36	37	38	39	40
41	42	43	44	45	46	47	48	49	50	51	52	53	54	55	56	57	58	59	60
61	62	63	64	65	66	67	68	69	70	71	72	73	74	75	76	77	78	79	80
81	82	83	84	85	86	87	88	89	90	91	92	93	94	95	96	97	98	99	00

Title to be printed on each page.

Bearing Data, One set per Bearing Cards 1-16 for Bearing 1. Followed by cards 1-16 for bearing 2, etc.
Card 1, One Card

BD(1)																BD(67)																BD(68)																BD(2)																																																															
1 2 3 4 5 6 7 8 9 10 11 12 13 14 15 16 17 18 19 20 21 22 23 24 25 26 27 28 29 30 31 32 33 34 35 36 37 38 39 40 41 42 43 44 45 46 47 48 49 50 51 52 53 54 55 56 57 58 59 60 61 62 63 64 65 66 67 68 69 70 71 72 73 74 75 76 77 78 79 80																																																																																																															
B A L L																M - S O																M - S O																S -																																																															
Bearing Type Ball or Cylindrical																Steel Designations																Outer Ring																Steel Life Factors																Orientation Angle in Degrees of Rolling Elements. 0.0 means first rolling element is on the Z-axis.																																															
																Inner Ring																																Outer																Inner																$0 \leq \phi_1 \leq \frac{2\pi}{N}$																															

(BALL "A" 13)

[illegible]

BD (4)		BD (11)		BD (5)		BD (7)		BD (6)		BD (17)		ROLLER BEARING	
Rolling Element Diameter	Roller Length End to End	Bearing Pitch (Mean) Diameter		Diametral Clearance		Number of Rolling Elements		Outer Ring Speed (RPM)					
1	2	3	4	5	6	7	8	9	10	11	12	13	14
15	16	17	18	19	20	21	22	23	24	25	26	27	28
29	30	31	32	33	34	35	36	37	38	39	40	41	42
43	44	45	46	47	48	49	50	51	52	53	54	55	56
57	58	59	60	61	62	63	64	65	66	67	68	69	70
71	72	73	74	75	76	77	78	79	80	81	82	83	84
85	86	87	88	89	90	91	92	93	94	95	96	97	98
99	100	101	102	103	104	105	106	107	108	109	110	111	112
113	114	115	116	117	118	119	120	121	122	123	124	125	126
127	128	129	130	131	132	133	134	135	136	137	138	139	140
141	142	143	144	145	146	147	148	149	150	151	152	153	154
155	156	157	158	159	160	161	162	163	164	165	166	167	168
169	170	171	172	173	174	175	176	177	178	179	180	181	182
183	184	185	186	187	188	189	190	191	192	193	194	195	196
197	198	199	200	201	202	203	204	205	206	207	208	209	210
211	212	213	214	215	216	217	218	219	220	221	222	223	224
225	226	227	228	229	230	231	232	233	234	235	236	237	238
239	240	241	242	243	244	245	246	247	248	249	250	251	252
253	254	255	256	257	258	259	260	261	262	263	264	265	266
267	268	269	270	271	272	273	274	275	276	277	278	279	280
281	282	283	284	285	286	287	288	289	290	291	292	293	294
295	296	297	298	299	300	301	302	303	304	305	306	307	308
309	310	311	312	313	314	315	316	317	318	319	320	321	322
323	324	325	326	327	328	329	330	331	332	333	334	335	336
337	338	339	340	341	342	343	344	345	346	347	348	349	350
351	352	353	354	355	356	357	358	359	360	361	362	363	364
365	366	367	368	369	370	371	372	373	374	375	376	377	378
379	380	381	382	383	384	385	386	387	388	389	390	391	392
393	394	395	396	397	398	399	400	401	402	403	404	405	406
407	408	409	410	411	412	413	414	415	416	417	418	419	420
COMMIT													

Card 3, Van Card

[illegible]

Zero is a valid entry:

Shim Width		Shim Angle	Free Contact: Ang.	Diametral Play Measured With Inner and Outer Ring Grooves Offset	End Play	Diametral Clearance With Inner and Outer Ring Grooves Aligned.	Outer Race Curvature	Inner Race Curvature
If the bearing is a ball bearing give an, two of ... first six pieces of data. Zero is a valid entry:								
							RO/D	RI/D
							Outer Race Radius Divided by the ball diameter	Inner Race Radius Divided by the ball diameter

[illegible]

Cylindrical Roller Bearings:

Cylindrical Roller Bearings:				
Outer Race	Flat Length	Crown Radius	Inner Race	Number of Slices
Effective Contact Length			Flat Length	(20 max) if left blank it is set to 10

RMS Surface Roughness (mm)		Asperity Slope Degrees		Rolling Element		Asperity Friction Coefficient	
Outer	Inner	Outer	Inner	Outer	Inner	Outer	Inner
0.0006	0.0016	2.4	2.0	2.0	0.1		
0.0013	0.0034	2.3	1.9	1.9	0.1		
0.0026	0.0068	2.2	1.8	1.8	0.1		
0.0051	0.0136	2.1	1.7	1.7	0.1		
0.0102	0.0272	2.0	1.6	1.6	0.1		
0.0204	0.0544	1.9	1.5	1.5	0.1		
0.0408	0.1088	1.8	1.4	1.4	0.1		
0.0816	0.2176	1.7	1.3	1.3	0.1		
0.1632	0.4352	1.6	1.2	1.2	0.1		
0.3264	0.8704	1.5	1.1	1.1	0.1		
0.6528	1.7408	1.4	1.0	1.0	0.1		
1.3056	3.4816	1.3	0.9	0.9	0.1		
2.6112	6.9632	1.2	0.8	0.8	0.1		
5.2224	13.9264	1.1	0.7	0.7	0.1		
10.4448	27.8528	1.0	0.6	0.6	0.1		
20.8896	55.7056	0.9	0.5	0.5	0.1		
41.7792	111.4112	0.8	0.4	0.4	0.1		
83.5584	222.8224	0.7	0.3	0.3	0.1		
167.1168	445.6448	0.6	0.2	0.2	0.1		
334.2336	891.2896	0.5	0.1	0.1	0.1		

Boeing Data
Card Type 7, one card 26
DD(25) XCAV

[illegible]

Card Type 1
 Bearing Data
 Only Cards 10-12 if operating clearances are not to be calculated.
 Card 10, One Card.

Card 10, One Card.										(48)										(49)										(50)										(51)										(52)																																																																																																																																																																																																																																																																																																																																																																																																																																																																																																																																																																																																																																																																																																																																																																																																																																																																																																																																																																																																																																																																																																																																																																																																																																																																																																																																																																																																																																																																																																																																																																																																																																																																																																																																																																																																																																																																																																																																																																																																																																																																																																																																																																																																																																																																																																																																																																																																																																																																																															
MAG. 14										17 18 19 20 21 22 23 24 25 26 27 28 29 30 31 32 33 34 35 36 37 38 39 40 41 42 43 44 45 46 47 48 49 50 51 52 53 54 55 56 57 58 59 60 61 62 63 64 65 66 67 68 69 70 71 72 73 74 75 76 77 78 79 80										17 18 19 20 21 22 23 24 25 26 27 28 29 30 31 32 33 34 35 36 37 38 39 40 41 42 43 44 45 46 47 48 49 50 51 52 53 54 55 56 57 58 59 60 61 62 63 64 65 66 67 68 69 70 71 72 73 74 75 76 77 78 79 80										17 18 19 20 21 22 23 24 25 26 27 28 29 30 31 32 33 34 35 36 37 38 39 40 41 42 43 44 45 46 47 48 49 50 51 52 53 54 55 56 57 58 59 60 61 62 63 64 65 66 67 68 69 70 71 72 73 74 75 76 77 78 79 80										17 18 19 20 21 22 23 24 25 26 27 28 29 30 31 32 33 34 35 36 37 38 39 40 41 42 43 44 45 46 47 48 49 50 51 52 53 54 55 56 57 58 59 60 61 62 63 64 65 66 67 68 69 70 71 72 73 74 75 76 77 78 79 80										17 18 19 20 21 22 23 24 25 26 27 28 29 30 31 32 33 34 35 36 37 38 39 40 41 42 43 44 45 46 47 48 49 50 51 52 53 54 55 56 57 58 59 60 61 62 63 64 65 66 67 68 69 70 71 72 73 74 75 76 77 78 79 80																																																																																																																																																																																																																																																																																																																																																																																																																																																																																																																																																																																																																																																																																																																																																																																																																																																																																																																																																																																																																																																																																																																																																																																																																																																																																																																																																																																																																																																																																																																																																																																																																																																																																																																																																																																																																																																																																																																																																																																																																																																																																																																																																																																																																																																																																																																																																																																																																																																																																															
INCLUDE BUT LEAVE BLANK										INCLUDE BUT LEAVE BLANK										INCLUDE BUT LEAVE BLANK										INCLUDE BUT LEAVE BLANK										INCLUDE BUT LEAVE BLANK										INCLUDE BUT LEAVE BLANK										INCLUDE BUT LEAVE BLANK										INCLUDE BUT LEAVE BLANK										INCLUDE BUT LEAVE BLANK										INCLUDE BUT LEAVE BLANK										INCLUDE BUT LEAVE BLANK										INCLUDE BUT LEAVE BLANK										INCLUDE BUT LEAVE BLANK										INCLUDE BUT LEAVE BLANK										INCLUDE BUT LEAVE BLANK										INCLUDE BUT LEAVE BLANK										INCLUDE BUT LEAVE BLANK										INCLUDE BUT LEAVE BLANK										INCLUDE BUT LEAVE BLANK										INCLUDE BUT LEAVE BLANK										INCLUDE BUT LEAVE BLANK										INCLUDE BUT LEAVE BLANK										INCLUDE BUT LEAVE BLANK										INCLUDE BUT LEAVE BLANK										INCLUDE BUT LEAVE BLANK										INCLUDE BUT LEAVE BLANK										INCLUDE BUT LEAVE BLANK										INCLUDE BUT LEAVE BLANK										INCLUDE BUT LEAVE BLANK										INCLUDE BUT LEAVE BLANK										INCLUDE BUT LEAVE BLANK										INCLUDE BUT LEAVE BLANK										INCLUDE BUT LEAVE BLANK										INCLUDE BUT LEAVE BLANK										INCLUDE BUT LEAVE BLANK										INCLUDE BUT LEAVE BLANK										INCLUDE BUT LEAVE BLANK										INCLUDE BUT LEAVE BLANK										INCLUDE BUT LEAVE BLANK										INCLUDE BUT LEAVE BLANK										INCLUDE BUT LEAVE BLANK										INCLUDE BUT LEAVE BLANK										INCLUDE BUT LEAVE BLANK										INCLUDE BUT LEAVE BLANK										INCLUDE BUT LEAVE BLANK										INCLUDE BUT LEAVE BLANK										INCLUDE BUT LEAVE BLANK										INCLUDE BUT LEAVE BLANK										INCLUDE BUT LEAVE BLANK										INCLUDE BUT LEAVE BLANK										INCLUDE BUT LEAVE BLANK										INCLUDE BUT LEAVE BLANK										INCLUDE BUT LEAVE BLANK										INCLUDE BUT LEAVE BLANK										INCLUDE BUT LEAVE BLANK										INCLUDE BUT LEAVE BLANK										INCLUDE BUT LEAVE BLANK										INCLUDE BUT LEAVE BLANK										INCLUDE BUT LEAVE BLANK										INCLUDE BUT LEAVE BLANK										INCLUDE BUT LEAVE BLANK										INCLUDE BUT LEAVE BLANK										INCLUDE BUT LEAVE BLANK										INCLUDE BUT LEAVE BLANK										INCLUDE BUT LEAVE BLANK										INCLUDE BUT LEAVE BLANK										INCLUDE BUT LEAVE BLANK										INCLUDE BUT LEAVE BLANK										INCLUDE BUT LEAVE BLANK										INCLUDE BUT LEAVE BLANK										INCLUDE BUT LEAVE BLANK										INCLUDE BUT LEAVE BLANK										INCLUDE BUT LEAVE BLANK										INCLUDE BUT LEAVE BLANK										INCLUDE BUT LEAVE BLANK										INCLUDE BUT LEAVE BLANK										INCLUDE BUT LEAVE BLANK										INCLUDE BUT LEAVE BLANK										INCLUDE BUT LEAVE BLANK										INCLUDE BUT LEAVE BLANK										INCLUDE BUT LEAVE BLANK										INCLUDE BUT LEAVE BLANK										INCLUDE BUT LEAVE BLANK										INCLUDE BUT LEAVE BLANK										INCLUDE BUT LEAVE BLANK										INCLUDE BUT LEAVE BLANK										INCLUDE BUT LEAVE BLANK										INCLUDE BUT LEAVE BLANK										INCLUDE BUT LEAVE BLANK										INCLUDE BUT LEAVE BLANK										INCLUDE BUT LEAVE BLANK										INCLUDE BUT LEAVE BLANK										INCLUDE BUT LEAVE BLANK										INCLUDE BUT LEAVE BLANK										INCLUDE BUT LEAVE BLANK										INCLUDE BUT LEAVE BLANK										INCLUDE BUT LEAVE BLANK										INCLUDE BUT LEAVE BLANK										INCLUDE BUT LEAVE BLANK										INCLUDE BUT LEAVE BLANK										INCLUDE BUT LEAVE BLANK										INCLUDE BUT LEAVE BLANK										INCLUDE BUT LEAVE BLANK										INCLUDE BUT LEAVE BLANK										INCLUDE BUT LEAVE BLANK										INCLUDE BUT LEAVE BLANK										INCLUDE BUT LEAVE BLANK										INCLUDE BUT LEAVE BLANK										INCLUDE BUT LEAVE BLANK										INCLUDE BUT LEAVE BLANK										INCLUDE BUT LEAVE BLANK										INCLUDE BUT LEAVE BLANK										INCLUDE BUT LEAVE BLANK										INCLUDE BUT LEAVE BLANK										INCLUDE BUT LEAVE BLANK										INCLUDE BUT LEAVE BLANK										INCLUDE BUT LEAVE BLANK										INCLUDE BUT LEAVE BLANK										INCLUDE BUT LEAVE BLANK										INCLUDE BUT LEAVE BLANK										INCLUDE BUT LEAVE BLANK										INCLUDE BUT LEAVE BLANK										INCLUDE BUT LEAVE BLANK										INCLUDE BUT LEAVE BLANK										INCLUDE BUT LEAVE BLANK										INCLUDE BUT LEAVE BLANK										INCLUDE BUT LEAVE BLANK										INCLUDE BUT LEAVE BLANK										INCLUDE BUT LEAVE BLANK										INCLUDE BUT LEAVE BLANK										INCLUDE BUT LEAVE BLANK										INCLUDE BUT LEAVE BLANK										INCLUDE BUT LEAVE BLANK										INCLUDE BUT LEAVE BLANK										INCLUDE BUT LEAVE BLANK										INCLUDE BUT LEAVE BLANK										INCLUDE BUT LEAVE BLANK										INCLUDE BUT LEAVE BLANK										INCLUDE BUT LEAVE BLANK										INCLUDE BUT LEAVE BLANK										INCLUDE BUT LEAVE BLANK										INCLUDE BUT LEAVE BLANK										INCLUDE BUT LEAVE BLANK										INCLUDE BUT LEAVE BLANK										INCLUDE BUT LEAVE BLANK										INCLUDE BUT LEAVE BLANK										INCLUDE BUT LEAVE BLANK										INCLUDE BUT LEAVE BLANK										INCLUDE BUT LEAVE BLANK										INCLUDE BUT LEAVE BLANK										INCLUDE BUT LEAVE BLANK										INCLUDE BUT LEAVE BLANK										INCLUDE BUT LEAVE BLANK										INCLUDE BUT LEAVE BLANK										INCLUDE BUT LEAVE BLANK										INCLUDE BUT LEAVE BLANK										INCLUDE BUT LEAVE BLANK										INCLUDE BUT LEAVE BLANK										INCLUDE BUT LEAVE BLANK										INCLUDE BUT LEAVE BLANK										INCLUDE BUT LEAVE BLANK										INCLUDE BUT LEAVE BLANK										INCLUDE BUT LEAVE BLANK										INCLUDE BUT LEAVE BLANK										INCLUDE BUT LEAVE BLANK										INCLUDE BUT LEAVE BLANK										INCLUDE BUT LEAVE BLANK										INCLUDE BUT LEAVE BLANK										INCLUDE BUT LEAVE BLANK										INCLUDE BUT LEAVE BLANK										INCLUDE BUT LEAVE BLANK										INCLUDE BUT LEAVE BLANK										INCLUDE BUT LEAVE BLANK										INCLUDE BUT LEAVE BLANK										INCLUDE BUT LEAVE BLANK										INCLUDE BUT LEAVE BLANK										INCLUDE BUT LEAVE BLANK										INCLUDE BUT LEAVE BLANK										INCLUDE BUT LEAVE BLANK										INCLUDE BUT LEAVE BLANK										INCLUDE BUT LEAVE BLANK										INCLUDE BUT LEAVE BLANK										INCLUDE BUT LEAVE BLANK										INCLUDE BUT LEAVE BLANK										INCLUDE BUT LEAVE BLANK										INCLUDE BUT LEAVE BLANK										INCLUDE BUT LEAVE BLANK										INCLUDE BUT LEAVE BLANK										INCLUDE BUT LEAVE BLANK										INCLUDE BUT LEAVE BLANK										INCLUDE BUT LEAVE BLANK										INCLUDE BUT LEAVE BLANK										INCLUDE BUT LEAVE BLANK										INCLUDE BUT LEAVE BLANK										INCLUDE BUT LEAVE BLANK										INCLUDE BUT LEAVE BLANK										INCLUDE BUT LEAVE BLANK										INCLUDE BUT LEAVE BLANK										INCLUDE BUT LEAVE BLANK										INCLUDE BUT LEAVE BLANK										INCLUDE BUT LEAVE BLANK										INCLUDE BUT LEAVE BLANK										INCLUDE BUT LEAVE BLANK										INCLUDE BUT LEAVE BLANK										INCLUDE BUT LEAVE BLANK										INCLUDE BUT LEAVE BLANK										INCLUDE BUT LEAVE BLANK										INCLUDE BUT LEAVE BLANK										INCLUDE BUT LEAVE BLANK										INCLUDE BUT LEAVE BLANK										INCLUDE BUT LEAVE BLANK										INCLUDE BUT LEAVE BLANK										INCLUDE BUT LEAVE BLANK										INCLUDE BUT LEAVE BLANK										INCLUDE BUT LEAVE BLANK										INCLUDE BUT LEAVE BLANK										INCLUDE BUT LEAVE BLANK										INCLUDE BUT LEAVE BLANK										INCLUDE BUT LEAVE BLANK										INCLUDE BUT LEAVE BLANK										INCLUDE BUT LEAVE BLANK										INCLUDE BUT LEAVE BLANK										INCLUDE BUT LEAVE BLANK										INCLUDE BUT LEAVE BLANK										INCLUDE BUT LEAVE BLANK										INCLUDE BUT LEAVE BLANK										INCLUDE BUT LEAVE BLANK										INCLUDE BUT LEAVE BLANK										INCLUDE BUT LEAVE BLANK										INCLUDE BUT LEAVE BLANK										INCLUDE BUT LEAVE BLANK										INCLUDE BUT LEAVE BLANK										INCLUDE BUT LEAVE BLANK										INCLUDE BUT LEAVE BLANK										INCLUDE BUT LEAVE BLANK										INCLUDE BUT LEAVE BLANK										INCLUDE BUT LEAVE BLANK										INCLUDE BUT LEAVE BLANK										INCLUDE BUT LEAVE BLANK										INCLUDE BUT LEAVE BLANK										INCLUDE BUT LEAVE BLANK										INCLUDE BUT LEAVE BLANK										INCLUDE BUT LEAVE BLANK										INCLUDE BUT LEAVE BLANK										INCLUDE BUT LEAVE BLANK</									

Card Type 2-
 Bearing Data
 Card 13, ONE CARD

Lubricant Properties

BD(71)										DD(72)										(73)										(74)										(75)										DD(76)																													
1	2	3	4	5	6	7	8	9	10	11	12	13	14	15	16	17	18	19	20	21	22	23	24	25	26	27	28	29	30	31	32	33	34	35	36	37	38	39	40	41	42	43	44	45	46	47	48	49	50	51	52	53	54	55	56	57	58	59	60	61	62	63	64	65	66	67	68	69	70	71	72	73	74	75	76	77	78	79	80
Lubricant Designation										VIS1 Dynamic Viscosity @ 100°F										VIS2 Dynamic Viscosity @ 210°F										R11000 Density Kg/Km ³ @ 15.5°C										C Coefficient of Thermal Expansion 1/°C										Cond Thermal Conductivity W/M°C																													

Lubricant N Code 1-4 right justified NCODE

— If NCODE is zero read this data —

Card Type 3---. .
Bearing Data
Card 14, One Card

[illegible]

These values should be non zero only if the lubricant code, card 13, item 1, is zero. These data define the friction model.

Card Type 1

LEGAL DATA

GENERAL DATA
COC 577/011105 5100. IF NO TEMP. CALCULATION IS OBTAINED, THEN LEAVE THE OINO BLANK.

[illegible]

GENERAL				STEADY STATE ONLY			TRANSIENT ONLY						
HIGHEST BITE NUMBER	HIGHEST LUNARON NUMBER SAME AS NUMBER OF UNION NUMBER	COPPER INITIAL TEMPERATURE SELECTED TEMPERATURES CAN BE DIFFER- ENT INITIAL VALUE USING CARD 17.	FLUX FLAG INITIALLY ZERO. IF $\neq 0$ FINAL TEMPERATURES WILL BE ACCORDING TO THE CARD 17. IF $\neq 0$, THEY CAN BE DIFFERENT INITIAL TEMPERATURES IN A LATER RUN.	OUTPUT FLAG INITIALLY ZERO. IF $\neq 0$ BEARING TEMPERATURE AND A TEMPERATURE WILL BE PRINTED EVERY TIME THE SHAFT- BEARING PROGRAM IS STOP CALLED.	MAXIMUM NO. OF THE SHAFT- BEARING PROGRAM.	ABSOLUTE FLUX NO. OF CARD 18 CONTAINS	ITERATION USUALLY LEFT BLANK IF $\neq 0$ THE INTER- MEDIATE ITERATION LIMIT. IF BLANK PRE-SET LIMIT IS USED	ACCURACY LEFT BLANK IF $\neq 0$ IT IS THE INTERMEDIATE REL. ACCURACY	STARTING TIME	STOPPING TIME	CALCULATION TIME STEP. IF LEFT THE BLOCKING WILL CALCUL- ATE A SUITABLE STEP.	TIME INTERVAL BETWEEN PRINTED TEMP. MAPS. THE INTERVAL WILL BE AT LEAST COUL TO THE GAO. TIME STEP.	TIME INTERVAL BETWEEN CALLS OF THE BEGINNING PROGRAM. ALWAYS AT LEAST EQUAL TO THE TIME STEP.

Card Type π
Thermal Data - Nodes where bearing frictional heat is generated

T5, One card/brg.

10	2	1	7
----	---	---	---

T6. as many cards as needed, followed by a blank card

T6. as many cards as needed, followed by a blank card

Node	Power
1	1
2	1
3	1
4	1
5	1
6	1
7	1
8	1
9	1
10	1
11	1
12	1
13	1
14	1
15	1
16	1
17	1
18	1
19	1
20	1
21	1
22	1
23	1
24	1
25	1
26	1
27	1
28	1
29	1
30	1
31	1
32	1
33	1
34	1
35	1
36	1
37	1
38	1
39	1
40	1
41	1
42	1
43	1
44	1
45	1
46	1
47	1
48	1
49	1
50	1
51	1
52	1
53	1
54	1
55	1
56	1
57	1
58	1
59	1
60	1
61	1
62	1
63	1
64	1
65	1
66	1
67	1
68	1
69	1
70	1
71	1
72	1
73	1
74	1
75	1
76	1
77	1
78	1
79	1
80	1
81	1
82	1
83	1
84	1
85	1
86	1
87	1
88	1
89	1
90	1
91	1
92	1
93	1
94	1
95	1
96	1
97	1
98	1
99	1
100	1

SPECIAL DATA - HEAT TRANSFER COEFFICIENTS

17. Give one of the following coefficients, as may be desired, followed by a blank card.

1-10 $h = \lambda / \delta$ (CONDUCTIVITY λ) (FILM THICKNESS δ)	11-20 $h = \lambda / \delta$ (FILM THICKNESS δ) (FORCED CONVECTION)	21-30 $h = \lambda / \delta$ (FILM THICKNESS δ) (NATURAL CONVECTION)	31-40 $h = \lambda / \delta$ (FILM THICKNESS δ) (NATURAL CONVECTION)	41-50 $h = \lambda / \delta$ (FILM THICKNESS δ) (NATURAL CONVECTION)	51-60 $h = \lambda / \delta$ (FILM THICKNESS δ) (NATURAL CONVECTION)	61-70 $h = \lambda / \delta$ (FILM THICKNESS δ) (NATURAL CONVECTION)	71-80 $h = \lambda / \delta$ (FILM THICKNESS δ) (NATURAL CONVECTION)	81-90 $h = \lambda / \delta$ (FILM THICKNESS δ) (NATURAL CONVECTION)	91-100 $h = \lambda / \delta$ (FILM THICKNESS δ) (NATURAL CONVECTION)
--	---	--	--	--	--	--	--	--	---

1-10 $h = \lambda / \delta$ (CONDUCTIVITY λ) (FILM THICKNESS δ)	11-20 $h = \lambda / \delta$ (FILM THICKNESS δ) (FORCED CONVECTION)	21-30 $h = \lambda / \delta$ (FILM THICKNESS δ) (NATURAL CONVECTION)	31-40 $h = \lambda / \delta$ (FILM THICKNESS δ) (NATURAL CONVECTION)	41-50 $h = \lambda / \delta$ (FILM THICKNESS δ) (NATURAL CONVECTION)	51-60 $h = \lambda / \delta$ (FILM THICKNESS δ) (NATURAL CONVECTION)	61-70 $h = \lambda / \delta$ (FILM THICKNESS δ) (NATURAL CONVECTION)	71-80 $h = \lambda / \delta$ (FILM THICKNESS δ) (NATURAL CONVECTION)	81-90 $h = \lambda / \delta$ (FILM THICKNESS δ) (NATURAL CONVECTION)	91-100 $h = \lambda / \delta$ (FILM THICKNESS δ) (NATURAL CONVECTION)
--	---	--	--	--	--	--	--	--	---

1-10 $h = \lambda / \delta$ (CONDUCTIVITY λ) (FILM THICKNESS δ)	11-20 $h = \lambda / \delta$ (FILM THICKNESS δ) (FORCED CONVECTION)	21-30 $h = \lambda / \delta$ (FILM THICKNESS δ) (NATURAL CONVECTION)	31-40 $h = \lambda / \delta$ (FILM THICKNESS δ) (NATURAL CONVECTION)	41-50 $h = \lambda / \delta$ (FILM THICKNESS δ) (NATURAL CONVECTION)	51-60 $h = \lambda / \delta$ (FILM THICKNESS δ) (NATURAL CONVECTION)	61-70 $h = \lambda / \delta$ (FILM THICKNESS δ) (NATURAL CONVECTION)	71-80 $h = \lambda / \delta$ (FILM THICKNESS δ) (NATURAL CONVECTION)	81-90 $h = \lambda / \delta$ (FILM THICKNESS δ) (NATURAL CONVECTION)	91-100 $h = \lambda / \delta$ (FILM THICKNESS δ) (NATURAL CONVECTION)
--	---	--	--	--	--	--	--	--	---

1-10 $h = \lambda / \delta$ (CONDUCTIVITY λ) (FILM THICKNESS δ)	11-20 $h = \lambda / \delta$ (FILM THICKNESS δ) (FORCED CONVECTION)	21-30 $h = \lambda / \delta$ (FILM THICKNESS δ) (NATURAL CONVECTION)	31-40 $h = \lambda / \delta$ (FILM THICKNESS δ) (NATURAL CONVECTION)	41-50 $h = \lambda / \delta$ (FILM THICKNESS δ) (NATURAL CONVECTION)	51-60 $h = \lambda / \delta$ (FILM THICKNESS δ) (NATURAL CONVECTION)	61-70 $h = \lambda / \delta$ (FILM THICKNESS δ) (NATURAL CONVECTION)	71-80 $h = \lambda / \delta$ (FILM THICKNESS δ) (NATURAL CONVECTION)	81-90 $h = \lambda / \delta$ (FILM THICKNESS δ) (NATURAL CONVECTION)	91-100 $h = \lambda / \delta$ (FILM THICKNESS δ) (NATURAL CONVECTION)
--	---	--	--	--	--	--	--	--	---

[illegible]

INDEX = 1	MODE J	l_1 mm	l_2 mm	l_3 mm	CONDUCTION BETWEEN 1 AND 2, AREA = $2\pi l_1 l_2$. IF INDEX 0, AREA = $l_1 l_2$, DISTANCE 1-2 = l_3 .
INDEX = 2	MODE J	l_1 mm	l_2	l_3	NATURAL CONVECTION BETWEEN 1 AND 2, AREA = $2\pi l_1 l_2$. IF INDEX 0, AREA = $l_1 l_2$.
INDEX = 3	MODE J	l_1	l_2	BLANK	FORCED CONVECTION BETWEEN 1 AND 2, AREA AS ABOVE. IF 7, 8, 9, 10, 11, 12.
INDEX = 4	MODE J	l_1	l_2	(l_3)	RADIATION BETWEEN 1 AND 2, AREA AS ABOVE. FOR DESCRIPTION OF l_3 , SEE USER'S MANUAL.
INDEX = 5	MODE J	l_1	l_2	BLANK	FLUID FLOW FROM MODE 1 TO MODE 2. FIRST INDEX IS INDEX OF FLUID FLOW AT MODE 1.
INDEX = 6	MODE J	MODE 1-2 FLUID FLOW AT MODE 1, 11.5 INDEX 5.50	BLANK	BLANK	CONDUCTION THROUGH A BEARING
INDEX = 7	MODE J	BEARING NUMBER ON 11.5 INDEX 5.5	PARTIAL PLATE CONTACT 1-2 AFTER SHAPE CONTACT	BLANK	PISTON, USUALLY = 1. IF 1 AND 2 IS A ROCKET IN THE OIL BETWEEN THE CONTACTING SURFACES, THE PISTON IS 0.5.

TO, The Card, Code

T ₀ , One Card/Node									
Node Number	Volume at Node: $V_1 = V_2 = V_3$			Density (KG/m ³)	Specific Heat WS/KG-°C				
	V_1 mm	V_2 mm	V_3 mm						
1	1	1	1						
2	2	2	2						
3	3	3	3						
4	4	4	4						
5	5	5	5						
6	6	6	6						
7	7	7	7						
8	8	8	8						
9	9	9	9						
10	10	10	10						
11	11	11	11						
12	12	12	12						
13	13	13	13						
14	14	14	14						
15	15	15	15						
16	16	16	16						
17	17	17	17						
18	18	18	18						
19	19	19	19						
20	20	20	20						
21	21	21	21						
22	22	22	22						
23	23	23	23						
24	24	24	24						
25	25	25	25						
26	26	26	26						
27	27	27	27						
28	28	28	28						
29	29	29	29						
30	30	30	30						
31	31	31	31						
32	32	32	32						
33	33	33	33						
34	34	34	34						
35	35	35	35						
36	36	36	36						
37	37	37	37						
38	38	38	38						
39	39	39	39						
40	40	40	40						
41	41	41	41						
42	42	42	42						
43	43	43	43						
44	44	44	44						
45	45	45	45						
46	46	46	46						
47	47	47	47						
48	48	48	48						
49	49	49	49						
50	50	50	50						
51	51	51	51						
52	52	52	52						
53	53	53	53						
54	54	54	54						
55	55	55	55						
56	56	56	56						
57	57	57	57						
58	58	58	58						
59	59	59	59						
60	60	60	60						
61	61	61	61						
62	62	62	62						
63	63	63	63						
64	64	64	64						
65	65	65	65						
66	66	66	66						
67	67	67	67						
68	68	68	68						
69	69	69	69						
70	70	70	70						
71	71	71	71						
72	72	72	72						
73	73	73	73						
74	74	74	74						
75	75	75	75						
76	76	76	76						
77	77	77	77						
78	78	78	78						
79	79	79	79						
80	80	80	80						
81	81	81	81						
82	82	82	82						
83	83	83	83						
84	84	84	84						
85	85	85	85						
86	86	86	86						
87	87	87	87						
88	88	88	88						
89	89	89	89						
90	90	90	90						
91	91	91	91						
92	92	92	92						
93	93	93	93						
94	94	94	94						
95	95	95	95						
96	96	96	96						
97	97	97	97						
98	98	98	98						
99	99	99	99						
100	100	100	100						

Shaft: Data - Shaft Geometry
Get: all shaft data cards if there are no bearings

151. as many cards as needed

[illegible]

\$3, as many cards as needed, followed by a blank card.

[illegible]

S2. As many cards as needed. Card needed only if any data is different from X-Y plane

S2. as many cards as needed. Card needed only if any data is different from X-Y plane

249

53. as many cards as needed, followed by a blank card.

250

APPENDIX C

SAMPLE BALL BEARING PROGRAM OUTPUT

1940 125. 110. 100. 90. 80. 70. 60. 50. 40. 30. 20. 10. 0. 10. 20. 30. 40. 50. 60. 70. 80. 90. 100. 110. 120. 130. 140. 150. 160. 170. 180. 190. 200. 210. 220. 230. 240. 250. 260. 270. 280. 290. 300. 310. 320. 330. 340. 350. 360. 370. 380. 390. 400. 410. 420. 430. 440. 450. 460. 470. 480. 490. 500. 510. 520. 530. 540. 550. 560. 570. 580. 590. 600. 610. 620. 630. 640. 650. 660. 670. 680. 690. 700. 710. 720. 730. 740. 750. 760. 770. 780. 790. 800. 810. 820. 830. 840. 850. 860. 870. 880. 890. 900. 910. 920. 930. 940. 950. 960. 970. 980. 990. 1000. 1010. 1020. 1030. 1040. 1050. 1060. 1070. 1080. 1090. 1100. 1110. 1120. 1130. 1140. 1150. 1160. 1170. 1180. 1190. 1200. 1210. 1220. 1230. 1240. 1250. 1260. 1270. 1280. 1290. 1300. 1310. 1320. 1330. 1340. 1350. 1360. 1370. 1380. 1390. 1400. 1410. 1420. 1430. 1440. 1450. 1460. 1470. 1480. 1490. 1500. 1510. 1520. 1530. 1540. 1550. 1560. 1570. 1580. 1590. 1600. 1610. 1620. 1630. 1640. 1650. 1660. 1670. 1680. 1690. 1700. 1710. 1720. 1730. 1740. 1750. 1760. 1770. 1780. 1790. 1800. 1810. 1820. 1830. 1840. 1850. 1860. 1870. 1880. 1890. 1900. 1910. 1920. 1930. 1940. 1950. 1960. 1970. 1980. 1990. 2000. 2010. 2020. 2030. 2040. 2050. 2060. 2070. 2080. 2090. 2100. 2110. 2120. 2130. 2140. 2150. 2160. 2170. 2180. 2190. 2200. 2210. 2220. 2230. 2240. 2250. 2260. 2270. 2280. 2290. 2300. 2310. 2320. 2330. 2340. 2350. 2360. 2370. 2380. 2390. 2400. 2410. 2420. 2430. 2440. 2450. 2460. 2470. 2480. 2490. 2500. 2510. 2520. 2530. 2540. 2550. 2560. 2570. 2580. 2590. 2600. 2610. 2620. 2630. 2640. 2650. 2660. 2670. 2680. 2690. 2700. 2710. 2720. 2730. 2740. 2750. 2760. 2770. 2780. 2790. 2800. 2810. 2820. 2830. 2840. 2850. 2860. 2870. 2880. 2890. 2900. 2910. 2920. 2930. 2940. 2950. 2960. 2970. 2980. 2990. 3000. 3010. 3020. 3030. 3040. 3050. 3060. 3070. 3080. 3090. 3100. 3110. 3120. 3130. 3140. 3150. 3160. 3170. 3180. 3190. 3200. 3210. 3220. 3230. 3240. 3250. 3260. 3270. 3280. 3290. 3300. 3310. 3320. 3330. 3340. 3350. 3360. 3370. 3380. 3390. 3400. 3410. 3420. 3430. 3440. 3450. 3460. 3470. 3480. 3490. 3500. 3510. 3520. 3530. 3540. 3550. 3560. 3570. 3580. 3590. 3600. 3610. 3620. 3630. 3640. 3650. 3660. 3670. 3680. 3690. 3700. 3710. 3720. 3730. 3740. 3750. 3760. 3770. 3780. 3790. 3800. 3810. 3820. 3830. 3840. 3850. 3860. 3870. 3880. 3890. 3900. 3910. 3920. 3930. 3940. 3950. 3960. 3970. 3980. 3990. 4000. 4010. 4020. 4030. 4040. 4050. 4060. 4070. 4080. 4090. 4100. 4110. 4120. 4130. 4140. 4150. 4160. 4170. 4180. 4190. 4200. 4210. 4220. 4230. 4240. 4250. 4260. 4270. 4280. 4290. 4300. 4310. 4320. 4330. 4340. 4350. 4360. 4370. 4380. 4390. 4400. 4410. 4420. 4430. 4440. 4450. 4460. 4470. 4480. 4490. 4500. 4510. 4520. 4530. 4540. 4550. 4560. 4570. 4580. 4590. 4600. 4610. 4620. 4630. 4640. 4650. 4660. 4670. 4680. 4690. 4700. 4710. 4720. 4730. 4740. 4750. 4760. 4770. 4780. 4790. 4800. 4810. 4820. 4830. 4840. 4850. 4860. 4870. 4880. 4890. 4900. 4910. 4920. 4930. 4940. 4950. 4960. 4970. 4980. 4990. 5000. 5010. 5020. 5030. 5040. 5050. 5060. 5070. 5080. 5090. 5100. 5110. 5120. 5130. 5140. 5150. 5160. 5170. 5180. 5190. 5200. 5210. 5220. 5230. 5240. 5250. 5260. 5270. 5280. 5290. 5300. 5310. 5320. 5330. 5340. 5350. 5360. 5370. 5380. 5390. 5400. 5410. 5420. 5430. 5440. 5450. 5460. 5470. 5480. 5490. 5500. 5510. 5520. 5530. 5540. 5550. 5560. 5570. 5580. 5590. 5600. 5610. 5620. 5630. 5640. 5650. 5660. 5670. 5680. 5690. 5700. 5710. 5720. 5730. 5740. 5750. 5760. 5770. 5780. 5790. 5800. 5810. 5820. 5830. 5840. 5850. 5860. 5870. 5880. 5890. 5900. 5910. 5920. 5930. 5940. 5950. 5960. 5970. 5980. 5990. 6000. 6010. 6020. 6030. 6040. 6050. 6060. 6070. 6080. 6090. 6100. 6110. 6120. 6130. 6140. 6150. 6160. 6170. 6180. 6190. 6200. 6210. 6220. 6230. 6240. 6250. 6260. 6270. 6280. 6290. 6300. 6310. 6320. 6330. 6340. 6350. 6360. 6370. 6380. 6390. 6400. 6410. 6420. 6430. 6440. 6450. 6460. 6470. 6480. 6490. 6500. 6510. 6520. 6530. 6540. 6550. 6560. 6570. 6580. 6590. 6600. 6610. 6620. 6630. 6640. 6650. 6660. 6670. 6680. 6690. 6700. 6710. 6720. 6730. 6740. 6750. 6760. 6770. 6780. 6790. 6800. 6810. 6820. 6830. 6840. 6850. 6860. 6870. 6880. 6890. 6900. 691

Julius & 7771 - (11) 'Gr. 21.1.155

***COMPUTER 720,PM 477.071 ** F CYCICAL SERVICES DIVISION 3MF INC. INC. ** COMPUTER PROGRAM AT74Y001 ***

END OF 170. NO. 00 35) TEST NO. 11 "TL L 7499 Q = 14679 "I = 25000

I N P U T D A T A I S O U N I T S

LINEAR DIMENSIONS INCLUDING SURFACE ROUGHNESS, LUBRICIT FILM THICKNESS AND LINEAR TACKING MOUNTING ERRORS ARE IN (MM), AREA IN (MM²), ANGLES INCLUDING ASPERITY SLOPES IN (DEG), GAP, GAPING ANGULAR MOUNTING ERRORS IN (RADIAN) ORBITAL SPACES IN (MM), LINEAR SPACES IN (MM/SEC), FORCE IN (NEWTONS) (N), MOMENTS IN (N-MM), PRESSURE AND ELASTIC MODULUS IN (N/MM²), DENSITY IN (KG/MM³), KINEMATIC VISCOSITY IN (MM²/SEC), TEMPERATURE IN (DEGREES C), COEFFICIENT OF THERMAL EXPANSION IN (1/DEGREES C), THERMAL CONDUCTIVITY IN (WATTS/MM²/DEGREES C)

BEARING NUMBER (1) TYPE - BALL BEARING

O U T P U T D A T A

NUMBER OF BALLS	AZIMUTH ANGLE ORIENTATION	DIAMETRAL CLEARANCE	TALL DIAMETER	PITCH DIAMETER	FREE CONTACT ANGLE	RACEWAY CURVATURE OUTER	SHAFT INNER SPEED	OUTER RING SPEED
21	-0.000	.130	29.5175	159.4995	26.00	.521	.516	25000.000

RMS SURFACE ROUGHNESS OUTLINE	INNER BALL	ASPERITY SLOPES OUTER	INNER BALL	ASPERITY COEF. FIRST	SMIN WIDTH	SHAFT DIAMETRAL PLAY	END PLAY
.01006	.00015	.00004	2.40	2.00	.103	.176	16.049
						.129	.489

C A G F D A T A

CAGE TYPE	CAGE ROCKET CLEARANCE	RAIL-LAND AREA	RAIL-LAND DIAMETER	RAIL-LAND CLEARANCE
IMNE - 4105 LAMID RACING	.303700	2.115	151.	.530

Reproduced from
Best available copy.

***COMPUTED 2405424 AT74101 ** 7 UNICAL SERVICES DIVISION SKF I.D. INS. ** COMPUTER PROGRAM AT74Y001 ***

END STUDY YES, NO. 42033 TEST NO. 11 MIL L 7993 Q = 14679 " = 25700

STILL DATA

INNER RING TYPE	LIFE FACTOR	OUTER RING TYPE	LIFE FACTOR
4-50	5.000	4-50	5.000

LUBRICANT DATA

DESIGNATION	VISCOSITY AT (17.74 C)	VISCOSITY AT (99.89)	DENSITY AT (15.56 C)	THERMAL EXPANSION COEFFICIENT	THERMAL CONDUCTIVITY
MTL-L-7493G	.13E-02	.32E-01	952.5100	.71E-03	.15E+00

FILM REPLACEMENT OUTER INNER	MAX. FRICTION COEFFICIENT	FRICTION RATIO BREAK-POINT	SLIDING SPEED AT MAX. FRICTION	SLIDING RATIO BREAK-POINT	PERCENT LUBE IN CAVITY
.10E-01	.10E-01	.3000	-0.00	-0.0000	2.50

***COMPUTER PROGRAM AT740001 ** TECHNICAL SERVICES DIVISION SKF INC. INC. ** COMPUTER PROGRAM AT740001 ***

END STUDY REG. NO. 46031 TEST NO. 11 MIL L 7504 G = 1.079 N = 29000

P I T C A T 2

BEARING NUMBER	COLL FITS SHAFT	INCHES RING	OUTER RING	HOUSING
1	.075290	35.0000	16.0000	32.4300 35.0000

BEARING NUMBER	SHAFT I.D.	WEARING SURF. I.D.	INNER RING AVE. I.D.	OUTER RING AVE. I.D.	GEARING SURF. I.D.	HOUSING O.D.
1	112.000	125.000	142.500	170.600	190.000	220.000

BEARING NUMBER (1)	SHAFT	INNER RING	OUTER RING	HOUSING
1	20.0000	23.0000	29.0000	20.0000

MODULUS OF ELASTICITY

POISSON'S RATIO

WEIGHT DENSITY

COEFF. OF THERMAL EXP.

***COMPUTER PROGRAM AT76001 ** TECHNICAL SERVICES DIVISION SFC INC. ** COMPUTER PROGRAM AT76001 ***

CMU STUDY 342. NO. 400489 TEST NO. 11 MILL L 7403 G = 1479 W = 25000

UNLESS OTHERWISE STATED, INTERNATIONAL UNITS ARE USED

GIVEN T-MATERIALS

1.0	231.00	2.0	210.00	3.0	241.30	4.0	241.00	5.0	221.00	6.0	210.00	7.0	200.00	8.0	190.00	9.0	180.00	10.0	170.00	11.0	160.00	12.0	150.00	13.0	140.00	14.0	130.00	15.0	120.00	16.0	110.00	17.0	100.00	18.0	90.00	19.0	80.00	20.0	70.00	21.0	60.00	22.0	50.00	23.0	40.00	24.0	30.00	25.0	20.00	26.0	10.00	27.0	0.00	28.0	0.00	29.0	0.00	30.0	0.00	31.0	0.00	32.0	0.00	33.0	0.00	34.0	0.00	35.0	0.00	36.0	0.00	37.0	0.00	38.0	0.00	39.0	0.00	40.0	0.00	41.0	0.00	42.0	0.00	43.0	0.00	44.0	0.00	45.0	0.00	46.0	0.00	47.0	0.00	48.0	0.00	49.0	0.00	50.0	0.00	51.0	0.00	52.0	0.00	53.0	0.00	54.0	0.00	55.0	0.00	56.0	0.00	57.0	0.00	58.0	0.00	59.0	0.00	60.0	0.00	61.0	0.00	62.0	0.00	63.0	0.00	64.0	0.00	65.0	0.00	66.0	0.00	67.0	0.00	68.0	0.00	69.0	0.00	70.0	0.00	71.0	0.00	72.0	0.00	73.0	0.00	74.0	0.00	75.0	0.00	76.0	0.00	77.0	0.00	78.0	0.00	79.0	0.00	80.0	0.00	81.0	0.00	82.0	0.00	83.0	0.00	84.0	0.00	85.0	0.00	86.0	0.00	87.0	0.00	88.0	0.00	89.0	0.00	90.0	0.00	91.0	0.00	92.0	0.00	93.0	0.00	94.0	0.00	95.0	0.00	96.0	0.00	97.0	0.00	98.0	0.00	99.0	0.00	100.0	0.00
-----	--------	-----	--------	-----	--------	-----	--------	-----	--------	-----	--------	-----	--------	-----	--------	-----	--------	------	--------	------	--------	------	--------	------	--------	------	--------	------	--------	------	--------	------	--------	------	-------	------	-------	------	-------	------	-------	------	-------	------	-------	------	-------	------	-------	------	-------	------	------	------	------	------	------	------	------	------	------	------	------	------	------	------	------	------	------	------	------	------	------	------	------	------	------	------	------	------	------	------	------	------	------	------	------	------	------	------	------	------	------	------	------	------	------	------	------	------	------	------	------	------	------	------	------	------	------	------	------	------	------	------	------	------	------	------	------	------	------	------	------	------	------	------	------	------	------	------	------	------	------	------	------	------	------	------	------	------	------	------	------	------	------	------	------	------	------	------	------	------	------	------	------	------	------	------	------	------	------	------	------	------	------	------	------	------	------	------	------	------	------	------	------	------	------	------	------	------	------	------	------	------	------	------	------	------	------	------	------	------	------	------	------	------	------	-------	------

***COMPUTER PROGRAM AT74001** TECHNICAL SERVICES DIVISION SKF INC. INC. ** COMPUTER PROGRAM AT74Y001 ***

PMU STUDY 16G. UN. 456333 TEST NO. 11 MIL L 7499 Q = 14679 N = 25000

SHAFT GEOMETRY, BEARING LOCATIONS AND SHAFT LOAD, PLANE X - 7.

2 GEOMETRIC SECTIONS 1 LOAD SECTION(S), 1 BEARINGS, MODULUS OF ELASTICITY = 2.100E+05

THRUST LOAD = 1.459E+04

POST- TION	INNER DIAM.		OUTER DIAM.		POINT FORCE	POINT MOMENT	LOAD INTENSITY		BEARING SEAT POS. ERR DEFL/FOR ANG. ERR DEFL/MOM
	LEFT	RIGHT	LEFT	RIGHT			LEFT	RIGHT	
1	-0.0	-0.0	90.0	-7.0	125.0				
2	25.0	90.0	90.0	125.0	125.0				
3	50.0	90.0	-0.0	125.0	-0.0				

***COMPUTER PROGRAM AT740001 ** TECHNICAL SERVICES DIVISION SKF IND. INC. ** COMPUTER PROGRAM AT74Y001 ***

END STUDY 3RG. NO. 456911 TEST NO. 11 MIL L 7304 Q = 1-679 H = 25000

RE A R I N G O U T P U T P L A K I N G N U M B E R 1 M E T R I C U N I T S

LINEAR (MM) AND ANGULAR (RADIANS) DEFLECTIONS				FORCES (N) AND MOMENTS (N-MM)						
DX	DY	DZ	GY	GZ	FX	FY	FZ	MX	MY	MZ
.104	0.	0.	-3.	0.	1.468E+04	0.	0.	0.	0.	0.

FRICTION HEAT GENERATION RATE (WATTS)				TORQUE (N-MM)	
OUTER	INNER	CAGE-R.E.	CAGE-LAND	ALL DRAG	TOTAL
2.349E+03	0.337E+03	65.0	127.	1.545E+04	2.633E+04
					1.013E+04

FATIGUE LIFE (HOURS)		H / SIGMA		LUBRICATION LIFE MULTIPLIERS		MATERIAL	
OUTER	INNER	BEARING	OUTER	INNER	OUTER	INNER	INNER
1-8.	3.243E+07	1-2.	1.46	.958	.958	5.00	5.00

***COMPUTER PROGRAM AT74V001 *** TECHNICAL SERVICES DIVISION SKF IND. INC. ** COMPUTER PROGRAM AT74V001 ***

END STUDY ARG. NO. 436933 TEST NO. 11 MIL L 7404 Q = 14679 N = 25000

BEARING OUTPUT TEARING NUMBER 1 METRIC UNITS

F M N FILM DATA FOR THE MOST HEAVILY LOADED ROLLING ELEMENT

FRICITION COEFFICIENT CORRECTED FILM (MM) THEORY, RED. FACTOR STANBY, RED. FACTOR MENISCUS DISTANCE (MM)

OUTER 3.141E-03 INNER 4.607E-03 OUTER 1.076E-04 INNER 7.177E-05 OUTER 1.00 INNER 1.00 OUTER 2.79 INNER 3.22

LUBRICANT TEMPERATURES AND PHYSICAL PROPERTIES

LOCATION TEMPERATURES (DEGREES C.) DENSITY (GM/CM3) KIN. VISC. (CP) DYN. VISC. (M2/M) PRESSURE VISCOSITY COEFFICIENT (M2/M)

OUTER 221.0007 0.869 0.957 0.034 0.264E-02
INNER 241.0000 0.7927 0.971 0.111 0.295E-02
BULK 174.0000 0.8402 1.3665 1.1492 0.650E-02

***COMPUTER PROGRAM AT74-001 ** TECHNICAL SERVICES DIVISION SKF IND. INC. ** COMPUTER PROGRAM AT74Y001 ***

END STUDY ARG. NO. 455913 TEST NO. 11 MILL 7404 0 0 0.0479 N 25000

P E A R I N G O U T P U T G E A R I N G N U M B E R 1 M E T R I C U N I T S

COMPONENT TEMPERATURES (DEGREES C.)

SHAFT 211.	INNER 210.	ROLL, ILM, 211.	OUTER 210.	HOUSING 210.

RING SPEEDS

OUTER (RPM) (RAD./SEC.)		INNER (RPM) (RAD./SEC.)		CALCULATED GAGE SPEED (RPM) (RAD./SEC.)		EPICYCLIC GAGE SPEED (RPM) (RAD./SEC.)		PERCENT DIFFERENCE	
0.	0.	2.616E+03	2.500E+04	1.217E+03	1.163E+04	1.142E+03	1.091E+04	6.53	

FIT PRESSURES (N/MM2)

SHAFT-COLD SHAFT-OPER. HSG.-COLD HSG.-OPER.	ORIGINAL CHANGE	DIAMETRAL CLEARANCES (MM)	SPEED GIVING ZERO FIT PRESSURE OPERATING BETWEEN SHAFT AND I.R. (RPM)
9.93 7.24	0. 0.	0.154	1.671E-02 3.988E+04

CMG JURY '126. 40. 450937 7:57 NO. 11 JUL 6 7179 0 = 10079 11 = 25309

REGULATORY. OUT PUT FOR GAINING HUMANITY

[illegible]

APPENDIX D

SAMPLE THERMAL ANALYSIS OUTPUT

INPUT SHAFT OF HELICOPTER ENGINE REDUCTION GEARBOX S/N 000-0, FULL OIL FLOW
 STEADY STATE TEMPERATURE CALCULATION. ITERATION LIMIT 5. ABSOLUTE ACCURACY .10 DEGREES
 UNLESS OTHERWISE STATED, INTERNATIONAL UNITS ARE USED

CONSTANT GENERATED HEATS

NODE	GEN. HEAT	NODE	GEN. HEAT	NODE	GEN. HEAT	NODE	GEN. HEAT	NODE	GEN. HEAT
5	505.00	8	170.00	10	500.00	14	397.00		
15	793.00	15	397.00	21	793.00	22	397.00		
25	397.00	26	793.00	32	397.00	33	793.00		
34	397.00	37	100.00						

INPUT SHAFT OF HELICOPTER ENGINE REDUCTION GEARBOX S/N 300-D, FULL OIL FLOW

HEAT TRANSFER COEFFICIENTS

TYPE	INDEX	COEFFICIENTS			
CONDUCTION	1	53.6517			34.0000
CONDUCTION	2	46.7209			25.0000
CONDUCTION	3	50.0291			12.5000
FORCED CONVECTION	21	300000	.570000	.000000	.000000
		170000	.000000	900.00	.700000-03
		210.330	.000000-03	.570000	103.45
		-4.0991	.000000-03	.000000	.250000
		30000	.570000	.000000	.000000
FORCED CONVECTION	22	200000-01	.200000-04	1.21000	.000000
		30000	.000000	.000000	.000000
		200000-01	.000000	.000000	187.707
		37.0000	.000000	.000000	.000000
FORCED CONVECTION	23	1000.00	.000000	.333000	40.0000
FORCED CONVECTION	24	27000.0-01	.000000	900.000	25.0000
FORCED CONVECTION	25	170000	.000000	.700000-03	421460+11
		100000-01	218.330	.000000	.000000
		-4.0991	.000000-03	.467000	.000000
		300000	.000000	.000000	.000000
RADIATION	31	0.00000			
RADIATION	32	0.00000			
RADIATION	33	100000+00			
FLUID FLOW	41	20.0000			
FLUID FLOW	42	42.0000			
FLUID FLOW	43	21.0000			
FLUID FLOW	44	63.0000			
FLUID FLOW	45	105.000			

1. PUT SHAFT OF HELICOPTER ENGINE REDUCTION GEARBOX S/H 000-0. FULL OIL FLOW

HEAT TRANSFER COEFFICIENTS

TYPE	INDEX	COEFFICIENTS
FLUID FLOW	46	107.000
FLUID FLOW	47	100.000

INPUT SUMMARY OF HELICOPTER ENGINE REDUCTION, GEARBOX S/N 000-D, FULL OIL FLOW

DESCRIPTION OF THE GEOMETRY AND INDICATION OF THE TYPES AND PATHS OF HEAT TRANSFER

ALL LENGTHS ARE IN MILLIMETERS, A NEGATIVE SIGN OF THE INDEX MEANS NO ROTATIONAL SYMMETRY

TYPE OF HEAT TR.	INDEX	WAVE	MODE	1ST LENGTH	2ND LENGTH	3RD LENGTH
CONDUCTION	1	BETWEEN	1 AND 2	60.0000	24.0000	44.0000
CONDUCTION	-1	BETWEEN	2 AND 3	20.0000	140.0000	150.0000
CONDUCTION	1	BETWEEN	2 AND 3	77.0000	26.0000	44.0000
CONDUCTION	1	BETWEEN	3 AND 13	95.0000	6.0000	73.0000
CONDUCTION	1	BETWEEN	12 AND 13	100.0000	6.0000	74.0000
CONDUCTION	1	BETWEEN	18 AND 20	104.0000	20.0000	53.0000
CONDUCTION	-1	BETWEEN	29 AND 30	20.0000	140.0000	150.0000
CONDUCTION	1	BETWEEN	29 AND 35	104.0000	22.0000	26.0000
CONDUCTION	1	BETWEEN	29 AND 36	92.0000	26.0000	22.0000
CONDUCTION	1	BETWEEN	30 AND 35	92.0000	26.0000	22.0000
CONDUCTION	1	BETWEEN	30 AND 36	104.0000	22.0000	26.0000
CONDUCTION	1	BETWEEN	34 AND 35	92.0000	26.0000	22.0000
CONDUCTION	1	BETWEEN	35 AND 36	170.0000	6.0000	276.0000
CONDUCTION	1	BETWEEN	17 AND 23	81.0000	22.0000	26.0000
CONDUCTION	1	BETWEEN	23 AND 24	81.0000	22.0000	26.0000
CONDUCTION	1	BETWEEN	28 AND 35	81.0000	22.0000	26.0000
CONDUCTION	1	BETWEEN	35 AND 36	81.0000	22.0000	26.0000
CONDUCTION	2	BETWEEN	8 AND 7	70.0000	26.0000	10.0000
CONDUCTION	2	BETWEEN	17 AND 16	74.0000	26.0000	13.0000
CONDUCTION	2	BETWEEN	23 AND 22	74.0000	26.0000	13.0000
CONDUCTION	2	BETWEEN	28 AND 27	74.0000	26.0000	13.0000
CONDUCTION	2	BETWEEN	35 AND 34	74.0000	26.0000	13.0000
CONDUCTION	3	BETWEEN	4 AND 5	36.0000	26.0000	7.0000
CONDUCTION	3	BETWEEN	9 AND 10	56.0000	12.0000	40.0000

Reproduced copy is available

INPUT SUMMARY OF HELICOPTER ENGINE REFINUTION, GEOLCA S/N 00-07, FULL OIL FLOW

DESCRIPTION OF THE GEOMETRY AND INDICATION OF THE TYPES AND PATHS OF HEAT TRANSFER

ALL LENGTHS ARE IN MILLIMETERS, ALL ANGLES ARE IN DEGREES, ALL SIGNS OF THE HEAT HEATS NO ROTATIONAL SYMMETRY

TYPE OF HEAT TRANSFER	INDEX	TYPE	1ST LENGTH	2ND LENGTH	3RD LENGTH
CONVECTION	1	CONVECTION	54.0000	14.0000	44.0000
CONVECTION	2	CONVECTION	43.0000	3.0000	35.0000
CONVECTION	3	CONVECTION	42.0000	5.0000	36.0000
CONVECTION	4	CONVECTION	35.0000	7.0000	35.0000
CONVECTION	5	CONVECTION	40.0000	20.0000	9.0000
CONVECTION	6	CONVECTION	30.0000	8.0000	26.0000
CONVECTION	7	CONVECTION	43.0000	8.0000	25.0000
CONVECTION	8	CONVECTION	40.0000	20.0000	9.0000
CONVECTION	9	CONVECTION	66.0000	8.0000	26.0000
CONVECTION	10	CONVECTION	80.0000	8.0000	26.0000
CONVECTION	11	CONVECTION	43.0000	8.0000	26.0000
CONVECTION	12	CONVECTION	36.0000	8.0000	26.0000
CONVECTION	13	CONVECTION	43.0000	8.0000	26.0000
CONVECTION	14	CONVECTION	36.0000	8.0000	26.0000
CONVECTION	15	CONVECTION	40.0000	8.0000	26.0000
CONVECTION	16	CONVECTION	43.0000	8.0000	26.0000
CONVECTION	17	CONVECTION	40.0000	8.0000	26.0000
CONVECTION	18	CONVECTION	40.0000	8.0000	26.0000
CONVECTION	19	CONVECTION	40.0000	8.0000	26.0000
CONVECTION	20	CONVECTION	40.0000	8.0000	26.0000
CONVECTION	21	CONVECTION	40.0000	8.0000	26.0000
CONVECTION	22	CONVECTION	40.0000	8.0000	26.0000
CONVECTION	23	CONVECTION	40.0000	8.0000	26.0000
CONVECTION	24	CONVECTION	40.0000	8.0000	26.0000
CONVECTION	25	CONVECTION	40.0000	8.0000	26.0000
CONVECTION	26	CONVECTION	40.0000	8.0000	26.0000
CONVECTION	27	CONVECTION	40.0000	8.0000	26.0000
CONVECTION	28	CONVECTION	40.0000	8.0000	26.0000
CONVECTION	29	CONVECTION	40.0000	8.0000	26.0000
CONVECTION	30	CONVECTION	40.0000	8.0000	26.0000
CONVECTION	31	CONVECTION	40.0000	8.0000	26.0000
CONVECTION	32	CONVECTION	40.0000	8.0000	26.0000
CONVECTION	33	CONVECTION	40.0000	8.0000	26.0000
CONVECTION	34	CONVECTION	40.0000	8.0000	26.0000
CONVECTION	35	CONVECTION	40.0000	8.0000	26.0000
CONVECTION	36	CONVECTION	40.0000	8.0000	26.0000
CONVECTION	37	CONVECTION	40.0000	8.0000	26.0000
CONVECTION	38	CONVECTION	40.0000	8.0000	26.0000
CONVECTION	39	CONVECTION	40.0000	8.0000	26.0000
CONVECTION	40	CONVECTION	40.0000	8.0000	26.0000
CONVECTION	41	CONVECTION	40.0000	8.0000	26.0000
CONVECTION	42	CONVECTION	40.0000	8.0000	26.0000
CONVECTION	43	CONVECTION	40.0000	8.0000	26.0000
CONVECTION	44	CONVECTION	40.0000	8.0000	26.0000
CONVECTION	45	CONVECTION	40.0000	8.0000	26.0000
CONVECTION	46	CONVECTION	40.0000	8.0000	26.0000
CONVECTION	47	CONVECTION	40.0000	8.0000	26.0000
CONVECTION	48	CONVECTION	40.0000	8.0000	26.0000
CONVECTION	49	CONVECTION	40.0000	8.0000	26.0000
CONVECTION	50	CONVECTION	40.0000	8.0000	26.0000
CONVECTION	51	CONVECTION	40.0000	8.0000	26.0000
CONVECTION	52	CONVECTION	40.0000	8.0000	26.0000
CONVECTION	53	CONVECTION	40.0000	8.0000	26.0000
CONVECTION	54	CONVECTION	40.0000	8.0000	26.0000
CONVECTION	55	CONVECTION	40.0000	8.0000	26.0000
CONVECTION	56	CONVECTION	40.0000	8.0000	26.0000
CONVECTION	57	CONVECTION	40.0000	8.0000	26.0000
CONVECTION	58	CONVECTION	40.0000	8.0000	26.0000
CONVECTION	59	CONVECTION	40.0000	8.0000	26.0000
CONVECTION	60	CONVECTION	40.0000	8.0000	26.0000
CONVECTION	61	CONVECTION	40.0000	8.0000	26.0000
CONVECTION	62	CONVECTION	40.0000	8.0000	26.0000
CONVECTION	63	CONVECTION	40.0000	8.0000	26.0000
CONVECTION	64	CONVECTION	40.0000	8.0000	26.0000
CONVECTION	65	CONVECTION	40.0000	8.0000	26.0000
CONVECTION	66	CONVECTION	40.0000	8.0000	26.0000
CONVECTION	67	CONVECTION	40.0000	8.0000	26.0000
CONVECTION	68	CONVECTION	40.0000	8.0000	26.0000
CONVECTION	69	CONVECTION	40.0000	8.0000	26.0000
CONVECTION	70	CONVECTION	40.0000	8.0000	26.0000
CONVECTION	71	CONVECTION	40.0000	8.0000	26.0000
CONVECTION	72	CONVECTION	40.0000	8.0000	26.0000
CONVECTION	73	CONVECTION	40.0000	8.0000	26.0000
CONVECTION	74	CONVECTION	40.0000	8.0000	26.0000
CONVECTION	75	CONVECTION	40.0000	8.0000	26.0000
CONVECTION	76	CONVECTION	40.0000	8.0000	26.0000
CONVECTION	77	CONVECTION	40.0000	8.0000	26.0000
CONVECTION	78	CONVECTION	40.0000	8.0000	26.0000
CONVECTION	79	CONVECTION	40.0000	8.0000	26.0000
CONVECTION	80	CONVECTION	40.0000	8.0000	26.0000
CONVECTION	81	CONVECTION	40.0000	8.0000	26.0000
CONVECTION	82	CONVECTION	40.0000	8.0000	26.0000
CONVECTION	83	CONVECTION	40.0000	8.0000	26.0000
CONVECTION	84	CONVECTION	40.0000	8.0000	26.0000
CONVECTION	85	CONVECTION	40.0000	8.0000	26.0000
CONVECTION	86	CONVECTION	40.0000	8.0000	26.0000
CONVECTION	87	CONVECTION	40.0000	8.0000	26.0000
CONVECTION	88	CONVECTION	40.0000	8.0000	26.0000
CONVECTION	89	CONVECTION	40.0000	8.0000	26.0000
CONVECTION	90	CONVECTION	40.0000	8.0000	26.0000
CONVECTION	91	CONVECTION	40.0000	8.0000	26.0000
CONVECTION	92	CONVECTION	40.0000	8.0000	26.0000
CONVECTION	93	CONVECTION	40.0000	8.0000	26.0000
CONVECTION	94	CONVECTION	40.0000	8.0000	26.0000
CONVECTION	95	CONVECTION	40.0000	8.0000	26.0000
CONVECTION	96	CONVECTION	40.0000	8.0000	26.0000
CONVECTION	97	CONVECTION	40.0000	8.0000	26.0000
CONVECTION	98	CONVECTION	40.0000	8.0000	26.0000
CONVECTION	99	CONVECTION	40.0000	8.0000	26.0000
CONVECTION	100	CONVECTION	40.0000	8.0000	26.0000

Reproduced from best available copy.

INPUT SHEET OF HELICOPTER ENGINE REDUCTION GEARBOX S/N 000-0, FULL OIL FLOW

DESCRIPTION OF THE GEOMETRY AND INDICATION OF THE TYPES AND PATHS OF HEAT TRANSFER

ALL LENGTHS ARE IN MILLIMETERS, A NEGATIVE SIGN OF THE INDEX MEANS NO ROTATIONAL SYMMETRY

TYPE OF HEAT TR.	INDEX	NODE	NODE	1ST LENGTH	2ND LENGTH	3RD LENGTH
FORCED CONVECTION	23	BETWEEN 3	A/D 00	70.0000	140.0000	
CONVECTION	33	BETWEEN 3	A/D 00	70.0000	140.0000	.0000
FORCED CONVECTION	23	BETWEEN 29	A/D 00	100.0000	20.0000	
CONVECTION	23	BETWEEN 29	A/D 00	80.0000	140.0000	
CONVECTION	33	BETWEEN 30	A/D 00	80.0000	140.0000	.0000
FORCED CONVECTION	23	BETWEEN 36	A/D 00	110.0000	30.0000	
CONVECTION	33	BETWEEN 36	A/D 00	110.0000	30.0000	.0000
FORCED CONVECTION	23	BETWEEN 38	A/D 00	32.0000	20.0000	
CONVECTION	33	BETWEEN 38	A/D 00	32.0000	20.0000	.0000
FORCED CONVECTION	23	BETWEEN 39	A/D 00	110.0000	45.0000	
CONVECTION	33	BETWEEN 39	A/D 00	110.0000	45.0000	.0000
FORCED CONVECTION	23	BETWEEN 12	A/D 00	110.0000	50.0000	
CONVECTION	33	BETWEEN 12	A/D 00	110.0000	50.0000	.0000
FORCED CONVECTION	23	BETWEEN 8	A/D 00	100.0000	60.0000	
CONVECTION	33	BETWEEN 8	A/D 00	100.0000	60.0000	.0000
FORCED CONVECTION	23	BETWEEN 10	A/D 00	50.0000	25.0000	
CONVECTION	33	BETWEEN 10	A/D 00	50.0000	25.0000	.0000
FORCED CONVECTION	24	BETWEEN 0	A/D 57	40.0000	100.0000	
CONVECTION	24	BETWEEN 10	A/D 57	66.0000	30.0000	
FORCED CONVECTION	24	BETWEEN 11	A/D 57	42.0000	5.0000	
CONVECTION	25	BETWEEN 12	A/D 13	32.0000	5.0000	
FORCED CONVECTION	25	BETWEEN 5	A/D 19	32.0000	5.0000	
CONVECTION	25	BETWEEN 42	A/D 44	32.0000	5.0000	
FORCED CONVECTION	25	BETWEEN 51	A/D 51	32.0000	5.0000	
CONVECTION	31	BETWEEN 10	A/D 12	66.0000	40.0000	94.0000

Revised 10/20/60

INPUT SHAFT OF HELICOPTER ENGINE REDUCTION GEARBOX S/N 000-0, FULL OIL FLOW

DESCRIPTION OF THE GEOMETRY AND INDICATION OF THE TYPES AND PATHS OF HEAT TRANSFER

ALL LENGTHS ARE IN MILLIMETERS, A NEGATIVE SIGN OF THE INDEX MEANS NO ROTATIONAL SYMMETRY

TYPE OF HEAT TR.	INDEX	MODE	MODE	1ST LENGTH	2ND LENGTH	3RD LENGTH
MAXIMIZATION.	32	RELAXED	5	A.D	7	48.0000
MAXIMIZATION.	32	RELAXED	14	A.D	16	48.0000
MAXIMIZATION.	32	RELAXED	20	A.D	22	48.0000
MAXIMIZATION.	32	RELAXED	25	A.D	27	48.0000
MAXIMIZATION.	32	RELAXED	32	A.D	34	48.0000
FLUID FLOW	41	FROM	51	TO	57	(INDEX 41)
FLUID FLOW	41	FROM	41	TO	47	(INDEX 47)
FLUID FLOW	42	FROM	61	TO	42	(INDEX 42)
FLUID FLOW	42	FROM	61	TO	45	(INDEX 42)
FLUID FLOW	42	FROM	61	TO	44	(INDEX 42)
FLUID FLOW	42	FROM	61	TO	44	(INDEX 42)
FLUID FLOW	42	FROM	61	TO	43	(INDEX 42)
FLUID FLOW	42	FROM	45	TO	44	(INDEX 42)
FLUID FLOW	42	FROM	46	TO	49	(INDEX 42)
FLUID FLOW	42	FROM	51	TO	52	(INDEX 42)
FLUID FLOW	42	FROM	43	TO	41	(INDEX 43)
FLUID FLOW	42	FROM	43	TO	57	(INDEX 43)
FLUID FLOW	42	FROM	46	TO	44	(INDEX 43)
FLUID FLOW	42	FROM	46	TO	47	(INDEX 43)
FLUID FLOW	42	FROM	49	TO	47	(INDEX 43)
FLUID FLOW	42	FROM	49	TO	50	(INDEX 43)
FLUID FLOW	42	FROM	52	TO	50	(INDEX 43)
FLUID FLOW	42	FROM	52	TO	53	(INDEX 43)
FLUID FLOW	42	FROM	53	TO	54	(INDEX 44)
FLUID FLOW	42	FROM	50	TO	54	(INDEX 44)

Best available copy.

INPUT SHEET OF HELICOPTER ENGINE REDUCTION GEARBOX S7: UND-O, FULL OIL FLOW

DESCRIPTION OF THE GEOMETRY AND INDICATION OF THE TYPES AND PATHS OF HEAT TRANSFER

ALL LENGTHS ARE IN MILLIMETERS, A NEGATIVE SIGN OF THE INDEX MEANS NO ROTATIONAL SYMMETRY

TYPE OF HEAT TR.	INDEX	NODE	NODE	1ST LENGTH	2ND LENGTH	3RD LENGTH
FLUID FLOW	42	FROM	47 TO 55	(INDEX 45)		
FLUID FLOW	44	FROM	54 TO 55	(INDEX 45)		
FLUID FLOW	44	FROM	54 TO 56	(INDEX 46)		
FLUID FLOW	45	FROM	55 TO 55	(INDEX 46)		
FLUID FLOW	46	FROM	56 TO 57	(INDEX 47)		
FLUID FLOW	47	FROM	57 TO 61	(INDEX 47)		

INPUT SHIPT OF HELICOPTER ENGINE REDUCTION GEARBOX S/1: 000-0, FULL OIL FLOW

TEMPERATURE MAP

TEMPERATURES ARE IN DEGREES CELSIUS. THE FIRST 57 TEMPERATURES ARE CALCULATED. THE OTHERS ARE KNOWN

STEADY STATE TEMPERATURE CALCULATION, INITIAL TEMPERATURES

CALCULATED TEMPERATURES

NODE	TEMPERATURE	NODE	TEMPERATURE	NODE	TEMPERATURE	NODE	TEMPERATURE	NODE	TEMPERATURE	NODE	TEMPERATURE
1	24.000	2	24.000	3	24.000	4	24.000	5	24.000	6	24.000
7	24.000	8	24.000	9	24.000	10	24.000	11	24.000	12	24.000
13	24.000	14	24.000	15	24.000	16	24.000	17	24.000	18	24.000
19	24.000	20	24.000	21	24.000	22	24.000	23	24.000	24	24.000
25	24.000	26	24.000	27	24.000	28	24.000	29	24.000	30	24.000
31	24.000	32	24.000	33	24.000	34	24.000	35	24.000	36	24.000
37	24.000	38	24.000	39	24.000	40	24.000	41	24.000	42	24.000
43	24.000	44	24.000	45	24.000	46	24.000	47	24.000	48	24.000
49	24.000	50	24.000	51	24.000	52	24.000	53	24.000	54	24.000
55	24.000	56	24.000	57	24.000						

274

KNOWN BOUNDARY TEMPERATURES

NODE	TEMPERATURE	NODE	TEMPERATURE	NODE	TEMPERATURE	NODE	TEMPERATURE	NODE	TEMPERATURE
58	24.000	59	24.000	60	24.000	61	70.000		
62	24.000	63	24.000	64	24.000	65	24.000	66	24.000
67	24.000	68	24.000	69	24.000	70	24.000	71	24.000
72	24.000	73	24.000	74	24.000	75	24.000	76	24.000
77	24.000	78	24.000	79	24.000	80	24.000	81	24.000
82	24.000	83	24.000	84	24.000	85	24.000	86	24.000
87	24.000	88	24.000	89	24.000	90	24.000	91	24.000
92	24.000	93	24.000	94	24.000	95	24.000	96	24.000
97	24.000	98	24.000	99	24.000	100	24.000		

0000000000 00 0 CP TIME = 4.134 SECONDS, CLOCK TIME = 14:00:40

0000000000 0000 0 CP TIME = 15.339 SECONDS, CLOCK TIME = 14:10:04

0000000000 00 0 CP TIME = 15.341 SECONDS, CLOCK TIME = 14:10:04

0000000000 0000 0 CP TIME = 19.790 SECONDS, CLOCK TIME = 14:11:02

